EFFECTS OF A REDUCTION IN RENAL FUNCTION ON CARDIOVASCULAR STRUCTURE AND FUNCTION: A PROSPECTIVE STUDY OF LIVING KIDNEY DONORS

WILLIAM EDWARD MOODY

A thesis submitted to the University of Birmingham for the degree of

DOCTOR OF PHILOSOPHY

Clinical and Integrated Cardiovascular Sciences

School of Clinical and Experimental Medicine

College of Medical and Dental Sciences

University of Birmingham

April 2015

ABSTRACT

Chronic kidney disease (CKD) is highly prevalent and recognised as a global public health problem. It has been consistently associated with hypertension and cardiovascular disease; many more patients with a glomerular filtration rate (GFR) below 60 ml/min/1.73m^2 die from cardiovascular causes than progress to end-stage renal disease. Nevertheless, observational studies of cardiovascular disease in CKD remain hard to interpret because renal impairment is forever accompanied by residual confounding factors. These may include the underlying disease process (e.g. diabetes mellitus), or the complications of CKD, such as hypertension, anaemia, bone mineral disease and inflammation. The prospective study of living kidney donors presented in this work provided an ideal experimental model to assess the longitudinal effects of reduced renal function in healthy subjects without manifest cardiovascular disease. Compared with healthy controls, the modest reduction in GFR in donors accompanying uninephrectomy caused increased left ventricular (LV) mass, LV dysfunction, and increased aortic stiffness. There was no change in blood pressure but there were increases in parathyroid hormone, uric acid and highly sensitive C-reactive protein. The size of the reduction in GFR independently predicted the extent of adverse LV remodelling. Reduced GFR should therefore be regarded as a causative risk factor for LV disease and increased arterial stiffness.

DEDICATION

To Lindsay, Rosie, Tom and Alice.

ACKNOWLEDGEMENTS

I would like to express my sincere thanks to all those who have helped me with this project. I am forever indebted to my lead supervisor Prof Jonathan Townend for his ongoing support, outstanding mentorship and expert scientific ideas; he has been a real inspiration. I am also extremely grateful for the unremitting advice and intellectual insight provided by my co-supervisors, Dr Charles Ferro, Dr Richard Steeds and Dr Melanie Madhani. Thanks must also go to Mrs Kathryn Adams, Mrs Donna Begg, Mrs Theresa McDonaugh, Mrs Theresa Brady and Mrs Elizabeth Dwenger, Research Nurses at the National Institute for Health Research / Wellcome Trust Clinical Research Facility, for their invaluable help with the day-to-day running of the study. I would also like to express my sincere thanks to my fellow clinical researchers, Dr Colin Chue, Dr Nicola Edwards and Dr Robin Taylor, in particular, for helping to run the MRI scanner. Thanks must also be extended to Dr Peter Nightingale and Mr James Hodson at the Queen Elizabeth Hospital Birmingham; the statistical support they provided was invaluable. I would like to thank the group in Oxford led by Dr Paul Leeson for sharing their expertise in how best to perform magnetic resonance assessment of flow mediated dilatation, and for the use of their in-house software program to compute automated cross-sectional area calculations of the brachial artery and aorta. Of course, the subjects that were recruited into this study deserve special mention, without them this project would not have been feasible. Finally, I wish to thank the British Heart Foundation for funding this investigator-led study.

EXTENT OF PERSONAL CONTRIBUTION

All work presented in this thesis was carried out by myself, with the following notable exceptions. The original idea for the observational, parallel group, blinded end point study of living kidney donors and healthy controls presented in this thesis was devised by Prof Jonathan Townend and Dr Charles Ferro, although the study protocol underwent extensive revisions following input from myself and Dr Richard Steeds. The application for the British Heart Foundation Clinical Research Training Fellowship that funded the work presented in this thesis was led by me and Professor Jonathan Townend with important contributions from Dr Charles Ferro, Dr Richard Steeds and Dr Melanie Madhani. Approval from the Research Ethics Committee (South Birmingham) and the study sponsor (Queen Elizabeth Hospital Birmingham) was sought by me and Prof Jonathan Townend. All cardiac magnetic resonance images were acquired by me with the assistance of Dr Colin Chue, Dr Richard Steeds, Dr Nicola Edwards and Dr Robin Taylor. Isotopic glomerular filtration rate studies were performed in the Nuclear Medicine Department at Queen Elizabeth Hospital Birmingham under the supervision of Dr Christopher Boivin. Assays for highly sensitive C-reactive protein were performed by Dr Lakhvir Assi at The Binding Site Group Ltd, Birmingham. Assays for N-terminal pro-brain natriuretic peptide were performed by Prof Leong Ng at Leicester Royal Infirmary. Assays for renin and aldosterone were performed by Dr Rachel Webster at the Queen Elizabeth Hospital Birmingham. Statistical advice was provided by Dr Peter Nightingale and Mr James Hodson at Queen Elizabeth Hospital Birmingham.

TABLE OF CONTENTS

LIST OF FIGURES

LIST OF TABLES

LIST OF ABBREVIATIONS

ACE	angiotensin converting enzyme
ACR	albumin : creatinine ratio
ADMA	asymmetric dimethylarginine
ADQI	acute dialysis quality initiative
ADH	antidiuretic hormone
AVPD	atrioventricular plane descent
AIx	augmentation index
AIx_{75}	augmentation index corrected for a heart rate of 75 beats per min
ANP	atrial natriuretic peptide
ARB	angiotensin II receptor blocker
BNP	B-type natriuretic peptide
CKD	chronic kidney disease
CKD-EPI	chronic kidney disease epidemiology collaboration
CMR-FT	cardiac magnetic resonance-feature tracking
^{51}Cr-EDTA	51-chromium ethylenediaminetetraacetic acid
DCM	dilated cardiomyopathy
E	lagrangian strain
Ea	arterial elastance
ECV	extracellular volume
Ees	elastance at end systole
EPO	erythropoietin
ESRD	end stage renal disease
ET-1	endothelin-1

eGFR	estimated glomerular filtration rate
FGF-23	fibroblast growth factor-23
FGFR-1	fibroblast growth factor receptor-1
FMD	flow mediated dilatation
FT	feature tracking
GCS	global circumferential strain
GLS	global longitudinal strain
GTN	glyceryl trinitrate
HARP	harmonic phase magnetic resonance imaging
HFpEF	heart failure with preserved ejection fraction
HLA	horizontal long axis
hsCRP	highly sensitive C-reactive protein
hsTnT	highly sensitive Troponin T
iGFR	isotopic glomerular filtration rate
ICC	intraclass correlation coefficient
ICV	intracellular volume
IMT	intima-media thickness
iPTH	intact parathyroid hormone
KDIGO	kidney disease improving global outcomes
LV	left ventricle or left ventricular
LVEDV	left ventricular end diastolic volume
LVEF	left ventricular ejection fraction
LVESV	left ventricular end systolic volume
LVM	LV mass
MDRD	modification of diet in renal disease

MR	mineralocorticoid receptor
MRI	magnetic resonance imaging
MRB	mineralocorticoid receptor blocker
NHANES	US National Health and Examination Survey
NKF K/DOQI	National Foundation Dialysis Outcome Quality Initiative
NO	nitric oxide
NOS	nitric oxide synthase
NT-proBNP	N-terminal pro-brain natriuretic peptide
PLAS	peak longitudinal atrial strain
preA-S	pre-atrial contraction longitudinal strain
PTH	parathyroid hormone
PWV	aortic pulse wave velocity
PWV_{adj}	aortic pulse wave velocity adjusted for mean arterial pressure
RAAS	renin-angiotensin-aldosterone system
SDC	smallest detectable change
SEM	standard error of the mean
SPAMM	spatial modulation of magnetization
SR	strain rate
SSFP	steady-state free precession imaging
T2DM	type 2 diabetes mellitus
TDI	tissue Doppler imaging
USRDS	United States Renal Database System
VLA	vertical long axis
VSMCs	vascular smooth muscle cells
vWF	von Willebrand Factor

1. INTRODUCTION: UNDERSTANDING THE EFFECTS OF CHRONIC KIDNEY DISEASE ON CARDIOVASCULAR RISK

1.1. The Kidneys

The kidneys are retroperitoneal organs located within the paravertebral gutters between the vertebral levels T12 and L3. Each kidney receives blood from the renal artery, and drains blood into the renal vein, which courses beside the ureter. The blood flow to the two kidneys under resting physiological conditions equates to roughly 25% of the cardiac output (approx. 1.25 L/min) despite the organs only constituting less than 0.5% of the total body weight. The basic functional unit of the kidney is the nephron and each human kidney contains between 1 and 1.5 million nephrons (Lote, 2012). The nephron consists of a glomerulus, a proximal tubule, a loop of Henle, a distal tubule and a collecting system. Ultrafiltration occurs at the glomerulus with passive movement of a protein-free fluid from the glomerular capillaries into Bowman's space. The amount of plasma that is filtered in the glomerulus over time is the glomerular filtration rate (GFR). Ultrafiltration is followed by selective reabsoprtion of water and electrolytes at the proximal tubule and concentration of the filtrate at the loop of Henle and collecting duct, ultimately resulting in the formation of urine (Berne, 1993).

By excretion of water and solutes, the kidneys are able to regulate body fluid osmolality and maintain the normal cell volume in all tissues. As well having an important excretory role,

the kidneys have several other major functions including: regulation of electrolyte and acid-base balance, and the production and secretion of hormones. Indeed, the kidneys are important endocrine organs that produce and secrete renin, prostaglandins, kinins, 1,25-dihydroxyvitamin D (calcitriol), and erythropoietin. Renin is produced by the granular cells of the juxtaglomerular apparatus and activates the renin-angiotensin-aldosterone system (RAAS), which has subsequent effects on salt and water retention and permits modulation of blood pressure. In conjunction with angiotensin II, prostaglandins and kinins also influence systemic blood pressure (Berne, 1993). In the proximal tubule of the nephron, the mitochondrial enzyme 25-hydroxyvitamin D3 1-alpha-hydroxylase converts 25-hydroxyvitamin D (calcidiol) to 1,25-dihydroxyvitamin D (calcitriol). Calcitriol circulates as the biologically active form of vitamin D, causing increased uptake of calcium from the gut into the blood, and increases the release of calcium into the blood from bone. Erythropoietin (EPO) is a glycoprotein hormone produced by interstitial fibroblasts in the kidney and serves as a cytokine for erythrocyte precursors in the bone marrow to stimulate red blood cell production (Berne, 1993).

1.2. The Cardiorenal Axis

Besides dynamic alterations in cardiac function, the regulation of intravascular volume is central to maintaining cardiovascular haemostasis and permitting adequate end-organ perfusion. To this end, the kidney integrates various haemodynamic, neural and endocrine factors as depicted in Figure 1-1. As part of the cardiorenal axis, changes in volume and pressure within the atria and ventricles initiate reflexes that affect renal function (Heywood, 2012). The heart can also affect the kidney by activating high-pressure arterial baroreceptors found in the carotid sinus, aortic arch and afferent arteriole of the glomerulus. A decline in arterial pressure results in vagal inhibition and an increase in sympathetic efferent activity stimulating RAAS via the beta-adrenergic pathway. When renal perfusion is lowered, renin is secreted which cleaves angiotensinogen to angiotensin I, which itself is cleaved by the angiotensin converting enzyme (ACE) to angiotensin II. Angiotensin II causes systemic vasoconstriction increasing blood pressure and preferentially vasoconstricts the efferent arteriole of the glomerulus, increasing renal perfusion pressure and the glomerular filtration rate. It also stimulates secretion of the mineralocorticoid aldosterone and release of anti-diuretic hormone (ADH) thereby promoting sodium and water retention. By contrast, increased cardiac filling pressures from an expanded extracellular fluid volume stimulates the release of ADH (so-called “Henry-Gauer reflex”) and atrial natriuretic peptide (ANP) from the atria and the release of B-type natriuretic peptide (BNP) from the ventricles. Their combined effect is to promote vasodilatation, sodium and water excretion, as well as to suppress aldosterone (Heywood, 2012, O'Connor, 2005).

The dysregulation of the cardiorenal axis and its negative feedback loop appears important for the development of left ventricular (LV) dysfunction, which is characterised by a deleterious sympathetic overactivation leading to excessive sodium and fluid retention. Although the exact mechanisms for this process remain poorly understood, it is fundamental in contributing to the evolution from asymptomatic to symptomatic LV dysfunction. The phenomenon may be explained by the "body volume regulation hypothesis" where despite an increase in total blood volume, arterial underfilling develops secondary to a decrease in cardiac output (Heywood, 2012). Under such circumstances, RAAS activation attenuates the normal renal response to the natriuretic peptides. Resistance to the natriuretic response of ANP and BNP appears to result from the neurohumoral-mediated diminished sodium delivery to their site of action, the collecting duct (Heywood, 2012).

In summary, there are many bidirectional physiological pathways whereby the heart and kidney may affect one another. In health, these are vital for maintaining optimal cardiorenal homeostasis under normal physiological conditions but in disease states, these compensatory mechanisms may prove maladaptive in the long-term. The term "cardio-renal syndrome" has been coined to describe a disorder of the heart and kidneys whereby acute or chronic dysfunction in one organ may induce acute or chronic dysfunction of the other. The five subtypes of this syndrome were originally described by Ronco *et al.* (2008) and their pathophysiological mechanisms are described in Figure 1-2. This classification has been subsequently endorsed by a consensus group under the auspices of the Acute Dialysis Quality Initiative (ADQI) (Ronco et al., 2010).

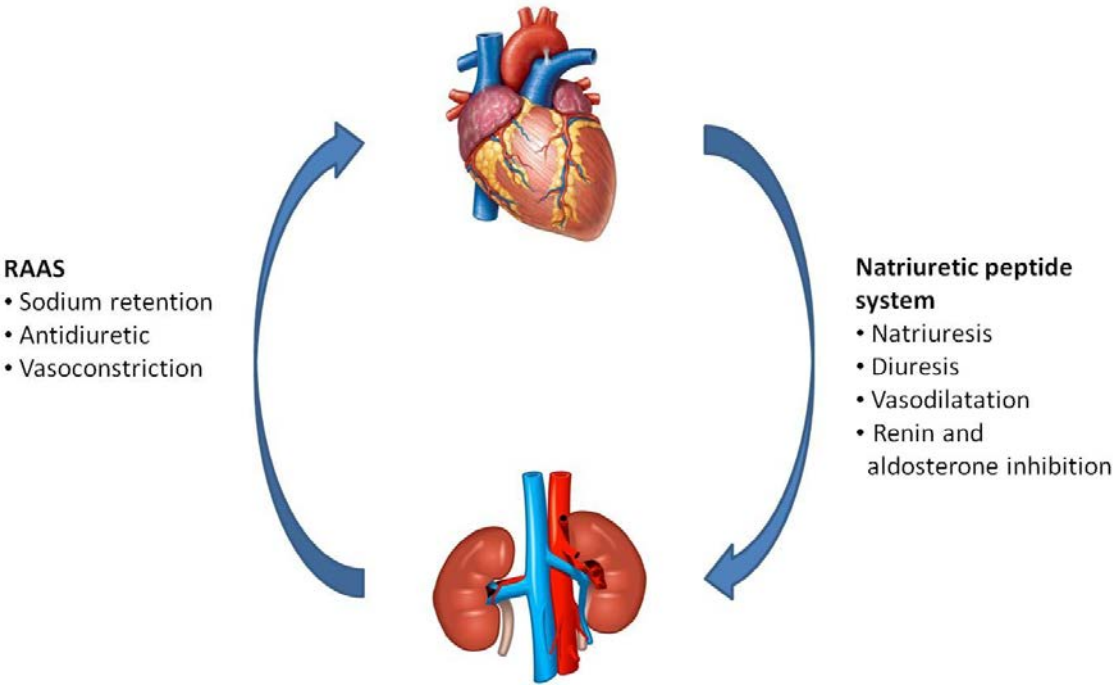

Figure 1-1. Schematic of the Cardiorenal Axis.

Abbreviation: RAAS, renin-angiotensin-aldosterone system. Adapted from Heywood, 2012.

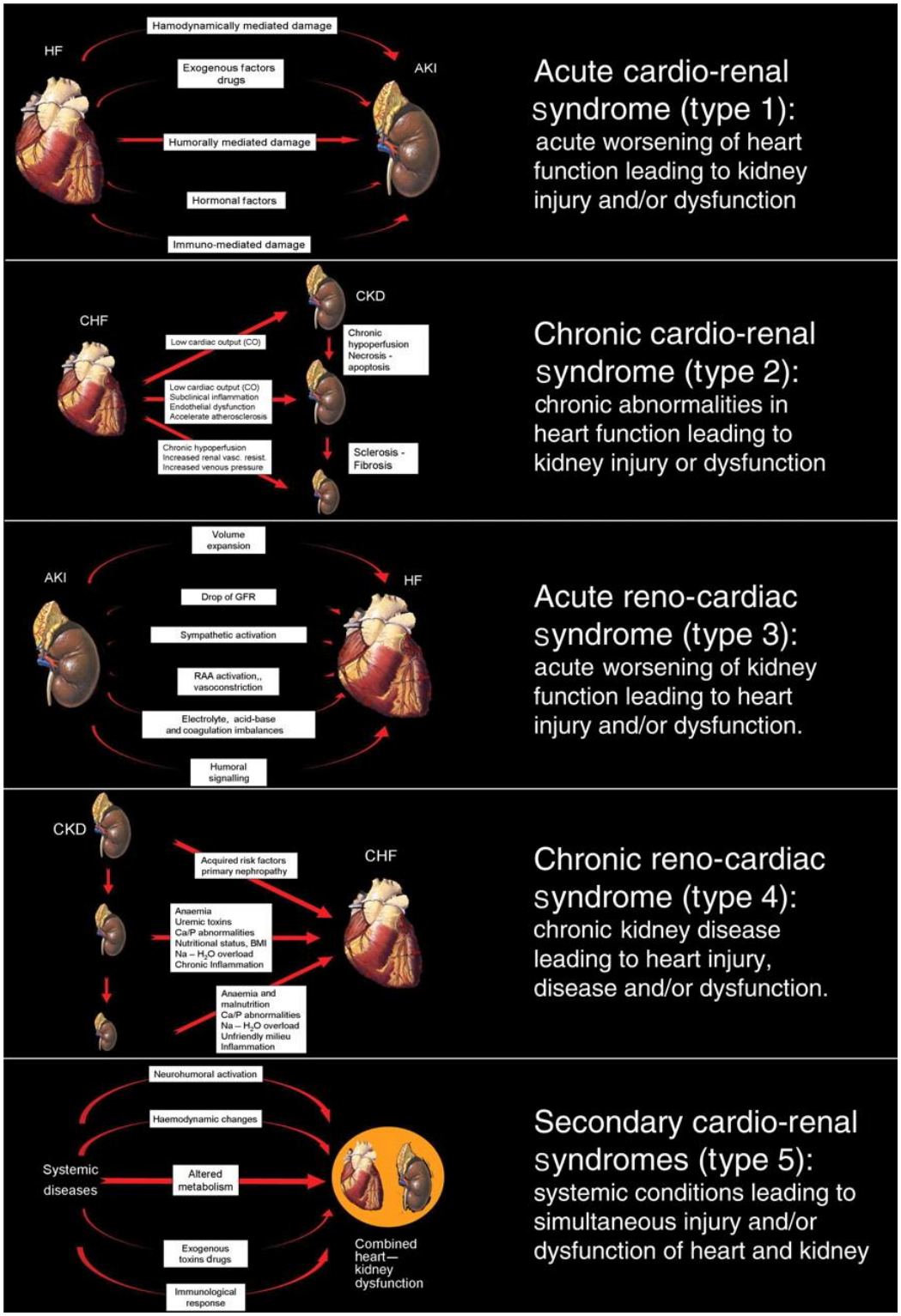

Figure 1-2. Pathophysiology of the Five Subtypes of Cardiorenal Syndrome.

Abbreviations: AKI, acute kidney injury; Ca, calcium CHF, congestive heart failure; CKD, chronic kidney disease; GFR, glomerular filtration rate;, P, phosphate (Ronco et al., 2010).

1.3. Definition of Chronic Kidney Disease

Chronic kidney disease is defined as abnormalities of kidney structure or function, present for more than 3 months. It can be classified according to the cause, GFR category, and albuminuria category, on the basis of their respective prognostic significance (KDIGO, 2012). There are 5 stages of CKD according to the GFR and evidence of structural or functional damage (Table 1-1).

The GFR cannot be directly measured but instead is indirectly quantified using clearance of a filtration marker into urine. As the reference standard, the GFR can be accurately measured using the clearance of intravenously administered radioisotopes such as 51Cr-ethylenediaminetetraacetic acid (51Cr-EDTA) (Martensson et al., 1998). More commonly, in clinical practice an estimated GFR (eGFR) is derived from measurement of endogenous serum creatinine and a number of equations are available. The Cockcroft-Gault equation was the first of these to be adopted after validation against 24-hour urinary creatinine clearance (Cockcroft and Gault, 1976), although it is no longer recommended because it systematically overestimates GFR. This relates to tubular creatinine secretion as well as the inclusion of weight as a variable, which in the presence of obesity and fluid overload is a poor reflection of lean body mass (Stevens et al., 2006). More commonly, eGFR is now calculated using either the Modification of Diet in Renal Disease (MDRD) equation or the Chronic Kidney Disease Epidemiology Collaboration (CKD-EPI) formula (Levey et al., 2009). Whilst both these methods calculate eGFR using the same 4 variables (age, race, gender and serum creatinine), it has been suggested that the CKD-EPI formula more accurately reflects measured GFR,

particularly in subjects with near-normal levels of renal function (GFR >60 ml/min/1.73m^2) (Michels et al., 2010). Nevertheless, the accuracy of eGFR remains limited by its dependence on muscle mass and dietary protein intake. Cystatin C is a cationic cysteine proteinase, produced by all cells at a constant rate which is freely filtered by the glomerulus and almost completely reabsorbed and degraded by the proximal tubule (Stevens et al., 2006). The recent addition of cystatin C to that of serum creatinine to determine eGFR gives further improved accuracy and moreover, strengthens the association between the eGFR and the risks of death and end-stage renal disease (Shlipak et al., 2013).

Data from the US National Health and Nutrition Examination Survey (NHANES) show the prevalence of CKD is both high and rising; over 13% of US citizens fulfil the National Kidney Foundation Dialysis Outcome Quality Initiative (NKF K/DOQI) criteria for stage 1 to 4 CKD (Coresh et al., 2007). Whilst this figure excludes patients with end stage renal disease (ESRD), a population associated with extreme cardiovascular risk, in public health terms the principal cardiovascular disease burden resides in early stage CKD which is over 50 times more prevalent (Figure 1-3), and affects up to 50% of community-dwelling subjects over the age of 70 years (Coresh et al., 2003).

Table 1-1. Stages of Chronic Kidney Disease as Defined by KDIGO Guidelines.

Stage	*Description*	*GFR (ml/min/1.73m^2)*
G1	Kidney damage* with normal or increased GFR	≥90
G2	Kidney damage* with mildly decreased GFR	60-89
G3	Moderately decreased GFR	30-59
G4	Severely decreased GFR	15-29
G5	Kidney failure	<15 or dialysis

*Evidence of functional or structural kidney abnormalities for ≥3 months. In the absence of evidence of kidney damage, neither GFR category G1 nor G2 fulfill the criteria for chronic kidney disease.

Abbreviations: GFR, Glomerular Filtration Rate; KDIGO, Kidney Disease Improving Global Outcomes.

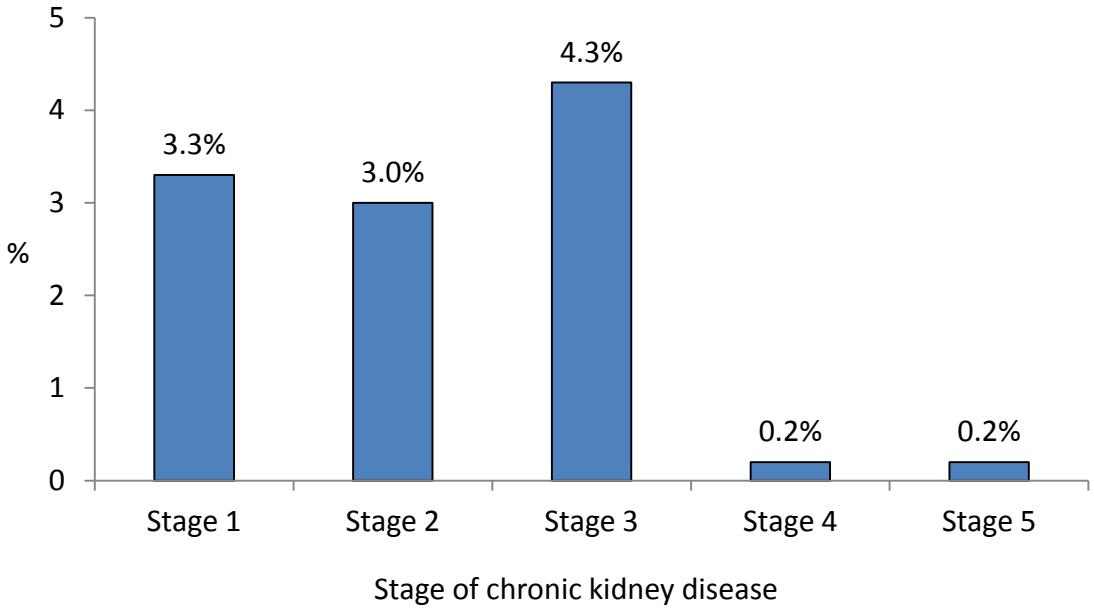

Figure 1-3. Estimated Prevalence of Chronic Kidney Disease in Adults in the United States according to the Third National Health and Examination Survey (NHANES III).

1.4. Chronic Kidney Disease and Cardiovascular Risk

Chronic kidney disease (CKD) is a major but poorly recognised and under-treated risk factor for cardiovascular disease (Best et al., 2004). Numerous observational studies have demonstrated the excess cardiovascular risk associated with CKD (Go et al., 2004, Schiffrin et al., 2007, Van Biesen et al., 2007, Mccullough et al., 2007, Kurth et al., 2009, Di Angelantonio et al., 2010, Matsushita et al., 2010). In a study of over a million US adults in whom serum creatinine was measured between 1996 and 2000, there was an independent, graded inverse relationship between eGFR at levels <60 ml/min/1.73m^2 and the risk of adverse cardiovascular events (Go et al., 2004). Although there is a consensus from international organisations (The National Kidney Foundation Kidney Disease Outcomes Quality Initiative (NKF K/DOQI) and Kidney Disease: Improving Global Outcomes (KDIGO)) that individuals with a GFR <60 ml/min/1.73m^2 are at increased risk of cardiovascular morbidity and mortality, (Eknoyan et al., 2004, KDIGO, 2012), whether it is appropriate to dichotomize patients based on this "threshold" is questionable. Many studies have simply used subjects with an eGFR of >60 ml/min/1.73m^2 as their reference population when considering cardiovascular risk. A more recent meta-analysis involving over a million participants taken from general population cohorts found all cause and cardiovascular mortality began rising at an eGFR of <75 ml/min/1.73m^2 (Matsushita et al., 2010). The Belgian Inter-University Research on Nutrition and Health Population Study followed 8,913 apparently healthy participants for a total of 10 years (Van Biesen et al., 2007). The results suggested excess cardiovascular mortality began even earlier at an eGFR of <90 mL/min/1.73m^2, a level commonly regarded as indicating near normal renal function. The cardiovascular mortality risk increased linearly

by 8% for every 10 mL/min/1.73m^2 fall in eGFR. This is a potentially very important finding given the high prevalence of eGFR values in this range, particularly in the elderly in whom the loss of renal function has hitherto been regarded as benign.

Several studies have also shown a graded relationship with cardiovascular risk and the level of albuminuria (Klausen et al., 2004, Arnlov et al., 2005, Matsushita et al., 2010). In the general population, even low levels of urinary albumin excretion, below the current diagnostic threshold for microalbuminuria, have been shown to predict future cardiovascular events including death, independent of other "traditional" cardiac risk factors (Klausen et al., 2004, Arnlov et al., 2005). This finding was recently confirmed by a CKD Prognosis Consortium meta-analysis where urinary albumin : creatinine ratio (ACR) was independently associated with adjusted risk of all cause and cardiovascular mortality with a log linear relationship but there was no evidence of the threshold effect which has been postulated for GFR (Matsushita et al., 2010). Indeed, the hazard ratio for all cause and cardiovascular mortality is already doubled within the ACR range of 0.3 – 3.0 mg/mmol, a level which is not detected by standard urinary dipsticks and has often been considered innocuous. Furthermore, the risks of cardiovascular and all cause mortality appear to be independently and multiplicatively associated with eGFR and albuminuria (Matsushita et al., 2010). Proteinuria is also associated with progression of renal disease (Jafar et al., 2003) and may even play a causal role through toxicity to tubular epithelial cells (Hostetter et al., 1981). Albuminuria is likely to be more than just a passive biomarker of cardiovascular disease making it an attractive target for risk reduction therapy. The PREVEND group have shown

that treating normotensive microalbuminuric individuals with an angiotensin-converting enzyme inhibitor resulted in a significant reduction in urinary albumin excretion and was also associated with a trend in reducing cardiovascular events compared to placebo (Asselbergs et al., 2004).

1.5. Pathophysiology of Cardiovascular Disease in Chronic Kidney Disease

The importance of detecting early stage CKD has been emphasised of late because it offers the potential to prevent or delay its progression and reduce the risk of cardiovascular disease on a global scale (NICE, 2015). The development of cardiovascular risk reduction therapies is however, hindered by the fact that whilst the epidemiological association between CKD and cardiovascular disease is strong, the underlying pathophysiological mechanisms remain ill-defined. There is abundant evidence suggesting that modification of "conventional" atherosclerotic risk factors in CKD does not improve cardiovascular outcomes to the same degree that would be expected for the general population. First, although in CKD there is a clustering of classical risk factors such as hypertension and diabetes mellitus, they perform very poorly in the prediction of cardiovascular risk in this population, particularly in late stage CKD (Coresh et al., 1998). Indeed, in ESRD there is an inverse relationship between cardiovascular event rates and risk factors such as total cholesterol, obesity and even blood pressure. These paradoxical associations may, at least in part, be explained by "reverse causality", a feature of chronic disease malnutrition-inflammation syndromes (Kalantar-Zadeh et al., 2003). Second, epidemiological studies suggest that whilst roughly 40% of all deaths in patients with ESRD are cardiovascular in origin, the majority of these deaths are attributable to sudden cardiac death, arrhythmia or congestive heart failure (Figure 1-4) with relatively few from atherosclerotic events such as myocardial infarction (USRDS, 2011). Heart failure is a major cause of morbidity and mortality in both early stage CKD and ESRD with incident rates 3-4 times higher than in non-CKD subjects (Foley et al., 2005). Thus, it is widely held that it is not atheromatous coronary artery disease

but myocardial disease - LV hypertrophy with fibrosis and diastolic dysfunction, often accompanied by systolic dysfunction - that is the principal cause of cardiovascular death and disease in CKD. The prevalence of LV hypertrophy is increased from the earliest stages of progressive renal disease and reaches over 70% in patients with ESRD (Stewart et al., 2005, Mark et al., 2006). Recent cardiac magnetic resonance imaging (MRI) data reported from the Birmingham Cardio-Renal Group demonstrate that a process of diffuse LV fibrosis begins in early stage CKD which is associated with important functional changes including abnormalities of regional systolic and diastolic ventricular function (Edwards et al., 2015). The result from the SHARP (Study of Heart And Renal Protection) trial of lipid lowering therapy in CKD, in which LDL reduction was associated with a significant decrease in major atherosclerotic events, but no reduction in total vascular mortality (Baigent et al., 2011) is consistent with this paradigm. These data are similar to those seen in lipid lowering trials in heart failure (Kjekshus et al., 2007); in both disease processes the majority of deaths appear to result from pump failure or arrhythmia as opposed to coronary events (USRDS, 2011).

1.5.1. Atheroma in Chronic Kidney Disease

Examination of the arterial system of patients with CKD reveals two distinct but overlapping arterial pathologies: atherosclerosis and arteriosclerosis (Edwards et al., 2006). Whilst atherosclerosis is primarily an intimal disease, patchy in distribution and occurring preferentially in medium-sized conduit arteries, arteriosclerosis is a diffuse disease of the media which leads to increased arterial stiffness (see Section 1.5.2). The morphological characteristics of atheroma in patients with CKD are distinct and include increased plaque

calcification and increased intimal and medial thickness (Schwarz et al., 2000). The prevalence of atheromatous disease in CKD is high, although it is not clear whether this is a direct result of renal dysfunction or the clustering of risk factors such as hypertension, diabetes and inflammation which invariably accompany CKD. A study of carotid intima-media thickness (IMT) from Finland showed a fourfold greater plaque score in CKD patients (pre-dialysis, dialysis and post transplant) compared to healthy controls (Leskinen et al., 2003). In a Canadian study, compared to a reference control group the adjusted relative risk of myocardial infarction was 1.4 in patients with non-diabetic CKD and 2.7 in diabetic stage 3 and 4 CKD compared to 2.0 for diabetes and 3.8 for subjects with previous myocardial infarction (Tonelli et al., 2012). When severe proteinuria was present, however, the relative risk of myocardial infarction in non-diabetic CKD equalled that of the diabetic population. There is also an increased prevalence of peripheral and cerebral vascular disease in CKD according to data from the US Renal Data System (Figure 1-5), though it must be remembered that these data are not controlled for co-morbidities such as diabetes and hypertension, known to be strongly associated with atheroma (Usrds, 2011). There is clear evidence of an adverse interaction between CKD and major atherosclerotic events; outcomes after acute coronary syndrome and stroke are much worse in CKD than in the general population (Macwalter et al., 2002, Hanna et al., 2011, Saltzman et al., 2011, Kumai et al., 2012). For instance, in ST elevation myocardial infarction, patients on dialysis (treated in the pre-primary angioplasty era) had a one year mortality rate of almost 60% with a one year cardiac mortality of 41% (Herzog et al., 1998).

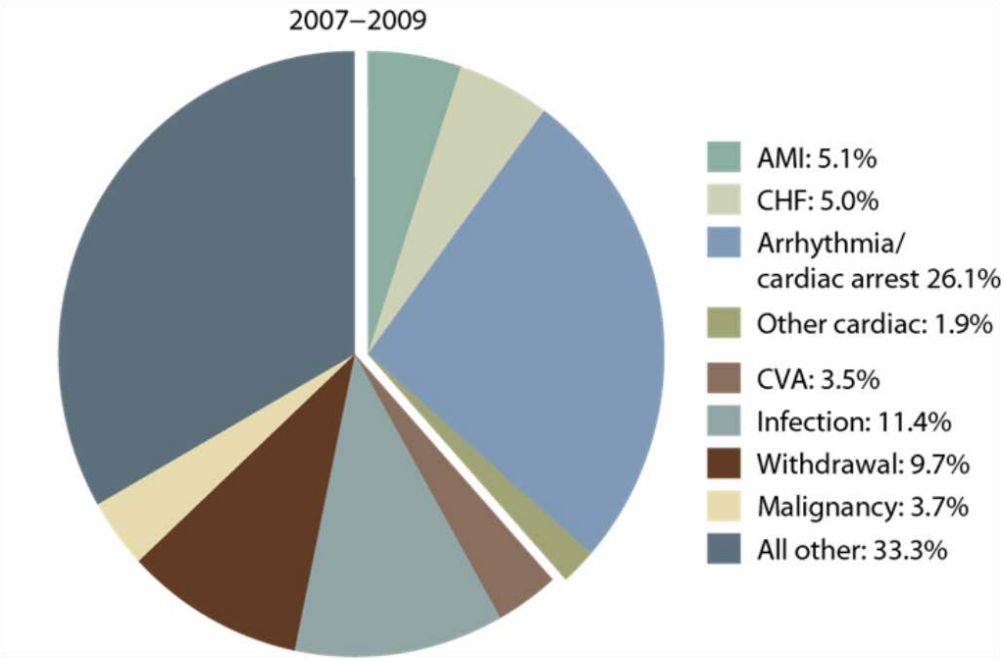

Figure 1-4. Causes of Death in Prevalent US Dialysis Patients.

Data are taken from 2007-2009. AMI; acute myocardial infarction; CHF, congestive heart failure; CVA, cerebrovascular accident. Figure is reproduced from Ch. 4 of the US Renal Data System annual report (2011).

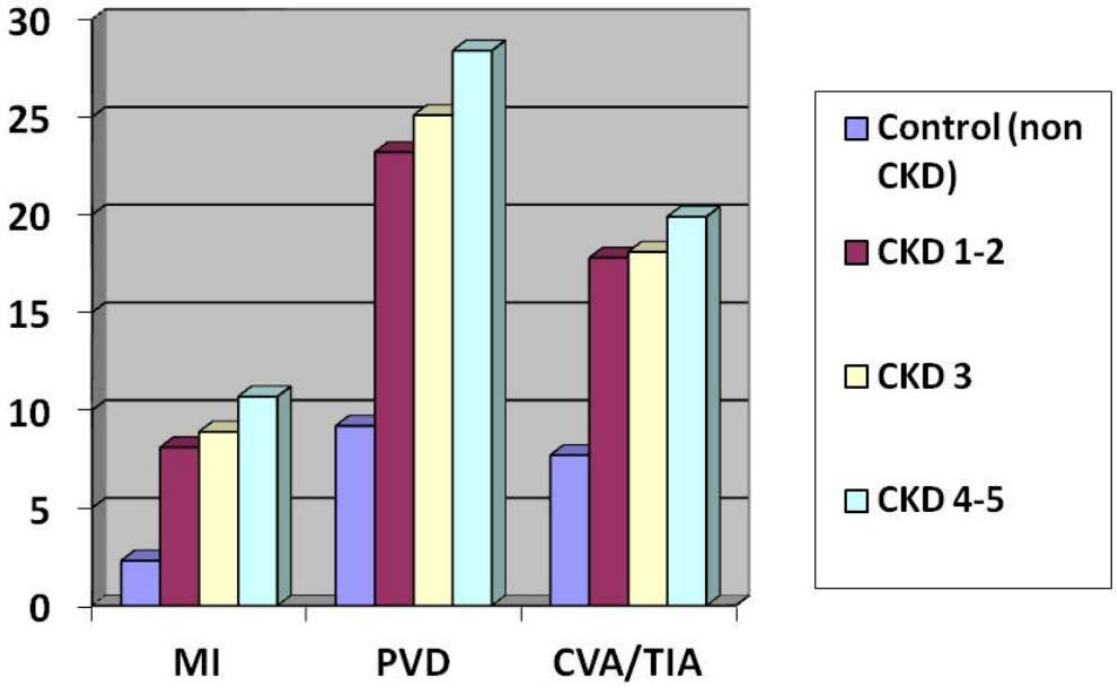

Figure 1-5. Cardiovascular Disease Prevalence Rates (%) by CKD Stage For Common Cardiovascular Diseases.

CKD, chronic kidney disease; CVA, cerebrovascular accident; MI, myocardial infarction; PVD, peripheral vascular disease; TIA, transient ischaemic attack. Figure reproduced from Ch. 4 of the US Renal Data System report (2011).

1.5.2. Arteriosclerosis in Chronic Kidney Disease

Arteriosclerosis is characterised by thickening and calcification of the medial arterial layer and is a hallmark feature of arterial disease in CKD. Medial calcification is concentric and does not extend into the arterial lumen unless there is co-existent atheroma. Increased collagen content, hyperplasia and hypertrophy of the vascular smooth muscle cells cause wall thickening which in combination with calcification results in increased arterial stiffness (Edwards et al., 2006). Although associations exist between the degree of arterial stiffness and atheromatous plaque burden (Van Popele et al., 2001), studies have failed to demonstrate a significant influence of traditional atherosclerotic risk factors on the development of arteriosclerosis (Cecelja and Chowienczyk, 2009), suggesting that alternative factors drive this process. There appears to be at least some degree of mechanistic overlap, however, as endothelial dysfunction (ED) and reduced NO bioavailability have been shown to contribute to arterial stiffening (Schmitt et al., 2005). Increased arterial stiffening appears to play a central role in the causation of cardiovascular disease in CKD. The strong association between arterial stiffening and mortality in ESRD was demonstrated over 10 years ago by London and colleagues (Guerin et al., 2001, Blacher et al., 1999, Blacher et al., 1998). Recent UK data (National Institute for Cardiovascular Outcomes Research) have demonstrated increased mortality after transcatheter aortic valve implantation in those subjects with an eGFR <45 ml/min/1.73m^2 (Ferro et al., 2015). These outcomes may in part, reflect the increased aortic calcification associated with worsening renal function (Chue et al., 2012b), which could predispose CKD subjects to peri-procedural complications such as paravalvular leak, aortic dissection and stroke. Whilst the process of arterial stiffening

appears to begin during early stage CKD, the prognostic significance of arterial stiffness in this specific population remains uncertain (Edwards et al., 2008a, Briet et al., 2006).

Before the pathophysiological effects of arterial stiffening can be fully appreciated, an understanding of the normal physiology of the aorta and large arteries is essential. Their major functions are not only to deliver blood around the body but to buffer the oscillatory changes in blood pressure that result from intermittent ventricular ejection. The highly distensible arterial system ensures that most tissues receive near steady flow with no exposure to peak systolic pressures; this mechanism is so efficient that there is almost no drop in peripheral mean arterial pressure compared to the ascending aorta (Avolio et al., 2009). Loss of arterial distensibility results in a more rigid aorta that is less able to accommodate the volume of blood ejected by the left ventricle, resulting in greater pressure augmentation in systole and higher pulse pressures (Davies et al., 2008). An often cited additional explanation for the elevated systolic pressure that accompanies an increase in arterial stiffness is that of an earlier return of reflected waves of ventricular contraction from distal arterial branch points (London et al., 1992, Latham et al., 1985). In healthy compliant arteries reflected waves were believed to return to the ascending aorta in diastole, augmenting diastolic pressure and coronary blood flow; in older and stiffer arteries, the reflected waves were thought to return earlier in systole increasing ventricular afterload and augmenting systolic and pulse pressures. Although an attractive hypothesis, there is now abundant evidence showing that reflected waves arrive in systole irrespective of age (Baksi et al., 2009). These data together with information available from techniques that separate

reflected waves from the reservoir pressure strongly suggest that the “cushioning effect” or Windkessel model appears to be the more important physiological explanation (Wang et al., 2003). In any case, as arterial stiffness increases, a loss in arterial distensibility exposes the myocardium, brain and kidneys to higher systolic pressures and greater pressure fluctuations resulting in myocardial, cerebral and renal microvascular damage and an increased risk of heart failure, arrhythmia, stroke and further renal impairment (Figure 1-6) (O'Rourke and Safar, 2005, Moody et al., 2013). Whilst higher systolic pressure increases LV afterload, lower diastolic pressure reduces diastolic coronary perfusion, promoting ischaemia and placing greater reliance on systolic coronary perfusion (London et al., 1996, Saeki et al., 1995).

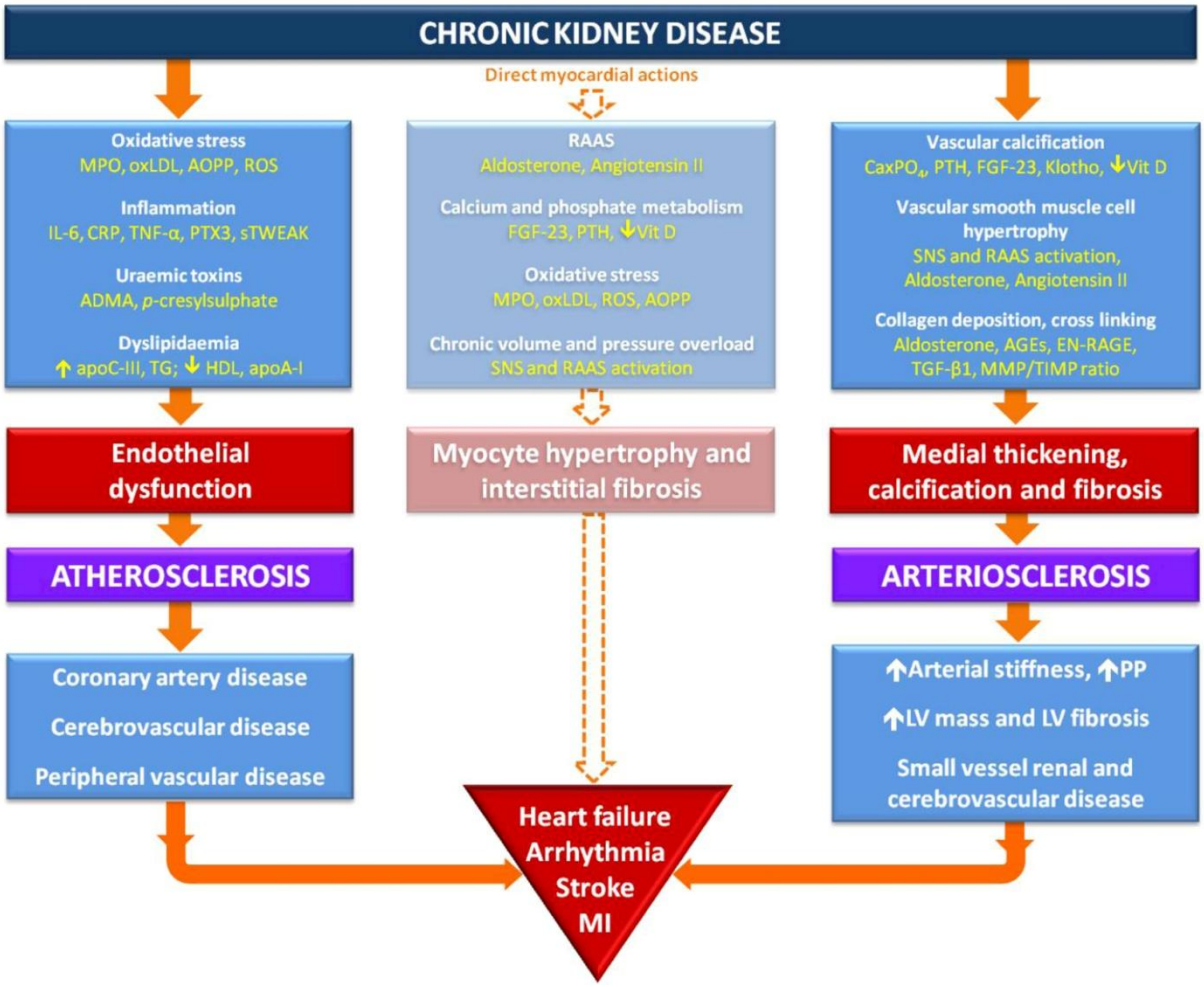

Figure 1-6. Proposed Mechanistic Pathways for Arterial and Myocardial Disease in Chronic Kidney Disease.

Abbreviations: ADMA, asymmetric dimethylarginine; AGEs, advanced glycation endproducts; AOPP, advanced oxidation protein products; apoA-I, apolipoprotein AI; apoC-III, apolipoprotein CIII; C1TP, carboxy-terminal telopeptide; $CaxPO_4$, calcium-phosphate product; CKD, chronic kidney disease; CRP, C-reactive protein; EN-RAGE, extracellular newly identified RAGE-binding protein; FGF-23, fibroblast growth factor-23; HDL, high-density lipoprotein; IL-6, interleukin-6; LV, left ventricular; MMP, matrix metalloproteinases; MPO, myeloperoxidase; oxLDL, oxidised low-density lipoprotein; NT-pro-BNP, N-terminal fragment pro-B-type natriuretic peptide; PIIINP, Procollagen III N-Terminal Propeptide; PP,

pulse pressure; PTH, parathyroid hormone; PTX3, pentraxin-3; RAAS, renin-angiotensin-aldosterone system; ROS, reactive oxygen species; TG, triglycerides; TGF-β1, transforming growth factor-beta1; TIMP, tissue inhibitors of metalloproteinases; TNF-α, tumour necrosis factor-alpha; sTWEAK, soluble tumour necrosis factor-like weak inducer of apoptosis; Vit D, 1,25 dihydroxyvitamin D.

1.5.3. Arterial-Ventricular Interaction in Chronic Kidney Disease

The central role of arterial stiffening has also focussed attention on the interaction between the left ventricle and arterial tree; termed arterial-ventricular interaction. In health, cardiac function is physiologically matched or coupled with arterial function to ensure maximum cardiac work and efficiency (Chen et al., 1998). This coupling is most commonly investigated and quantified by the measurement of arterial and ventricular elastances, either invasively with conductance catheters or non-invasively using echocardiographic parameters. LV systolic elastance (Ees) is a measure of chamber stiffness at end systole and arterial elastance (Ea) is a measure of net ventricular afterload (incorporating resistance, pulsaltile load and blood pressure) determined by the ratio of end-systolic pressure to stroke volume. When LV function is normal, the coupling ratio is generally between 0.7 and 1.0 (Ea is smaller than Ees) so that work efficiency is maximised but stroke work is sub-maximal for a given preload. With systolic dysfunction, Ees falls so that in mild dysfunction, the ventricle performs at maximum stroke work. When the heart is coupled to a stiff vascular system, the heart must increase systolic stiffness (Ees) to maintain cardiac metabolic efficiency ensuring transfer of blood to the arterial tree without excessive changes in pressure. Thus the arterial-ventricular coupling ratio is maintained but both Ea and Ees are considerably elevated. These compensatory adaptations maintain cardiac performance with enhanced contractility at rest, but at a price: cardiac reserve is reduced, diastolic function is impaired and the cardiovascular responses to alterations in pressure and volume load are blunted leading to haemodynamic instability and a susceptibility to “flash” pulmonary oedema (Chen et al., 1998).

The abnormalities of arterial and LV function which are so highly prevalent in ESRD may begin in early stage CKD. In a population-based study of 742 individuals, mildly reduced eGFR was significantly associated with greater LV mass in a process dependent upon increased arterial stiffness (Henry et al., 2005). In a cross-sectional study of patients with stage 2 and 3 CKD, the Birmingham Cardio-Renal Group found delayed ventricular relaxation, increased LV systolic and end diastolic stiffness and elevated left atrial volumes compared to healthy matched controls (Edwards et al., 2008a). Arterial elastance was also elevated such that the arterial-ventricular coupling ratio was preserved. This suggests that the two processes occur in parallel and is consistent with the theory that aortic stiffness drives the development of LV stiffness in CKD (Edwards et al., 2008a). This pattern, similar to that found in heart failure with preserved ejection fraction (Edwards et al., 2008b), suggests that early stage CKD is likely to be associated with reduced cardiovascular reserve and increased haemodynamic instability, although further work is required in this area. The level of GFR at which arterial stiffening begins to increase is not clear but elevated pulse wave velocity (PWV), the current reference standard marker of aortic stiffness, is already evident in stage 2 CKD (Wang et al., 2005). A stepwise increase in PWV corresponding with advancing stages of CKD suggests that arterial stiffness increases as a graded relationship with declining GFR.

1.6. Mechanisms of Arterial Stiffening and Left Ventricular Hypertrophy in Chronic Kidney Disease

Understanding the potential mechanisms underlying increased arterial stiffness in CKD is important, particularly if we are to begin devising strategies to prevent or reverse this pathophysiology. Arterial stiffening is a result of both functional and structural abnormalities of the arterial wall. Endothelial dysfunction provides a dynamic component that may be amenable to treatment with conventional agents such as statins, antihypertensives and novel treatments that increase nitric oxide bioavailability. The structural vascular changes of CKD are however likely to prove harder to reverse. The various potential molecular causes of arteriosclerosis in CKD are summarised in Table 1-3. Recent work has highlighted the importance of both aldosterone and disordered bone mineral metabolism in the causation of arterial stiffness in CKD. Preventive therapy is available for both factors; such treatment might reduce arterial stiffness and prevent many of the pathological cardiovascular changes seen in CKD including LV hypertrophy and fibrosis. Reduction of arterial stiffness is an attractive target for it has the potential to slow the decline in renal function and thereby interrupt the spiralling progression of renal and vascular disease (Figure 1-6).

Table 1-2. Key Human Studies Investigating Molecular Mechanisms of A*therosclerosis* in Chronic Kidney Disease.

Factor/Mechanism	Study population	Study type	Study outcomes	Reference
Endothelial dysfunction				
Reduced NO Secondary to reduced eNOS activity, increased ADMA and peroxynitrite formation	Plasma creatinine 770±250µmol/L (n=33)	Cross-sectional	Whole body basal NO production (determined by *in vivo* arginine-to-citrulline conversion) was reduced compared to healthy controls.	(Wever et al., 1999)
	Non-diabetic CKD stages 2-4 (n=106)	Cross-sectional	Abnormal FMD demonstrated in early stage CKD compared to healthy controls.	(Thambyrajah et al., 2000)
ADMA Endogenous inhibitor of eNOS principally excreted by the kidney, decreases NO bioavailability	Non-diabetic CKD (IgA nephropathy and ADPKD) (n=60)	Cross-sectional	Increase in ADMA associated with primary chronic renal disease at an early stage, even when GFR was within the normal range.	(Kielstein et al., 2002)
	CKD stage 5 on HD (n=90)	Prospective cohort	When combined, ADMA and CRP levels predicted the progression of carotid IMT on a multivariate regression analysis.	(Zoccali et al., 2002)
	CKD, GFR 31±15 ml/min/1.73m^2 (n=131)	Prospective cohort	Plasma ADMA levels inversely correlated with GFR and predicted progression to ESRD and all-cause mortality.	(Ravani et al., 2005)
	T1DM with diabetic nephropathy, GFR 76±34 ml/min/1.73m^2 (n=397)	Prospective cohort	ADMA levels predicted fatal and nonfatal CV events as well as progression of renal dysfunction over a median of 11.3 years.	(Lajer et al., 2008)
EMP Vesicles shed from the plasma membrane in response to endothelial cell injury/activation	CKD stage 5 (n=76)	Cross-sectional	Increased numbers of circulating EMP correlated with reduced FMD and increased arterial stiffness determined by aortic PWV.	(Amabile et al., 2005)
	CKD stage 5 (n=64)	Cross-sectional	Circulating apoptotic EMPs and VEGF were significantly higher in HD patients compared with non-dialysis CKD patients and those patients on PD. Serum VEGF levels were significantly elevated in CKD compared with healthy controls.	(Merino et al., 2010)
Angiogenic factors				
VEGF Cytokine involved in endothelial proliferation, migration, tube formation, and induces eNOS	CKD stage 5 on HD (n=228)	Prospective cohort	Increased VEGF levels were associated with LV systolic dysfunction (reduced fractional shortening of LV midwall) and mortality in HD patients.	(Mallamaci et al., 2008)

sVEGFR-1 (or sFlt-1) An endogenous antagonist for VEGF and a negative regulator of post-ischaemic angiogenesis	CKD stage 5 on HD (n=185)	Prospective cohort	A high level of sVEGFR-1 predicted all cause mortality over a median duration of 31 months.	(Guo et al., 2009)
	CKD stage 3-5 (n=186)	Cross-sectional	Levels of sVEGFR-1 were higher in CKD patients compared with healthy controls.	(Di Marco et al., 2009)
EPC Circulating, bone-marrow derived cells involved in endothelial cell regeneration	CKD stage 5 on HD (n=74)	Cross-sectional	Lower EPC numbers were demonstrated which correlated with endothelial dysfunction and Framingham's risk factor score.	(Choi et al., 2004)
	Early-moderate CKD, eGFR 37±19ml/min/1.73m^2 (n=82)	Cross-sectional	Reduction in EPC demonstrated even in early stage CKD with increase in VEGF levels and smooth progenitor cells with increasing renal dysfunction.	(Jie et al., 2010)
	CKD stage 5 on HD (n=265)	Prospective cohort	The number of functionally active EPCs predicted adverse CV events over a median follow up of 36 months.	(Lorenzen et al., 2010)
Uraemic toxins				
***p*-cresylsulphate** End-product of phenol metabolism, uraemic retention solute	Non-diabetic CKD stage 5 on HD (n=175)	Prospective cohort	*p*-cresylsulphate, indirectly quantified as *p*-cresol, was associated with all cause mortality and CVD after a mean follow up of 56 months.	(Meijers et al., 2008)
	CKD stages 2-5 (n=139)	Prospective cohort	Total and free *p*-cresylsulphate were inversely correlated with renal function and were significantly associated with vascular calcification. Free *p*-cresylsulphate predicted overall and CV death over a mean of 25 months.	(Liabeuf et al., 2010)
Oxidative stress				
MPO Enzyme that uses H_2O_2 to oxidise tyrosine to tyrosyl radical which cross-links proteins	CKD stage 5 on HD (n=356)	Prospective cohort	Serum MPO levels correlated with levels of markers of inflammation (CRP, IL-6, TNF-alpha, CRP) and overall mortality over a median duration of 26 months.	(Kalantar-Zadeh et al., 2006)
AOPP Carried by oxidized plasma proteins, especially albumin	Non-diabetic CKD, 20-40 ml/min (n=80)	Prospective cohort	AOPP, CRP and fibrinogen levels independently predicted incident vasculo-occlusive atherosclerotic CV events over a median follow up of 7 years.	(Descamps-Latscha et al., 2005)
oxLDL Chemotactic to monocytes, activates collagenases, promotes apoptosis of endothelial cells	CKD stages 3-5 (n=44)	Cross-sectional	Endothelial function determined using plethysmography was related to intracellular oxidative stress in patients with CKD.	(Annuk et al., 2005)

Homocysteine A non-protein amino acid synthesised from methionine	CRIB study, CKD stages 1-5 CrCl 6 to 105 mL/min (n=369)	Cross-sectional	Among CKD patients with prevalent LVH (21%) and vascular disease (34%), those with more severe renal impairment had higher plasma homocysteine levels.	(Wheeler et al., 2003)
Coagulation/fibrinolysis				
vWF Large plasma glycoprotein, produced by endothelial cells and megakaryoctyes, binds to Factor VIII/collagen/platelet GpIb	Hoorn study, population-based study (n=613)	Prospective cohort	eGFR was inversely associated with vWF and VCAM-1 which predicted CV mortality over a median follow-up of 12.5 years.	(Stam et al., 2006)
	Non-diabetic CKD stages 2-4 (n=106)	Cross-sectional	Abnormal FMD and increased vWF was demonstrated in early stage CKD compared with healthy controls.	(Thambyrajah et al., 2000)
Fibrinogen Soluble plasma glycoprotein, produced in the liver, converted by thrombin into fibrin	ARIC and CHS studies eGFR 51±9ml/min/1.73m^2 (n=1,678)	Prospective cohort	Levels of fibrinogen, albumin, TG and CRP predicted composite CV events in an adult general population cohort over median duration of 108 months.	(Weiner et al., 2008)
	CKD stages 3-4 (n=128)	Prospective cohort	Elevated fibrinogen independently predicted all cause mortality stage 3-4 CKD.	(Goicoechea et al., 2008)
Inflammation				
TNF-alpha Cytokine involved in acute phase reaction, produced chiefly by activated macrophages	Pre-dialysis and dialysis CKD (n=87)	Cross-sectional	Raised circulating levels of TNF-alpha, IL-6 and CRP were associated with reduced FMD compared with controls.	(Bolton et al., 2001)
CRP Acute phase response protein, member of the pentraxin superfamily	Pre-dialysis CKD, CrCl 7+/-1 ml/min (n=109)	Cross-sectional	During stepwise multivariate analysis, adjusting for age and gender, CRP remained associated with an increased carotid intima-media area.	(Stenvinkel et al., 1999)
	CKD stage 5, HD (n=757)	Prospective cohort	A synergistic effect of proinflammatory cytokines (CRP, IL-6, IL-8, albumin) was demonstrated in predicting all cause and CV mortality over 30 months.	(Panichi et al., 2008)
	MDRD study, CKD stages 3-4 (n=697)	Prospective cohort	High CRP independently predicted all cause and CV mortality over a median of 125 months.	(Menon et al., 2005)
IL-6 Inflammatory cytokine, key factor in the acute phase response	CKD stage 5 on dialysis (n=217)	Prospective cohort	IL-6 was a stronger predictor of all cause and CV mortality than CRP over an average duration of 41 months.	(Tripepi et al., 2005)
	CKD stage 5 on dialysis (n=45)	Prospective cohort	In a stepwise multiple regression model, IL-6 predicted changes in the carotid-intima media area independently of traditional risk factors.	(Stenvinkel et al., 2002)

PTX3 Member of the pentraxin superfamily, released by monocytes, fibroblasts and endothelial cells	CKD stages 3-4 (n=71)	Prospective cohort	In a p*ost hoc* analysis, PTX3 positively correlated with CV events and mortality.	(Tong et al., 2007)
	CKD stage 5, dialysis and non-dialysis (n=132)	Cross-sectional	PTX3 levels were significantly higher in patients with a history of coronary artery disease and peripheral artery disease as well as those on HD.	(Boehme et al., 2007)
sTWEAK Binds to Fn14 receptor to induce expression of cell adhesion molecules and cytokines, downregulated in atheroma	Non-diabetic, non-dialysis CKD stages 1-5 (n=257)	Prospective cohort	PTX3 and carotid IMT increased, whereas FMD and sTWEAK decreased with worsening renal function. sTWEAK levels predicted mortality after a median of 39 months independent of traditional risk factors and FMD.	(Yilmaz et al., 2011a)
	CKD stage 5 on chronic HD (n=120)	Cross-sectional	Serum sTWEAK concentrations were lower in HD patients compared with controls and lowest in patients with both ESRD *and* T2DM.	(Kralisch et al., 2008)
CD14++ & CD16+ monocytes "Pro-inflammatory" monocyte subset	Non-dialysis CKD patients (n=119)	Prospective cohort	CD14(++)CD16(+) monocytes were independently associated with CV events over a median of 4.9 years.	(Rogacev et al., 2011)
AGEs Product of irreversible covalent cross-linking of collagen and elastin with carbohydrates or carbonyls	Diabetic and non-diabetic CKD (n=27)	Cross-sectional	Levels of AGE peptides inversely correlated with creatinine clearance and were elevated in patients with diabetes.	(Makita et al., 1991)
	CKD stage 5 on HD (n=312)	Prospective cohort	Total serum fluorescent AGEs were 3-fold higher compared to healthy controls although were associated with better survival over 32 months.	(Schwedler et al., 2002)
sRAGE and EN-RAGE (S100A12) The soluble receptor of AGE and its proinflammatory ligand	CKD stage 5 on HD (n=234)	Prospective cohort	sRAGE and EN-RAGE levels were significantly elevated compared to healthy controls. EN-RAGE, but not sRAGE, was independently and positively associated with CV mortality over a median follow up of 41 months.	(Nakashima et al., 2010)

Abbreviations: ADMA, asymmetric dimethylarginine; AGEs, advanced glycation endproducts; ADPKD, adult polycystic kidney disease; AOPP, advanced oxidation protein products; ARIC, Atherosclerosis Risk in Communities; CD, cluster of differentiation; CHS, Cardiovascular Health Study; CKD, chronic kidney disease; CrCl, creatinine clearance; CRIB, Chronic Renal Impairment in Birmingham study; CRP, C-reactive protein; CV, cardiovascular; CVD, cardiovascular disease; EMP, endothelial microparticle; EN-RAGE, extracellular newly identified RAGE-binding protein; EPC, endothelial progenitor cell; ESRD, end-stage renal disease; sFlt-1, soluble fms-like tyrosine kinase-1; FMD, flow mediated dilatation; Fn14, fibroblast growth factor-inducible 14; eGFR, estimated glomerular filtration rate; Gp1b, glycoprotein 1b; HD, haemodialysis; H_2O_2, hydrogen peroxide; IL-6, interleukin-6; IL-8, interleukin-8; IMT, intima-media thickness; LV, left ventricular; LVH, left ventricular hypertrophy; MDRD, Modification of Diet in Renal Disease; MPO, myeloperoxidase, eNOS, endothelial nitric oxide synthase; NO, nitric oxide; oxLDL, oxidised low-density lipoprotein; PD, peritoneal dialysis; PTX3, pentraxin-3; PWV, pulse wave velocity; sRAGE, soluble receptor for advanced glycation endproducts; TNF-alpha, tumour necrosis factor-alpha; sTWEAK, soluble tumour necrosis factor-like weak inducer of apoptosis; T1DM, type 1 diabetes mellitus; T2DM, type 2 diabetes mellitus; VCAM; vascular cell adhesion molecule-1; sVEGFR-1, soluble vascular endothelial growth factor receptor-1; VEGF, vascular endothelial growth factor; vWF, von Willebrand factor.

Table 1-3. Key Human Studies Investigating Molecular Mechanisms of A*rteriosclerosis* in Chronic Kidney Disease.

Factor/Mechanism	Study population	Study type	Study outcomes	Reference
Vascular calcification				
Ca, PO_4, PTH Key mediators of bone metabolism and vascular calcification	CaNPREDDICT study CKD stage 4 (n=4,321)	Retrospective	Mortality was associated with higher PO_4, higher PTH and reduced Vitamin D over a median follow up of 31 months.	(Levin et al., 2008)
	MESA study, CKD stage 3 (n=439)	Cross-sectional	Modest elevation of PO_4 (even within the normal reference range) was associated with a greater prevalence of coronary, aortic and valvular calcification, independent of PTH, vitamin D and traditional risk factors.	(Adeney et al., 2009)
	CKD stage 5 on HD (n=12,833)	Prospective cohort	Elevated serum PO_4, Ca x PO4 product and PTH product was strongly associated with cardiac mortality (especially sudden cardiac death) over 2 years.	(Ganesh et al., 2001)
	Non-diabetic CKD stages 2-4 (n=208)	Cross-sectional	Serum PO_4 was independently associated with LV mass.	(Chue et al., 2012a)
Vitamin D The kidney converts 25-(OH)D to its active hormonal form 1,25-$(OH)_2D_3$	CKD stage 5 on HD (n=1,000)	Case control	Decreased levels of 25-(OH)D and 1,25-$(OH)_2D_3$ were associated with increased all cause mortality within 90 days of starting dialysis.	(Wolf et al., 2007)
	PRIMO study, CKD stages 3-4 (n=227)	Randomised controlled trial	Forty-eight weeks' therapy with active vitamin D did not reduce LV mass on cardiac MRI or improve LV diastolic function on echocardiography.	(Thadhani et al., 2012)
FGF-23 Secreted by osteoblasts and osteocytes, regulates levels of phosphate and 1,25-$(OH)_2D_3$	CKD stage 5 on HD (n=219)	Prospective cohort	High FGF-23 levels were associated with all cause mortality and vascular calcification independent of serum phosphate.	(Jean et al., 2009)
	Pre-dialysis CKD (n=149)	Prospective cohort	Elevated FGF-23 predicted CV events over a mean follow up of 5 years.	(Seiler et al., 2010)
	CKD stages 2-3 (n=177)	Cross-sectional	FGF-23 was independently associated with Gensini score, a measure of coronary atheroma.	(Kanbay et al., 2010)
	CRIC study, CKD (n=411) eGFR 20-70ml/min/1.73m^2	Prospective cohort	Baseline FGF-23 levels independently predicted new onset LVH on echocardiography at 2.9 ± 0.5 years.	(Faul et al., 2011)
α-Klotho A cofactor for FGF-23 and an endogenous inhibitor of vascular calcification	CKD stage 5 (n=21)	Cross-sectional	Western blot showed reduced vascular Klotho protein expression associated with extensive medial calcification in explanted human renal and epigastric arteries.	(Lim et al., 2012)

Fetuin-A Inhibitor of mineralisation, downregulated in the acute phase response	CKD stage 5 on HD (n=312)	Cross-sectional	Lower levels of fetuin-A were associated with CV and all cause mortality over 32 months.	(Ketteler et al., 2003)
OPG Member of the TNF receptor superfamily, osteoclastogenesis inhibitory factor	CKD stage 5 on HD (n=26)	Prospective cohort	Increased OPG levels were associated with progression of aortic calcification over a mean period of 5 years.	(Nitta et al., 2003)
	CKD stage 5 on HD (n=185)	Prospective cohort	Elevated OPG levels predicted CV and all cause mortality over 2 years.	(Morena et al., 2006)
Collagen/Fibrosis				
PIIINP Circulating biomarker of collagen synthesis, degradation product of type III collagen	CRIB II study, CKD stages 2-4 (n=112)	Randomised controlled trial	PIIINP levels were increased in CKD in association with LV diastolic dysfunction; this increase was attenuated by 40 weeks treatment with spironolactone.	(Edwards et al., 2010)
C1TP Marker of type I collagen degradation	RRI-CKD study, CKD stages 3-5 (n=242)	Cross-sectional	Both PIIINP and C1TP values were significantly higher in more advanced stages of CKD. PIIINP was associated with PWV.	(Dellegrottaglie et al., 2011)
Renin-angiotensin-aldosterone system				
Angiotensin II Vasoconstrictor, promotes inflammation by stimulating VSMC to generate oxygen free radicals, induces VSMC hypertrophy and collagen synthesis	CKD stage 5 on HD (n=150)	Prospective cohort	Blood pressure lowering with an ACEI in combination with decreased PWV was associated with reduced all cause and CV mortality.	(Guerin et al., 2001)
	CRIB II study, CKD stages 2-4 (n=112)	Randomised controlled trial	The addition of spironolactone to ACEI/ARB treatment significantly reduced PWV and LV mass.	(Edwards et al., 2009)
Endothelial dysfunction, Oxidative stress and Inflammation				
Please refer to Table 1-2.				

Abbreviations: ACEI, angiotensin-converting-enzyme inhibitor; ARB, angiotensin receptor blocker; Ca, calcium; CaNPREDDICT, Canadian study of prediction of risk and evolution to dialysis, death and interim cardiovascular events over time; CKD, chronic kidney disease; CV, cardiovascular; CRIB II; chronic renal impairment in Birmingham study II; C1TP, carboxy-terminal telopeptide; 25-(OH)D, 25-hydroxyvitamin D (calcifidiol); $1,25(OH)_2D_3$, 1,25-dihydroxyvitamin D_3 (calcifitriol); FGF-23, fibroblast growth factor-23; HD, haemodialysis; LV, left ventricular; MESA, multi-ethnic study of atherosclerosis; OPG, osteoprotegerin; PIIINP, Procollagen III N-Terminal Propeptide; PO_4, phosphate, PRIMO, Paricalcitol Capsules Benefits in Renal Failure Induced Cardiac Morbidity in Subjects With Chronic Kidney Disease Stage 3/4; PTH, parathyroid hormone; PWV; pulse wave velocity; RRI; Renal Research Institute; VSMC, vascular smooth muscle cell.

1.6.1. Endothelial Dysfunction

The vascular endothelium is recognised as having multiple, complex functions which regulate vascular tone, thrombosis, haemostasis, permeability and cell adhesion. It releases vasodilatory substances such as nitric oxide (NO), prostacyclin, C-type natriuretic peptide and endothelium-derived hyperpolarizing factor, as well as vasoconstrictors including endothelin-1 (ET-1), angiotensin II and thromboxane A_2 (Endemann and Schiffrin, 2004). Endothelial dysfunction or, more correctly "endothelial activation", is considered a key initiating step in atherogenesis (Table 1-2) and also contributes to arterial stiffening (Table 1-3). Indeed, ED due to chronic inflammation and oxidative stress is thought to be an early and important feature of CKD (Schiffrin et al., 2007). It has been implicated as one of the chief pathophysiological mechanisms contributing to the association of cardiovascular disease and CKD (Stam et al., 2006) and may, in part, explain the strength of the graded correlation between worsening renal function and increasing cardiovascular risk (Schiffrin et al., 2007, Go et al., 2004).

Measuring endothelial function in carefully defined cohorts of subjects with CKD offers promise as a method to examine the pathogenesis of atheroma in CKD. There remains however, a lack of clinical studies examining ED in subjects specifically with reduced GFR, particularly in those with early-stage CKD. Where data on ED in CKD does exist, reports are often conflicting. Early studies using flow-mediated-dilatation and circulating biomarkers suggested that patients with early stage CKD had deranged endothelial function (Thambyrajah et al., 2000, Stam et al., 2006, Bolton et al., 2001). More recent work has

suggested that this may have been due to the inclusion of patients with other risk factors such as hypertension, vasculitis, smoking and even established vascular disease, and that if these factors are excluded as far as possible, endothelial function is abnormal only in more advanced (stages 4 and 5) CKD (Lilitkarntakul et al., 2011). This inference is however, difficult to reconcile with the evidence that early stage CKD patients have multiple factors known to cause ED such as inflammation, oxidative stress, increased circulating asymmetrical dimethylarginine (ADMA) and RAAS activation (Moody et al., 2012b, Yilmaz et al., 2009, Yilmaz et al., 2010b). The precise relationship between GFR and ED remains to be elucidated and many potential mechanisms are still under investigation (Table 1-2 and Table 1-3).

Abnormalities in vascular endothelial function amongst patients with CKD were originally described in patients with ESRD maintained on dialysis. In a cross-sectional analysis, endothelium-dependent, but not endothelium-independent, vasodilatation of the brachial artery was markedly reduced in 28 chronic haemodialysis subjects compared with 28 healthy controls (Van Guldener et al., 1997). The same investigators then showed FMD was similarly reduced in a group of peritoneal dialysis patients compared with age-matched controls (Van Guldener et al., 1998). A later cross-sectional study demonstrated both lower FMD and endothelium-independent dilatation in 114 chronic haemodialysis patients compared with 49 age- and sex-matched controls (Yildiz et al., 2003). Flow-mediated-dilatation was independently associated with LV mass index, suggesting ED might cause decreased elasticity of the arterial vasculature and contribute to the development of LV hypertrophy.

Subsequent studies have also demonstrated the presence of ED in patients with ESRD (Luksha et al., 2011).

The first published study to include early-stage CKD patients in an assessment of endothelial function involved measurement of FMD by ultrasound assessment of the brachial artery in 80 non-diabetic CKD patients (eGFR 14 – 54 ml/min/1.73m^2); FMD was significantly reduced compared with 26 normal controls (median (interquartile range), 2.6% (0.7 to 4.8%) vs. 6.5% (4.8 to 8.3%); $p < 0.001$) (Thambyrajah et al., 2000). There was no significant difference in FMD between GFR quartiles (1st quartile median GFR 49 (46 to 54); 4th quartile median GFR 16 (14 to 18)), however, suggesting that ED occurs early in the course of renal disease. Similar findings were reported by another UK group who compared endothelial function in patients with angina, patients with pre-dialysis CKD (creatinine clearance <50 ml/min) and those on dialysis with healthy controls (Bolton et al., 2001). Flow-mediated-dilatation was severely reduced in all groups compared to controls (patients with both pre-dialysis and dialysis dependent CKD had similar values to those with angina) whilst endothelial-independent dilatation was preserved in each group. Circulating levels of inflammatory cytokines (IL-6 and TNF-alpha), C-reactive protein and VCAM-1 were elevated in pre-dialysis patients compared with controls.

In the Hoorn population cohort study, a series of biomarkers of ED were measured at baseline in 613 subjects aged 50 to 75 years in whom renal function was only mildly impaired (mean eGFR 68 ± 12 ml/min/1.73m^2) (Stam et al., 2006). Estimated GFR was

inversely associated with soluble VCAM-1, von Willebrand Factor (vWF) and urinary ACR but not markers of inflammation. Over a median follow up period of 12.5 years, sixty-seven individuals from the original cohort died from cardiovascular causes. The relative risks (95% CI) of cardiovascular and all-cause mortality associated with a decrease of 5 ml/min/1.73m^2 of eGFR were 1.22 (1.09 to 1.36) and 1.12 (1.05 to 1.20), respectively. After adjustment for biomarkers of endothelial function, the strength of this association was markedly attenuated.

The concept that ED is present even in patients with minor renal dysfunction and contributes to increased cardiovascular risk, was further supported by a large prospective cohort study (Yilmaz et al., 2011b). In 304 non-dialysis outpatients attending renal clinics, uniformly distributed across stages 1-5 CKD, a cross-sectional analysis showed highly sensitive C-reactive protein (hsCRP) and carotid IMT had a graded inverse relationship with eGFR, whilst FMD decreased with declining renal function. After a median follow-up of 42 months, FMD was shown to predict adverse cardiovascular outcomes even after adjustment for age, sex, blood pressure, total cholesterol, eGFR, diabetes, and medical history of cardiovascular disease at baseline. In a Cox regression model containing FMD, hsCRP and carotid IMT, both FMD and hsCRP but not IMT were significant predictors of adverse cardiovascular events. The authors concluded the clinical use of FMD is preferred over IMT measurements to monitor early-stage CKD patients at risk. Nonetheless, there is abdundant evidence supporting carotid IMT as an important prognostic indicator. Indeed, a series of paediatric studies used carotid IMT as a surrogate marker of ED, demonstrating increases in as early as

stage 2 CKD and often within the first decade of life (Litwin and Niemirska, 2009, Litwin et al., 2008). Likewise, in an adult cross-sectional study of 38 pre-dialysis (stage 3 to 4 CKD), 18 haemodialysis and 22 kidney-transplant patients, FMD was impaired whilst CRP and IMT were increased when compared with controls (Recio-Mayoral et al., 2011). There was a significant positive correlation between eGFR and FMD although in pre-dialysis patients, there was only a non significant trend towards impaired FMD (predialysis 3.2% vs. controls 5.6 %).

Endothelial dysfunction is a prerequisite for atherogenesis. Disruption of signalling of endothelium-derived relaxing factors occurs at an early stage in atherosclerosis and precedes development of lipid streaks and plaques (Schiffrin et al., 2007). Progressive deterioration of renal function in CKD is associated with the accumulation of uraemic toxins (Table 1-4) which may stimulate oxidative stress and inflammation, and in turn contribute to ED and progression of atheroma. Dyslipidaemia associated with CKD also contributes to the inflammatory response in renal failure with changes in blood-lipid composition (Schiffrin et al., 2007). Cardiovascular calcification in CKD patients is more prevalent, progressive, extensive and severe compared with the non-CKD population, and results from both disturbed mineral metabolism (see Section 1.6.3) and a complex, active process of osteogenesis in vascular smooth muscle cells (VSMCs) (Chue et al., 2010).

Table 1-4. Potential Uraemia-related Risk Factors Predicting Cardiovascular Disease or Outcome in Patients with Chronic Kidney Disease.

Category of risk factor	Biomarkers
Endothelial dysfunction	ADMA, EMP, PTX3, VCAM, EPC, albuminuria, vWF
Inflammation	IL-6, IL-18, S-albumin, WBC, fibrinogen hyaluronan TNF-α, MPO, CRP, PTX3, PAI-1
Oxidative Stress	MPO, oxLDL, AOPP, homocysteine
Protein-energy wasting	serum albumin, serum creatinine, prealbumin
Uraemic toxins	S-creatinine, *p*-cresylsulphate
Vascular calcification	PO4, Ca, Mg, PTH, fetuin-A, OPG, OPN, FGF-23
Sympatho-activation	Norepinephrine
Coagualtion/fibrinolysis disorders	Fibrinogen, vWF
Adipokines	Adiponectin, visfatin, leptin
Subclinical hypothyroidism “low T3 condition”	fT3, T3
Insulin resistance	HOMA, AGEs
Cardiac	NT-pro-BNP, Troponin T
Anaemia	Haemoglobin

Abbreviations: ADMA, asymmetric dimethylarginine; AGEs, advanced glycation end-products; AOPP, advanced oxidation protein products; CKD, chronic kidney disease; CRP, C-reactive protein; EMP, endothelial cell-derived microparticle; EPC, endothelial progenitor cell; FGF-23, fibroblast growth factor 23; HOMA, homeostasis model assessment method; IL, interleukin; MPO, myeloperoxidase; OPG, osteoprotegerin; OPN, osteopontin; oxLDL, oxidized low-density lipoprotein; PAI-1, plasminogen activator inhibitor 1; PTH, parathyroid hormone; PTX3, pentraxin-3; NT-pro-BNP, N-terminal pro-brain natriuretic peptide; T3, triiodothyronine; TNF-α, tumour necrosis factor-α; vWF, von Willebrand factor; VCAM, vascular cell adhesion molecule; WBC, white blood cell count. (Moody et al., 2012b).

Endothelial dysfunction also contributes to arteriosclerosis, a disease affecting the media of large and middle sized arteries with an increased calcification, an increased collagen : elastin ratio, and hyperplasia and hypertrophy of VSMCs (see Section 1.5.2). Whilst increased arterial stiffness is caused primarily by structural changes, there appears to also be an important major functional contribution from the vascular endothelium. Marked increases in arterial stiffness as measured by PWV have been demonstrated in response to NOS inhibitors, with reductions in response to exogenous NO donors (Chue et al., 2010).

The potential pathophysiological mechanisms responsible for ED in CKD are diverse and a more detailed account of these biological mechanisms is available elsewhere (Endemann and Schiffrin, 2004, Stenvinkel et al., 2008). A list of proposed mediators is given in Table 1-4. Systemic inflammation and oxidative stress are almost universal in CKD and result in ED by decreasing the bioavailablity of NO via reductions in nitric oxide synthase (NOS) activity and the production of peroxynitrite, a cytotoxic oxidant which leads to oxidation of LDL and uncoupling of endothelial NOS (eNOS) (Endemann and Schiffrin, 2004). There is also growing evidence to support a role for ADMA, a product of protein turnover and potent endogenous inhibitor of eNOS (Endemann and Schiffrin, 2004). Plasma ADMA levels are elevated in CKD because the kidney is the principal organ for excretion of ADMA and there is reduced activity of the enzyme dimethylarginine dimethylaminohydrolase. Increased ADMA levels are strongly associated with ED, carotid IMT, concentric LV hypertrophy and LV dysfunction (Endemann and Schiffrin, 2004). Higher ADMA levels have also been shown to predict faster rates of decline in GFR in subjects with early-moderate CKD as well as overall mortality (Endemann and Schiffrin, 2004). Numerous other uraemic toxins have been implicated in

causing adverse changes in endothelial function including the protein-bound solute *p*-cresol. More recently, its conjugate *p*-cresylsulphate, the principal end product of phenol metabolism, has emerged as the primary culprit for toxicity; it predicts mortality in ESRD and triggers an increase in endothelial microparticle release (Liabeuf et al., 2010).

A number of studies have examined interventions aimed at improving endothelial function in CKD although results have been disappointing. Most trials have been small-scale and many have lacked a control group. In a small, unblinded, uncontrolled study of ESRD patients, administration of soy proteins improved endothelial function and decreased ADMA levels (Cupisti et al., 2007). A reduction in ADMA has also been reported in a small but randomized study of lipoic acid in 50 patients with ESRD (Chang et al., 2007). Whilst a reduction in ADMA levels also occurred following statin therapy in patients with hypercholesterolaemia (Lu et al., 2004), no such effect was seen in the Antioxidant Therapy in Chronic Renal Insufficiency (ATIC) study of patients with stage 2-4 CKD (Nanayakkara et al., 2009). This randomized double blind controlled trial did, however, demonstrate increased FMD, reduced carotid IMT and reduced urinary albumin excretion after 18 months of a regimen including pravastatin, vitamin E supplementation and homocysteine-lowering therapy (Nanayakkara et al., 2007). Statins have also been shown to improve FMD in non-diabetic patients undergoing peritoneal dialysis (Han et al., 2011) and may exert pleiotropic effects by increasing the number of circulating EPC (Tousoulis et al., 2011). In contrast, a randomised double blind controlled study of children with stage 3-4 CKD failed to show any improvement in FMD after 8 weeks of atorvastatin (Mackie et al., 2010). A randomized,

double blind placebo controlled study including both non-diabetic and diabetic patients with CKD stage 3-4 showed short-term rosiglitazone therapy reduced vWF but had no effect on FMD or arterial stiffness (Chan et al., 2011).

1.6.2. The Renin-Angiotensin-Aldosterone System

It is unclear as to the exact mechanism but there appears to be RAAS activation in CKD which has deleterious effects on the cardiovascular system as a result of the actions of both angiotensin II and aldosterone (Brown, 2008, Quarles, 2013). Elevated aldosterone levels are the result of two mechanisms; aldosterone "escape" describes inappropriately elevated plasma levels relative to salt and fluid overload (Struthers, 2004) while aldosterone "breakthrough" refers to persistently high levels despite treatment with ACE inhibitors and angiotensin receptor blockers (Schrier, 2010). It is now well recognised that aldosterone, probably produced locally as well as by the adrenal cortex, exerts injurious actions directly on the myocardium and vasculature. Aldosterone mediated oxidative stress and inflammation result in structural fibrotic change within the arterial wall and myocardium (Brown, 2008). These features may result from both genomic actions via mineralocortcoid receptor (MR) activation and non genomic actions. The adverse inflammatory effects of aldosterone are powerfully potentiated and may be dependent upon the presence of sodium excess. The combination of high levels of aldosterone and sodium overload is unusual as aldosterone production is usually suppressed by sodium overload but aldosterone "escape" is a characteristic of both heart failure (in which mineralocorticoid

receptor blockers (MRB) have proven efficacy (Zannad et al., 2011, Pitt et al., 1999)) and CKD (Struthers, 2004).

Aldosterone causes a range of other adverse vascular effects including ED, autonomic dysfunction, vasoconstriction and hypertension (Farquharson and Struthers, 2000, Funder, 2010). Aldosterone decreases endothelial NO by increasing NADPH oxidase activity and generation of reactive oxygen species (Struthers and Macdonald, 2004). In a rabbit model, aldosterone decreased tetrahydrobiopterin, an important cofactor for eNOS activity and NO production, whilst the MRB eplerenone improved tetrahydrobiopterin levels and restored NO synthesis (Rajagopalan et al., 2002). Angiotensin II infusion in rats caused ED by oxidant stress from the stimulation of NADPH oxidase and uncoupling eNOS (Lobysheva et al., 2011). All of these deleterious actions, including inflammation and fibrosis, occur in the myocardium and in the kidney itself thereby causing further glomerular injury and setting up a toxic feed-forward loop of renal and vascular damage (Del Vecchio et al., 2007).

Aldosterone and angiotensin II have also been associated with adverse LV geometry in small cross-sectional studies of patients with reduced GFR resulting from essential arterial hypertension (Muscholl et al., 1998, Nakahara et al., 2007). In a large community-based sample of 2119 Framingham Offspring Study participants, increased aldosterone-to-renin ratio independently predicted both concentric and eccentric hypertrophy in multivariable models (Velagaleti et al., 2008). Taken together, these data support a major role for RAAS activation in adverse LV remodelling.

Myography studies have shown that RAAS blockade in hypertensive type 2 diabetic patients with an ACE inhibitor or an angiotensin II receptor blocker (ARB) restored endothelial function and improved resistance artery remodelling (Rizzoni et al., 2001, Savoia et al., 2006). This effect was thought to be independent of blood pressure since beta-1 adrenoreceptor blockade with a similar degree of blood pressure lowering did not have an effect on endothelium-dependent vasodilatation. In subtotally nephrectomised rats, MRB therapy reduces arterial stiffness (Lacolley et al., 2002) as well as proteinuria and LV hypertrophy (Greene et al., 1996). These animal data are consistent with the theory that RAAS inhibition reduces risk at least in part, via a blood pressure independent mechanism.

In further support of this paradigm, a recent study involving hypertensive diabetic patients with stage 1 CKD (24-h protein excretion ≥ 500 mg/d, systolic blood pressure ≥ 140 mmHg and/or diastolic blood pressure ≥ 90 mmHg) showed that treatment with valsartan improved FMD and normalized proteinuria, PTX3, and TWEAK (Yilmaz et al., 2010a) although the study was uncontrolled. In a similar longitudinal study of diabetic patients, the same investigators showed a beneficial effect of ramipril on FMD and proteinuria, accompanied by a reduction in levels of ADMA (Yilmaz et al., 2010b). Finally, in a study of 150 patients with CKD stage 5D given ACE inhibitor therapy over an average of 4 years, mortality benefit was only evident in those subjects with reduced PWV and absent in those subjects with unchanged PWV despite similar reductions in blood pressure (Guerin et al., 2001).

In patients with reduced GFR in association with chronic heart failure, the addition of a MRB to an ACE inhibitor improved endothelial function as measured by the vasodilator response to acetylcholine (Farquharson and Struthers, 2000). Several studies of CKD patients have shown spironolactone also reduces proteinuria (Struthers and Macdonald, 2004), and slows the progression of carotid IMT (Vukusich et al., 2010). Possible mechanisms of action of MRBs on endothelial function include reduced concentration of macrophage oxidized LDL cholesterol, increased NO bioavailability, up-regulation of endothelial-dependent vasodilators such as prostacyclin and endothelium-derived hyperpolarising factor, attenuation of angiotensin I-mediated vasoconstriction and improved endothelial signalling pathways leading to NO synthase synthesis (Struthers and Macdonald, 2004).

The use of MRB therapy prevents many of the adverse effects of aldosterone both *in vitro* and in live animal studies (Luther et al., 2012) suggesting that providing these agents can be tolerated without serious hyperkalaemia in patients with CKD, they may be able to prevent or even reverse arterial stiffening and LV hypertrophy and fibrosis. In a preliminary proof of concept study of patients with early-moderate CKD, the effects of spironolactone on PWV (determined by SphygmoCor) and LV mass (determined by cardiac MRI) were compared with placebo (Edwards et al., 2009). After 40 weeks, significant reductions in both PWV and LV mass were observed in the spironolactone group. Adverse effects such as hyperkalaemia were very infrequent suggesting that treatment is safe so long as appropriate monitoring is in place (Edwards et al., 2012). Further work is currently underway in the SPIRO-CKD study (EudraCT: 2013-002636-25) with the aim of confirming safety and to clarify the degree to

which these improvements in LV and arterial function were specific to MR blockade or secondary to blood pressure reduction.

Data are beginning to emerge on the effects RAAS blockade on hard outcomes in CKD. A meta-analysis of RAAS blockade either by an ACE inhibitor or ARB in CKD demonstrated a significant reduction in cardiovascular events and incident rate of heart failure compared to placebo, although no survival benefit was observed (Balamuthusamy et al., 2008). More recently, in a 3-year randomized trial of 309 haemodiaysis patients, subjects randomized to receive 25 mg spironolactone had a reduction in the composite primary outcome of cardiovascular death or hospitalization from cardiovascular cause compared to placebo (Matsumoto et al., 2014). There is now a call for larger studies such as the BARACK D (Benefits of Aldosterone Receptor Antagonism in Chronic Kidney Disease) trial to confirm the efficacy of MRB agents in CKD patients (Hill et al., 2014).

1.6.3. Vitamin D, Parathyroid Hormone and Fibroblast Growth Factor-23

Two of the key hormones involved in the regulation of calcium and phosphate homeostasis are parathyroid hormone (PTH) and fibroblast growth factor-23 (FGF-23). In response to hypocalcaemia or a phosphate load, PTH is secreted by the parathyroid glands serving to increase renal calcium reabsorption and increase phosphate excretion. Parathyroid hormone also raises the plasma calcium level by releasing calcium from the bones and stimulates the renal enzyme 1-α-hydroxylase to increase levels of the active form of vitamin D (1,25-

dihydroxvitamin D) thereby promoting gastrointestinal absorption of phosphate and calcium. Fibroblast growth factor-23 is a phosphatonin hormone secreted primarily by osteocytes in bone in response to increased serum phosphate levels. It serves to reduce the expression and activity of Na/Pi co-transporters in the proximal renal tubules (Shimada et al., 2004), lowers serum levels of 1,25-dihydroxyvitamin D by inhibiting renal expression of 1-α-hydroxylase (Saito et al., 2003), and suppresses synthesis of PTH (Martin et al., 2012a). It also stimulates expression of the catabolic enzyme 24-hydroxylase, resulting in reduced gastrointestinal phosphate absorption (Saito et al., 2003). The renal tubular effects of FGF-23 are mediated by FGF receptors (chiefly FGFR-1); the interaction between FGF-23 and FGFR-1 is facilitated by α-Klotho, a transmembrane protein co-receptor which increases the binding affinity of FGF-23 (Martin et al., 2012a, Urakawa et al., 2006).

As well as having effects on the "classical" PTH target organs (the kidney, gut and bone), it appears that PTH may also have direct biological actions on the heart (Bro and Olgaard, 1997). This is inferred from the presence of PTH receptors in the myocardium and further, the induction of cardiomyocyte hypertrophy with PTH *in vitro* (Schluter and Piper, 1998). Parathyroid hormone is recognised to stimulate the protein kinase C pathway, which has been implicated in the hypertrophy of cardiomyocytes (Ferreira et al., 2011). There are also clinical data supporting PTH as a key mediator in the development of left ventricular hypertrophy. Parathyroid hormone was originally proposed as a potential mediator of LVH among patients with ESRD and secondary hyperparathyroidism (Harnett et al., 1988). Perhaps the strongest evidence for PTH having a causal role in the development of LV

hypertrophy is available from an elegant case-control study of patients with primary hyperparathyroidism; at baseline there was a high prevalence of LV hypertrophy that significantly improved following parathyroidectomy without an accompanying change in mean blood pressure (Piovesan et al., 1999). This relationship is also evident among community-dwelling subjects in whom serum PTH levels are independently associated with higher LV mass (Saleh et al., 2003). In the Cardiovascular Health Study, 25-hydroxyvitamin D deficiency in conjunction with elevated concentrations of PTH observed in elderly patients with early-moderate CKD were associated with adverse cardiovascular events over 14 years of follow up (Kestenbaum et al., 2011). Whilst deficiency in 25-OHD deficiency was associated with myocardial infarction and mortality, PTH excess was associated with incident heart failure, a finding supported by the data which links PTH to adverse LV remodelling. Parathyroid hormone may also accelerate cardiovascular calcification, including mineralisation of the aortic valve (Hekimian et al., 2013). Most recently, it has been shown that those subjects with CKD post aortic valve replacement (eGFR <60 ml/min/1.73m^2) were more likely to have insufficient levels of 25-hydroxyvitamin D together with increased circulating levels of PTH (Laflamme et al., 2014). Once again, the elevated PTH in these subjects was independently associated with LV mass.

There has also been increasing interest in the potential role of FGF-23 as a novel cardiovascular risk marker. Increased circulating levels of FGF-23 predict decline in renal function in community-based individuals (Rebholz et al., 2015). Moreover, FGF-23 levels are independently associated with the incident rate of atrial fibrillation (Mathew et al., 2014), heart failure, coronary heart disease, and cardiovascular and all-cause mortality (Lutsey et

al., 2014, Ix et al., 2012). However, the proposed mechanisms by which FGF-23 is linked to these adverse outcomes are contentious. There is powerful evidence from translational work that elevated FGF-23 has a direct causal role in the pathogenesis of LV hypertrophy (Faul et al., 2011). In an ethnically diverse cohort of 3,070 participants with CKD enrolled in the Chronic Renal Insufficiency Cohort (CRIC) study, circulating FGF-23 levels were increased in CKD and independently associated with LVH. In the same report, it was demonstrated *in vitro* that FGF-23 directly induces pathological hypertrophy of isolated cardiomyocytes and t *in vivo* that mice injected with either intraventricular or intravenous injection of FGF-23 develop significantly more LV hypertrophy compared with vehicle-injected mice. Left ventricular hypertrophy was evident in α-Klotho-deficient mice, an accepted animal model for constitutively elevated FGF-23 levels. Furthermore, the klotho heterozygotes manifested FGF-23 levels and LV remodelling that were intermediate between those of wild-type and klotho-deficient mice. Finally, it was shown in the 5/6 nephrectomy rat model of CKD that pharmacological inhibition of FGFR with PD173074 attenuated the severity of LV hypertrophy without a reduction in blood pressure.

Despite this robust series of experiments, the exact cellular mechanism for the adverse LV remodelling associated with increased FGF-23 remains contentious because α-Klotho has not been found in the myocardium (Faul et al., 2011). Another potential explanation is that FGF-23 activates FGFR/α-Klotho co-receptors in the kidney, which indirectly leads to LV hypertrophy and cardiovascular mortality through RAAS activation (Quarles, 2013). In keeping with this theory, FGF-23 appears to be a potent inhibitor of angiotensin converting

enzyme-2 expression in the kidney (Dai et al., 2012), thereby preventing degradation of angiotensin I and II. This complex feedback system is further influenced by 1,25-dihydroxyvitamin D, which itself inhibits renin gene transcription and blocks RAAS but also stimulates FGF-23 production in bone (Simpson et al., 2007). Thus, the action of 1,25-dihydroxyvitamin D causing increased circulating levels of FGF-23 but inhibiting RAAS might have contradictory effects on the myocardium; this may explain the results of the PRIMO study in which calcitriol treatment (1,25-dihydroxyvitamin D) had no significant effect on LV remodelling (P = 0.06) (Thadhani et al., 2012). Furthermore, there are data from *in vivo* animal models showing angiotensin II suppresses renal α-Klotho expression and that α-Klotho overexpression can mitigate angiotensin II–induced proteinuria (Mitani et al., 2002). Finally, in klotho-hypomorphic (*kl*/*kl*) mice, aldosterone directly stimulated vascular calcification by inducing Pit-1-dependent phosphate transport in vascular smooth muscle cells via direct activation of the MR receptor (Voelkl et al., 2013). In this model of α-Klotho deficiency, spironolactone increased life span in association with reduced vascular calcification lending further support to the notion that MRB therapy confers vascular protection at least in part, via blood pressure independent effects.

In simple terms, the increased afterload caused by arterial calcification and stiffening together with hypertension should lead to LV hypertrophy. In truth, however, this concept maybe a gross over-simplification; the pathophysiology behind the development of LV hypertrophy and vascular calcification in relation to bone mineral disturbances in CKD (Chronic Kidney Disease–Mineral and Bone Disorder (CKD-MBD)) is undoubtedly complex,

and this is reflected by refractoriness to current therapies. Indeed, the recent results from clinical trials aimed at improving cardiovascular endpoints by correcting disturbances in mineral metabolism have thus far proved disappointing (Thadhani et al., 2012, Chertow et al., 2012, Chue et al., 2013b). A multifaceted strategy that includes targeting the proximate pathogenic factors such as PTH, FGF-23 and aldosterone may offer greater potential to improve cardiovascular outcomes in CKD.

1.6.4. Erythropoietin and Anaemia

Anaemia in CKD is typically normocytic, normochromic, and hypoproliferative (Babitt and Lin, 2012). Although generally normal or slightly increased in anaemia of CKD, EPO levels are considered inappropriately low relative to the degree of anaemia, because similarly anaemic patients with normal kidney function have 10–100 times higher EPO levels (Mcgonigle et al., 1984, Garcia et al., 1982). As well as the relative EPO deficiency, there are a number of other factors which contribute to anaemia of CKD including shortened erythrocyte survival, the presence of uraemic-induced inhibitors of erythropoiesis, and disordered iron homeostasis (Babitt and Lin, 2012).

The effects of anaemia on the development of LV hypertrophy are well established in subjects with ESRD. In chronic anaemia, prolonged volume and fluid overload and increased cardiac work lead to progressive cardiac enlargement and LVH (Parfrey et al., 1996, Harnett et al., 1988). The extent of adverse left ventricular remodelling progresses in parallel with

changes in haemoglobin level (London, 2001). Importantly, the effects of chronic anaemia on the LV may not be limited to subjects with ESRD. In a prospective study of 246 patients with mild-moderate CKD and a baseline prevalence of LV hypertrophy of 36%, a 12-month decline in haemoglobin level independently predicted the increase in LV mass index measured using two-dimensional-targeted M-mode echocardiography (Levin et al., 1999).

Early data from small-scale observational studies suggested that the correction of anaemia with EPO decreased cardiac output and heart rate, and might induce at least a partial regression of LV mass and delay the development of LV dilatation (Foley et al., 2000, Pascual et al., 1991). In subsequent randomized controlled trials however, the use of EPO stimulating agents have not been shown to reduce adverse outcomes associated with anaemia, such as mortality, nonfatal cardiovascular events, hospitalizations, and progression of kidney disease (Kdoqi, 2006). Moreover, recent trials in both haemodialysis and predialysis CKD patients demonstrate an increased risk of death, adverse cardiovascular events, and stroke by administering EPO stimulating agents to target haemoglobin levels >110 g/L (Pfeffer et al., 2009, Singh et al., 2006, Besarab et al., 1998, Parfrey et al., 2005). Similarly, in a meta-analysis of 1731 ESRD and anaemic CKD subjects, conventional haemoglobin targets for EPO therapy of >100 g/L were associated with a reduction in LV mass index, but a target level of >120 g/L did not have a beneficial impact on adverse LV remodelling (Parfrey et al., 2009).

1.6.5. Uric acid

Uric acid is generated during the metabolism of nucleotides and adenosine triphosphate (ATP) and represents the end-product of purine metabolism in humans, which is produced chiefly in the liver and intestines, but also by the endothelium, skeletal muscle and the kidneys (Kanbay et al., 2013). Under normal physiological conditions, two-thirds of the uric acid produced is excreted via the kidneys with one third eliminated via the biliary tract. In the kidney, urate is filtered readily by the glomerulus and then reabsorbed by the proximal tubules. The exact details of urate transport are poorly elucidated but it appears that, the efficiency with which the kidney reabsorbs urate contributes to hyperuricaemia. A number of factors play a role in elevating uric acid levels in CKD including the reduced GFR, frequent use of diuretics, increased renal vascular resistance, and co-existent insulin resistance (Jalal et al., 2013).

Uric acid has a number of deleterious cellular actions which could explain the association between hyperuricaemia and adverse cardiovascular and renal outcomes. It is accepted that entry of uric acid into the cell induces oxidative stress and this is mediated by its direct reactions with superoxide and peroxynitrite (Sautin et al., 2007, Kuzkaya et al., 2005). This process generates several radicals, including the aminocarbonyl radical and the triuretcarbonyl radical (Imaram et al., 2010), as well as intermediates with alkylating activity (Gersch et al., 2008). Uric acid has also been implicated in the development of ED. Numerous studies show that the presence of intracellular uric acid is associated with a reduction in nitric oxide bioavailability via a number of pathways, including blocking uptake of L-arginine,

stimulating L-arginine degradation via arginase, and the scavenging of nitric oxide by uric acid or from uric acid generated oxidants (Kanbay et al., 2013). Treatment with L-arginine in rats blocks the adverse effects of hyperuricaemia on systemic hypertension and prevents preglomerular arteriolopathy. (Sanchez-Lozada et al., 2007). There is also evidence that uric acid may have a role in both systemic and intrarenal RAAS activation. In a renal histology study of the remnant kidney rat model of progressive renal failure, levels of uric acid were associated with the percentage of renin positive juxtaglomerular cells (Kang et al., 2001).

Observational data have consistently demonstrated higher uric acid levels are associated with a greater risk of ischaemic heart disease, elevated blood pressure, and an adverse cardiovascular risk profile (Fang and Alderman, 2000, Liese et al., 1999, Sundstrom et al., 2005, Bos et al., 2006). It remains possible however, that these findings result from unmeasured confounding or the phenomenon of reverse causality, whereby preclinical arteriosclerosis might lead to increased circulating levels of urate before a diagnosis of hypertension or LV hypertrophy is made. In a recent Mendelian randomisation analysis that used variation in the SLC2A9 gene (solute carrier family 2, facilitated glucose transporter member 9) as an instrument for uric acid (Vitart et al., 2008), there was no strong evidence for causal associations between uric acid and ischaemic heart disease or blood pressure among the 58702 participants assessed (Palmer et al., 2013).

Nonetheless, evidence is emerging albeit from small interventional studies, that uric acid may represent a true cardiovascular risk factor and play a causal role in the pathogenesis of cardiovascular disease. Lowering uric acid levels with allopurinol reduced both office and

ambulatory blood pressure in hyperuricaemic adolescents with newly diagnosed hypertension (Feig and Johnson, 2003). A subsequent unblinded study performed in adult subjects with asymptomatic hyperuricaemia demonstrated only small benefits of allopurinol on blood pressure but improved endothelial function and eGFR after just 4 months of treatment (Kanbay et al., 2011). In a *post hoc* analysis of the RENAAL (Reduction of Endpoints in Non-insulin dependent diabetes mellitus with the Angiotensin II Antagonist Losartan) study it was suggested that one fifth of the protective renoprotective effect of losartan among patients with diabetic nephropathy could be attributed to the decrease in serum uric acid levels (Miao et al., 2011). Finally, in a randomised double-blind placebo-controlled trial of CKD stage 3 patients with LV hypertrophy, lowering uric acid with a xanthine oxidase inhibitor resulted in a significant reduction in LV mass as measured by cardiac MRI but had no effect on blood pressure, implying that uric acid may have direct adverse effects on myocardial structure (Kao et al., 2011). After 9 months of treatment, there were also accompanying improvements in augmentation index (AIx) on pulse wave analysis and endothelial function as determined by FMD. Larger randomised studies are warranted to confirm these preliminary findings but the fact that uric acid levels can already be effectively and safely modified in CKD with low doses of allopurinol is encouraging.

1.7. Limitations to Studies of Cardiovascular Disease in Chronic Kidney Disease

Lower estimated glomerular filtration rate (eGFR) has been consistently associated with an increased risk of major vascular events and death and a recent meta-analysis suggests that if this relationship is causal, up to one fifth of vascular events among those over 70 years could be attributed to reduced renal function (Mafham et al., 2011). Yet despite the wealth of evidence associating reduced GFR with an elevated cardiovascular risk, it is difficult to prove causality. Cross-sectional studies of CKD are almost invariably confounded by factors such as the underlying disease (e.g. hypertension, diabetes mellitus, systemic vasculitis) and the harmful sequelae of CKD which include hypertension, anaemia and inflammation. Thus, it remains possible that renal disease itself does not cause cardiovascular disease and merely represents a clustering of cardiovascular risk factors. A prospective longitudinal study of subjects who develop a decline in GFR and or albuminuria is required to examine the effects of new onset renal dysfunction on the cardiovascular system. In human studies this is difficult because the duration of kidney disease is seldom evident at the time of presentation. Kidney donors, however, provide a near ideal experimental model as they are a healthy population, screened to exclude confounding co-morbidity, in whom renal function declines suddenly at a known time point. Two thirds of donors will fall into the category of stage 3 CKD after donation (Moody et al., 2012a) and whilst initial survival data have been largely reassuring (Segev et al., 2010, Fehrman-Ekholm et al., 1997), a small adverse cardiovascular influence cannot be excluded because donors are “super-selected” for health and, therefore, have better predicted cardiovascular risk than healthy control populations.

1.8. Living Kidney Donors

1.8.1. Current Status of Living Donor Kidney Transplantation

Renal transplantation is the optimal treatment for patients with ESRD but demand continues to exceed the supply of cadaveric organs. This has led to a substantial growth in the practice of living kidney donation such that every year more than 27,000 adult subjects worldwide elect to donate a kidney (Horvat et al., 2009). In the UK, there has been an increase in the number of annual living donor kidney transplants (Table 1-5); in 2012-13, living donations represented 36% of the total kidney transplant programme (NHSBT, 2013). Similarly, in the US and Canada, the number of living donor kidney operations performed has doubled over the last decade and accounts for over 40% of all kidney transplants (Knoll, 2008). This increased activity can be attributed to a number of factors including: improved patient education (BTS, 2005), recognition of its cost-effectiveness (Laupacis et al., 1996, Baltzan et al., 1997), use of minimally invasive laparoscopic nephrectomy reducing donor morbidity (Chin et al., 2009), evidence that pre-emptive transplants performed from living kidney donors have better graft survival than those from cadaveric donors (Meier-Kriesche and Kaplan, 2002) and the acceptance that outcomes from living genetically unrelated donors are equivalent to traditional genetically related donations (Terasaki et al., 1995). Another key aspect has been the surge in the number of non-directed altruistic donors. In 2012-13, of the 1,068 people receiving a living donor kidney transplant in the UK, 76 were from altruistic living donors (NHSBT, 2013).

Table 1-5. UK Living Donor Kidney Transplantation.

Year	*N*
2007-08	804
2008-09	903
2009-10	1,037
2010-11	1,045
2011-12	1,009
2012-13	1,068

Data from *www.uktransplant.org.uk* (2013)

The criteria for "fitness" to undergo donor nephrectomy were initially very strict in an attempt to minimise both operative and long-term risks in subjects undergoing surgery for no personal physical benefit. Subjects were intensively screened prior to surgery so that kidney donors comprised a super fit population with lower levels of co-morbidity and cardiovascular risk than the general population. Recently however, with an ever growing waiting list for kidney transplantation, exclusion criteria for living donors have become more relaxed. Centres are now accepting subjects with a lower GFR than may have been considered appropriate in the past in addition to older age groups, those with controlled hypertension, and those with raised body mass index (Bia et al., 1995, Knoll, 2008). Indeed, nearly a fifth of all living kidney donors (199 out of 1068; 18%) proceeding to nephrectomy last year in the UK were aged over 60 years (NHSBT, 2013). The potential long-term renal

and cardiovascular effects of kidney donation may be most relevant to these donors with higher cardiovascular risk profiles.

1.8.2. Renal Function after Kidney Donation

Glomerular filtration rate. Uninephrectomy is associated with an acute 50% reduction in GFR followed by an improvement to about 70% of baseline within 2-3 weeks secondary to glomerular hypertrophy and hyperfiltration in the remaining kidney (Krohn et al., 1966, Anderson et al., 1991). Long-term longitudinal studies comparing early and late post donation GFR have found no evidence of a further decline in mean function over periods of between 10 and 30 years (Saran et al., 1997). In a meta-analysis of 48 cross-sectional studies involving over 3,000 patients and 1,703 controls, uninephrectomy was associated with a reduction in GFR of 17.1 ml/min/1.73m^2 (95% CI -20.2 to -14.0 ml/min/1.73m^2) that tended to improve slightly with each 10 years of follow-up (Garg et al., 2006). These findings are difficult to interpret as GFR was measured by a variety of methods including creatinine clearance by timed collection and estimated values derived from serum creatinine concentration, both of which are known to be inaccurate particularly at the modestly sub-normal GFR levels expected post-donation (Poggio et al., 2005, Barri et al., 2010, Tan et al., 2010). Ibrahim measured GFR by iohexol clearance in a randomly selected sample of 255 donors at a mean of 12 years after donation and found a mean GFR of 63.7 +/- 11.9 ml/min/1.73m^2, 76% of the estimated level at the time of donation (Ibrahim et al., 2009). Fifteen percent of donors fulfilled criteria for stage 3 CKD although in no case was the value

<30 ml/min/1.73m^2. In a recent study using ^{125}I-iothalamate GFR, a more accurate assessment of renal function, the overall prevalence of stage 3 CKD in 196 donors at 3 months after nephrectomy was higher at 27%; this proportion was heavily age dependent, however, with only 10% of donors under 30 years falling into this category but 91% of those aged 60–69 years (Barri et al., 2010). The figures for stage 3 CKD according to eGFR are even higher (Figure 1-7) and it should be remembered the graded association between CKD and cardiovascular risk emerged from observational studies which used eGFR as their index of renal function. These data are supported by my own analysis of 71 donors transplanted in 2009 at Queen Elizabeth Hospital, Birmingham (Moody et al., 2012a). Despite a mean baseline iGFR of 100 ml/min/1.73m^2 using ^{51}Cr-EDTA clearance and a mean donor age of only 47 years, 65% had an eGFR <60 ml/min/1.73m^2 at 3–12 months post-nephrectomy (Figure 1-8).

The risk of developing CKD of any category after donation is dependent upon race and age. In a large US study of health outcomes after kidney donation (Lentine et al., 2010), older age at donation was associated with an increased risk of 4% per year of age of “medically coded” CKD. Black and Hispanic donors were approximately twice as likely to develop CKD after nephrectomy as white donors. Of more concern was the finding that black donors were at increased risk of progressing to ESRD over 20 years with an incidence of nearly 1% (2 out of 271) compared to <0.5% in Hispanics and 0% in whites. However, in the largest US study of donors to date, a difference in the cumulative incidence of ESRD was observed in both black and white donors (Muzaale et al., 2014). Black donors had an estimated risk of 75 per 10,000 at 15 years after donation compared with 24 per 10,000 black nondonors; the risk in white

donors was estimated at 23 per 10,000 versus 0 per 10,000 white nondonors. Thus, there was a significant increased relative risk of developing ESRD following live kidney donation although the magnitude of the absolute risk increase was small, even among black donors.

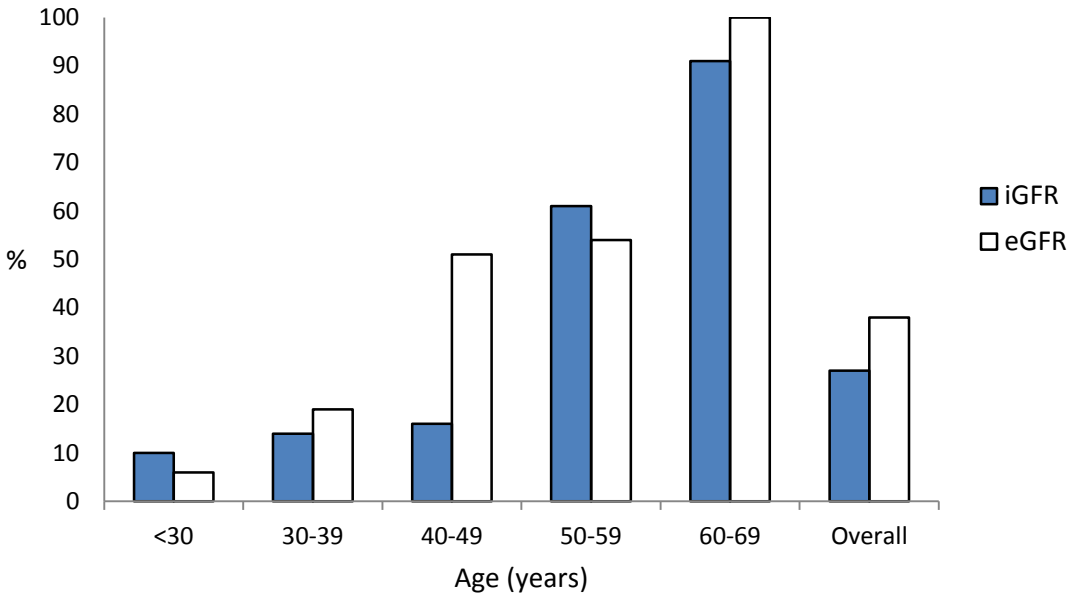

Figure 1-7. Percentage Proportion of Stage 3 Chronic Kidney Disease in Living Kidney Donors 3 Months Post-Nephrectomy According To Age and Method Used for GFR Measurement.

(Barri et al., 2010)

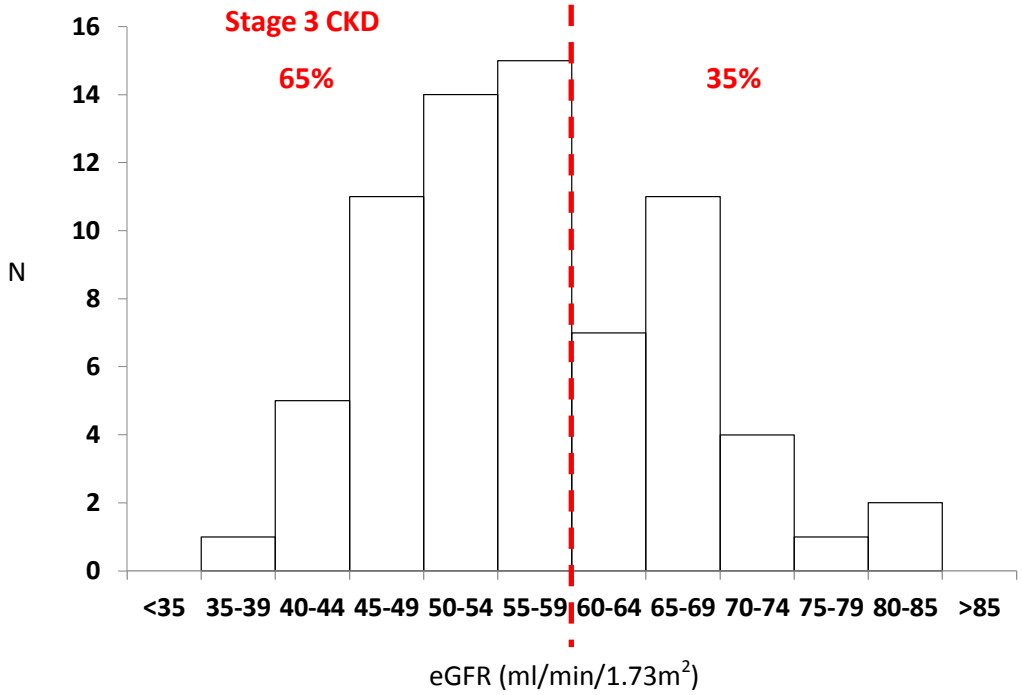

Figure 1-8. Living Donor Estimated Glomerular Filtration Rate at 3–12 Months Post-Nephrectomy.

(Moody et al., 2012a)

Proteinuria. A number of studies have demonstrated an increase in protein excretion following kidney donation. In a meta-analysis of 48 studies involving 5,048 donors, at an average of 7 years after donation, the average 24-h urinary protein excretion was 154 mg/day (above the upper limit of normal protein excretion; see Table 1-6) (Garg et al., 2006). The pooled incidence of clinical proteinuria (>300 mg/day) was 12% and compared to controls, the pooled risk of microalbuminuria was increased at 3.9 (relative risk 3.9, 95% CI 1.2 to 12.6). The effect of normal ageing was investigated by analysing 3 studies with controls involving 129 donors and 59 controls. At an average of 11 years after donation, 24-h urinary protein was higher in donors compared to controls (147 vs. 83 mg/day). This difference increased with time from donation suggesting a progressive effect. Higher levels of proteinuria are seen in donors with hypertension (Gossmann et al., 2005, Hakim et al., 1984, Chavers et al., 1985) and males appear to be at greater risk than females (Furchgott and Zawadzki, 1980). More recently, Ibrahim *et al.* reported that in 255 donors selected randomly from 3,698 nephrectomies performed at the University of Minnesota between 1963 and 2007, 11.5% had microalbuminuria and 1.2% had macroalbuminuria at a mean of 12.2 years after donation (Ibrahim et al., 2009). There was a log linear increase in ACR with time following donation although in the absence of a control group, it was not possible to distinguish this from an effect of ageing.

Table 1-6. Equivalents for 24 h Urinary Albumin and Protein Excretion, Albumin : Creatinine Ratio (ACR) and Protein : Creatinine ratio (PCR).

Albuminuria*		Proteinuria**	
ACR *mg/g; (mg/mmol)*	24 h urinary albumin *(mg/24 h)*	PCR *mg/g; (mg/mmol)*	24 h urinary protein *(mg/24 h)*
30 (3.4)	30	150 (17.0)	150
300 (33.9)	300	500 (56.8)	500
700 (79.5)	700	1000 (113.0)	1000

**Microalbuminuria* is defined as a 24 h albumin excretion rate of 30-300 mg/24 h (ACR > 3.0 mg/mmol). *Macroalbuminuria* is defined as a 24 h albumin excretion rate of >300 mg/24 h (ACR > 30 mg/mmol) **There is no consistent definition for *proteinuria*. The upper limit of normal protein excretion is usually defined as a 24 h urinary protein of 150 mg/24 h (PCR 15 mg/mmol). To convert mg/g to mg/mmol multiply by 0.113. Data adapted from www.nice.org.uk/CG73

1.8.3. Risk of Hypertension after Kidney Donation

A meta-analysis of 48 studies from 28 countries (11 prospective, 37 retrospective) examined blood pressure changes following kidney donation in 5,145 donors (Boudville et al., 2006). Roughly a third of the donors had incomplete follow-up data and only 10 of the studies selected had a control group with comparable age, sex and ethnicity. Most individual reports failed to detect a statistically significant change in blood pressure but were almost certainly underpowered. The pooled estimates, however, did show that compared to controls, systolic blood pressure increased by 5 mmHg and diastolic blood pressure by 4 mmHg at approximately 10 years after donation. The Norwegian Living Donor Registry of 256 donors

also demonstrated an increase in systolic blood pressure of about 5 mmHg at 5 years after nephrectomy, and an increased prevalence of hypertension at 27% compared to 3% before donation (Mjoen et al., 2010). Similarly, a retrospective cohort study of 1,278 donors showed an increase in diagnosed hypertension compared to controls (16.3% vs. 11.9%, hazard ratio 1.4, 95% CI 1.2-1.7) at a mean of 6.2 years (Garg et al., 2008). The same study also noted that donors were seen more often by their primary care physicians, raising the possibility that the increased prevalence might have been due to increased monitoring. In the University of Minnesota study, mean "office" systolic blood pressure in the 255 patients following nephrectomy was 122 mmHg, significantly lower than an age matched control population (Ibrahim et al., 2009). The prevalence of hypertension requiring drug therapy was 25%, not significantly different from the figure of 29% in the control population. A longitudinal study of 75 donors followed over 10 years did show an increased prevalence of hypertension in donors when compared with age/sex matched data from epidemiological studies of the general population (Saran et al., 1997). The prevalence of hypertension was 36% at an initial visit 1–21 years after donation increasing to 75%. This effect was especially strong in those donors over the age of 55 years. It appears that baseline blood pressure influences the magnitude of the observed increase in blood pressure in donors. Higher pre-donation blood pressure, even that regarded as being within normal limits, is associated with higher rates of hypertension post-donation (Ludmer et al., 1986, Rizvi et al., 2005). Older age at donation is also associated with an increased risk of post-donation hypertension with an effect size of 6% per year (Lentine et al., 2010). In a recent retrospective Canadian cohort study published in the *New England Journal of Medicine*, gestational hypertension or preeclampsia were reported to be more common in living kidney donors than in nondonors

with comparable baseline health (11% vs. 5%; odds ratio, 2.4) although there were no reports of maternal death, stillbirth, or neonatal death among the 131 donors (Garg et al., 2015). In the general population, it is accepted that subjects with a history of preeclampsia are at a significantly heightened risk for cardiovascular disease (Ahmed et al., 2014) and this might in part, relate to the development of left ventricular dysfunction, as evidenced by impaired myocardial longitudinal strain (Shahul et al., 2012).

The well recognised racial disparities which affect the development and progression of hypertension in the general population are also evident among living kidney donors. In a large retrospective study of 4,650 donors the prevalence of hypertension at 5 years from donation varied from 13.9% in young white women to 47.9% in black men over 50 years of age (Lentine et al., 2010). At a median of 7 years, the risk of hypertension in black and Hispanic donors was greater than that of white donors with an adjusted hazard ratio of 1.52. The risk of hypertension in Hispanics exceeded control values from NHANES data and there was a similar trend in black donors that could not be accounted for by socioeconomic factors. These data are further supported by a study demonstrating hypertension in as many as 41% of black donors at a mean follow up of 7 years post-nephrectomy (Nogueira et al., 2009). In a single centre retrospective cohort study, hypertension was diagnosed more frequently among 38 indigenous North American donors compared with 76 randomly selected white donor controls (NA 42% vs. white 19%, p=0.02) (Storsley et al., 2010).

1.8.4. Risk of Diabetes Mellitus after Kidney Donation

To date, there is no evidence to confirm an increased risk of developing type 2 diabetes mellitus (T2DM) in humans following kidney donation. No effect on insulin resistance was detected in an uncontrolled observational cohort study of 58 living donors at 6 months post-donation (Prasad et al., 2008). In a retrospective survey of 3,777 kidney donors at a mean of 18 years after donation, 154 of the 2,954 respondents (6%) had developed T2DM (Ibrahim et al., 2010). This proportion is roughly equivalent to that observed in the general population suggesting it probably represents an effect of ageing but the lack of control group might have concealed an excess risk associated with donation. Those who did develop T2DM were more likely to have hypertension (70.8% vs. 36.2%, $p = 0.005$) and proteinuria (18.8% vs. 3.9%, $p < 0.0001$) but had a similar eGFR when compared to matched controls. As for the general population, risk factors associated with an increased risk of developing T2DM post donation include male gender and body mass index >30 kg/m^2 at baseline. Black, Hispanic (Ibrahim et al., 2010) and native North American donors (Storsley et al., 2010) also appear to be at increased risk of developing T2DM following nephrectomy compared with white donors.

1.8.5. Other Cardiovascular Consequences of Kidney Donation

Two cross-sectional studies have examined PWV in kidney donors (Bahous et al., 2006, Abhayaratna et al., 2010), a well-validated measure of arterial function that is independently predictive of cardiovascular mortality in a range of populations including hypertension and

CKD (Laurent et al., 2006). Increased arterial stiffness in CKD is believed to play a central role in promoting the adverse changes in cardiac structure and function which predispose to an increased risk of cardiovascular death. Its mechanistic importance is discussed in section 1.5.2 and has also been reviewed in detail elsewhere (Moody et al., 2013). Aortic PWV was found to be significantly higher in 101 donors at a mean of 111 ± 42 months post-nephrectomy relative to a healthy volunteer group, even after adjustment for age, sex, and blood pressure (Bahous et al., 2006). The second study of 40 living kidney donors included echocardiographic assessment at an average of 7 years post-nephrectomy (Abhayaratna et al., 2010). When compared with controls, donation was associated with increased PWV as well as increased LV relative wall thickness and left atrial size.

In a retrospective cross-sectional study, echocardiography was used to determine LV mass among patients with CKD stage 2-3 and compared to a group of healthy subjects with a similarly reduced iGFR as a consequence of renal donation (Rugale et al., 2013). The LVM index among patients with early-stage CKD was higher than in donors and associated with lower haematocrit, an increased plasma renin activity and higher aldosterone levels. A more recent longitudinal study of 45 normotensive healthy donor subjects, reported that increased baseline carotid-femoral PWV measured using the SphygmoCor system was associated with decreased post donation compensatory hyperfiltration independent of age, blood pressure and baseline GFR (Fesler et al., 2015). There was no significant change in PWV or office blood pressure at 12 months post-donation although it is notable that the study was not blinded and lacked a control group.

There is some weak evidence from two other small longitudinal cohort studies that the reduction in GFR accompanying nephrectomy is also associated with ED (Rossi et al., 2014, Yilmaz et al., 2014). A progressive reduction in endothelium dependent (FMD) and independent (glyceryl trinitrate (GTN)) brachial reactivity was observed in 42 living donors over the 2 years following nephrectomy, together with sustained increases in uraemic toxins including indoxyl sulfate and *p*-cresyl sulphate. An increase in the carotid IMT was also observed at 2 years. However, the magnitude of the absolute change in both these functional and structural parameters was small and comparable to that which has been observed with "normal" ageing (Howard et al., 1993, Celermajer et al., 1994). Similarly, in a study including 38 living kidney donors, FMD was significantly reduced at 3 and 12 months as compared to baseline and associated with increases in mean serum IL-6, ADMA and VCAM levels (Yilmaz et al., 2014). In keeping with these findings, significant increases in ADMA and FGF-23 at 6 months post-donation were reported in a longitudinal study involving 34 living kidney donors, although no change in blood pressure was demonstrated (Huan et al., 2013). However, it is notable that all of the aforementioned cohort studies have lacked a control group, and so it becomes difficult to draw any firm conclusions from these data.

To date, only one other prospective, controlled pathophysiological study of human kidney donors exists (Kasiske et al., 2013). For each donor in this study, healthy siblings with 2 kidneys were originally recruited as the "ideal" controls. After one year however, only 23 pairs had enrolled despite the involvement of 7 US transplant centres and therefore, the inclusion criteria for controls were relaxed to include any healthy individual who theoretically could have been a donor. It was not until 2013 that the study released its first

report (seven years after its inception), which reflects the difficulty in executing large scale prospective controlled studies of living kidney donors. In the 203 pairs that completed a 6 month follow up visit, there was a 23% increase in PTH in donors compared with controls, as well as an increase in uric acid, and a small but significant reduction in haemoglobin. All of these serological indices have been associated with adverse LV remodelling and increased arterial stiffness (Laflamme et al., 2014, Kao et al., 2011, Levin et al., 1999), although no assessment of large artery or LV structure and function was undertaken.

1.8.6. Animal Studies Assessing the Cardiovascular Effects of Uninephrectomy

There are limited animal studies addressing the effects of reduced renal function on the cardiovascular system but those data which are available are in keeping with the literature in humans. Investigators have shown that subtotal nephrectomy causing severe renal dysfunction causes major abnormalities of cardiovascular structure and function (Sviglerova et al., 2010). Burnett Jr. and co-authors have shown that even mildly reduced renal function caused by unilateral nephrectomy in Wistar rats resulted in increased myocardial collagen content and induced changes in LV gene profiles in the absence of hypertension (Martin et al., 2008). In the same model, the investigators have since shown that uninephrectomy is associated with a persistent increase in LV mass and myocardial fibrosis when compared with Sham control at 4 and 16 weeks (Martin et al., 2012b). Cardiac fibrosis was significantly associated with urinary protein excretion, and increases in circulating aldosterone and plasma BNP, together with impairment of both systolic and diastolic function demonstrated by strain echocardiography. Animal work has also suggested that kidney donation might be

associated with an increased risk of type 2 diabetes mellitus (T2DM). Sprague-Dawley rats develop glucose intolerance and islet beta cell loss 8 months after uninephrectomy (Sui et al., 2007).

1.8.7. Survival and Health Status after Kidney Donation

In general, the results of existing long-term follow up studies suggest that far from suffering an increased risk of early mortality, kidney donors have an excellent prognosis (Figure 1-9). A number of previous large single centre studies provide reassurance that nephrectomy does not adversely affect donor survival. Indeed, a widely quoted Swedish study which followed the health status of 430 kidney donors between 1964 and 1994, suggested that donors tend to live longer than the general population (Fehrman-Ekholm et al., 1997). A case series of 601 Japanese subjects donating a kidney between 1970 and 2006, found a 20-year survival rate of 86%, which was more or less equivalent to that reported by Fehrman-Ekholm et al. (Okamoto et al., 2009). Similarly, Ibrahim and colleagues from the University of Minnesota found no significant difference in survival between 3,698 donors who donated kidneys between 1963 and 2007 and a NHANES cohort matched for age, sex and race (Ibrahim et al., 2009). At 30 years, these proportions were 83% versus 76%, and at 40 years, they were 50% in donors versus 56% in controls. In addition, this study randomly selected 255 donors from its sample and measured various health and quality of life outcomes as well as iohexol GFR measurements, demonstrating that compared with age-, sex-, race-, and body mass index–matched controls, donor outcomes were not inferior. The above reports are limited

however, by the fact that they are all single centre studies with racial homogeneity among donors.

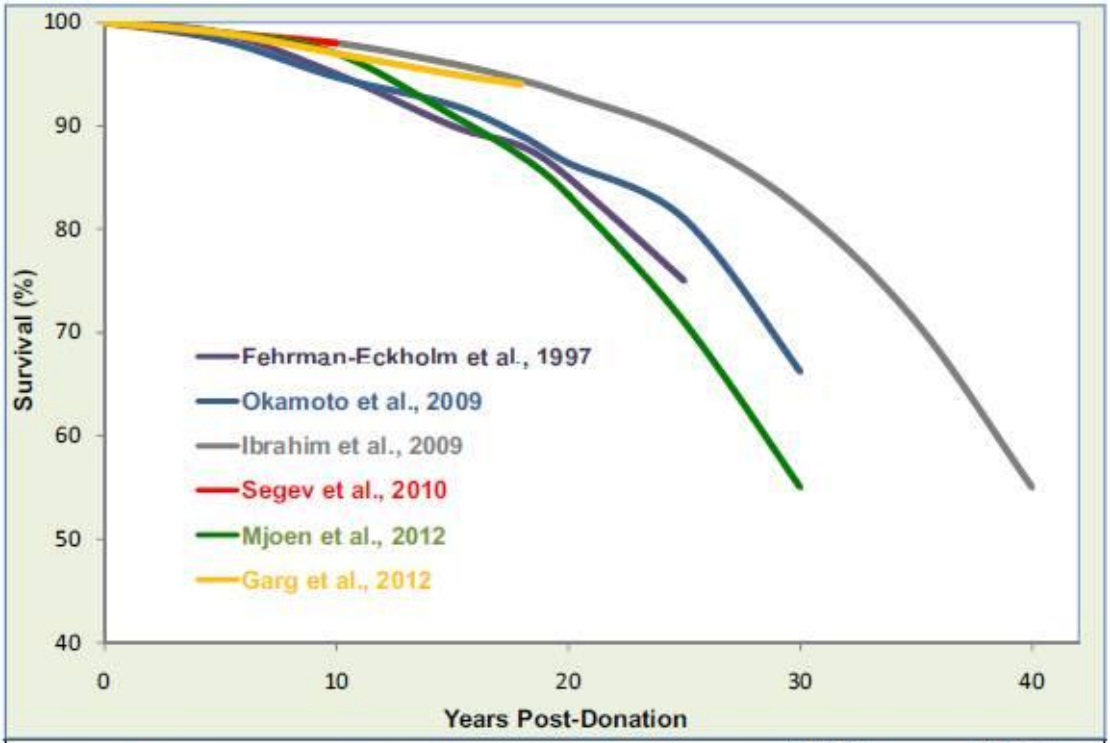

Study	Follow Up	Controls	Age at Donation	Donor Survival
Fehrman-Eckholm et al (1964-1994, n=459)	12 y (mean)	Swedish Population	78% < 59 y	85% at 20 y
Okamoto et al (1970-2006, n=601)	13.7 y (median)	Japanese Population	52 ± 10 y	86.4% at 20 y
Ibrahim et al (1963-2007, n=3,698)	12.2 y (median)	Human Mortality Database	41.1 ± 11 y	93.5% at 20 y
Segev et al (1994-2009, n=80,347)	6.3 y (median)	NHANES III/DMF	79.5% < 50 y	97.9% at 12 y
Mjoen et al (1963-2007, n=2,269)	14.7 y (median)	Norwegian Population	47.6 ± 12.6 y	83.3% at 20 y
Garg et al (1992-2009, n=2,028)	6.5 y (median)	Canadian Population	43 y (median)	95% at 18 y

Figure 1-9. Studies Examining Living Kidney Donor Survival.

Combined survival donor estimates are based on Kaplan-Meier curves from the individual studies.

(Reule et al., 2013)

Nevertheless, these results are in agreement with a large scale registry study of over 80,000 US donors between 1994 and 2009 with a median follow up period of over 6 years, in which the mortality of live kidney donors was slightly lower than that of matched controls from the NHANES III cohort (Segev et al., 2010). In this study, admirable efforts were made to identify a suitable control population that closely matched the relatively healthy status of kidney donors. Quality of life was better than population norms and co-existent health problems were not significantly different.

1.8.8. Limitations to Studies of Cardiovascular Disease in Living Kidney Donors

The general lack of excess morbidity and mortality amongst kidney donors represents a paradox in the face of strong evidence from epidemiological studies which show a clear and graded association between reduced GFR and cardiovascular risk (Mahmoodi et al., 2012, Fox et al., 2012, Matsushita et al., 2010). If the relationship between GFR and cardiovascular risk is causative, a 30% lower eGFR confers a 20% – 30% higher risk of major vascular events and all-cause mortality (Mafham et al., 2011), yet there is an equivalent decline in GFR accompanying the reduction in glomerular mass after nephrectomy (Barri et al., 2010). This discrepancy may be explained by residual confounding related to difficulties in identifying an equivalent control group to kidney donors. Prior to selection for transplantation, potential donors undergo intensive health screening and because the finding of almost all disease states (apart from mild hypertension) leads to exclusion from donation they are not representative of the general population. Indeed, based on accepted living kidney donor

exclusion criteria, more than half of the NHANES cohort would have been ineligible as donors (Segev et al., 2010, Ibrahim et al., 2009). In the absence of detailed physiological assessments, epidemiological donor studies will continue to suffer a selection bias with residual confounding arising from unrecognized medical problems in the nondonor group. For instance, the Canadian Donor Nephrectomy Outcomes Research Network have published extensively using a "universal healthcare administrative database" as their baseline data source for nondonor controls, although these data were heavily reliant on community subjects rating their own health and lacked information on blood pressure, serological indices or imaging parameters (Garg et al., 2015, Garg et al., 2012, Moody and Townend, 2014, Moody et al., 2012c). Further confounding may arise from the fact that donors are well motivated often making substantial healthy lifestyle modifications both before and after surgery. It is noteworthy that thus far, with the exception of two recent US reports (Segev et al., 2010, Muzaale et al., 2014), virtually all studies of kidney donors are either retrospective or have low inclusion rates making them heavily subject to selection and follow-up biases.

Elevated blood pressure is a key risk factor for cardiovascular disease accounting for approximately 8 million premature deaths per year worldwide (Lawes et al., 2008). If it is confirmed that nephrectomy for kidney transplantation increases the risk of developing hypertension (Boudville et al., 2006, Moody et al., 2014b), kidney donors would be the *only* group of patients yet studied, in which a rise in blood pressure has not been accompanied by an increase in mortality. In the general population, even a 2 mmHg increase in systolic blood

pressure confers a long-term increase in mortality from stroke and cardiovascular disease of 10% and 7%, respectively (Lewington et al., 2002). Thus, it is likely that either the data on blood pressure or on morbidity and mortality in kidney donors are incorrect.

Despite initially reassuring findings from a Norwegian registry study (Mjoen et al., 2012), after an extended median follow up of 15.1 years, it was suggested for the first time that there may be a small increase in the risk of cardiovascular events in donors compared to controls (Mjoen et al., 2013). The selection process for identifying nondonor controls in this study was however subject to question (Mjoen et al., 2013, Moody and Townend, 2014). A significant difference in the mean age between donors and controls of almost 10 years (46.0 ± 11.5 yr vs. 37.6 ± 11.7 yr) may have contributed to the increased cardiovascular death rate observed in donors despite adjusting for age in the survival analyses. Furthermore, this report was also limited by the lack of information on renal function in the nondonor controls.

It remains possible that the cross-sectional studies which imply reduced eGFR causes cardiovascular disease have drawn wrong conclusions because of residual confounding by disease states that tend to co-exist with CKD (e.g. diabetes, hypertension), which have not been adequately corrected for by the investigators. Further, since age is a factor in the calculation of eGFR using the MDRD formula, these two entities are inextricably linked. It is conceivable, therefore, that the epidemiological association of CKD with cardiovascular disease is at least, in part, an effect of increasing age (Lindeman et al., 1985, Moynihan et al.,

2013). Employing accurate measures of GFR using isotopic methods would allow further qualification of the level of reduced renal function at which excess cardiovascular risk begins and also help distinguish the effects of reduced renal function from those of ageing.

1.9. Summary

In summary, there is strong cross-sectional evidence of an association between cardiovascular disease and CKD although proof that a reduction in GFR is a causative factor in cardiovascular disease remains lacking. Chronic kidney disease has a powerful clustering effect for other cardiovascular risk factors such as hypertension, diabetes, dyslipidaemia and inflammation and together these processes may confound this association as well as heighten the possibility of "reverse causality". Increasing rates of living kidney donation provide an ideal opportunity to examine the effects of an isolated reduction in renal function on the cardiovascular system, free from the confounding co-morbidity present in many patients with CKD. Although large scale retrospective studies have in the main revealed no evidence of excess mortality in kidney donors, adverse effects on cardiovascular health may be hidden by (1) the careful selection of healthy donors without diabetes and with low levels of hypertension and obesity relative to the general population, and (2) the inappropriate selection of nondonor controls with unrecognized medical disorders owing to inadequate screening. These factors could conceal an adverse impact of reduction in GFR upon cardiovascular parameters since resulting values could still be within those of a "normal" unselected control population. A prospective, controlled study examining hard outcomes in kidney donors would prove very challenging because of low event rates, making it expensive as well as taking a long time to report. An alternative is to undertake a detailed prospective pathophysiological study of living kidney donors with comparison against an appropriate control population, and with the ability to detect adverse effects on well-recognised surrogate markers of cardiovascular disease following a reduction in GFR.

1.10. Experimental Hypotheses

The following *a priori* hypotheses were therefore proposed. A reduction in GFR accompanying surgical uninephrectomy in human living kidney donors is associated with adverse cardiac and vascular effects which include:

(1) An increase in LV mass

(2) An impairment in LV systolic and diastolic function

(3) A blood pressure-independent increase in aortic stiffness (PWV)

(4) An increase in central and peripheral blood pressure

(5) An increase in biomarkers of inflammation, myocardial stretch and myocyte injury

(6) A reduction in endothelial function measured by FMD

2. METHODS

The following chapter describes in detail the techniques used for the forthcoming studies. Table 2-1 lists the major data collection methods employed and includes the key outcomes of interest.

2.1. Cardiac Magnetic Resonance Imaging

Cardiac MRI was performed using a 1.5-T scanner (Magnetom Verio, Siemens, Erlangen, Germany) (Figure 2-1). Serial contiguous short axis cines were piloted from the vertical long axis and horizontal long axis images of the left and right ventricles (ECG R-wave gated, steady-state free precession imaging (SSFP) [True-FISP]; matrix size 256 x 158, temporal resolution 40-50 ms, repetition time 3.2 ms, echo time 1.7 ms, flip angle 60°, slice thickness 7 mm with 3 mm gap) in accordance with previously validated methodology (Maceira et al., 2006).

2.1.1. Left Ventricular Volumes, Function and Mass

Cardiac MRI is the reference standard for the determination of ventricular mass, volumes and function and as compared with transthoracic echocardiography, has higher interstudy reproducibility, thereby reducing the number of participants required to adequately power studies such as those described in the following chapters (Grothues et al., 2002).

Table 2-1. Summary of Main Data Collection Methods and Outcomes of Interest.

Outcome	Method
Primary outcome	
Left ventricular mass	Images were acquired using 1.5T cardiac magnetic resonance imaging (Magnetom Avanto, Siemens, Erlangen, Germany). Analysis will be performed offline (Circle Cardiovascular Imaging Software, cvi[42], Vers. 4.2.1, Calgary, Canada).
Secondary outcomes	
Aortic stiffness (aPWV)	Aortic pulse wave velocity (SphygmoCor, AtCor Medical, Sydney) were performed following 15 minutes of supine rest using a high-fidelity micromanometer (SPC-301, Millar Instruments, Texas). Path length is taken as sternal notch-to-femoral pulse distance minus sternal notch-to-carotid pulse distance.
Mean 24h ambulatory peripheral blood pressure	Mean blood pressure from the non-dominant arm using a 24 hour monitoring system (Mobil-O-Graph NG, IEM, Stolberg). Readings taken every 30 min during the day (08:00-22:00) and every 60 min overnight.
Office systolic and diastolic blood pressure	Three separate measurements taken after at least 5 minutes of seated rest using a BHS validated automated device, mean of last two recorded.
Augmentation index and central haemodynamics	A micromanometer (SPC-301, Millar Instruments, Texas) was used to flatten, but not occlude the radial artery using gentle pressure. An averaged peripheral waveform and corresponding central waveform will be generated after 11 seconds of data capture. The central waveform will then be analysed to determine augmentation index and central aortic pressures.
Left ventricular systolic and diastolic function	CMR-FT analysis of SSFP cine images was undertaken offline by a single blinded observer (TomTec 2D, Cardiac Performance Analysis, Munich, Germany). Myocardial tagging (SPAMM) was performed and analysis performed offline by a single blinded observer (CIMTag2D, Auckland, NZ). Transthoracic echocardiography was undertaken (iE33, Philips, Eindhoven, Netherlands) and analysis performed offline on an Xcelera workstation (Philips, Eindhoven, Netherlands).

Endothelial function	Magnetic resonance imaging (Magnetom Avanto, Siemens, Erlangen, Germany) to calculate flow-mediated dilatation as the proportional change in brachial artery area in response to hyperaemia. Analysis will be performed offline using semi-automated contour tracking software (MATLAB R2008b, MathWorks Inc., Massachusetts, USA).
Renal function	Isotopic GFR using the renal clearance of ^{51}Cr-EDTA.
Bloods	Haemoglobin, creatinine, calcium, albumin, glucose, phosphate, parathyroid hormone, hsTnT, hsCRP, NT-proBNP and uric acid.
Urine	Albumin: creatinine ratio

Abbreviations: aPWV, aortic pulse wave velocity; BHS, British Hypertension Society; CMR-FT, cardiac magnetic resonance-feature tracking; EDTA, Ethylenediaminetetraacetic acid; GFR, glomerular filtration rate; hsCRP, highly sensitive C-reactive protein, hsTnT, highly sensitive Troponin T; LV, left ventricular; NT-proBNP, N-terminal prohormone of brain natriuretic peptide; SPAMM, spatial modulation of magnetization imaging; SSFP, steady state free precession; TDI, tissue doppler imaging.

Analysis was made off-line in a Core laboratory by a single observer (W.E.M.) blinded to subject donor/control status (Circle Cardiovascular Imaging Software, cvi[42], Vers. 4.2.1, Calgary, Canada). Each cardiac MRI dataset was anonymised and saved under a unique random identifier blinded to the observer. Unblinding was performed at the end of the study once analysis had been completed for all study participants.

Manual planimetry of the short axis epicardial and endocardial contours in end-diastole and end-systole was performed using standardised methods for determination of ventricular ejection fraction, volumes and mass (Maceira et al., 2006). The LV basal short axis slice was identified as the image containing at least 50% of circumferential myocardium in end-diastole. Papillary muscles were included in the mass and excluded from volumetric analyses. Mass was calculated as end-diastolic epicardial − endocardial volume × 1.05. LV mass was indexed to body surface area using the Mosteller formula: BSA (m^2) = √((weight (kg)×height (cm))/3600). Left ventricular hypertrophy was defined as LV mass >2SDs above the mean for age and sex (Maceira et al., 2006). The mass-to-volume ratio calculated as LV mass / LV end-diastolic volume, was used as an index of concentric LV remodelling (Zile et al., 2011, Cheng et al., 2009).

To cross-check LV volumetric data, aortic forward flow measurements at the level of the pulmonary artery were performed along with assessment of right ventricular stroke volume by manual tracing of the right ventricular endocardial border in end-diastole and end-systole. Values for LV volumes and mass were only accepted for subsequent analysis if *all* of

the following conditions had been satisfied: (1) LV stroke volume is within 10 mL of right ventricular stroke volume; (2) LV stroke volume is within 10 mL of the total aortic forward flow; and (3) LV end-diastolic and end-systolic masses are within 10% of each other.

Assessment of intra-observer and inter-study reproducibility for the measurement of LV mass, volumes and function using cardiac MRI is described in detail in Chapter 3 (Moody et al., 2015).

2.1.2. Assessment of Left Ventricular Systolic and Diastolic Function

In addition to gross volumetric measures of systolic LV function (ejection fraction and stroke volume), both systolic and diastolic function were assessed using cardiac MRI measurement of myocardial deformation by feature tracking (TomTec 2D Cardiac Performance Analysis, Munich, Germany). A validation of this technique against dynamic tissue-tagging MRI, the reference standard non-invasive methodology for strain calculation, is described in detail in Chapter 4 (Moody et al., 2014a). A normal reference range for cardiac magnetic resonance-feature tracking (CMR-FT) strain parameters has also recently been published using data from this study (Taylor et al., 2015). Briefly, the endocardial borders of the LV steady-state free-precession horizontal long-axis cine and mid LV short-axis cines were manually contoured in the end-diastolic frame. The software then automatically tracked the motion of related features adjacent to the endocardial border, such as the cavity-tissue boundary or individual tissue patterns, throughout the remainder of the cardiac cycle to produce

endocardial strain parameters. The average of the segmental strains from the short-axis view was computed as the global endocardial circumferential strain (GCS), and the average of segmental strains in the horizontal long-axis view was recorded as the global endocardial longitudinal strain (GLS). Global strain rate (SR) signals were also recorded during systole and early filling as peak systolic SR and early diastolic SR, respectively (Figure 2-2).

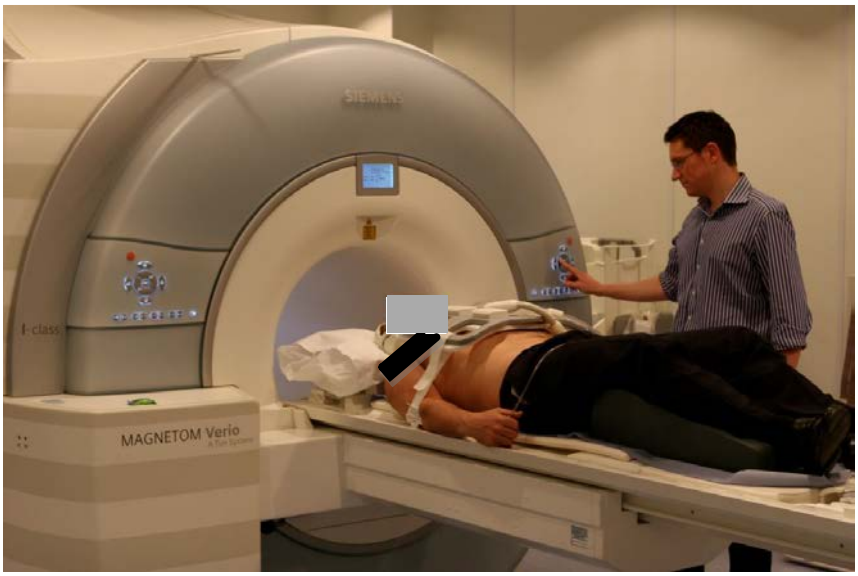

Figure 2-1. 1.5T Cardiac Magnetic Resonance Scanner Used to Perform Imaging in Subjects.

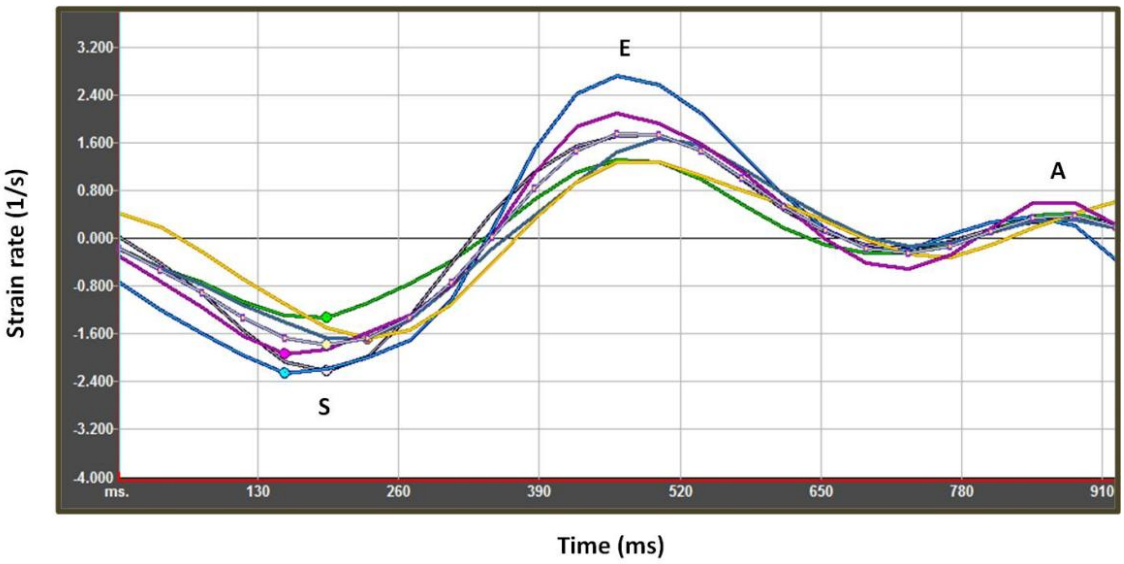

Figure 2-2. Representative Circumferential Strain Rate Profile From Cardiac Magnetic Resonance-Feature Tracking at the Mid Left Ventricular Level of a Healthy Control.

This example demonstrates a typical strain rate pattern with S (systolic), E (early diastolic) and A (late diastolic) waves. The dotted white line represents the global subendocardial circumferential strain rate.

Longitudinal atrioventricular plane descent (AVPD) was also measured in the septum and lateral wall as the distance travelled by the respective annulus from end-diastole to end-systole (Maceira et al., 2006). The biplane area-length method was used to assess left atrial volumes using the horizontal and vertical long axis images in end-systole: Volume = (0.848 x $Area_{4ch}$ x $Area_{2ch}$)/ [($Length_{2ch}$ + $Length_{4ch}$)/2] (Hudsmith et al., 2007). The left atrial appendage was included but the pulmonary veins were excluded from area measurements. The longitudinal axis of the left atrium was defined by measuring the distance from the center of the mitral valve annulus to the posterior left atrial wall.

In asymptomatic subjects without manifest heart disease at baseline, lower peak longitudinal atrial strain (PLAS) measured using CMR-FT, is an independent predictor of incident heart failure (Habibi et al., 2014). Left atrial function was therefore also assessed using CMR-FT, as previously described (Habibi et al., 2014). The software (TomTec 2D Cardiac Performance Analysis, Munich, Germany) generates longitudinal strain curves for each atrial wall segment from the horizontal and vertical long axis images. Global longitudinal atrial strain was generated by averaging all LA segmental values in each time frame. Global peak longitudinal atrial strain (PLAS) and pre-atrial contraction longitudinal strain (preA-S) were derived from the global longitudinal strain profile as shown in Figure 2-3.

Dynamic tissue-tagging MRI also allowed direct non-invasive assessment of regional systolic and diastolic function and is a previously validated technique (Yeon et al., 2001). Spatial modulation of magnetization was used to generate a uniform grid pattern with 8 mm tag

separation on the LV myocardium at three short axis sections (basal, mid and apex) and the horizontal long axis image using a fast filed echo multi-shot sequence (temporal resolution 30 ms, repetition time 3.9 ms, echo time 1.7 ms, voxel size 1.99/2.04/8.00 mm^3, flip angel 5°, tag grid angle 45° with slice thickness 8 mm and a minimum number of 15 phases per cardiac cycle) with prospective ECG gating, as previously described (Young et al., 1994). Blinded analysis was performed offline (SIMTAG, University of Auckland, New Zealand) for LV longitudinal and circumferential shortening as previously described (Young et al., 1994).

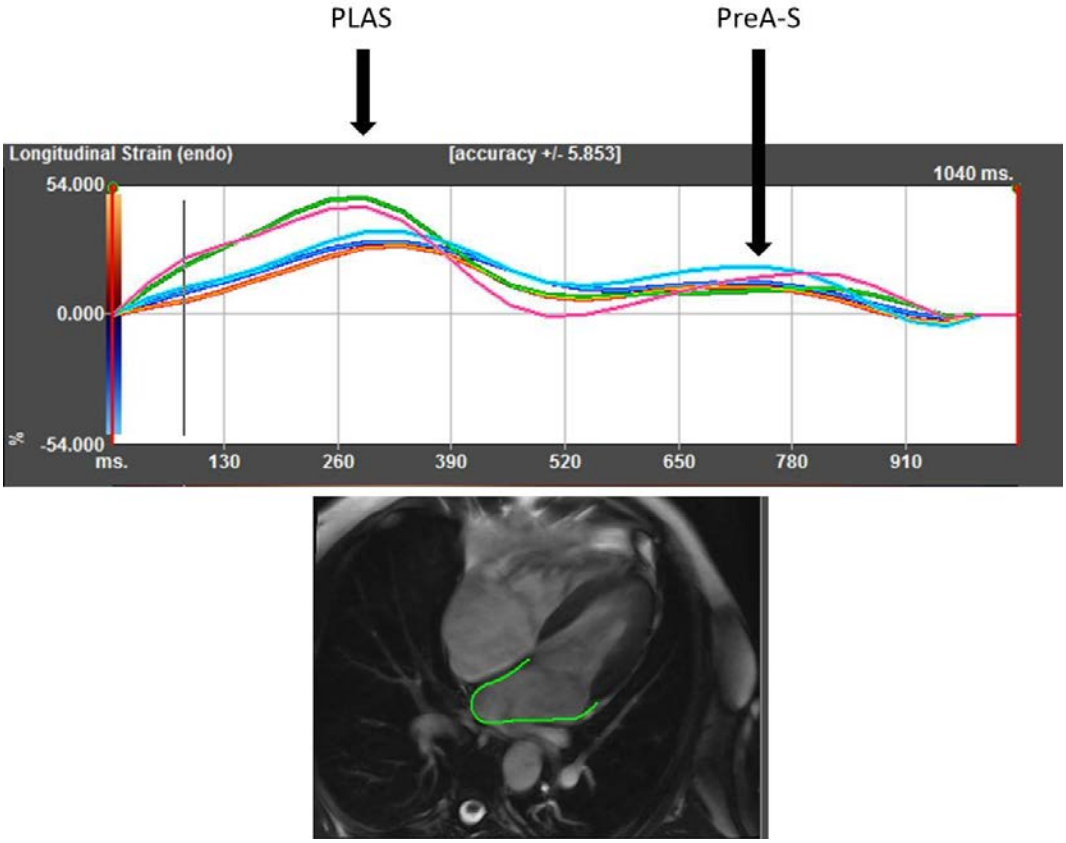

Figure 2-3. Representative Left Atrial Longitudinal Strain Profile in a Healthy Control Subject.

Abbreviations: PLAS, peak longitudinal atrial strain; preA-S, pre-atrial contraction longitudinal strain.

2.1.3. Aortic Distensibility

Measurement of aortic distensibility using MRI has low intra-observer variability and good reproducibility (Forbat et al., 1995). Aortic distensibility was assessed at the ascending aorta, the proximal descending aorta at the level of the pulmonary artery (Figure 2-4), and the distal descending aorta at the level of the diaphragm on held end-expiration. Measurements were calculated using the previously validated formula (Chue et al., 2013a, Groenink et al., 1998):

$$\text{Aortic distensibility} = \Delta \text{ aortic area} / (\text{minimum aortic area} \times \text{pulse pressure})$$

Peripheral blood pressure was measured synchronously, in triplicate, at the brachial artery at the time of scanning for determination of pulse pressure. The measurement of aortic cross-sectional area in systole and diastole was made off-line using automated in house software within Matlab 6.5© (MathWorks Inc., Massachusetts, USA) (Jackson et al., 2009).

2.1.4. Endothelial Function

The term “endothelial dysfunction” was originally coined to describe impaired endothelium-dependent vasodilatation to specific stimuli such as acetylcholine (ACh) and bradykinin (Endemann and Schiffrin, 2004). A much wider definition of ED has now been accepted, encompassing the presence of a pro-inflammatory and pro-thrombotic state. Despite expansion of this term, the overwhelming majority of clinical investigators continue to use techniques employing endothelium-dependent vasodilatation as their index of ED. *Ex vivo,*

using the small vessel myograph, an increasing number of studies have been performed using resistance arteries from human subcutaneous fat to assess endothelium-dependent relaxation (Endemann and Schiffrin, 2004). *In vivo* methods include strain-gauge plethysmography to measure changes in forearm blood flow during infusion of intra-arterial endothelial-dependent and -independent vasodilators such as ACh and sodium nitroprusside (NO donor), respectively. Arguably, this remains the clinical "gold standard" (Wilkinson and Webb, 2001). The measurement of FMD of the brachial artery using ultrasound and more recently magnetic resonance imaging is less invasive and, although a process not completely dependent on the release of NO in response to increased shear stress (Joannides et al., 1995), has become increasingly prominent (Wiesmann et al., 2004, Celermajer et al., 1992).

Flow mediated dilatation of the brachial artery was measured using MRI measurement of brachial artery area before and after 5 minutes of arterial occlusion and also following GTN control (400mcg, sub-lingual) (Wiesmann et al., 2004). Brachial artery measurements were performed off-line using semi-automated contour tracking software (MATLAB R2008b, MathWorks Inc., Massachusetts, USA; Figure 2-5). The FMD was calculated as the proportional change in cross-sectional area in response to hyperaemia (Jackson et al., 2009).

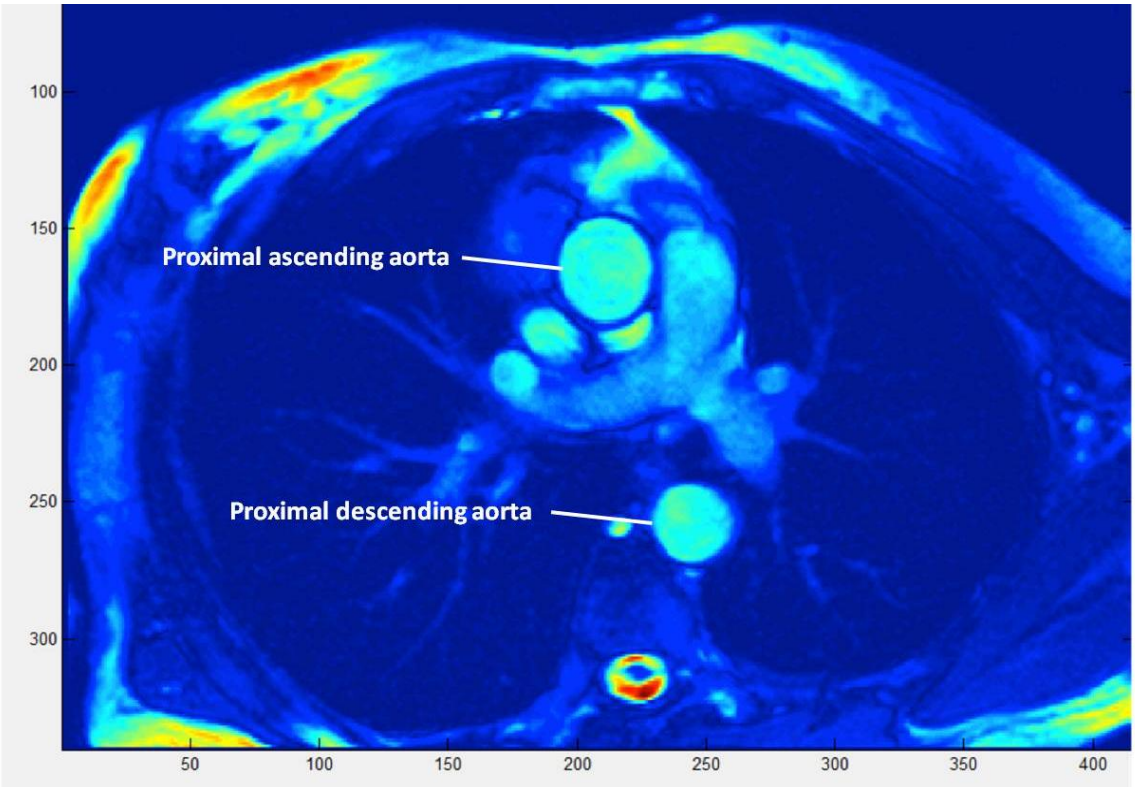

Figure 2-4. Measurement of Aortic Cross-Sectional Area Made Off-line Using Automated In-House Software Within Matlab 6.5© (MathWorks Inc., Massachusetts, USA).

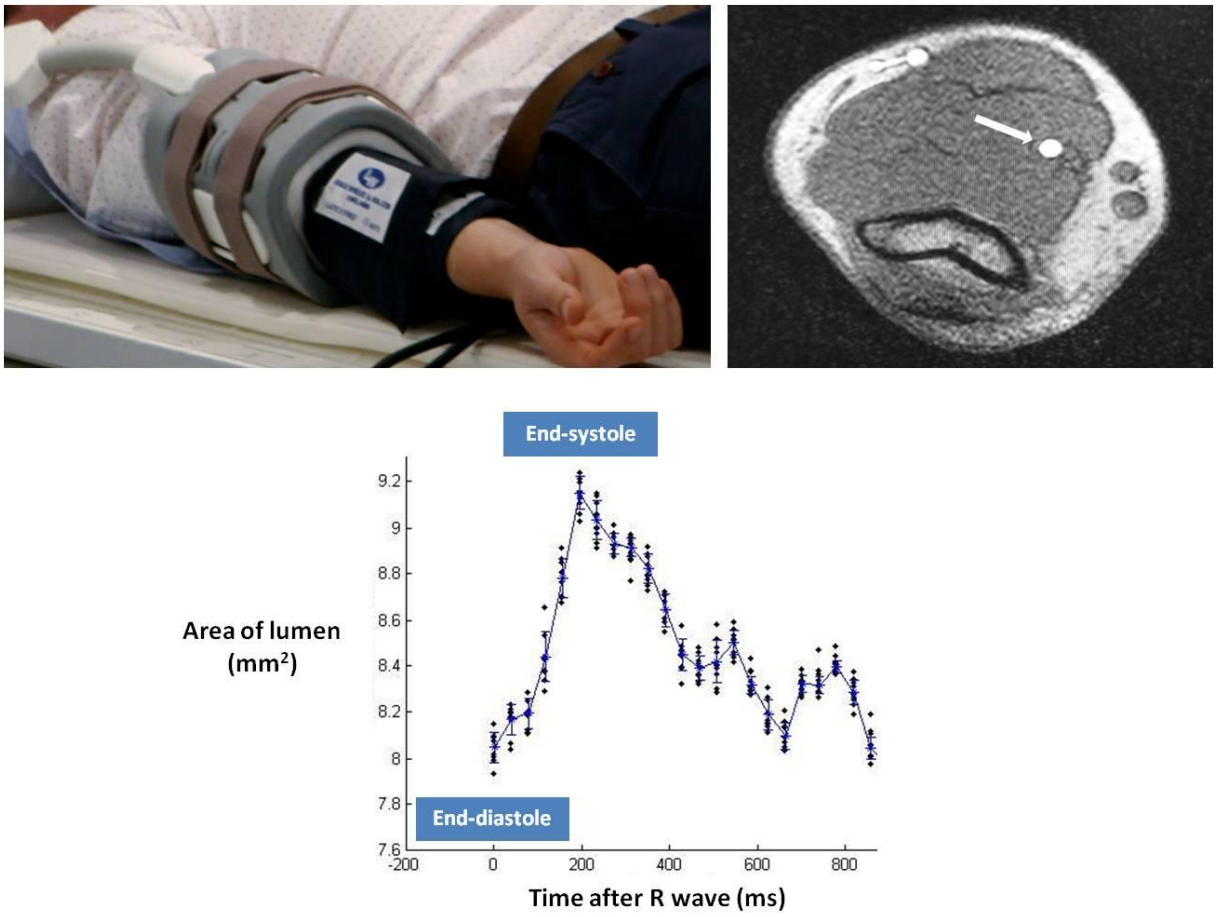

Figure 2-5. Magnetic Resonance Assessment of Flow Mediated Dilatation at the Brachial Artery.

Brachial artery cross-sectional area was measured off line within Matlab 6.5© (MathWorks Inc., Massachusetts, USA) at baseline, after functional hyperaemia and after 400 mcg glyceryl trinitrate control.

2.1.5. Assessment of Extracellular Volume Fraction

Following a substantial amendment to the protocol, patients were also consented to receive intravenous gadolinium 0.15mmol/kg for the purpose of assessing the extracellular volume fraction (ECV). A SSFP single breath hold modified Look-Locker (MOLLI) inversion recovery sequence was used for T1 mapping in the LV basal and mid-ventricular short axis levels before and between 15-20 minutes after contrast administration (8mm slice with a 192 read-out matrix, 6/8 phase partial Fourier with 81% phase resolution, FOV 320 x 320, TR 2.4ms, TE 1.01ms, 11 phases (3, 3, 5 scheme), total breath hold 17 R-R intervals). Late gadolinium enhancement imaging was performed 7-10 minutes after 0.15 mmol/Kg of gadolinium contrast bolus (Gadovist Bayer Health Care).

Quantitative parametric T1 images were generated using Argus software (Siemens®) with manual contouring to define a region of interest (ROI) in the LV septum at basal and mid myocardial levels. Global native (non-contrast) myocardial T1 time (ms) was calculated from the averaged T1 times in the LV septum basal and mid ventricular regions of interest (ROI) before contrast administration and global ECV after contrast using validated formulae (Moon et al., 2013, Ugander et al., 2012):

$$ECV = [\Delta R1_{myocardium} - \Delta R1_{blood\ pool}] * [1 - Hct]$$

Hct refers to the haematocrit recorded on a venous blood sample at the time of scan, ΔR1 = 1/T1 time post contrast – 1/T1 time pre contrast. Myocardial intracellular volume (ICV) was

also calculated as; 1-ECV providing a measure of cell volume which is important when interpreting the composition of the myocardium with LV hypertrophy (Moon et al., 2013).

2.2. Assessment of Blood Pressure

Office blood pressure was measured with the patient seated on 3 occasions using a validated automated device. The first measurement was made following at least 5 minutes of seated rest. Two further readings were made with at least one minute between each reading and the average of these was used for analysis. All measurements were made from the non-dominant arm using the same cuff size between visits. Participants also underwent 24-h ambulatory blood pressure monitoring using a British Hypertension Society validated oscillometric recorder (Mobil-O-Graph NG, IEM, Stolberg, Germany) which provided data on both peripheral and central blood pressure (Wei et al., 2010, Weiss et al., 2012).

2.3. Assessment of Arterial Stiffness

2.3.1. Pulse Wave Velocity

Aortic PWV is the current reference standard non-invasive technique for measuring aortic stiffness (Laurent et al., 2006). Subjects were studied in a quiet, temperature-controlled laboratory after 15 minutes of lying supine. Pulse wave velocity (SphygmoCor, AtCor Medical, Sydney) was determined by sequential acquisition of pressure waveforms from the carotid and femoral arteries by use of a micromanometer (SPC-301, Millar Instruments, TX,

USA;) as previously described (Wilkinson et al., 1998, Frimodt-Moller et al., 2008). The path length was calculated by subtracting the distance between the sternal notch and the carotid recording site from the distance between the sternal notch and the femoral site. Transit time is calculated using the foot-to-foot method, which determines the time difference between the onset of the pulse wave at the carotid and femoral sites. The foot of the pulse wave was defined as the onset of the steep rise of the pulse wave at end diastole. Carotid and femoral arterial waveforms were sequentially recorded using the high fidelity micromanometer whilst an ECG was simultaneously obtained. A representative output is depicted in Figure 2-6.

Aortic PWV is a blood pressure-dependent variable and therefore PWV values were adjusted for mean arterial pressure as described previously (Ford et al., 2010). Adjustment was made based on a linear regression of PWV with mean arterial pressure as the determinant. Unstandardised residuals derived from this regression model were added to the mean PWV to derive adjusted PWV (PWV_{adj}).

2.3.2. Pulse Wave Analysis

Blood pressure measurement was performed in subjects lying supine before undertaking applanation tonometry to record high fidelity arterial pressure waveforms from which indices relating to large artery stiffness could be calculated. Central pressure waveforms were derived and analysed using the technique of pulse wave analysis as previously

described (Wilkinson et al., 1998, Savage et al., 2002). A micromanometer was used to flatten, but not occlude the radial artery using gentle pressure (Figure 2-7). An averaged peripheral waveform and corresponding central waveform was generated after 11 seconds of data capture. The central waveform was then analysed to determine the augmentation index (AIx: the difference between the second and first peaks of the central pressure waveform, expressed as a percentage of the pulse pressure and central aortic pressures (Figure 2-8). This method has been shown to be reproducible in both healthy subjects and in patients with CKD (Wilkinson et al., 1998, Savage et al., 2002).

Figure 2-6. Representative Ouput From Pulse Wave Velocity.

Figure 2-7. Applanation Tonometry of the Radial Artery.

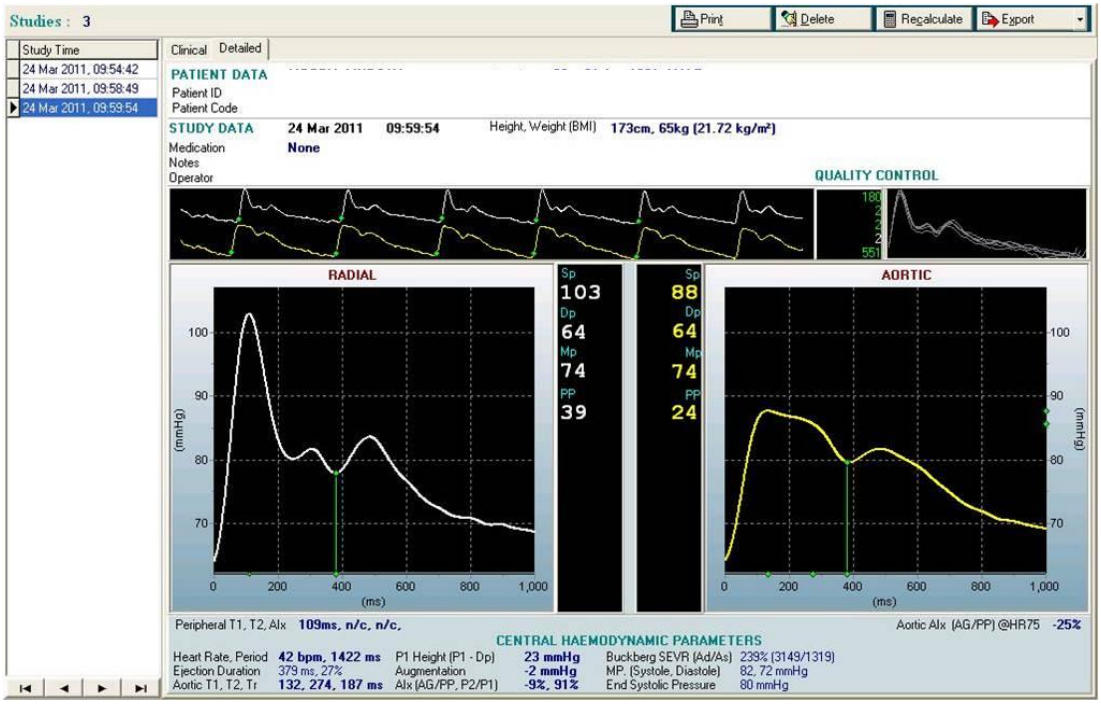

Figure 2-8. Representative Output From Pulse Wave Analysis.

2.4. Assessment of Carotid-Intima Media Thickness

Subjects were examined supine with the head rotated at 45 degrees. Right and left common carotid arteries were imaged using high resolution ultrasound (Philips iE33, L9-3 MHz linear array transducer) 1 cm proximal to the carotid bifurcation with images optimized to demonstrate the posterior wall intima-media in accordance with published guidelines (Touboul et al., 2012). Common carotid IMT was measured as the distance between lumen-intima and media-adventitia interfaces using automated wall tracking software (IMT plug-in, QLAB). The mean of the right and left carotid measurements was used for analysis.

2.5. Echocardiography

A comprehensive transthoracic echocardiogram (iE33, Philips, Eindhoven, Netherlands) was performed at rest with the subject in the left lateral decubitus position by a single experienced sonographer (W.E.M.) using second harmonic imaging and an S5-1 multi-frequency transducer. All parameters were measured in triplicate and averaged as per the American Society of Echocardiography guidelines (Schiller et al., 1989). Analysis was performed offline by a single blinded observer on an Xcelera workstation (Philips, Eindhoven, Netherlands). Ventricular dimensions, wall thickness, chamber volumes and stroke volume were determined using standard methods (Lang et al., 2005). Left ventricular diastolic function was determined using standard techniques (Nagueh et al., 2009). Peak systolic (s'), early diastolic (e') and late diastolic (a') mitral annular velocities were measured at end expiration with real time pulsed wave tissue Doppler (TDI) (Alam et al., 1999).

2.5.1. Calibrated Integrated Backscatter

The ultrasonic reflectivity of tissue has long been used to non-invasively characterize myocardial tissue and is well validated against histologically quantitated collagen (Jellis et al., 2010, Shapiro et al., 1984, Picano et al., 1990). A higher (less negative) calibrated integrated backscatter (cIBS) value is indicative of a greater amount of LV interstitial fibrosis.

Measurements of tissue intensity were obtained offline from sample volumes placed within the pericardium, posterior wall, and anteroseptum from standard gray-scale 2-D parasternal long-axis view images. A fixed 5 x 5 mm region of interest was positioned in the mid-myocardium of the antero-septal and posterior walls of the LV and a fixed 2 x 2mm region of interest was positioned in the pericardium. A resultant integrated backscatter curve was derived with standard commercial software (QLAB, Philips, Eindhoven, Netherlands). Calibrated integrated backscatter was calculated by subtracting pericardial integrated backscatter intensity from the mean integrated backscatter intensity of the posterior wall and anteroseptum in end-diastole.

2.6. Assessment of Renal Function

Isotopic GFR (iGFR) studies were performed using the renal clearance of 51Cr-EDTA (Martensson et al., 1998) under the supervision of Dr. Christopher Boivin in the Nuclear Medicine Department at the Queen Elizabeth Hospital Birmingham. Venous blood samples

were drawn at 2, 3 and 4 hours after a single intravenous injection of the isotope. The CKD-EPI equation was used to determine $eGFR_{cr}$ with serum creatinine recalibrated to be traceable to an isotope derived mass spectroscopy method (Levey et al., 2009). Urinary ACR was determined from a spot morning urine sample (Gansevoort et al., 2005).

2.7. Biochemical Assays

Highly sensitive Troponin T was measured by a sandwich principle immunoassay (cobas 8000 modular analyzer, Roche Diagnostics, Burgess Hill), with a lower limit of detection of 5 ng/L and a 99th percentile value in apparently healthy individuals of 14 ng/L (Giannitsis et al., 2010). Serum N-terminal pro B Natriuretic peptide was measured by sandwich immunoassay with magnetic particle separation and chemiluminescent detection (Roche Diagnostics, Burgess Hill) with a lower limit of detection of 0.6 pmol/L (Downie et al., 1999). Serum C-reactive protein was measured using a highly sensitive assay by latex-enhanced nephelometry (Full Range CRP, SPA_{PLUS} analyser, The Binding Site Group Ltd, Birmingham, UK). Plasma intact PTH was measured by a sandwich immunoassay method (Roche Diagnostics, reference range, 3.5-6.5 pmol/L). Plasma 25-hydroxyvitamin D was measured by liquid chromatomography tandem mass spectrometry. Renin was measured using the Cis-Bio immunoradiometric (IRMA) kit (Codolet, France) and aldosterone was determined by tandem mass spectrometry on an AB Sciex 6500 triple quad mass spectrometer coupled to a Shimadzu Nexera XR UPLC (Warrington, UK). Serum calcium, phosphate and uric acid were measured by standard automated methods.

Assays for high sensitive C-reactive protein and cystatin C were performed by Dr Lakhvir Assi at The Binding Site Group Ltd, Birmingham. Assays for N-terminal pro-brain natriuretic peptide were performed by Prof Leong Ng at Leicester Royal Infirmary. Assays for renin and aldosterone were performed by Dr Rachel Webster at the Queen Elizabeth Hospital Birmingham.

2.8. Overview of Statistical Methodology

All data presented in this thesis were analysed using SPSS version 21 (SPSS Inc., Chicago, Illinois, USA). Normality of data distribution for each variable was determined using the Kolmogorov-Smirnov test and normality plots. Normally distributed variables were presented as mean ± standard deviation and analysed using parametric tests. Any non-normally distributed variables were log-transformed prior to analysis to achieve normality and the logs were analysed using parametric tests; such variables were quoted as median (interquartile range). If normality was not achieved with log transforming, non-parametric analyses were performed. Between-group comparisons were performed using independent t-tests (two groups) or a one-way analysis of variance (more than two groups). Within-group comparisons across different time points were assessed using paired samples t-tests. The primary analysis performed between-group comparisons across different time points using a repeated measures analysis of variance, with the time point (month 0 and month 12) as the

within-subjects factor and the group (donor, control) as the between-subjects factor, thus testing the difference in change over time between the two groups. To account for the effect of missing data, a further quantitative analysis was performed using a last observation carried forward principle. Independent predictors of changes in variables were determined using multivariable logistic regression. Generalised estimating equations were used to compare groups (donors, controls) for the likelihood of developing detectable variables over time (0 and 12 months). Linear regression analysis was performed to determine the relationship between continuous variables; parametric variables were assessed using Pearson's correlation and any non-parametric variables assessed using Spearman's correlation. Categorical variables were presented as frequency (percentage) and analysed using the chi-square test. A Type I error rate below 5% ($P<0.05$) was considered statistically significant.

2.9. Regulatory Approvals and Authorisations

Professor Jonathan N. Townend was the designated Principal Investigator for this study. This project did not constitute a Clinical Trial of an Investigational Medicinal Product (IMP) as defined by the EU Directive 2001/20/EC. The South Birmingham Research Ethics Committee granted approval for the human research studies described in this thesis (Ref: 10/H1207/70). The project was also given local Research and Development and Site Specific Assessment approval from University Hospitals Birmingham NHS Foundation Trust. The University Hospital Birmingham NHS Foundation Trust acted as sponsor (Ref. RRK3922). Approval from the Administration of Radioactive Substances Advisory Committee was given to authorise

use of 51Cr-EDTA for determination of isotopic GFR (Ref. RPC 290/1051/126569). University Hospital Coventry and Warwickshire agreed to act as a Participant Identification Centre (PIC). The study was conducted in accordance with the recommendations for physicians involved in research on human subjects adopted by the 18th World Medical Assembly, Helsinki 1964 and later revisions. Informed written consent was sought prior to any study procedures being conducted. The study was supported by a British Heart Foundation Clinical Research Fellowship under Dr William Moody (FS/11/17/28700). The study was subject to inspection and audit by University Hospital Birmingham NHS Foundation Trust under their remit as sponsor and was found to adhere to Good Clinical Practice.

3. REPRODUCIBILITY OF LEFT VENTRICULAR MEASUREMENTS

3.1. Background

Cardiac MRI is considered the gold standard technique to monitor changes in LV dimensions and function in both congenital and acquired heart disease (Fratz et al., 2013, Hendel et al., 2006). Reference ranges normalized for gender, age and body surface area help clinicians discriminate between normality and pathology (Hudsmith et al., 2005, Maceira et al., 2006), and by including assessments of *short-term* inter-study variability (test-retest after 1 week) can account for differences in LV measurements arising from physiological variation (load alterations and time of day effects). Most clinical imaging however, is repeated at much greater time intervals; physicians frequently monitor ventricular size and function in patients with valvular heart disease or cardiomyopathy on an annual basis, although there are no longitudinal cardiac MRI data quantifying the effect of biological and technical variability over this time frame. Without such information, it is difficult to determine what represents a clinically significant change, particularly when the observed difference is small.

In this study, we therefore sought to examine the *within-subject* changes in LV volumes, mass and ejection fraction (EF) using cardiac MRI over 12 months in subjects identified from the control arm of the CRIB-Donor study (see Chapter 5), a well-characterized cohort of normal healthy adults.

3.2. Methods

3.2.1. Patient Selection

We retrospectively identified 42 healthy control subjects (45 ± 13 yr, male 43 %) who did not proceed to nephrectomy from the Chronic Renal Impairment in Birmingham – Donor study (CRIB-Donor, NCT01028703), the results of which are described in detail in Chapter 5. All subjects included in the current study had a 10-year risk of a cardiovascular event of < 7.5%, a normal exercise stress echocardiogram and normal haematology and biochemistry blood profiles (JBS3, 2014). Exclusion criteria included any of the following: a history of cardiovascular disease, including hypertension; diabetes; glucose intolerance; chronic kidney disease; or a first degree relative with a proven or potentially inheritable cardiac condition.

3.2.2. Cardiac Magnetic Resonance Imaging

The full cardiac MRI study protocol is described in detail in Section 2.1 and has been published elsewhere (Moody et al., 2014b). Briefly, subjects underwent cardiac MRI imaging (1.5 T Magnetom Verio, Siemens) at baseline and 12 months. Analysis of SSFP images was performed manually offline (Argus Software) by a single blinded observer (W.E.M., 5 years experience) for the assessment of LV ejection fraction (LVEF), LV end-diastolic volume (LVEDV), LV end-systolic volume (LVESV), and LV mass (LVM). The LV basal short axis slice was identified as the image containing at least 50% of circumferential myocardium in end-diastole (Figure 3-1). Papillary muscles were included in the mass and excluded from volumetric analyses.

.

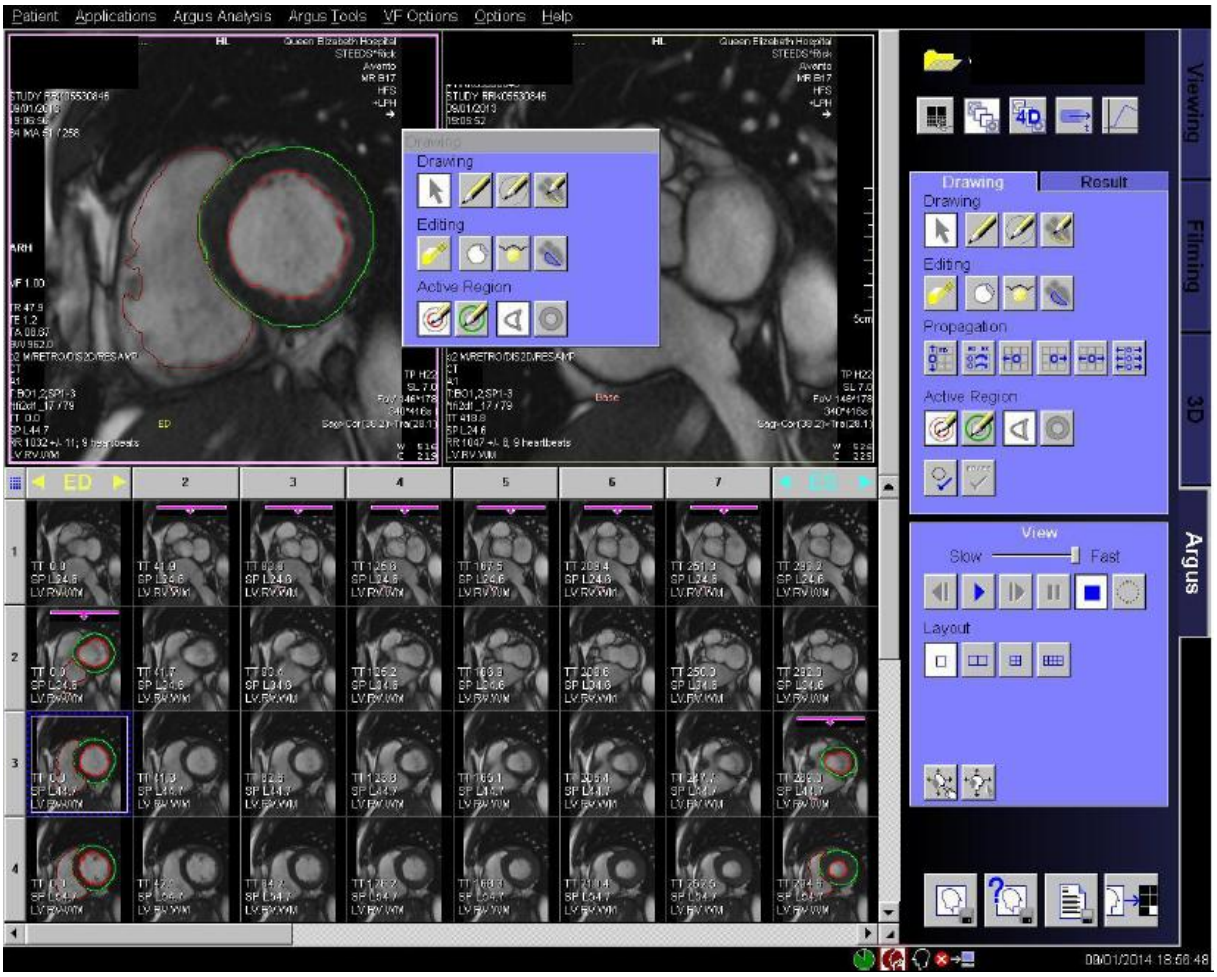

Figure 3-1. Example of the Offline Analysis Performed Using Argus Software on Left Ventricular Short Axis Steady State Free Precession Cine Images.

3.2.3. Reproducibility

To assess intraobserver report variability, baseline studies were re-analyzed by the same observer 4 weeks later, blinded to the original data. A random subset of participants (n = 10) also underwent repeat imaging within 7 days to determine short-term interstudy reproducibility; both scans were analyzed by the same blinded observer.

3.2.4. Statistical Analysis

Data were analyzed using SPSS (v. 21, Chicago, IL). Data are expressed as mean ± SD, median (interquartile range) or frequency (%). The normality of distribution was determined using normality plots and the Kolmogorov-Smirnov test. The within-patient changes were compared with a Student's paired t-test. The mean short-term change in LV parameters was compared with the mean 12-month change using an unpaired t-test.

Reliability was assessed using the intraclass correlation coefficient (ICC) with a model of absolute agreement; absolute measurement error was estimated by the standard error of measurement (SEM) and smallest detectable change (SDC) (Weir, 2005). The SEM is defined as SEM = SD*d* / √ 2, where SD*d* is the standard deviation of the mean difference between two measurements, and takes the amount of measurement error into consideration and quantifies the within-subject variability. The SDC is calculated as SDC = 1.96 x SEM x √2, where 1.96 corresponds to the 95% confidence interval and the square root of 2 is to adjust for sampling from two different measurements, and represents the 95% confidence that a change in the measurement exceeding this threshold is true and reliable and not just a

measurement error (Weir, 2005). For all statistical comparisons, $P < 0.05$ was considered significant.

3.3. Results

The demographics and cardiovascular risk profiles of the healthy control subjects identified for this study are presented in Table 1. All subjects remained well with no clinical events over the 12 month study period. There were no significant changes in any LV parameter on repeat cardiac MRI at 12 months (Table 3-2). Moreover, the short-term interstudy biases (mean differences) were not significantly different from the long-term changes observed at 1 year (LVEF, LVEDV, LVESV, LVM; P = 0.81, 0.63, 0.97, 0.72, respectively). On the basis of our interstudy reproducibility, the SDC for LVEF, LVEDV, LVESV and LVM, which could be recognized with 95% confidence are 6%, 13ml, 7ml and 6g, respectively (Table 3-3).

Table 3-1. Patient Characteristics.

Patient variable	N = 42
Age (yr)	45 ± 13
Gender (male:female)	18:24
Height (m)	1.70 ± 0.90
Weight (kg)	74.5 ± 11.5
Body mass index (kg/m^2)	26.2 ± 4.0
Office systolic blood pressure (mmHg)	120.7 ± 11.7
Office diastolic blood pressure (mmHg)	74.1 ± 8.4
Cardiovascular medications	0 (0)
Hemoglobin (g/L)	135.2 ± 10.2
eGFR <60 ml/min/1.73m^2	0 (0)
Fasting cholesterol (mg/dL)	191.4 ± 40.2
Fasting glucose (mg/dL)	84.4 ± 7.2
Urinary ACR (µg/mg)	0.89 (0.89 – 2.65)
10 yr cardiovascular risk < 7.5%*	42 (100)

Data are expressed as mean ± SD, median (interquartile range) or frequency (%). Dividing the urinary ACR by 8.84 converts the units from µg/mg to mg/mmol. ACR, albumin : creatinine ration; eGFR, estimated glomerular filtration rate.

*Calculated using the JBS-3 heart risk calculator available at www.jbs3risk.com

Table 3-2. Annual Change in Left Ventricular Ejection Fraction, Volumes and Mass.

Parameter	Month 0	Month 12	Mean difference	*p*
LVEF (%)	70.3 ± 6.9	71.2 ± 6.4	0.9 ± 4.3	0.18
LVEDV (mL)	121.2 ± 28.2	121.3 ± 26.9	0.1 ± 10.4	0.91
LVESV (mL)	37.0 ± 14.7	35.8 ± 13.7	-1.2 ± 6.6	0.26
LVM (g)	111.4 ± 31.7	109.5 ± 32.0	-2.0 ± 8.6	0.14

Data are mean ± SD. Changes in LV parameters compared using a paired Student's *t* test.

Abbreviations: LVEF, left ventricular ejection fraction; LVEDV, left ventricular end diastolic volume; LVESV, left ventricular end systolic volume; LVM, left ventricular mass.

Table 3-3**.** Intraobserver and Short-Term Interstudy Variability Using Cardiac Magnetic Resonance in Normal Healthy Adults.

Parameter	Variability	Mean difference	*p*	Limits of agreement	ICC (95% CI)	SDC
LVEF (%)	Intraobserver	1.00 ± 1.27	0.11	-1.48 to 3.48	0.99 (0.94 to 1.00)	-
	Interstudy	0.57 ± 2.94	0.63	-5.19 to 6.33	0.93 (0.62 to 1.00)	5.8
LVEDV (mL)	Intraobserver	0.67 ± 3.62	0.67	-6.43 to 7.77	0.99 (0.95 to 1.00)	-
	Interstudy	-1.57 ± 6.47	0.43	-14.25 to 11.11	0.99 (0.97 to 1.00)	12.7
LVESV (mL)	Intraobserver	-0.83 ± 2.79	0.50	-6.30 to 4.64	0.99 (0.93 to 1.00)	-
	Interstudy	-1.29 ± 3.65	0.37	-8.44 to 5.86	0.98 (0.91 to 1.00)	7.2
LVM (g)	Intraobserver	-0.33 ± 2.16	0.21	-4.56 to 3.90	0.99 (0.95 to 1.00)	-
	Interstudy	-1.00 ± 3.03	0.50	-6.94 to 4.94	0.98 (0.91 to 1.00)	5.9

Data are mean ± SD. Changes in LV parameters compared using a paired Student's *t* test.

Abbreviations: ICC, intraclass correlation coefficient; SDC, smallest detectable change. All other abbreviations as in Table 3-2.

3.4. Discussion

To our knowledge, this is the first longitudinal cardiac MRI study to perform a repeat annual assessment in individuals free of cardiovascular disease. The data presented herein suggest the effect healthy ageing at 1 year is negligible and need not be taken into account by clinicians when reporting cardiac MRI studies performed in patients over this time frame.

As for any imaging modality, cardiac MRI is subject to variability because of technical, procedural, observer, and biological factors (Iskandrian et al., 2014). The intrinsic variability of cardiac MRI becomes important in interpreting serial tests in both research (such as in the CRIB-Donor study), and in the clinical setting to be able to define a true pathological change in a given patient. Therefore, in order to calculate a SDC for each LV parameter, we opted to include an assessment of short-term interstudy reproducibility. Despite recent improvements in MRI scanner performance and pulse sequences, it has been over a decade since the test, re-test (interstudy) reproducibility of LV mass and volume measurements made in normal adult subjects using manual contouring has been reported (Grothues et al., 2002, Moon et al., 2002). Our interstudy reproducibility was excellent which may in part reflect implementation of contemporary imaging hardware and potentially improved cine sequences.

For completeness, both relative and absolute indices of agreement are presented: ICC and SDC, respectively. However, when interpreting clinical tests it becomes more intuitive and appropriate to calculate a SDC because this index can account for both random and systematic error in measurements (Vaz et al., 2013). The SDC is based on a statistical computation and is distinct from the minimally clinically important difference (MCID) which

is set on clinical grounds and represents how large the change in an outcome should be, to be deemed clinically important. Establishing a MCID for LV parameters was beyond the scope of the current study.

All images in this study were acquired using a standardized imaging protocol on a single scanner at one center, conditions which might often be replicated in routine practice. Studies were also performed however, by the same technician and analysed by a single trained observer which may approximate less to standard clinical circumstances. Nevertheless, this scenario provides the optimal setting to maximize test-retest reliability and derive the lowest achievable SDC for respective LV parameters. It should also be remembered that as an index of test-retest reliability, the ICC is affected by the characteristics of the individuals being tested and will therefore likely be higher in this healthy cohort as compared to diseased populations (Moon et al., 2002). Indeed, these results may be less generalisable to patients with heart disease where the reliability of SSFP cine imaging may be hampered by gating issues (e.g. atrial fibrillation or frequent ectopy) or the inability to perform adequate breath holds (e.g. heart failure).

The current study was not designed or indeed powered, to examine changes in LV structure or function due to “normal” ageing; cross-sectional data provided from the Multi-Ethnic Study of Atherosclerosis study suggest that LV mass decreases incrementally with increasing age by -0.3 g per year (Cheng et al., 2009). By contrast, the novelty of the current study lies in its longitudinal design which has enabled an assessment of within-subject variability of LV functional metrics over a 12 month period. Importantly, the data presented

herein demonstrate that in health, the size of any change to the LV observed at 1 year is not significantly different in magnitude to the respective SDC.

In conclusion, the results of this study have demonstrated high reproducibility for the measurements of LV mass and function. These findings support the hypothesis that measured differences in the LV are due to “real” changes in the cardiovascular system. By emphasising the reproducibility and reliability of cardiac MRI data, these data have particular importance for the interpretation of routine clinical reports, as well as longitudinal research studies presented in this thesis (Chapter 5, CRIB-Donor study). In patients undergoing repeat annual assessment by cardiac MRI, even small changes in LV function, size and mass (which are greater than the SDC for the given parameter) may be attributable to disease progression and/or a treatment response.

4. VALIDATION OF CARDIAC MAGNETIC RESONANCE FEATURE-TRACKING METHODOLOGY FOR THE ASSESSMENT OF MYOCARDIAL STRAIN

4.1. Introduction

Myocardial strain is a sensitive measure of regional and global LV contractile function (Mor-Avi et al., 2011). Recognising abnormal strain allows the early detection of subtle LV dysfunction which precedes decreases in ejection fraction in conditions such as dilated cardiomyopathy (DCM) (Poterucha et al., 2012, Hankiewicz et al., 2008). Early identification of myocardial dysfunction is important for clinical risk stratification, prompt initiation of treatment and guides therapeutic decision-making (Donal et al., 2012). We recently used dynamic tissue-tagging cardiac MRI to identify improvements in longitudinal strain parameters following treatment with spironolactone in patients with early-stage chronic kidney disease (Edwards et al., 2010).

Myocardial tagging by cardiac MRI has been widely accepted as the reference standard non-invasive imaging technique for quantifying strain after validation against sonomicrometry in dogs (Yeon et al., 2001) and non-homogenous strain phantoms (Young et al., 1993). Most MR tagging techniques create a visible pattern of magnetisation saturation in a grid or with parallel lines on the magnitude reconstructed images which are then analysed, e.g. spatial modulation of magnetization (SPAMM), or by extracting information about myocardial tags in k-space, e.g. harmonic phase (HARP) (Young et al., 2012b). All tagging pulse sequences have at least one disadvantage which may include tag fading, low signal to noise ratio, long

acquisition times requiring prolonged breath-holds, limited availability of validated post-processing software and protracted retrospective analysis. Moreover, each tagging technique requires the acquisition of additional sequences to those which are routinely performed, a factor limiting clinical applicability.

Cardiac magnetic resonance feature-tracking analysis offers a fast and practical method to calculate strain from routinely acquired SSFP cine images without the need to perform additional tagged sequences (Hor et al., 2011). In a large study of boys with Duchenne muscular dystrophy, CMR-FT was proposed as an accurate method for measuring strain in a comparison with HARP although quantification was limited to average circumferential systolic strain in the mid-LV short axis slice (Hor et al., 2010). Despite recent reports addressing inter-study (Morton et al., 2012), and inter and intra-observer variability for CMR-FT (Schuster et al., 2011b, Schuster et al., 2011a), there has been no attempt to validate this technique for diastolic SR calculation against a reference standard myocardial tagging analysis (Harrild et al., 2012). Furthermore, according to one previous study the CMR-FT framework cannot yet be reliably extended to assess long axis function (Augustine et al., 2013). Therefore, the aim of the current study was to compare CMR-FT with SPAMM tissue tagging for the computation of longitudinal and circumferential systolic *and* diastolic strain measures in a group of healthy adult controls and patients with DCM.

4.2. Methods

This study was approved by the West Midlands Research Ethics Committee and carried out in accordance with the principles of the Declaration of Helsinki. All patients provided informed written consent.

4.2.1. Study Population

Control subjects. Normal healthy adults were prospectively identified from CRIB-Donor, a study which aimed to examine the effects of living kidney donation on cardiovascular structure and function (Chapter 5). The current UK exclusion criteria for living kidney donation are given in Table 5-2. Prior to nephrectomy, all potential kidney donors that underwent normal baseline cardiac MR studies from March 2011 to June 2012 were included as healthy controls. Control subjects also had normal 12-lead electrocardiography, stress echocardiography and routine haematology and biochemistry profiles.

DCM subjects. Patients with DCM were prospectively identified as part of a detailed pathophysiological study assessing the effects of myocardial fibrosis on cardiac mechanics (REC: 12/WM/0157). The diagnosis of idiopathic DCM was made on the basis of LV dilatation and systolic dysfunction in the absence of valvular heart disease, congenital heart disease and ischaemic heart disease sufficient to cause ventricular impairment, following gadolinium contrast-enhanced cardiac MRI (Assomull et al., 2006), and normal coronary angiography.

4.2.2. Imaging Protocol

Cardiac MRI studies were conducted using a 1.5-T scanner (Magnetom Verio, Siemens, Erlangen, Germany). The time taken to acquire images for each patient was recorded. All cardiac magnetic resonance images were acquired by me with the assistance of Dr. Colin Chue, Dr. Richard Steeds, Dr. Nicola Edwards and Dr. Robin Taylor.

Steady State Free Precession Cine Imaging. Vertical long axis (VLA) and horizontal long axis (HLA) SSFP cine imaging of the left and right ventricles was performed and these images were used to pilot the LV short axis stack as described in section 2.1 (Maceira et al., 2006).

Myocardial tagging. As described in Section 2.1.2, three short axis tagged images at the LV base (mitral valve), middle (papillary muscle) and apex, as well as a HLA image were acquired using prospective electrocardiographic gating. Tagging was performed prior to the administration of gadolinium.

4.2.3. Myocardial Strain and Strain Rate Analysis

A timed off-line analysis was performed on tagged and SSFP images at identical slice positions by two independent blinded observers (R.J.T and W.E.M.; 4 and 5 years' experience, respectively). Both tagged and SSFP slices were reviewed by an independent expert (R.P.S; 13 years' experience) and only high quality MR studies were included for analysis.

CIMTag dynamic tissue-tagging. Tagged images were analyzed with CIMTag2D software (Cardiac Image Modelling, University of Auckland, Auckland, NZ). An overview of the generalized analysis framework is depicted in Figure 1. The model geometry was initialized in the first frame (end-diastole) using guide-point modelling (Young et al., 2000). Briefly, guide points placed by the user on the endocardial and epicardial border of the LV in the end-diastolic frame were fitted by the model using linear least squares optimization, resulting in an initial segmentation of the LV with minimal user interaction (Figure 4-1a). The reference model was then automatically warped to fit the tissue displacement map given by the SPAMM images. The tissue displacement map was given from a nonrigid registration tracking procedure as previously described (Young et al., 2012b, Li et al., 2008, Li et al., 2010). Points were tracked from frame to frame using the incremental displacement maps. A texture map of model stripes was overlaid on the display to provide a graphical representation of the tracking result (Figure 4-1b). The initial tag locations, spacing and orientation were automatically determined by interrogating the location of the harmonic peaks in the k-space data. The user corrected any tracking errors by placing guide points on the texture map overlay, thereby interactively warping the model to provide a best fit between image tags and model stripes (Figure 4-1c). The HLA image sequence was used to determine LV longitudinal strain and SR. Left ventricular circumferential strain and SR were measured from the 3 short axis views. Whole wall global peak systolic strain and SR values were obtained and subdivided according to wall thickness into respective thirds: subepicardium, midwall and subendocardium.

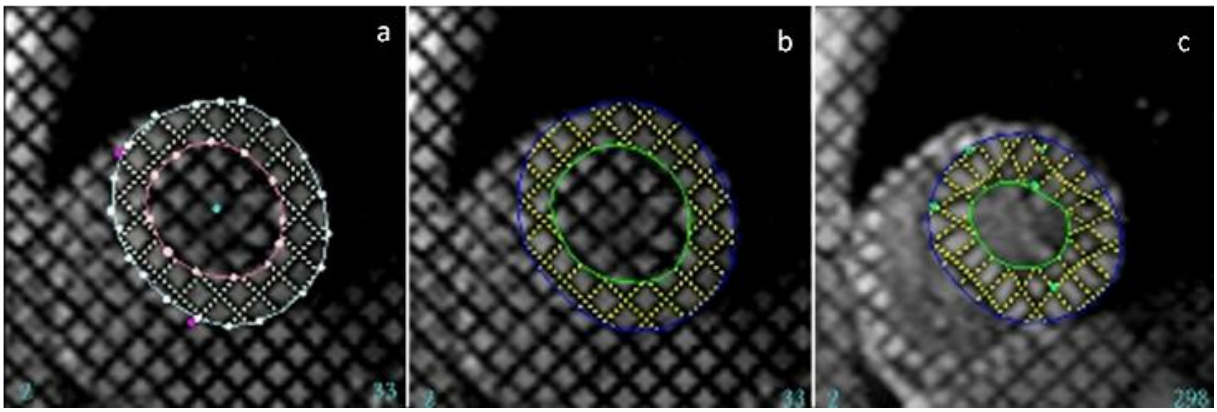

Figure 4-1. Overview of the Generalized CIMTag2D Analysis Framework.

a) Guide points placed by the user on the endocardial and epicardial border of the LV in the first frame (end-diastole) were fitted by the model using linear least squares optimization, resulting in an initial segmentation of the LV with minimal user interaction and subsequent initialization of the finite element model in the first frame of the SPAMM sequence.

b) Visual depiction of the tissue displacement map provided by non-rigid registration image tracking process at end-diastole.

c) User corrected texture map overlay as seen after placing guide points in end-systole, thereby interactively warping the model to provide a best fit between image tags and model stripes.

CMR-FT analysis. Diogenes CMR-FT software (TomTec Imaging Systems, Munich, Germany), a vector-based analysis tool, was used to perform subendocardial strain analysis in the corresponding SSFP images (Figure 4-2). Endocardial borders were drawn manually in the end-diastolic frame for each image. The CMR-FT software automatically propagated the contour and followed its features (brightness gradient at the tissue-cavity interface, dishomogeneties of the tissue, spatial coherence) throughout the remainder of the cardiac cycle. Global measures of subendocardial longitudinal strain were derived from the HLA view. Global subendocardial circumferential strain parameters were derived from the three short axis views. As for tagging analysis, global diastolic SR signals were recorded during early filling. CMR-FT segmental strain parameters were not extracted for comparison with tagging because a series of reports demonstrate high intra- and inter-observer variability for regional data (Kempny et al., 2012, Morton et al., 2012, Schuster et al., 2011a, Schuster et al., 2011b).

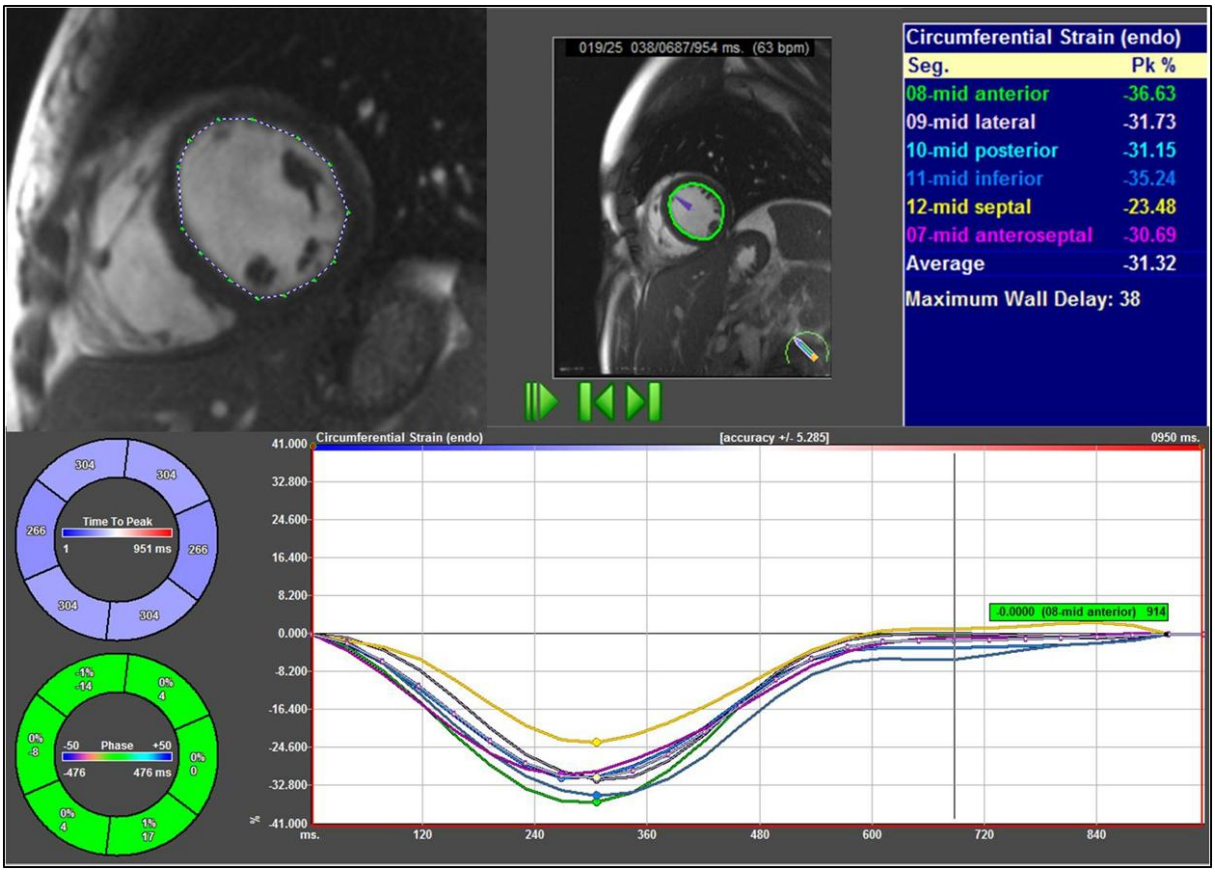

Figure 4-2. Acquisition of Circumferential Strain with FT Software in a Normal Subject.

The endocardial contour of a midventricular SSFP image is drawn manually. The first segment is always set in the anterior septum for consistency.

4.2.4. Left Ventricular Function, Volumes, Mass and Wall Thickness

Analysis of LV function, volume and LV mass was performed offline (Argus Software, Siemens, Erlangen, Germany) as described in Section 2.1.1. Left ventricular wall thickness was also measured in the short axis in each of the six segments of the mid LV according to the AHA standardized model, and at the identical slice position from which mid LV circumferential strain parameters were derived.

4.2.5. Statistical Analysis

Data are presented as mean ± standard deviation, median (interquartile range) or frequency (percentage). Data distribution for continuous variables was assessed using normality plots and the Kolmogorov-Smirnov test. Non-parametric data were log-transformed prior to analysis to achieve normality. Individual strain and SR values obtained using the two different methods were compared using the Bland-Altman technique and Pearson's correlation. A Spearman's rank correlation of the differences with the means of parameters derived from FT and CIMTag was performed. The mean strain parameters derived from the two techniques were compared using paired *t* tests if normally distributed. Continuous variables from controls and DCM patients were compared using independent *t* tests. An ANOVA with repeated measures with a Greenhouse-Geisser correction was used to compare differences in tagging derived strain parameters across the 3 myocardial layers. Statistical analysis was performed using SPSS v21. A type I error rate <5% ($p<0.05$) was considered statistically significant.

4.2.6. Variability of CIMTag2D and CMR-FT Strain Measurements

Inter-observer and intra-observer variability assessments were performed using a paired *t* test and reported as a bias (mean difference) and standard deviation (SD). The coefficient of variability, defined as the SD of the differences divided by their mean, and the ICC for absolute agreement were also calculated (Grothues et al., 2002).

4.3. Results

4.3.1. Study Population

A total of 45 subjects were identified (35 controls, 10 DCM); age was 44 ± 14 years. Baseline characteristics are shown in Table 4-1. Compared with healthy controls, DCM patients were older (58 ± 14 vs. 41 ± 12 years, $p<0.01$) and had higher body weight (87 ± 17 vs. 77 ± 11 kg, $p<0.01$). No other demographic data were significantly different.

All participants completed the full imaging protocol. Two controls were however, excluded from the imaging analysis because of poor tagging imaging quality due to breathing artefacts (n = 1) and electrocardiogram gating issues (n=1); these participants were therefore only included in volumetric and LV mass assessments. All SSFP images were of excellent image quality and compatible with CMR-FT software.

Table 4-1. Baseline Characteristics of the Study Population.

Baseline characteristics	Controls (n= 35)	DCM (n= 10)	Overall (n=45)
Age (years)	41 ± 12	58 ± 14*	44 ± 14
Male gender (%)	26 (62)	6 (60)	32 (63)
Ethnicity			
Caucasian (%)	36 (90)	8 (80)	45 (88)
Asian (%)	3 (8)	1 (10)	4 (8)
Afro-Caribbean (%)	1 (2)	1 (10)	2 (4)
Weight (kg)	77 ± 11	87 ± 17*	79 ± 13
Heart rate (bpm)	66 ± 10	70 ± 10	67 ± 10
Systolic blood pressure (mmHg)	120 ± 11	112 ± 14**	119 ± 12
Diastolic blood pressure (mmHg)	72 ± 6	72 ± 11	72 ± 7
Left ventricular ejection fraction (%)	71 ± 6	33 ± 15†	69 (64 – 74)‡
End-diastolic volume (mL)	124 ± 25	205 ± 51†	137 ± 43
End-systolic volume (mL)	37 ± 13	140 ± 60†	39 (30 – 59)
Stroke volume (mL)	87 ± 14	64 ± 21†	84 ± 17
Left ventricular mass (g)	122 ± 27	161 ± 21	123 (106 – 141)
Left ventricular mass index (g/m^2)	64 ± 11	82 ± 20	64 (59 – 73)
Late gadolinium enhancement result	-	All negative	-

Data are mean ± standard deviation, frequency (percentage) or median (interquartile range). DCM, dilated cardiomyopathy. *p<0.01; **p<0.05; †p<0.001 (compared with controls using an independent two-tailed Student's *t* test). ‡ Range of left ventricular ejection fraction for overall cohort was 19-79%.

4.3.2. Myocardial Strain and Strain Rate Analysis

A detailed summary of the statistical comparison of FT versus tagging for all global strain and SR parameters is presented in Table 4-2.

Global longitudinal strain (E_{II}). Tagged imaging revealed a transmural longitudinal strain gradient; there was a progressive increase in longitudinal deformation from the subepicardium through the midwall and into the subendocardium ($p<0.001$; Figure 4-3). In an analysis of all subjects, CMR-FT peak systolic global longitudinal strain (E_{II}) correlated most strongly with CIMTag E_{II} values derived from tagging of the subendocardium ($r=0.70$, $p<0.001$; Figure 4-4a). A Bland Altman plot (Figure 4-4b) demonstrates agreement but with a small systematic overestimation from CMR-FT (-18.1 ± 5.0% vs. -16.7 ± 4.8%, bias 1.3 ± 3.8%, $p=0.03$). Whilst in DCM patients mean peak global E_{II} values were not significantly different between the two techniques (-9.7 ± 4.5% vs. -8.8 ± 3.9%, $p=0.44$), among healthy controls there was a small but significant difference in E_{II} values derived from CMR-FT versus tagged imaging (-19.5 ± 3.5% vs. -18.0 ± 3.5%, $p=0.04$; Figure 4-5).

Table 4-2. Comparison of CMR-FT versus Tagging Derived Global Strain and Strain Rate Parameters for the Overall Cohort, in Healthy Controls and in Dilated Cardiomyopathy Subjects.

HEALTHY CONTROLS (n=35)	**Feature Tracking**	**Tagging whole Wall**	**Tagging sub-epicardium**	**Tagging mid wall**	**Tagging sub-endocardium**
Long axis function (HLA)					
Peak systolic longitudinal E					
Mean value ± SD (%)	-19.5 ± 3.5	-18.0 ± 3.5	-15.9 ± 3.0	-17.7 ± 3.2	-18.0 ± 3.5
p-value*	-	0.01	<0.001	0.002	0.04
Pearson's correlation coefficient	-	0.29	0.25	0.27	0.35
p-value**	-	0.09	0.15	0.11	0.04
Bias ± SD (%)	-	2.51 ± 4.0	3.6 ± 4.0	3.6 ± 4.0	1.42 ± 4.0
Peak systolic longitudinal SR					
Mean value ± SD (1/s)	-1.12 ± 0.22	-0.95 ± 0.24	-0.90 ± 0.23	-0.97 ± 0.24	-1.03 ± 0.26
p-value*	-	0.001	<0.001	0.002	0.07
Pearson's correlation coefficient	-	0.27	0.27	0.27	0.31
p-value**	-	0.12	0.12	0.11	0.06
Bias ± SD (1/s)	-	0.17 ± 0.28	0.22 ± 0.27	0.16 ± 0.28	0.09 ± 0.28
Early diastolic longitudinal SR					
Mean value ± SD (1/s)	1.19 ± 3.5	0.69 ± 0.30	0.67 ± 0.30	0.70 ± 0.30	0.72 ± 0.30
p-value*	-	<0.001	<0.001	<0.001	<0.001
Pearson's correlation coefficient	-	0.20	0.22	0.19	0.19
p-value**	-	0.25	0.20	0.27	0.27
Bias ± SD (1/s)	-	-0.50 ± 0.40	-0.51 ± 0.40	-0.49 ± 0.40	-0.47 ± 0.40
Short axis function (mid LV)					
Peak systolic circumferential E					
Mean value ± SD (%)	-24.8 ± 2.9	-18.6 ± 2.5	-12.9 ± 2.0	-18.3 ± 2.6	-24.9 ± 3.0
p-value*	-	<0.001	<0.001	<0.001	0.90
Pearson's correlation coefficient	-	0.15	0.02	0.10	0.26
p-value**	-	0.39	0.92	0.55	0.13
Bias ± SD (%)	-	6.2 ± 3.5	11.9 ± 3.5	6.6 ± 3.7	-0.08 ± 4.0
Peak systolic circumferential SR					
Mean value ± SD (1/s)	-1.48 ± 0.27	-1.01 ± 0.18	-0.72 ± 0.13	-0.98 ± 0.18	-1.34 ± 0.31
p-value*	-	<0.001	<0.001	<0.001	0.02
Pearson's correlation coefficient	-	0.22	0.01	0.18	0.28
p-value**	-	0.21	0.99	0.31	0.09
Bias ± SD (1/s)	-	0.48 ± 0.29	0.76 ± 0.30	0.50 ± 0.30	0.14 ± 0.06
Early diastolic circumferential SR					
Mean value ± SD (1/s)	1.34 ± 0.32	0.79 ± 0.16	0.48 ± 0.11	0.76 ± 0.16	1.15 ± 0.24
p-value*	-	<0.001	<0.001	<0.001	0.001
Pearson's correlation coefficient	-	0.53	0.44	0.52	0.45
p-value**	-	0.001	<0.01	0.001	<0.01
Bias ± SD (1/s)	-	-0.55 ± 0.27	-0.85 ± 0.29	-0.58 ± 0.28	-0.19 ± 0.30
DILATED CARDIOMYOPATHY (n=10)					
Long axis function (HLA)					
Peak systolic longitudinal E					
Mean value ± SD (%)	-9.7 ± 4.7	-8.2 ± 3.5	-7.6 ± 3.0	-8.3 ± 3.6	-8.8 ± 3.9
p-value*	-	0.26	0.16	0.30	0.44

Pearson's correlation coefficient	-	0.77	0.73	0.75	0.80
p-value**	-	0.08	0.10	0.09	0.05
Bias ± SD (%)	-	1.5 ± 2.9	2.1 ± 3.1	1.4 ± 3.0	0.9 ± 2.7
Peak systolic longitudinal SR					
Mean value ± SD (1/s)	-0.56 ± 0.19	-0.45 ± 0.19	-0.46 ± 0.15	-0.46 ± 0.19	-0.47 ± 0.23
p-value*	-	0.04	0.16	0.05	0.08
Pearson's correlation coefficient	-	0.88	0.65	0.87	0.91
p-value**	-	0.02	0.16	0.03	0.01
Bias ± SD (1/s)	-	0.11 ± 0.10	0.10 ± 0.15	0.10 ± 0.10	0.09 ± 0.10
Early diastolic longitudinal SR					
Mean value ± SD (1/s)	0.49 ± 0.20	0.31 ± 0.22	0.28 ± 0.18	0.31 ± 0.23	0.35 ± 0.26
p-value*	-	0.07	0.05	0.07	0.17
Pearson's correlation coefficient	-	0.57	0.45	0.59	0.60
p-value**	-	0.24	0.38	0.22	0.21
Bias ± SD (1/s)	-	-0.19 ± 0.20	-0.22 ± 0.20	-0.19 ± 0.19	-0.14 ± 0.22
Short axis function (mid LV)					
Peak systolic circumferential E					
Mean value ± SD (%)	-9.6 ± 4.8	-7.2 ± 2.4	-6.3 ± 1.8	-7.2 ± 2.2	-8.1 ± 1.9
p-value*	-	0.15	0.07	0.15	0.36
Pearson's correlation coefficient	-	0.70	0.76	0.73	0.61
p-value**	-	0.12	0.08	0.10	0.20
Bias ± SD (%)	-	2.5 ± 3.5	3.3 ± 3.6	2.4 ± 3.5	1.6 ± 3.8
Peak systolic circumferential SR					
Mean value ± SD (1/s)	-0.57 ± 0.23	-0.41 ± 0.10	-0.36 ± 0.09	-0.40 ± 0.10	-0.50 ± 0.23
p-value*	-	0.06	0.04	0.05	0.37
Pearson's correlation coefficient	-	0.80	0.67	0.82	0.73
p-value**	-	0.06	0.14	<0.05	0.10
Bias ± SD (1/s)	-	0.16 ± 0.17	0.20 ± 0.19	0.17 ± 0.16	0.07 ± 0.17
Early diastolic circumferential SR					
Mean value ± SD (1/s)	0.48 ± 0.26	0.46 ± 0.20	0.30 ± 0.13	0.44 ± 0.20	0.63 ± 0.26
p-value*	-	0.89	0.23	0.79	0.41
Pearson's correlation coefficient	-	0.18	0.20	0.20	0.20
p-value**	-	0.73	0.71	0.71	0.71
Bias ± SD (1/s)	-	-0.03 ± 0.36	-0.18 ± 0.32	-0.04 ± 0.36	0.15 ± 0.41

E, Lagrangian strain; HLA, horizontal long axis; LV,left ventricle; SD, standard deviation; SR, strain rate

*Feature tracking derived means compared with tagging measurements using a paired Student's *t* test. **Using Pearson's *r*, correlation coefficient.

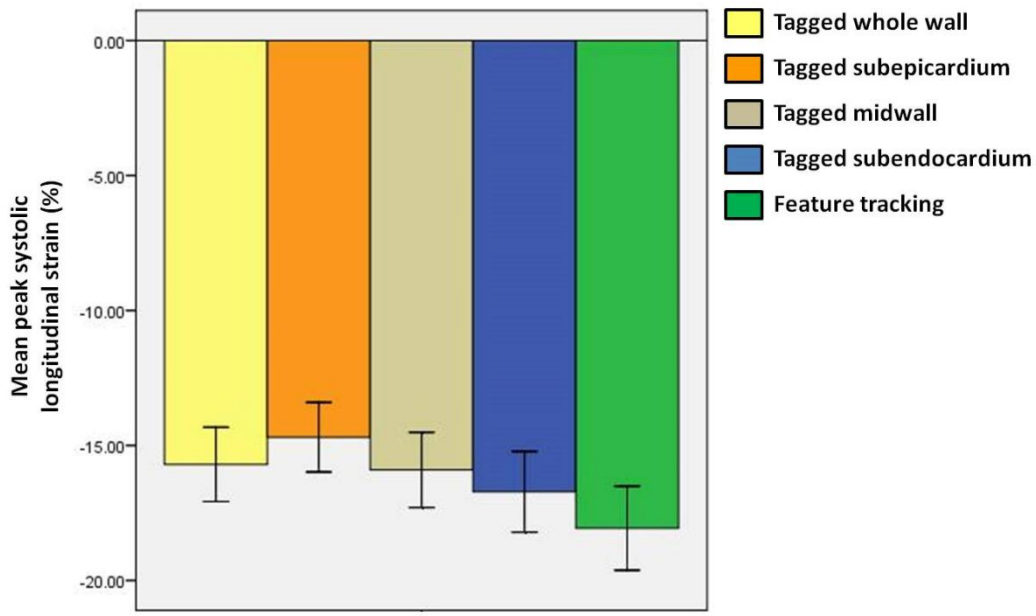

Figure 4-3. Global Longitudinal Strain Measures Calculated From CMR-FT and a Targeted Tagging Analysis Across the Three Layers of the Myocardium.

When using an ANOVA with repeated measures with a Greenhouse-Geisser correction, the mean scores for peak systolic global longitudinal strain across the 3 layers of the myocardium were statistically different ($F(1.2, 49.9)=54.8$, $P<0.001$).

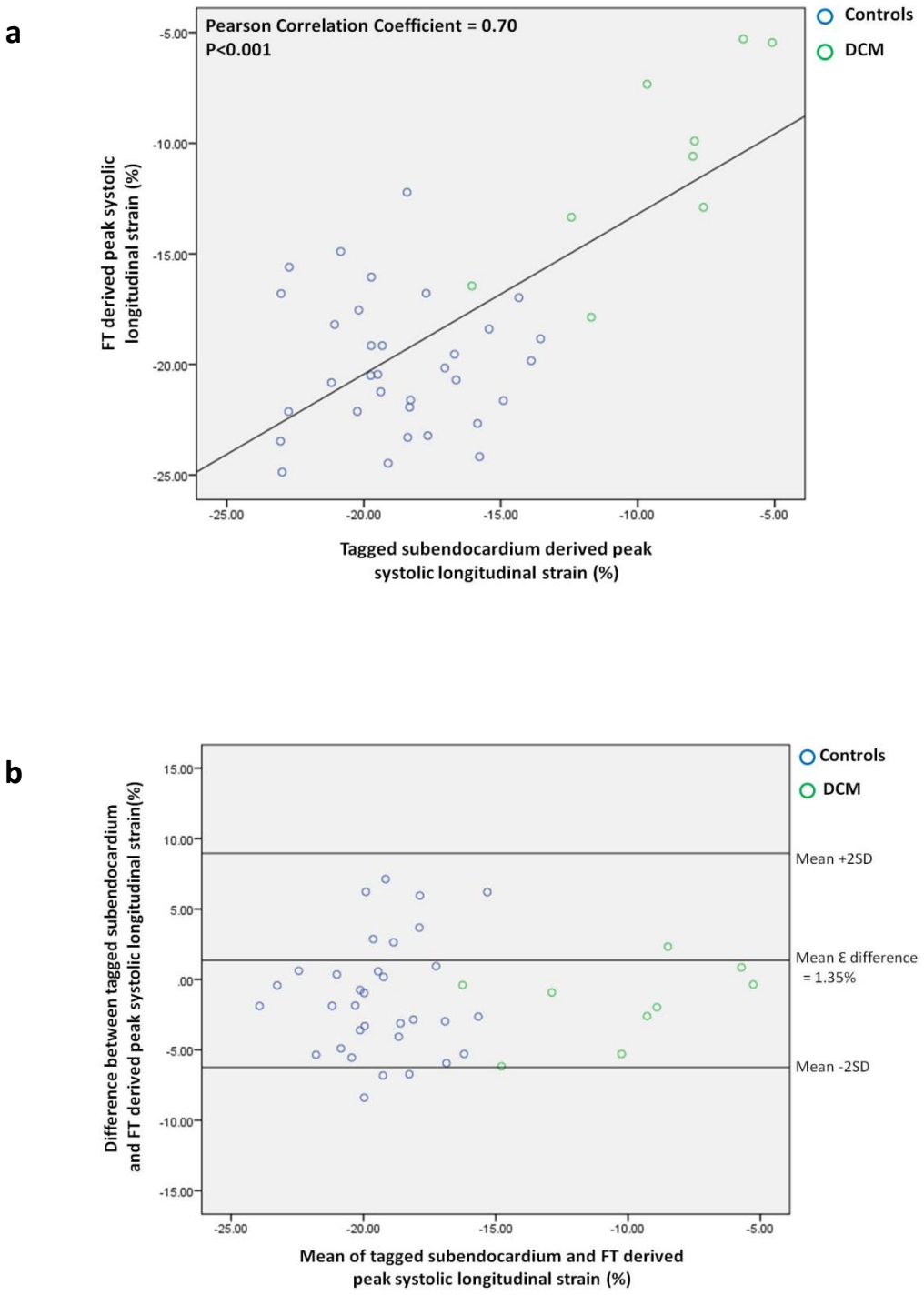

Figure 4-4. (a) Pearson Correlation and (b) Bland Altman Plots Demonstrating Agreement for Peak Systolic Global Longitudinal Strain Calculation Using CMR-FT versus Tagging.

Spearman's rank correlation of the differences and the means was non-significant (ρ=0.078, P=0.625).

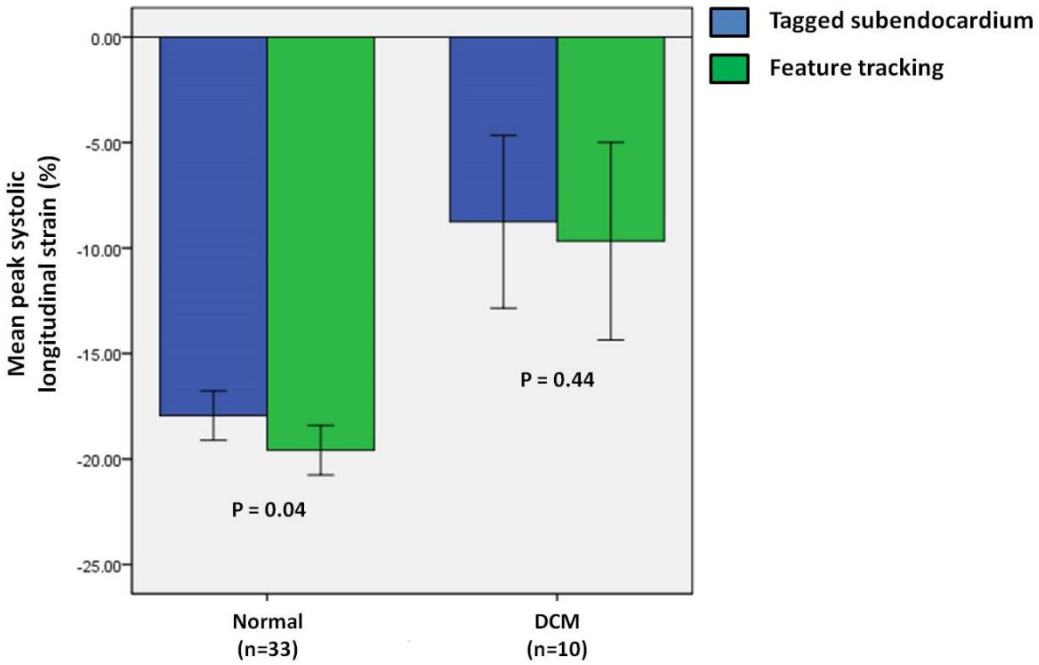

Figure 4-5. Comparison of CIMTag versus CMR-FT Derived Peak Systolic Global Longitudinal Strain Between Control and DCM subjects.

Longitudinal strain rate. The subendocardial layer also had the highest values for peak systolic longitudinal SR derived from tagging (Table 4-2). Among all participants, FT-peak systolic global longitudinal SR correlated with corresponding CIMTag derived measurements from the subendocardium (r=0.64, p<0.001; Figure 4-6a). There was agreement between the two techniques for peak systolic global longitudinal SR values with a small tendency towards higher values from CMR-FT compared with tagging (-1.04 ± 0.29 1/s vs. -0.95 ± 0.32 1/s, bias 0.09 ± 0.26 1/s, p=0.04; Figure 4-6b). Although the correlation remained significant (r=0.42, p=0.007), the weakest agreement between the two techniques was for early diastolic global longitudinal SR (1.10 ± 0.40 1/s vs. 0.67 ± 0.32 1/s, bias -0.42 ± 0.40 1/s, p<0.001; Figure 4-7).

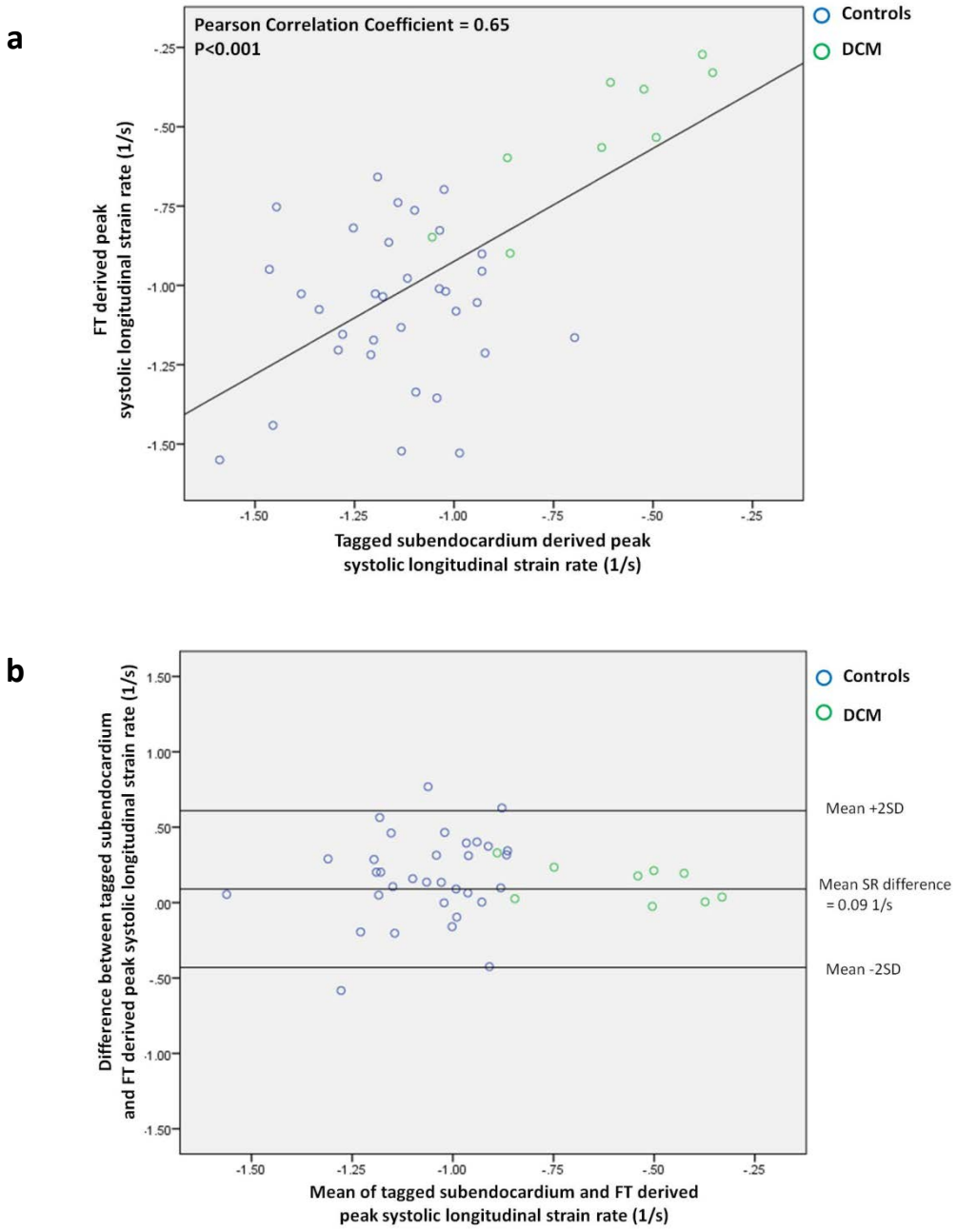

Figure 4-6. (a) Pearson Correlation and (b) Bland Altman Plots Demonstrating Agreement for Peak Systolic Global Longitudinal Strain Rate Calculation Using CMR-FT versus Tagging.

Spearman's rank correlation of the differences and the means was non-significant (ρ=0.196, P=0.213).

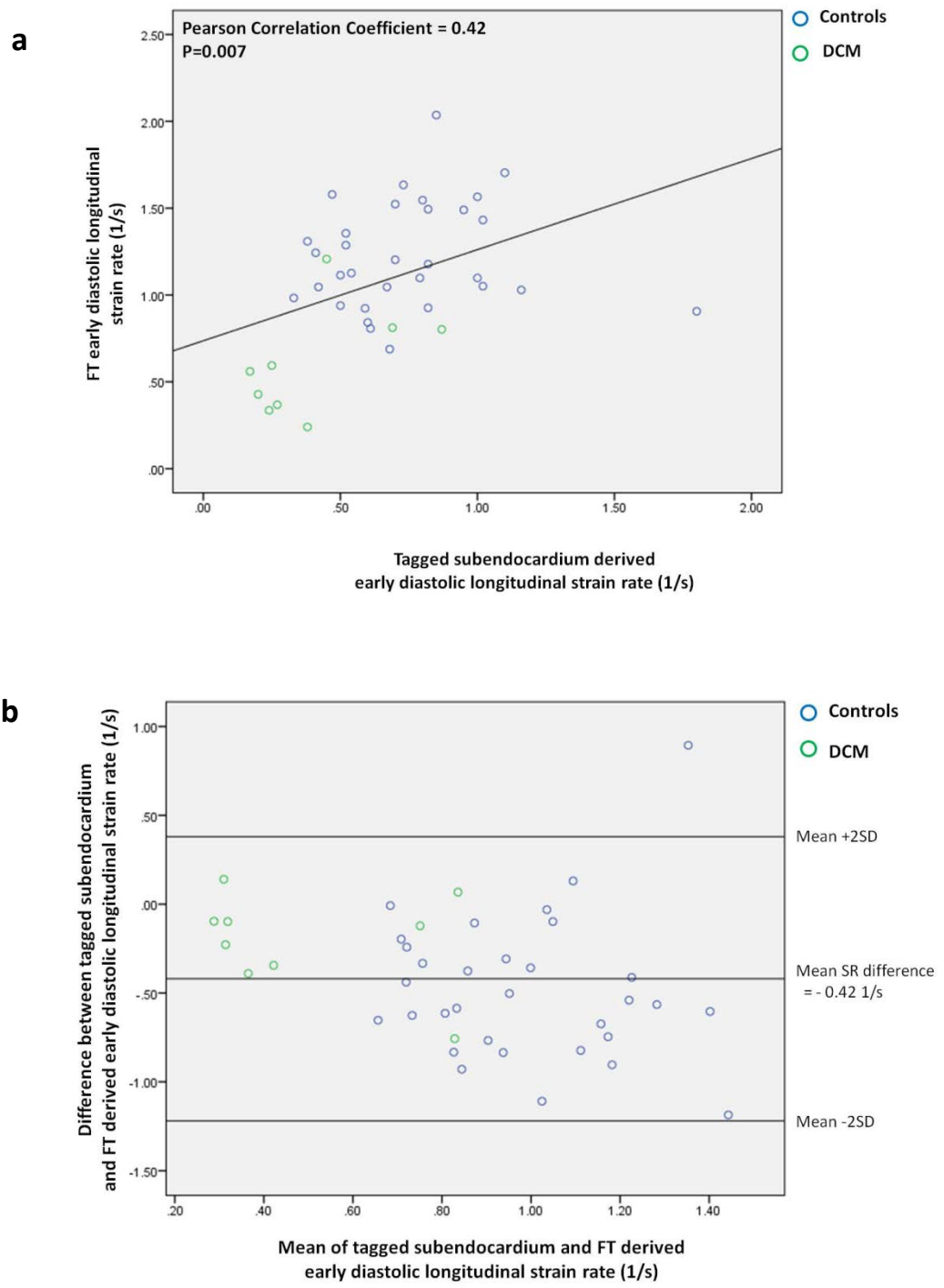

Figure 4-7. (a) Pearson Correlation and (b) Bland Altman Plots Demonstrating Agreement for Early Diastolic Global Longitudinal Strain Rate Calculation Using CMR-FT versus Tagging.

Spearman's rank correlation of the differences and the means was significant (ρ=-0.329, P=0.036) suggesting a proportional error with a downward trend.

Circumferential strain (E_{cc}). Across all subjects, CMR-FT derived peak systolic global circumferential strain measurements at the mid LV slice were not significantly different from those calculated via tagging (Figure 4-8). As with the long axis analysis, FT-E_{cc} values correlated most strongly with CIMTag-E_{cc} values derived from the subendocardium (r=0.83, p<0.001; Figure 4-9 and Figure 4-10a). A Bland-Altman plot shows close agreement between the two techniques across the entire cohort with neither systemic overestimation nor underestimation and a bias of only 0.2 ± 4.0% (-22.7 ± 6.2% vs. -22.5 ± 6.9%, p=0.80; Figure 4-10b).

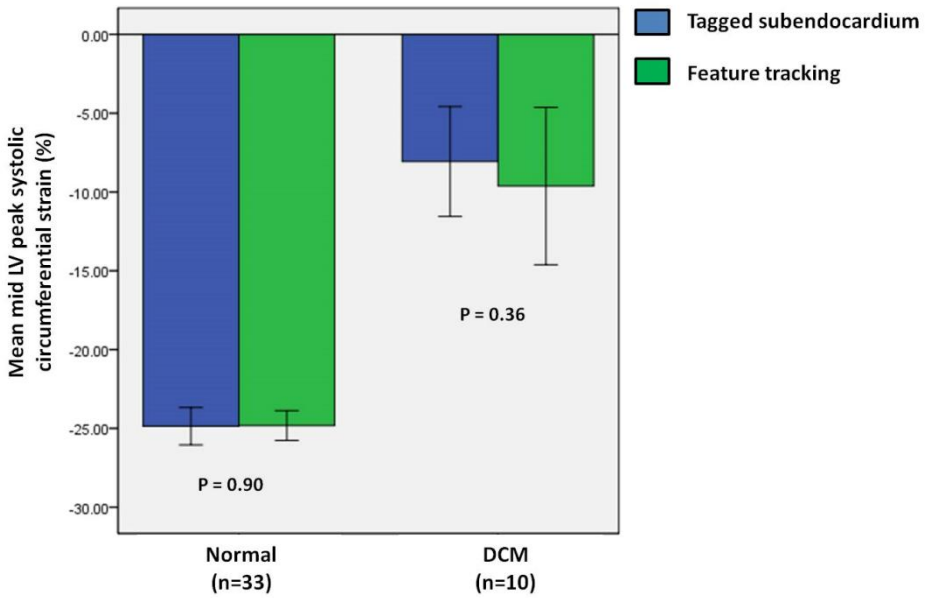

Figure 4-8. Comparison of CIMTag versus CMR-FT Derived Peak Systolic Global Circumferential Strain between Control and DCM Subjects.

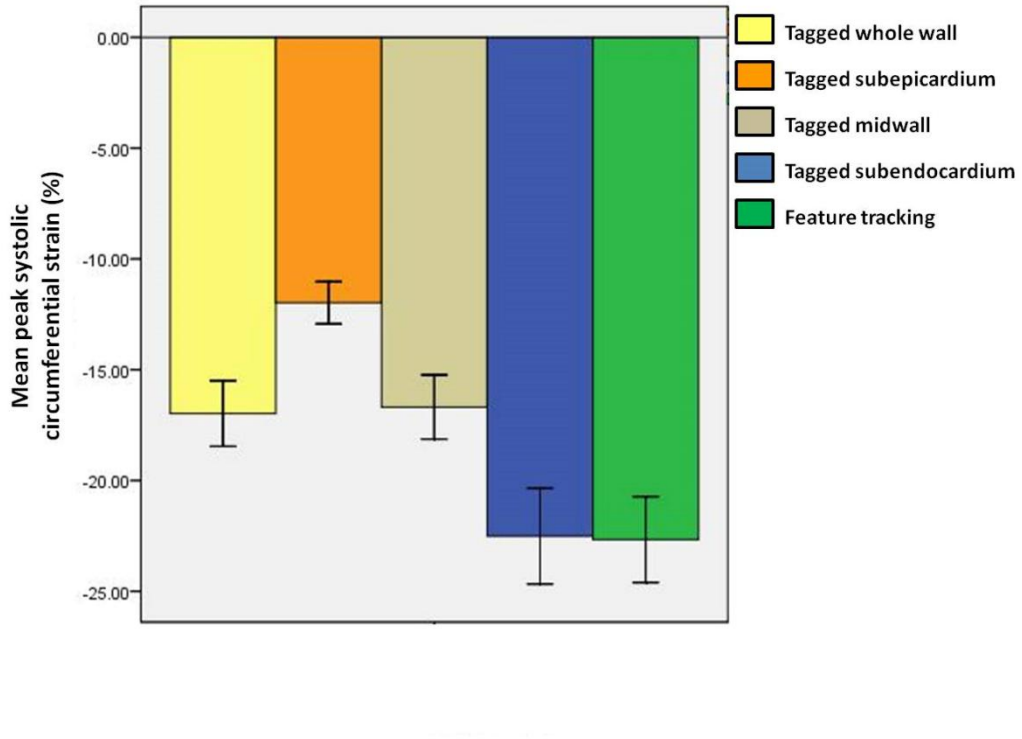

Figure 4-9. Global Circumferential Strain Measures Calculated from CMR-FT and a Targeted Tagging Analysis Across the Three Layers of the Myocardium.

Using an ANOVA with repeated measures with a Greenhouse-Geisser correction, the mean scores for peak systolic global circumferential strain across the myocardium were statistically different ($F(1.0, 41.8)=218.4$, $P<0.001$).

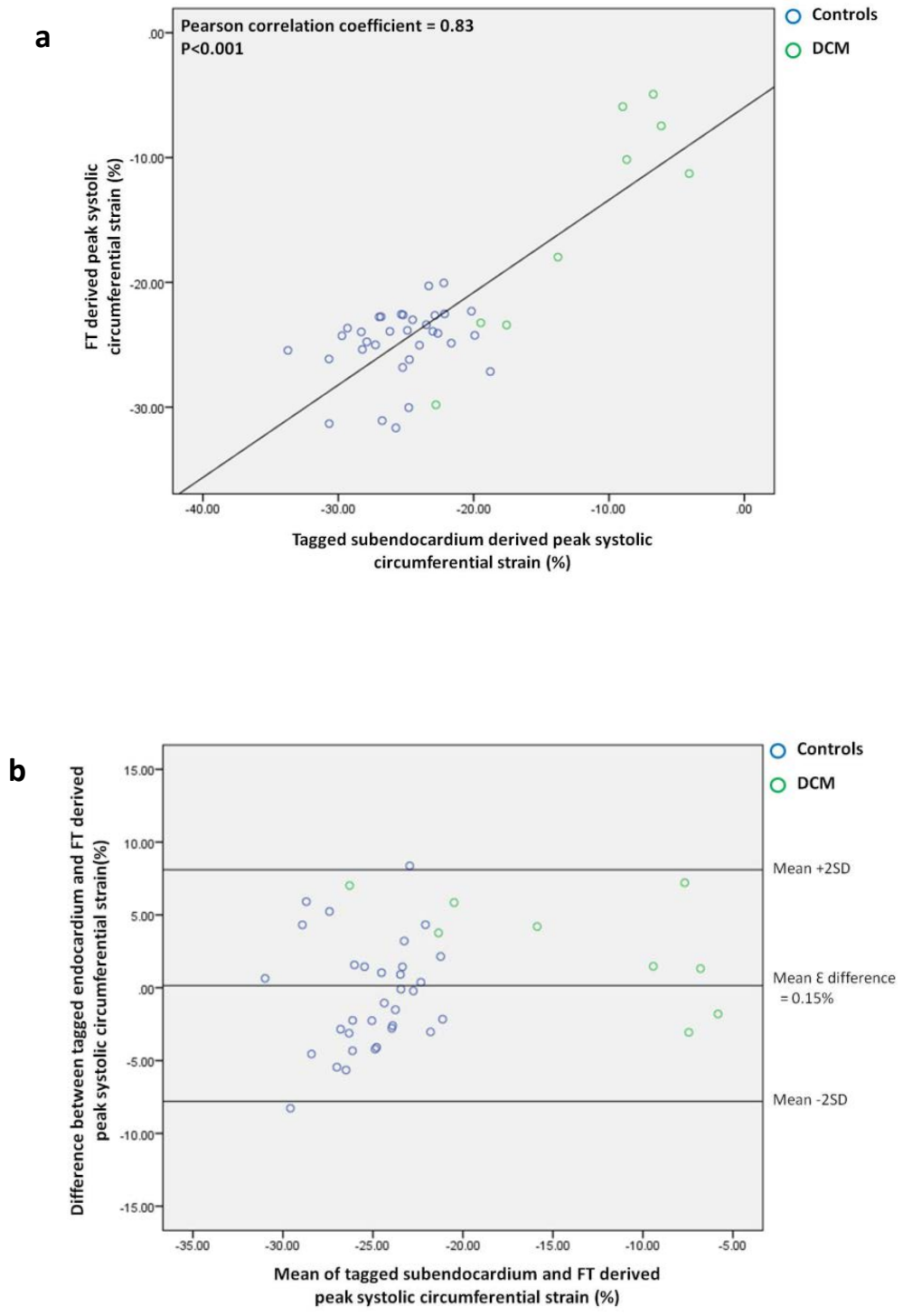

Figure 4-10. (a) Pearson Correlation and (b) Bland Altman Plots Demonstrating Agreement for Peak Systolic Global Circumferential Strain Calculation Using CMR-FT versus Tagging.

Spearman's rank correlation of the differences and the means was non-significant (ρ=0.292, P=0.06).

Measures of circumferential strain from the mid LV slice showed better agreement between CMR-FT and CIMTag compared with measures derived from the LV base and apex (Table 4-3). Tagged imaging also showed a graded increase in circumferential shortening from the base towards the apex.

Circumferential strain rate. Among all participants, FT-peak systolic global circumferential SR correlated closely with corresponding CIMTag derived measurements from the subendocardium (r=0.69, p<0.001; Figure 4-11a). As for longitudinal SR, Bland-Altman analysis also showed agreement between the two techniques for calculation of peak systolic global circumferential SR (-1.35 ± 0.42 1/s vs. -1.22 ± 0.42 1/s, bias 0.13 ± 0.33 1/s; Figure 4-11). FT-early diastolic global circumferential SR also correlated with tagging derived values from the subendocardium (r=0.64, p<0.001; Figure 4-12a) and showed satisfactory agreement (1.21 ± 0.44 vs. 1.07 ± 0.30, bias -0.14 ± 0.34 1/s; Figure 4-12b).

Influence of wall thickness. There was no significant difference between the mid LV ventricular wall thickness of DCM patients and healthy controls (7.2 ± 1.1 mm vs. 7.3 ± 1.0 mm, p=0.7). The limits of agreement for calculation of peak systolic circumferential strain in patients with DCM versus healthy controls were comparable (-7.76 to 7.92 % vs. -5.85 to 9.05 %). For calculation of peak systolic circumferential strain across the overall cohort, there was no association between ventricular wall thickness and the size of the bias relative to its mean value (r = -0.15, p=0.33).

Table 4-3. Comparison of CMR-FT versus Tagging Derived Global Circumferential Strain in the Short Axis at the Apex and Base for the Overall Cohort.

	Feature tracking	**Tagging whole wall**	**Tagging sub epicardium**	**Tagging mid wall**	**Tagging sub endocardium**
Short axis function (base)					
Peak systolic circumferential E					
Mean value ± SD (%)	-23.9 ± 6.4	-12.8 ± 4.1	-9.6 ± 2.8	-12.6 ± 4.0	-16.7 ± 5.9
p-value*	-	<0.001	<0.001	<0.001	<0.001
Pearson's *r*	-	0.63	0.52	0.64	0.63
p-value**	-	<0.001	<0.001	<0.001	<0.001
Bias ± SD (%)	-	11.1 ± 5.0	14.4 ± 5.5	11.3 ± 4.9	7.3 ± 5.3
Short axis function (apex)					
Peak systolic circumferential E					
Mean value ± SD (%)	-26.2 ± 9.2	-18.5 ± 4.7	-12.7 ± 3.3	-18.2 ± 4.6	-24.9 ± 7.0
p-value*	-	<0.001	<0.001	<0.001	0.27
Pearson's *r*	-	0.56	0.39	0.56	0.59
p-value**	-	<0.001	0.01	<0.001	<0.001
Bias ± SD (%)	-	7.7 ± 7.6	13.5 ± 8.5	7.9 ± 7.6	1.3 ± 7.6

E, Lagrangian strain; SD, standard deviation.

*FT derived means compared with tagging measurements using a paired Student's *t* test.

**Using Pearson's *r*, correlation coefficient.

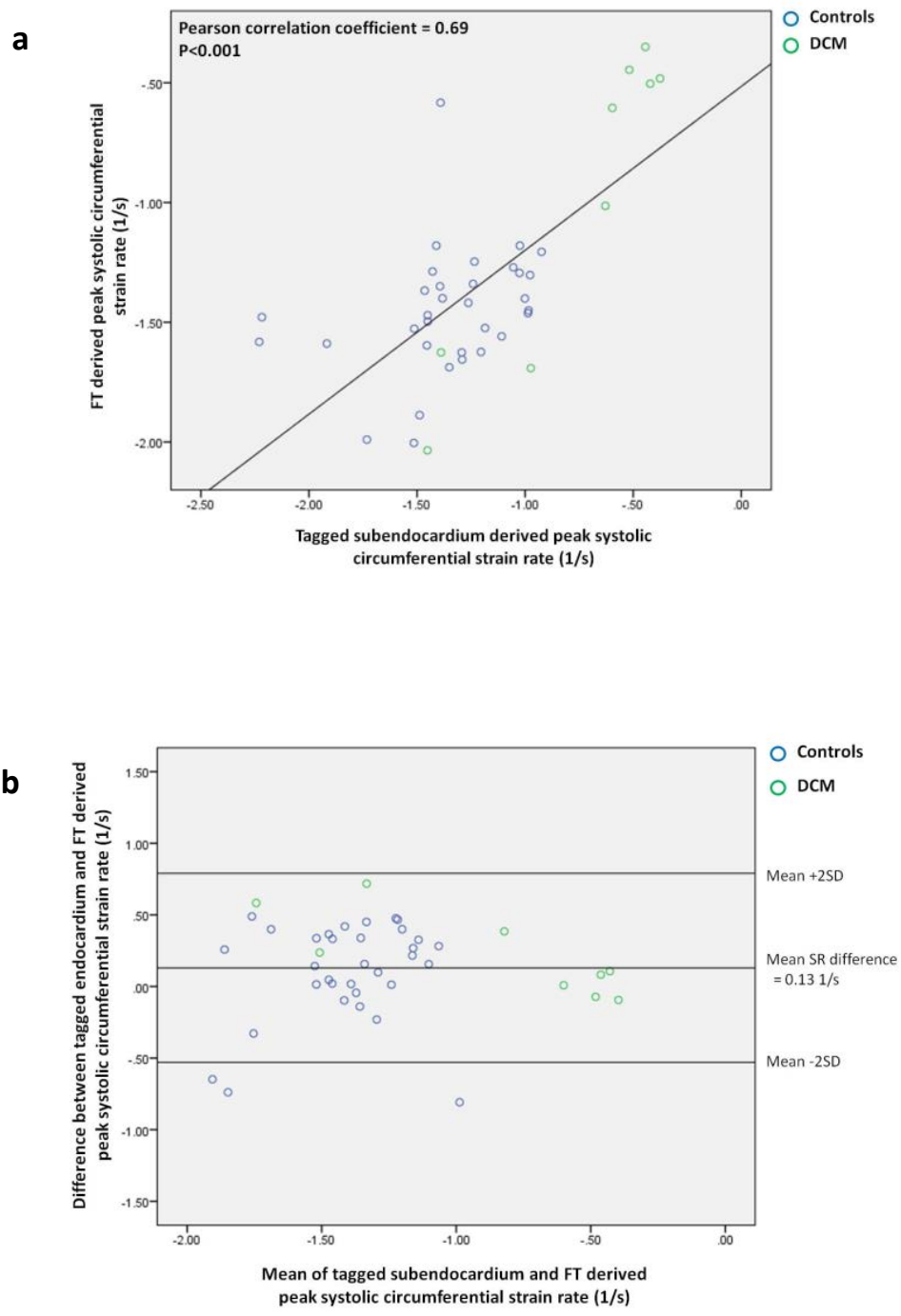

Figure 4-11. (a) Pearson Correlation and (b) Bland Altman Plots Demonstrating Agreement for Peak Systolic Global Circumferential Strain Rate Calculation Using CMR-FT versus Tagging.

Spearman's rank correlation of the differences and the means was non-significant (ρ=-0.034, P=0.833).

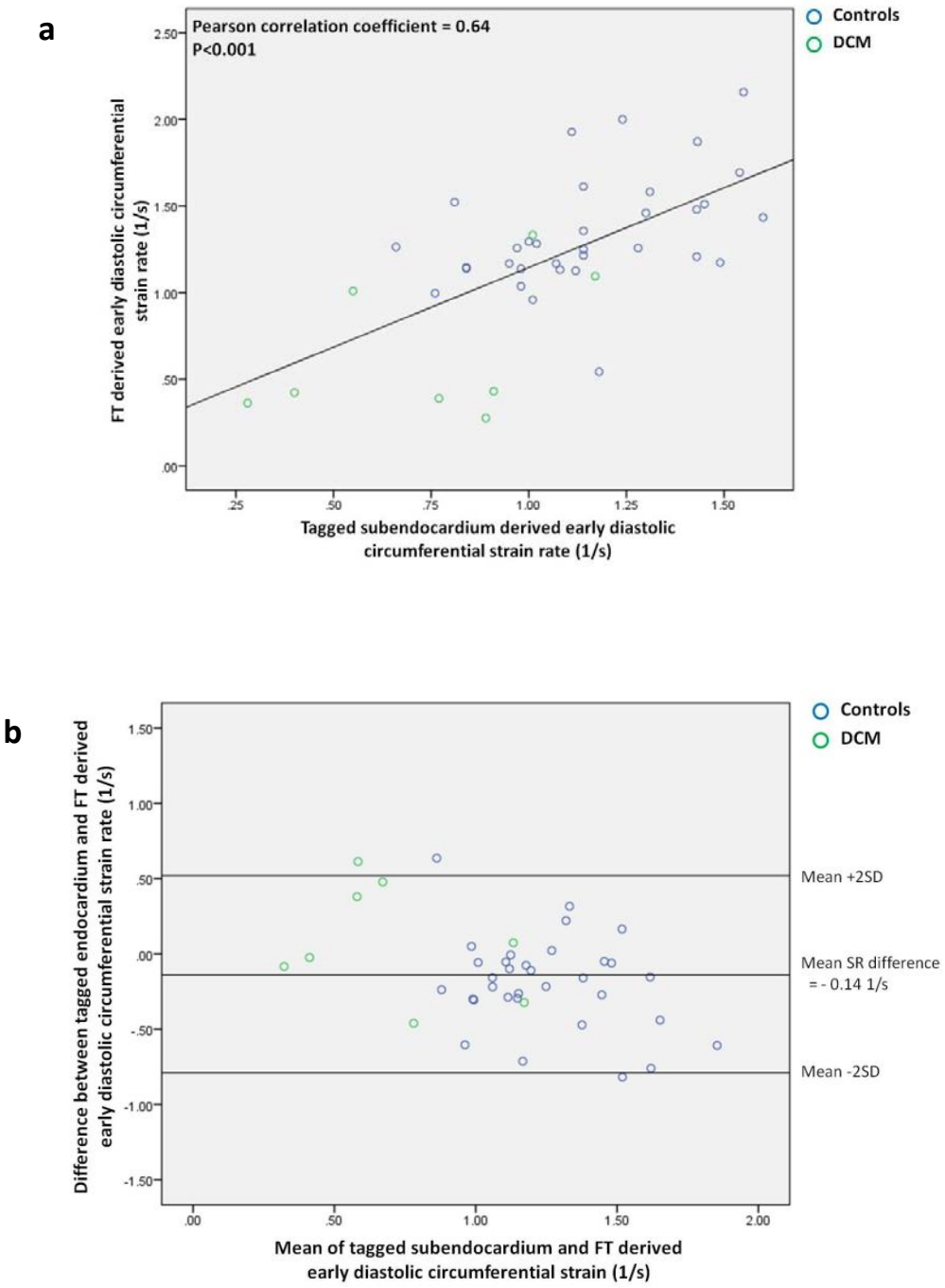

Figure 4-12. (a) Pearson Correlation and (b) Bland Altman Plots Demonstrating Agreement for Early Diastolic Global Circumferential Strain Rate Calculation using CMR-FT versus Tagging.

Spearman's rank correlation of the differences and the means was significant (ρ=-0.315, P=0.045) suggesting a proportional error with a downwards trend.

Table 4-4 shows the large difference in post-processing time taken between the two techniques (5.9 ± 0.8 vs. 23.2 ± 3.5 min, p<0.001).

Table 4-4. Time Taken for Image Acquisition and Post-processing Analysis.

	Feature tracking	**Tagging**
SSFP acquisition time (min)	12.1 ± 3.4	12.1 ± 3.4
SPAMM acquisition time (min)	-	8.4 ± 2.3
Post-processing time (min)	5.9 ± 0.8*	23.2 ± 3.5

Data are mean ± SD. SSFP, steady-state free precession; SPAMM, spatial modulation of magnetization.

*p<0.001 (means compared using a paired Student's *t* test).

4.3.3. Interobserver and Intraobserver Variability for Strain and Strain Rate

Intraobserver and interobserver variability for CMR-FT analysis of peak systolic global longitudinal strain was small (bias -0.49 ± 1.83 % and 0.22 ± 1.13 %; respectively). The reproducibility of CMR-FT strain measurements compared favourably with CIMTag, particularly with respect to interobserver variability (Table 4-5 and Table 4-6).

Table 4-5. Intraobserver and Interobserver Variability for CMR-FT Derived Global Strain Parameters.

Parameter	Variability	Bias ± SD	p value	Limits of Agreement	Coefficient of Variation (%)	Intra-class Correlation Coefficient (95% CI)
E_{ll} (%)	Intraobserver	-0.49 ± 1.83	0.29	-4.08 to 3.11	7.68	0.88 (0.72 to 0.96)
	Interobserver	0.22 ± 1.13	0.42	-1.99 to 2.42	5.48	0.98 (0.94 to 0.99)
SSR_{ll} (1/s)	Intraobserver	0.02 ± 0.18	0.70	-0.34 to 0.38	17.89	0.89 (0.72 to 0.96)
	Interobserver	0.02 ± 0.16	0.61	-0.30 to 0.33	12.95	0.86 (0.67 to 0.95)
DSR_{ll} (1/s)	Intraobserver	0.05 ± 0.18	0.27	-0.30 to 0.40	14.84	0.85 (0.64 to 0.94)
	Interobserver	0.01 ± 0.28	0.90	-0.53 to 0.55	20.99	0.85 (0.63 to 0.94)
E_{cc} (%)	Intraobserver	-0.34 ± 0.87	0.09	-2.05 to 1.36	3.55	0.96 (0.90 to 0.99)
	Interobserver	0.63 ± 1.29	0.06	-1.90 to 3.16	4.95	0.93 (0.81 to 0.97)
SSR_{cc} (1/s)	Intraobserver	-0.02 ± 0.08	0.21	-0.18 to 0.13	5.36	0.96 (0.90 to 0.98)
	Interobserver	0.02 ± 0.11	0.56	-0.20 to 0.23	6.68	0.94 (0.84 to 0.98)
DSR_{cc} (1/s)	Intraobserver	0.00 ± 0.07	0.92	-0.13 to 0.13	5.29	0.97 (0.93 to 0.99)
	Interobserver	-0.01 ± 0.11	0.63	-0.24 to 0.21	7.82	0.96 (0.89 to 0.98)

E_{cc}, Peak systolic global circumferential strain; E_{ll}, Peak systolic global longitudinal strain; SSR_{cc}, Peak systolic global circumferential strain rate; SSR_{ll}, Peak systolic global longitudinal strain rate; DSR_{cc}, Early diastolic circumferential strain rate; DSR_{ll}, Early diastolic longitudinal strain rate.

Table 4-6. Intraobserver and Interobserver Variability for Myocardial Tagging Derived Global Strain Parameters.

Parameter	Variability	Bias ± SD	p value	Limits of Agreement	Coefficient of Variation (%)	Intra-class Correlation Coefficient (95% CI)
E_{ll} (%)	Intraobserver	-0.47 ± 0.62	0.04	-1.68 to 0.74	3.41	0.97 (0.83 to 0.99)
	Interobserver	-0.47 ± 2.02	0.49	-4.42 to 3.49	11.44	0.75 (0.29 to 0.93)
SSR_{ll} (1/s)	Intraobserver	0.00 ± 0.06	0.91	-0.11 to 0.11	6.64	1.00 (0.98 to 1.00)
	Interobserver	-0.01 ± 0.17	0.90	-0.33 to 0.32	17.27	0.60 (-0.04 to 0.89)
DSR_{ll} (1/s)	Intraobserver	0.05 ± 0.10	0.14	-0.14 to 0.24	14.15	0.89 (0.62 to 0.97)
	Interobserver	0.11 ± 0.20	0.12	-0.28 to 0.49	31.59	0.45 (-0.11 to 0.82)
E_{cc} (%)	Intraobserver	-0.39 ± 1.22	0.39	-2.79 to 2.09	4.79	0.92 (0.74 to 0.98)
	Interobserver	-0.53 ± 1.53	0.30	-3.54 to 2.48	6.01	0.86 (0.56 to 0.96)
SSR_{cc} (1/s)	Intraobserver	0.00 ± 0.06	0.92	-0.12 to 0.12	4.63	0.95 (0.82 to 0.99)
	Interobserver	-0.02 ± 0.18	0.71	-0.37 to 0.33	13.86	0.46 (-0.25 to 0.83)
DSR_{cc} (1/s)	Intraobserver	0.03 ± 0.08	0.25	-0.13 to 0.19	7.38	0.95 (0.81 to 0.99)
	Interobserver	0.09 ± 0.19	0.15	-0.27 to 0.46	16.75	0.78 (0.36 to 0.94)

E_{cc}, Peak systolic global circumferential strain; E_{ll}, Peak systolic global longitudinal strain; SSR_{cc}, Peak systolic global circumferential strain rate; SSR_{ll}, Peak systolic global longitudinal strain rate; DSR_{cc}, Early diastolic circumferential strain rate; DSR_{ll}, Early diastolic longitudinal strain rate.

4.4. Discussion

In this study, we have principally compared a SSFP FT-based algorithm against a reference standard tagged image analysis (SPAMM) for the assessment of Lagrangian strain and SR. This report builds upon recent validation work by including comparisons of 2D longitudinal and circumferential strain and SR during systole and diastole; only systolic strain parameters have previously been validated (Hor et al., 2010, Harrild et al., 2012, Augustine et al., 2013). We have compared the ability of the two techniques to accurately measure diastolic SR during early filling, a sensitive marker of LV diastolic dysfunction which is an important precursor of incident heart failure (Kane et al., 2011). On the basis of our analysis performed in the subendocardium and in the circumferential direction, CMR-FT could realistically be extended to the computation of early diastolic SR. From a technical viewpoint, the current study benefits from having performed all sequences on a 1.5T MR scanner; a previous validation utilised a mix of acquisitions from 1.5T and 3T MR scanners (Hor et al., 2010). The validation described herein was also undertaken on corresponding SSFP and tagging images acquired from identical slice positions, a method which has not always been adopted (Hor et al., 2010). Finally, by performing a timed analysis, this report highlights that CMR-FT can generate strain data over four-times more rapidly than myocardial tagging and this has obvious clinical implications.

Our results contrast with a recent report from Augustine *et al.* which demonstrated that CMR-FT measurements of longitudinally directed strain showed poor agreement with tagging (Augustine et al., 2013). There are a number of differences between the studies which could account for this discrepancy. In our analysis, strain parameters derived from CMR-FT versus tagging were compared for *all* patients entered into the study, which included healthy subjects as well as those with DCM; the validation by Augustine was more modest and included only 20 healthy volunteers out of a total of 145 subjects (13.8%). More importantly, Augustine *et al*. compared measurements of longitudinal strain derived from tagging across the whole myocardial wall with CMR-FT measures derived from the blood-tissue interface, which effectively select subendocardial deformation information. In order to perform a valid comparison between the two techniques, it is imperative to measure strain from the equivalent myocardial layer, namely the subendocardium. Indeed, the longitudinal myocardial fibres are principally located in the subendocardium (Geyer et al., 2010). For this reason, in our Bland-Altman analyses, we made the *a priori* decision to compare CMR-FT strain parameters with tagged subendocardial values, which likely explains the improved agreement between the two techniques reported in the current study.

Results of the two methods for calculation of subendocardial strain measures are correlated and, with the exception of early diastolic longitudinal SR, Bland-Altman assessments displayed good agreement, although there are small differences in the measurements between techniques. Some of the variability in CIMTag strain

measurements may relate to the requirement to manually contour both endocardial and epicardial borders, together with the need to make a visual assessment of the tissue displacement map before making corrections to provide a best fit between image tags and model stripes. In contrast, only endocardial contours were constructed in the CMR-FT platform in this study, after which the process was fully automated without an option to modify tracking. These differences may account for CIMTag measurements having poorer inter-observer variability as compared with CMR-FT as well as tagging post-processing taking considerably longer. Another potential disadvantage of SPAMM tagging, which may also contribute to increased variability in strain outputs, is the potential for image quality to be affected by changes in heart rate. Furthermore, measurement of strain throughout the cardiac cycle to include diastolic parameters is not always achievable with 1.5T MRI scanners because of loss of tags caused by T1 relaxation (Edvardsen et al., 2006). CMR-FT offers a potentially more robust calculation of diastolic strain data because it relies on standard cine images whose spatial resolution is not adversely affected by T1 relaxation.

In general, the CMR-FT derived longitudinal strain and SR data were more variable than the circumferential data calculated from the short axis. This may be due to difficulty tracking at the blood-tissue interface and a tendency to track the mitral valve apparatus. In keeping with previous reports, circumferential strain showed the strongest agreement between the two techniques and was particularly robust for the mid-LV slice (Augustine et al., 2013, Hor et al., 2010). At the LV apex, however, less

muscle is available for creating the tag grid upon which the guide point modelling for CIMTag is based which may have led to increased variability. CMR-FT may lose some of its ability to track the features in each voxel at the tissue-cavity interface at the apex (where there is a potential for cavity obliteration in end-systole) which may also account for increased error. The variability in circumferential strain at the LV base could be explained by a relative increase in the through plane motion typically observed at this level. The extent to which this degree of variability in CMR-FT measurements might relate to clinical use requires further exploration. There is already evidence that regional assessment by CMR-FT may not be as robust as existing tagging modalities but the potential advantages in ease of acquisition and time for analysis suggest that this method of assessing global deformation could still be of clinical utility.

This study has confirmed a transmural strain gradient which exists across the myocardial wall (Moore et al., 2000); both longitudinal and circumferential strain values from tagging increased from subepicardial through to subendocardial layers. This likely explains the better agreement of CMR-FT with tagging values from the subendocardium. It also offers a potential explanation for the reduced sensitivity and slightly higher strain values derived from CMR-FT. The CMR-FT algorithm only tracked deformation at the endocardial border therefore potentially losing important trans-mural information captured in tag grids that span the entire thickness of the ventricular wall. Mechanistically, this is in keeping with the pathology of dilated cardiomyopathy, which is characterized by epicardial injury on *ex vivo* histopathology and demonstrable

in vivo with late post gadolinium imaging (Simonetti and Raman, 2010). In this study, ventricular wall thickness was not significantly different between DCM and controls. In DCM, the ventricles are dilated but often with normal ventricular wall thickness, imparting an appearance of thin ventricular walls (Maron et al., 2006). Nonetheless, in an analysis which included all study subjects, wall thickness did not appear to affect the agreement between strain measures calculated using CMR-FT and myocardial tagging.

By design, this study did not attempt to validate regional measures because of ongoing concerns over the reproducibility of CMR-FT segmental data. CMR-FT applies 2D B-mode tracking such that the motion components parallel to tissue boundaries responsible for segmental information are much more affected by noise compared to the perpendicular components from which global strain measures are derived. This relates to the gradients in backscatter amplitude being much higher between tissue and blood than within the myocardium.

A number of limitations to the current study deserve mention. There were a comparatively low number of subjects included with pathology; however this cohort enabled a validated assessment of the CMR-FT based technique over a broad range of LV function. Only subendocardial global measures of deformation could be measured on CMR-FT and a comprehensive assessment of SR during late diastolic filling was not possible because of constraints over temporal resolution and loss of tags. Assessment of myocardial deformation by strain and SR is sensitive to differences in sampling rate.

Even though considerable effort was made to ensure all tagging sequences were acquired with more than 15 phases (and many over 20 phases), there will almost inevitably be a difference in temporal resolution between a prospectively-gated sequence and retrospectively-gated sequence, specifically when confined by the resting heart rate and breath-holding of the patient. The issue of temporal resolution is such that whilst results may correlate, values recorded are unlikely to be the same – in a clinical situation, it would be important to compare results using the same method in any single patient. All scans were performed on a 1.5T scanner for consistency, although employing a 3T scanner may have resulted in improved tag persistence. Finally, differences in breath-hold requirements may have contributed to variability between acquisitions.

4.5. Conclusion

In a study population with a wide range of LV function, CMR-FT systolic and diastolic global circumferental strain measures and systolic global longitudinal strain measured at the subendocardium show satisfactory agreement with corresponding values from tagged imaging. The CMR-FT global algorithm is a reliable tool in the research arena and also offers the potential for clinical utility, because it can be performed without the need for additional imaging and lengthy post-processing.

5. CARDIOVASCULAR EFFECTS OF UNILATERAL NEPHRECTOMY IN HUMAN LIVING KIDNEY DONORS

5.1. Hypothesis

The CRIB (Chronic Renal Impairment in Birmingham) – Donor study was designed to test the hypothesis that compared to control subjects, the reduction in GFR in living kidney donors causes adverse structural and functional cardiovascular effects including LV remodelling coupled with increases in LV mass and increased aortic stiffness.

5.2. Methods

5.2.1. Study Design

The CRIB-Donor protocol has been reported previously in detail (Moody et al., 2014b). The study had a prospective, longitudinal, parallel group, blinded end point design comparing living kidney donors with similarly healthy controls, and was conducted between March 2011 and July 2014. The study was approved by the West Midlands Research Ethics Committee (Ref: 10/H1207/70), adhered to the principles set out by the Declaration of Helsinki, and was registered with the U.S. National Institutes of Health database (NCT01769924). The conduct and reporting of this study was guided by the STROBE (Strengthening the Reporting of Observational Studies in Epidemiology)

Statement (Von Elm et al., 2007). Written informed consent was obtained from all subjects.

5.2.2. Setting and Participants

Subjects were recruited from two University-hospital based UK transplant centres (Queen Elizabeth Hospital Birmingham and University Hospital Coventry and Warwickshire). The inclusion and exclusion criteria are listed in Table 5-1 and adhere to the UK living kidney donor guidelines compiled by the Joint Working Party of The British Transplantation Society and The Renal Association (British Transplantation Society / the Renal Association, 2005). Where possible, control patients were recruited from the same living donor clinics at which donors were identified, by identifying individuals who after screening were found to be fit for donation but did not proceed to surgery (e.g. because of arterial anatomy, immunological mismatch or recipient-related health issues). If they also fulfilled donor criteria, donor-related family members were also invited to participate in the study as healthy controls. The remainder of healthy controls were recruited following advertisement made at blood donation and community care facilities using the identical inclusion and exclusion criteria for donors. In order to provide a closely matched control population with equivalent baseline health status to the donor cohort, both donor and control subjects underwent identical screening tests.

Table 5-1. Study Inclusion and Exclusion Criteria.

Inclusion criteria
Age 18-80 yrs
Acceptable GFR by donor age prior to donation*
Exclusion criteria
Hypertensive end-organ damage, uncontrolled hypertension or the requirement for more than 2 anti-hypertensive medications
Significant proteinuria†
Left ventricular dysfunction
Diabetes mellitus
Atrial fibrillation
Any history of cardiovascular or pulmonary disease that would preclude kidney donation

Abbreviation: GFR, glomerular filtration rate

*Based on the anticipation of having an eGFR of >50ml/min/1.73m^2 aged 70 years.

†Urinary albumin – creatinine ratio >30 mg/mmol, protein – creatinine ratio >50 mg/mmol or 24-hour total protein >300 mg/day.

5.2.3. Study Protocol

A flow chart of the study protocol is presented in Figure 5-1. Investigations were performed in each participant at baseline (within 6 weeks prior to nephrectomy in donors), with subsequent follow-up studies performed at 6 and 12 months. Kidney donors underwent routine follow up by their local medical and surgical team with no alteration to normal care.

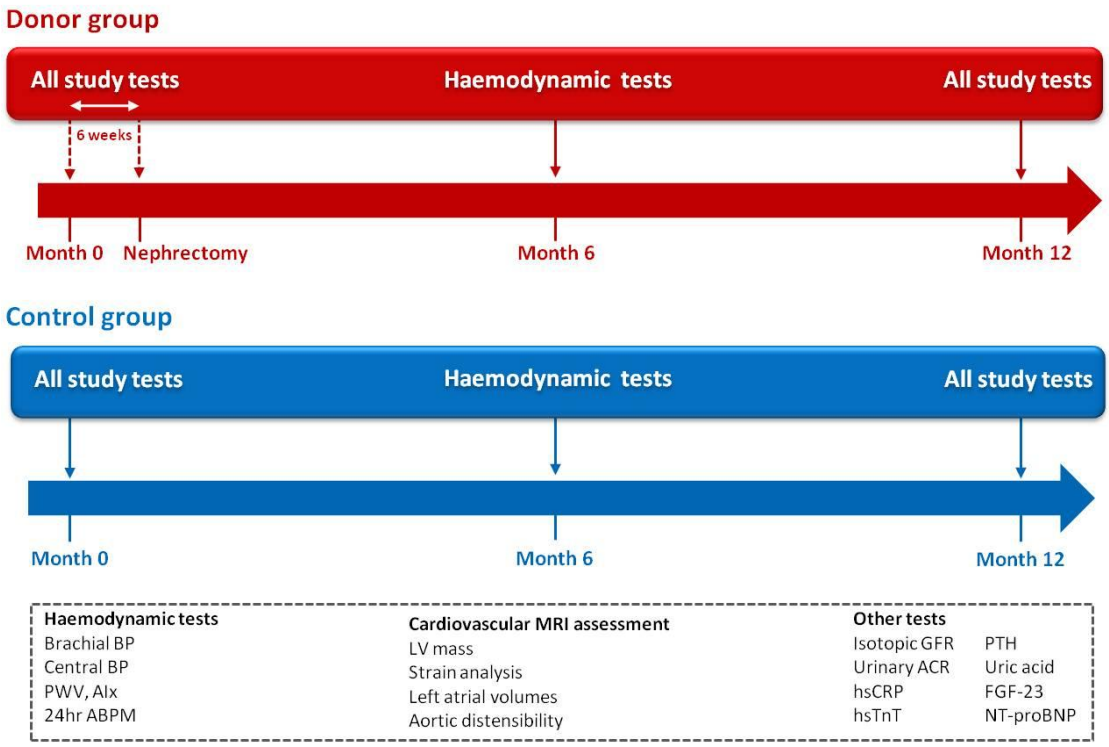

Figure 5-1. Study Protocol

Abbrevations: ACR, albumin – creatinine ratio; ABPM, ambulatory blood pressure monitor; AIx, augmentation index; BP, blood pressure; FGF-23, fibroblast growth factor-23; GFR, glomerular filtration rate; hsCRP, high sensitivity C-reactive protein; hsTnT, highly sensitive Troponin T; LV left ventricular; NT-proBNP, N-terminal pro B Natriuretic peptide; PTH; parathyroid hormone; PWV, aortic pulse wave velocity.

5.2.4. Subject Withdrawal.

Withdrawal criteria are listed in Table 5-2. In general, living kidney donors are a highly motivated population and it was therefore expected that the drop-out rate would be low.

Table 5-2. Study Withdrawal Criteria.

Withdrawal criteria
Pregnancy
Occurrence of any serious adverse or cardiovascular event which in the opinion of the investigators, warrants the subject's permanent withdrawal from the study
Repeated non-attendance to study visits
Subject decision to withdraw
Subject loss to follow up (loss of contact before final study visit)

5.2.5. Outcomes

The primary end point was change in LV mass at 12 months, as measured by cardiac MRI. Secondary end points were changes in (1) glomerular filtration rate by isotopic and creatinine based methods; (2) LV mass-volume ratio by cardiac MRI; (3) LV strain indices by MRI feature tracking; (4) brachial blood pressure, (5) central blood pressure, aortic PWV and AIx by SphygmoCor; (6) aortic distensibility by cardiac MRI; (7) T1 mapping derived ECV by cardiac MRI; (8) FMD of the brachial artery by MRI; (9) cIBS by transthoracic echocardiography; and (10) cardiac biomarkers including hsCRP, serum NT-proBNP, hs-cTnT and urinary ACR. Potential mediators of increased LV mass were also measured including renin; aldosterone; uric acid; and PTH. The rationale for selecting the above end points is given in Chapters 1 and 2.

5.2.6. Investigations

The techniques used to examine the above outcomes have already been described in detail in Chapter 2.

5.2.7. Monitoring and Safety Assessments

All adverse events, including SAEs, were recorded and followed up for the duration of the study or until resolution. Assessment of adverse events was performed by the study investigators. All SAEs were graded and reported to the sponsor. Any suspected unexpected serious adverse reactions were reported by the Chief Investigator within 15 days of the event to the sponsor, and National Research Ethics Committee (NRES), using the NRES SAE form for a non-Clinical Trial of an IMP.

5.2.8. Reproducibility

Reproducibility was determined using the same technique described in Chapter 3. Briefly, to assess intra-observer report variability of LV mass measurement, ten baseline studies were re-analyzed by the same observer 4 weeks later, blinded to the original data (W.E.M). A random subset of participants (n = 10) also underwent repeat imaging within 7 days to determine inter-study reproducibility; both scans were analyzed by the same observer blinded to temporal sequence and patient identity (W.E.M). Reliability

was assessed using the intra-class correlation coefficient (ICC) with a model of absolute agreement.

5.2.9. Sample Size Determination

Sample size calculation was based on the primary outcome of change in LV mass. In a previous intervention study in CKD, the standard deviation of change in LV mass was 12 g (Edwards et al., 2009). A sample size of 55 subjects per group provided 90% power to detect a change in LV mass of 7.5 g with an alpha value of 0.05. I therefore aimed to recruit 70 patients per group to allow for drop-outs.

5.2.10. Statistical Analysis

Statistical analysis was performed as described in Section 2.8. The primary analysis tested differences between groups over 12 months using repeated-measures ANOVA. A further quantitative analysis was performed using a last observation carried forward principle. Independent predictors of changes in LV mass and renal function were determined using multivariable logistic regression models. Generalised estimating equations were used to compare donors with controls for the likelihood of developing detectable serum and urinary biomarkers over 12 months.

5.3. Results

5.3.1. Recruitment

Recruitment for the study began in March 2011 and was completed in July 2013. During this period, a total of 216 subjects were screened (Figure 5-2). Of those, 40 were ineligible based on the inclusion and exclusion criteria, 32 declined, and 20 did not respond. In total, 124 subjects were recruited (68 donors, 54 controls). The decision to end recruitment before reaching our target number was based on cessation of research funding and the recruitment of adequate numbers to achieve the required power with respect to LV mass.

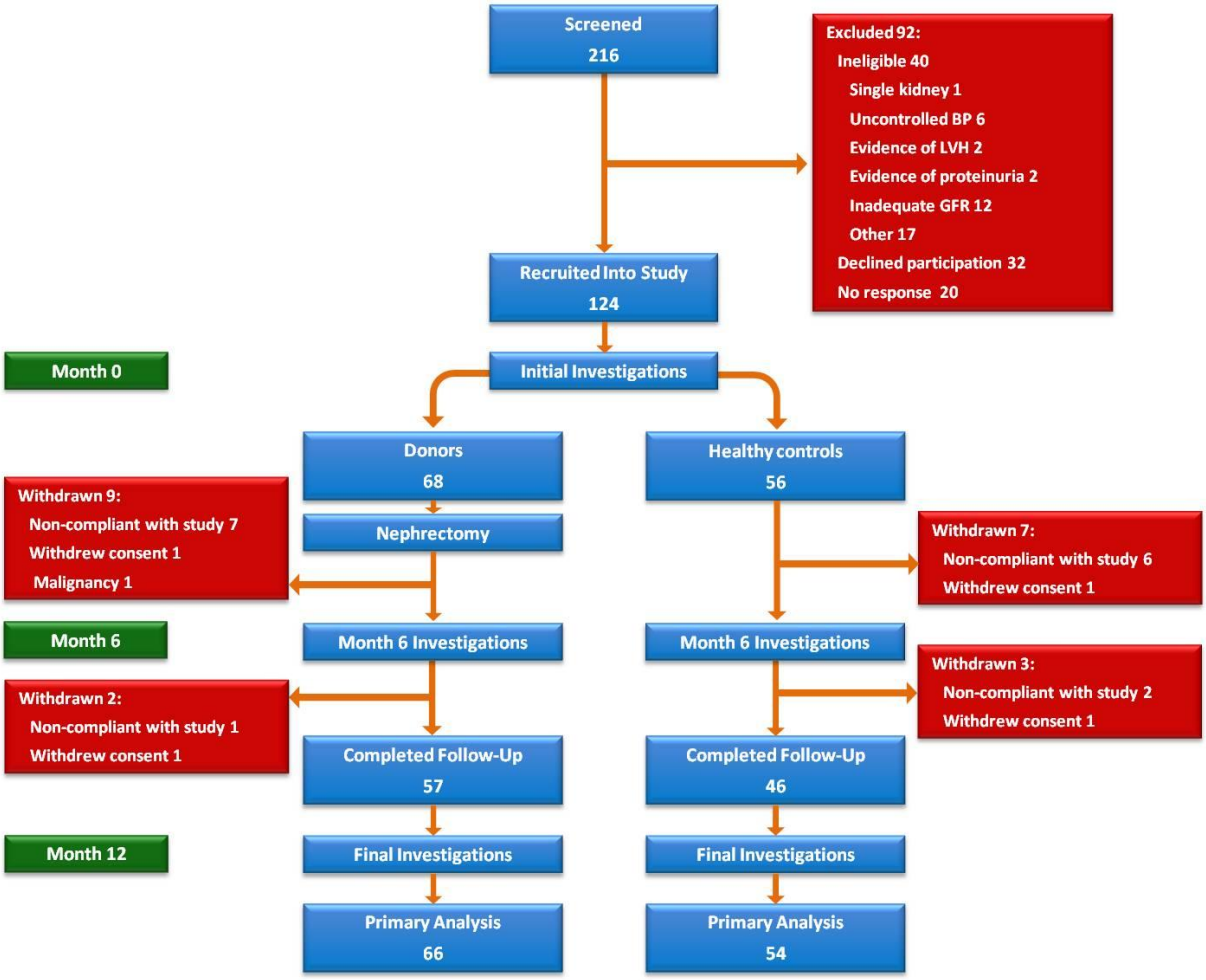

Figure 5-2. Study Timeline.

Abbreviations: BP, blood pressure; LVH, left ventricular hypertrophy; GFR, glomerular filtration rate.

5.3.2. Baseline Data

Baseline characteristics of the two study groups are shown in Table 5-3. There were no significant differences between groups with respect to age, sex, ethnicity, cardiovascular risk factors, medication and renal function. Seven subjects (6%) were on anti-hypertensive therapy at baseline. For all participants, blood pressure was <140/90 mmHg.

Table 5-3. Demographic and Clinical Characteristics at Baseline.

Variable	Donor (N = 68)	Controls (N = 56)	P Value
Demographics			
Age (yrs)	46.5 ± 12.1	44.1 ± 12.8	0.28
Male sex	23 (34)	27 (48)	0.14
Race or ethnic group			
White	62 (90)	47 (86)	0.27
Asian	5 (7)	5 (9)	0.75
Black	2 (3)	3 (6)	0.66
Body mass index (kg/m2)	26.8 ± 4.1	26.0 ± 3.6	0.22
Risk factors			
Hypertension	3 (5)	4 (7)	0.70
Diabetes	0 (0)	0 (0)	1.00
Current smoker	8 (12)	3 (5)	0.34
Ex-smoker	21 (30)	13 (24)	0.42
Family history of cardiovascular disease†	19 (28)	11 (20)	0.30
Medication			
Statin	2 (3)	4 (7)	0.41
Antihypertensive agent	3 (5)	4 (7)	0.70
ACE inhibitor or Angiotensin-receptor blocker	1 (2)	3 (5)	0.33
Beta-blocker	1 (2)	1 (2)	1.00
Calcium channel blocker	1 (2)	1 (2)	1.00
Levothyroxine	3 (5)	2 (4)	1.00
Non-steroidal anti-inflammatory agent	1 (2)	1 (2)	1.00

Haematology and Biochemistry			
Haemoglobin (g/dL)	13.7 ± 1.2	13.6 ± 1.2	0.66
Serum creatinine (μmol/L)	73 ± 14	72 ± 14	0.95
Estimated GFR_{Cr} (mL/min/1.73m^2)	88 ± 18	89 ± 19	0.72
Isotopic GFR (mL/min/1.73m^2)	93 ± 12	91 ± 14	0.64
Cholesterol (mmol/L)	5.2 ± 1.1	5.0 ± 1.1	0.33
Fasting glucose (mmol/L)	4.7 ± 0.5	4.7 ± 0.4	0.56

Data are presented as mean ± SD or number (%).

†Defined as a first degree relative with a history of myocardial infarction or ischaemic stroke aged younger than 55 years in men and younger than 65 years in women.

There were no significant differences between donor and control groups analyzed using independent samples Student's t or Fisher's exact tests. A two-tailed P value<0.05 was considered statistically significant.

5.3.3. Follow up and Events

Eleven donors did not complete follow up to 12 months (Figure 5-2); 2 declined continued participation because of the travelling involved and 8 could not be contacted. One subject was withdrawn after diagnosis of a malignancy, which was subsequently reported as a SAE. No subjects died or suffered a cardiovascular event during the study.

5.3.4. Change in Renal function and Biochemical Effects

The changes in biochemical indices and cardiac biomarkers are presented in Table 5-4. There was a mean decrease in iGFR in donors of −30 ± 12 ml/min/1.73m^2 with no change in controls (−1 ± 10 ml/min/1.73m^2; P < 0.001). At 12 months, over a third of donors (35%) had an iGFR <60 ml/min/1.73m^2 while more than half (53%) had an eGFR <60 ml/min/1.73m^2. Compared with controls, donors had significant increases in uric acid (+56 ± 35 μmol/L vs. +2 ± 33 μmol/L; P < 0.001); iPTH (+1.1 ± 1.6 pg/ml vs. +0.4 ± 1.3 pg/ml; P = 0.03) and hsCRP (+1.7 ± 5.3 mg/dl vs. −0.7 ± 5.2 mg/dl; P < 0.01). Donors also had significantly greater numbers with detectable hs-cTnT (odds ratio, 16.2 [95%CI, 2.6 – 100.1]; P < 0.01) and microalbuminuria (odds ratio, 3.74 [95%CI, 1.09 – 12.75]; P = 0.04). There were no significant changes in NT-proBNP or in circulating levels of renin and aldosterone.

Table 5-4. Haematological and Biochemical Effects of a Reduction in Renal Function.

Biomarker	**Donor (N = 57)**		**Control (N = 46)**		**P Value**
	Month 0	**Month 12**	**Month 0**	**Month 12**	
Haemoglobin (g/L)	137 ± 12	134 ± 11	136 ± 12	137 ± 13	0.06
Estimated GFR_{Cr} (mL/min/1.73m^2)	89 ± 19	59 ± 13	87 ± 17	86 ± 19	<0.001
Isotopic GFR (mL/min/1.73m^2)	92 ± 12	63 ± 9	90 ± 13	89 ± 12	<0.001
Urinary ACR ≥ 3.0 mg/mmol†	0%	7%	0%	0%	0.04
Serum hs-cTnT ≥ 5 ng/L†	0%	21%	9%	2%	<0.01
Serum NT-proBNP (pmol/L)‡	0.3 (0.3 – 7.7)	0.3 (0.3 – 18.9)	0.3 (0.3 – 16.0)	0.3 (0.3 – 4.0)	0.23
Serum hsCRP (mg/dL)‡	1.20 (0.40 – 2.28)	1.90 (0.70 – 3.25)	0.85 (0.40 – 1.83)	1.0 (0.58 – 1.68)	<0.01
Serum calcium (mmol/L)	2.31 ± 0.11	2.33 ± 0.08	2.30 ± 0.09	2.33 ± 0.09	0.70
Serum phosphate (mmol/L)	1.07 ± 0.18	1.05 ± 0.17	1.09 ± 0.17	1.13 ± 0.25	0.15
Serum intact parathyroid hormone (pg/mL)	4.5 ± 1.5	5.6 ± 1.7	4.2 ± 1.3	4.6 ± 1.5	0.03
25-hydroxyvitamin D (nmol/L)	50 ± 27	57 ± 32	52 ± 23	53 ± 21	0.20
Serum uric acid (µmol/L)	276 ± 74	332 ± 72	289 ± 55	291 ± 54	<0.001
Renin (ng/L) ‡	9.4 (7.1 – 13.2)	7.9 (5.1 – 11.4)	9.2 (7.1 – 14.3)	10.1 (6.8 – 15.1)	0.24

Aldosterone (pmol/L) ‡	129 (60 – 192)	120 (77 – 187)	111 (67 – 187)	189 (80 – 271)	0.22
Total cholesterol (mmol/L)	5.3 ± 1.1	5.3 ± 1.0	4.9 ± 1.1	4.9 ± 1.1	0.74
HDL cholesterol (mmol/L)‡	1.6 (1.3 – 1.8)	1.5 (1.3 – 1.9)	1.5 (1.3 – 1.8)	1.5 (1.3 – 1.9)	0.26
LDL cholesterol (mmol/L)	3.1 ± 1.0	3.2 ± 0.9	2.9 ± 0.9	2.8 ± 0.9	0.18
Glucose (mmol/L)	4.7 ± 0.5	4.9 ± 1.0	4.7 ± 0.4	4.8 ± 0.6	0.50

Data are presented as mean ± SD, or %. N is the number of subjects with available baseline and 12 month data. A repeated-measures ANOVA with time point (month 0 or 12) as the within-subjects factor and group (control or donor) as the between-subjects factor tested the difference in change over time between groups.

† Generalised estimating equations were used to compare donors with controls for the likelihood of developing detectable serum and urinary biomarkers between month 0 and 12.

‡ Data presented as median (interquartile range), log transformed prior to repeated-measures ANOVA analysis.

A two-tailed P value <0.05 was considered statistically significant.

Abbreviations: ACR, albumin – creatinine ratio; GFR, glomerular filtration rate; GFR_{Cr}, glomerular filtration rate according to the CKD-EPI equation; HDL, high-density lipoprotein; hsCRP; high sensitivity C-reactive protein; hs-cTnT, high sensitivity cardiac Troponin T; LDL, low-density lipoprotein; NT-proBNP, N-terminal pro B Natriuretic peptide

5.3.5. Effects on Ventricular Mass, Volumes and Function

A summary of the data on the effects of nephrectomy on cardiac structure and function is presented in Table 5-5. In donors but not controls, LV mass increased significantly (+7 ± 10 g vs. −3 ± 8 g; P < 0.001; Figure 5-3 and Figure 5-4). In donors compared with controls, there were analogous increases in the LV mass index (+3.5 ± 5.0 g/m^2 vs. -1.6 vs. 4.3 g/m^2; P < 0.001) and LV mass – volume ratio (+0.06 ± 0. 12 g/ml vs. −0.01 ± 0.09 g/ml; P < 0.01). Nephrectomy did not affect LV volumes or ejection fraction but was associated with a reduction in long axis function determined by septal AVPD compared to controls (−1 ± 2 mm vs. 0 ± 2 mm; P = 0.03). There were no effects of kidney donation on right ventricular volumes or function.

Table 5-5. Myocardial Effects of a Reduction in Renal Function by Cardiac MRI.

	Donor (N = 50)		Control (N =45)		
	Month 0	**Month 12**	**Month 0**	**Month 12**	**P Value**
LV mass (g)	114 ± 26	121 ± 29	117 ± 30	114 ± 29	<0.001
LV mass index by BSA (g/m^2)	61 ± 9	65 ± 11	63 ± 13	61 ± 11	<0.001
LV mass-to-volume ratio (g/ml)	0.94 ± 0.16	1.00 ± 0.19	0.91 ± 0.16	0.90 ± 0.14	<0.01
LV ejection fraction (%)	70 ± 6	69 ± 5	67 ± 7	68 ± 6	0.48
LV end diastolic volume index (ml/m^2)	66 ± 11	66 ± 12	70 ± 14	69 ± 14	0.43
LV end systolic volume index (ml/m^2)	19 ± 6	20 ± 7	22 ± 8	22 ± 7	0.38
LV stroke volume (ml)	86 ± 16	85 ± 16	89 ± 20	88 ± 19	0.67
Aortic forward flow (ml)†	83 ± 21	81 ± 16	86 ± 19	89 ± 23	0.26
Septal AVPD (mm)	15 ± 2	14 ± 3	15 ± 2	15 ± 2	0.03
Lateral AVPD (mm)	15 ± 3	14 ± 3	15 ± 2	15 ± 2	0.12
LA volume (ml)	78 ± 22	81 ± 16	84 ± 20	80 ± 23	0.10

LA volume index (ml/m^2)	43 ± 9	44 ± 8	45 ± 10	44 ± 9	0.27
RV stroke volume (ml)	81 ± 14	80 ± 14	84 ± 17	82 ± 17	0.61
RV end diastolic volume index (ml/m^2)	61 ± 11	63 ± 12	66 ± 13	65 ± 12	0.10
RV end systolic volume index (ml/m^2)	17 ± 7	20 ± 7	21 ± 8	20 ± 6	0.22

Data are presented as mean ± SD. N is the number of subjects with available baseline and 12 month data. Repeated-measures ANOVA with time point (month 0 or 12) as the within-subjects factor and group (control or donor) as the between-subjects factor tested the difference in change over time between groups. A two-tailed P value <0.05 was considered statistically significant. †Left ventricular stroke volume as determined by aortic flow mapping; data available in 45 donors, 41 controls. Abbreviations: AVPD; atrioventricular plane displacement; BSA, body surface area; LA, left atrium; LV left ventricle; MRI, magnetic resonance imaging; RV right ventricle.

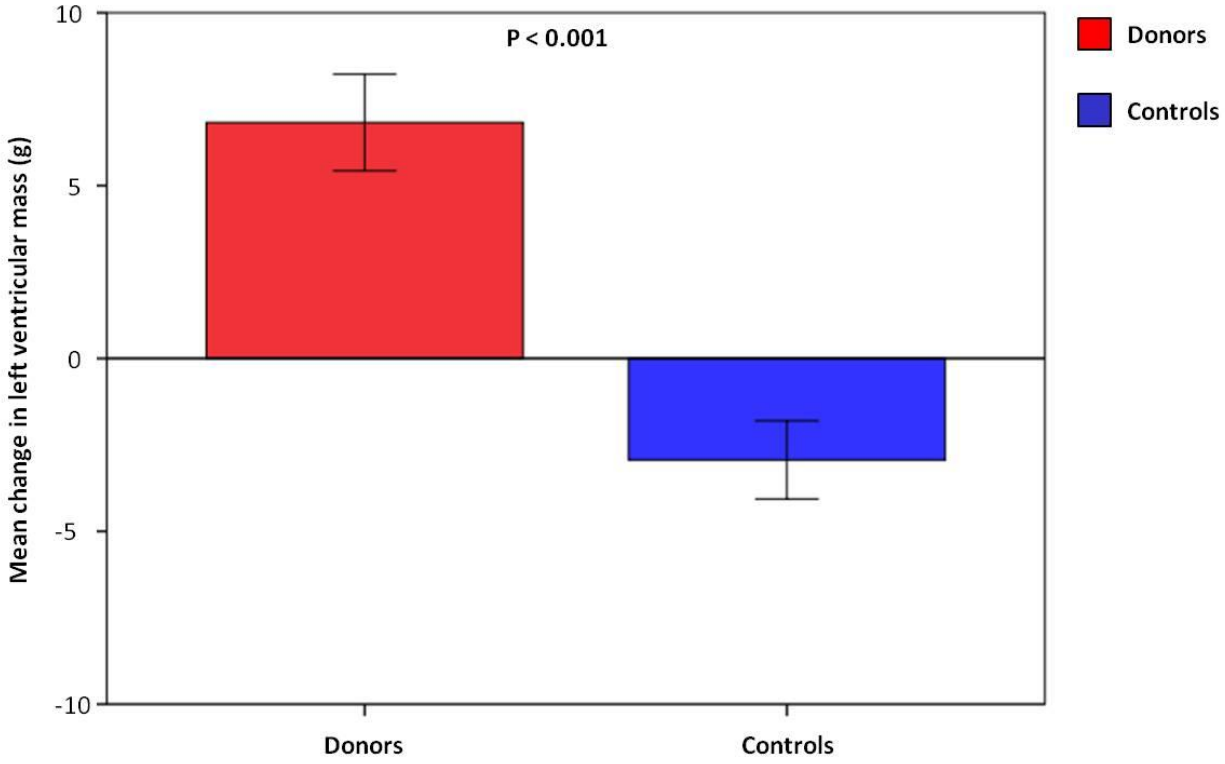

Figure 5-3. 12-Month Change in Left Ventricular Mass in Donors versus Controls.

Error bars (S.E.M.). Repeated-measures ANOVA with time point (month 0 or 12) as the within-subjects factor and group (control or donor) as the between-subjects factor tested the difference in change over time between groups.

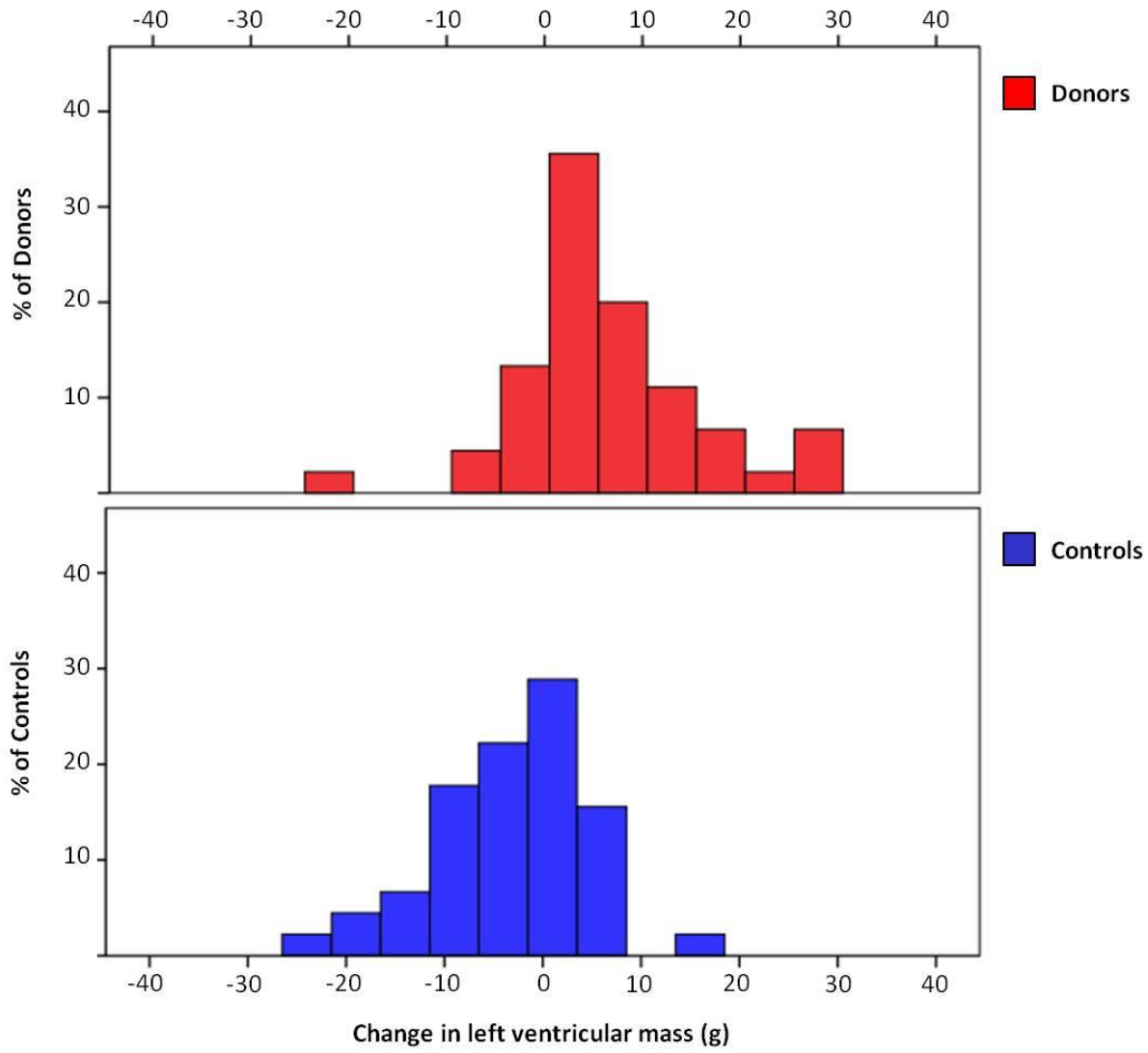

Figure 5-4. Spread of 12-Month Change in Left Ventricular Mass in Donors and Controls.

Left ventricular systolic function as measured by global circumferential strain was reduced (Figure 5-5) with directionally similar but non-significant changes in global longitudinal strain (Table 5-6). There were no significant differences in left atrial volume or parameters of left atrial strain between donors and controls.

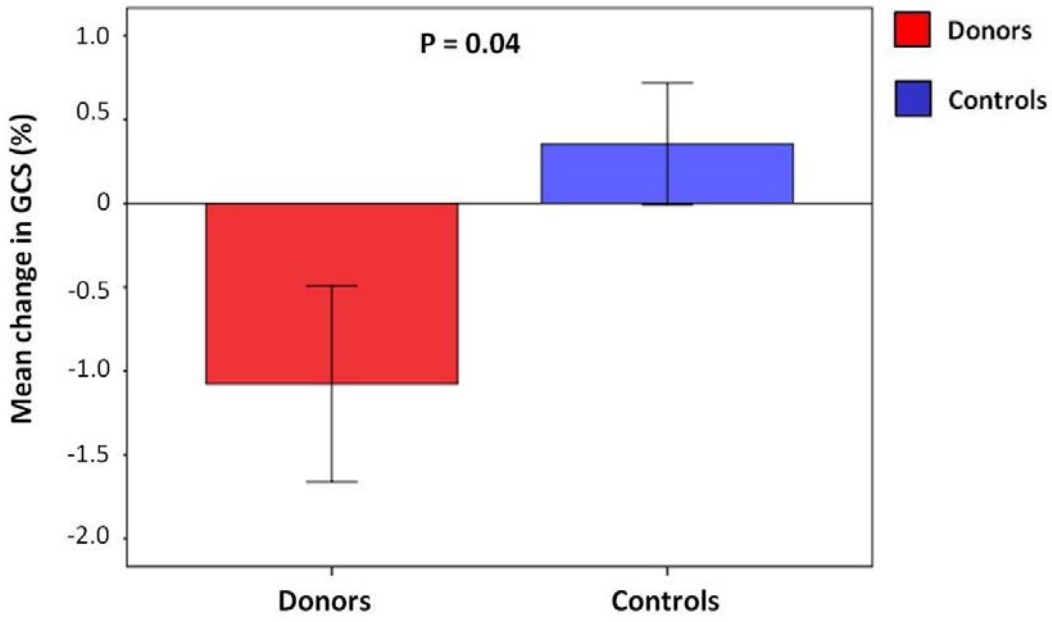

Figure 5-5. 12-Month Change in Global Circumferential Strain in Donors versus Controls.

Error bars (S.E.M.). Repeated-measures ANOVA with time point (month 0 or 12) as the within-subjects factor and group (control or donor) as the between-subjects factor tested the difference in change over time between groups.

Abbreviation: GCS, peak systolic global circumferential strain.

Table 5-6. Effects of a Reduction in Renal Function on Myocardial Strain Parameters.

	Donor (N = 50)		**Control (N = 45)**		
	Month 0	**Month 12**	**Month 0**	**Month 12**	**P**
Global short axis function (mid LV slice)					
Peak systolic circumferential E, GCS (%)	-27.14 ± 4.29	-26.07 ± 4.22	-25.35 ± 3.95	-25.71 ± 3.69	0.04
Peak systolic circumferential SR (s^{-1})	-1.63 ± 0.32	-1.60 ± 0.34	-1.51 ± 0.33	-1.53 ± 0.32	0.39
Early diastolic circumferential SR (s^{-1})	1.44 ± 0.53	1.29 ± 0.57	1.30 ± 0.52	1.37 ± 0.34	0.07
Global long axis function (HLA slice)					
Peak systolic longitudinal E, GLS (%)	-22.3 ± 5.3	-21.2 ±3.9	-20.4 ± 3.2	-21.1 ± 3.6	0.07
Peak systolic longitudinal SR (s^{-1})	-1.30 ± 0.39	-1.28 ± 0.43	-1.16 ± 0.28	-1.17 ± 0.44	0.68
Early diastolic longitudinal SR (s^{-1})	1.29 ± 0.45	1.21 ± 0.40	1.16 ± 0.30	1.17 ± 0.33	0.30
Left atrial long axis function					
Global PLAS (%)	35.5 ± 9.1	32.9 ± 9.9	39.7 ± 12.6	33.8 ± 9.5	0.25
PreA-S (%)	14.4 ± 5.3	13.3 ± 5.4	15.1 ± 5.6	13.0 ± 4.3	0.52

Data are presented as mean ± SD. N is the number of subjects with available baseline and 12 month data. Repeated-measures ANOVA with time point (month 0 or 12) as the within-subjects factor and group (control or donor) as the between-subjects factor tested the difference in change over time between groups. A two-tailed P value <0.05 was considered statistically significant. Abbreviations: E, Lagrangian strain, HLA, horizontal long axis; GCS, global subendocardial circumferential strain; GLS, global subendocardial longitudinal strain; LV left ventricle; PLAS, peak longitudinal atrial strain; PreA-S, peak longitudinal strain before atrial contraction; SR, strain rate

5.3.6. Effects on Blood Pressure

There were no significant differences at 12 months between donors and controls in any parameter of blood pressure including brachial, central or ambulatory measures (Table 5-7).

Table 5-7. Effect of a Reduction in Renal Function on Blood Pressure.

	Donor (N = 57)		Control (N = 46)		
	Month 0	**Month 12**	**Month 0**	**Month 12**	**P Value**
Brachial systolic BP (mmHg)	124 ± 11	123 ± 10	124 ± 12	121 ± 11	0.38
Brachial diastolic BP (mmHg)	75 ± 8	78 ± 8	76 ± 9	76 ± 8	0.09
Central systolic BP (mmHg)	112 ± 10	112 ± 11	112 ± 13	111 ± 13	0.43
Central diastolic BP (mmHg)	76 ± 8	78 ± 9	77 ± 9	77 ± 9	0.25
Ambulatory brachial systolic BP (mmHg)†	121 ± 8	122 ± 12	122 ± 11	121 ± 10	0.55
Ambulatory brachial diastolic BP (mmHg)†	75 ± 6	76 ± 9	74 ± 8	76 ± 9	0.68

Data are presented as mean ± SD. N is the number of subjects with available baseline and 12 month data. Repeated-measures ANOVA with time point (month 0 or 12) as the within-subjects factor and group (control or donor) as the between-subjects factor tested the difference in change over time between groups. A two-tailed P value <0.05 was considered statistically significant. †Data available in 46 donors, 36 controls; daytime brachial blood pressure measured between 08:00 and 22:00. Abbreviation: BP, blood pressure.

5.3.7. Effects on Arterial Stiffness

In donors, there was a graded increase in aortic PWV observed at 6 and 12 months post-nephrectomy (Figure 5-6).

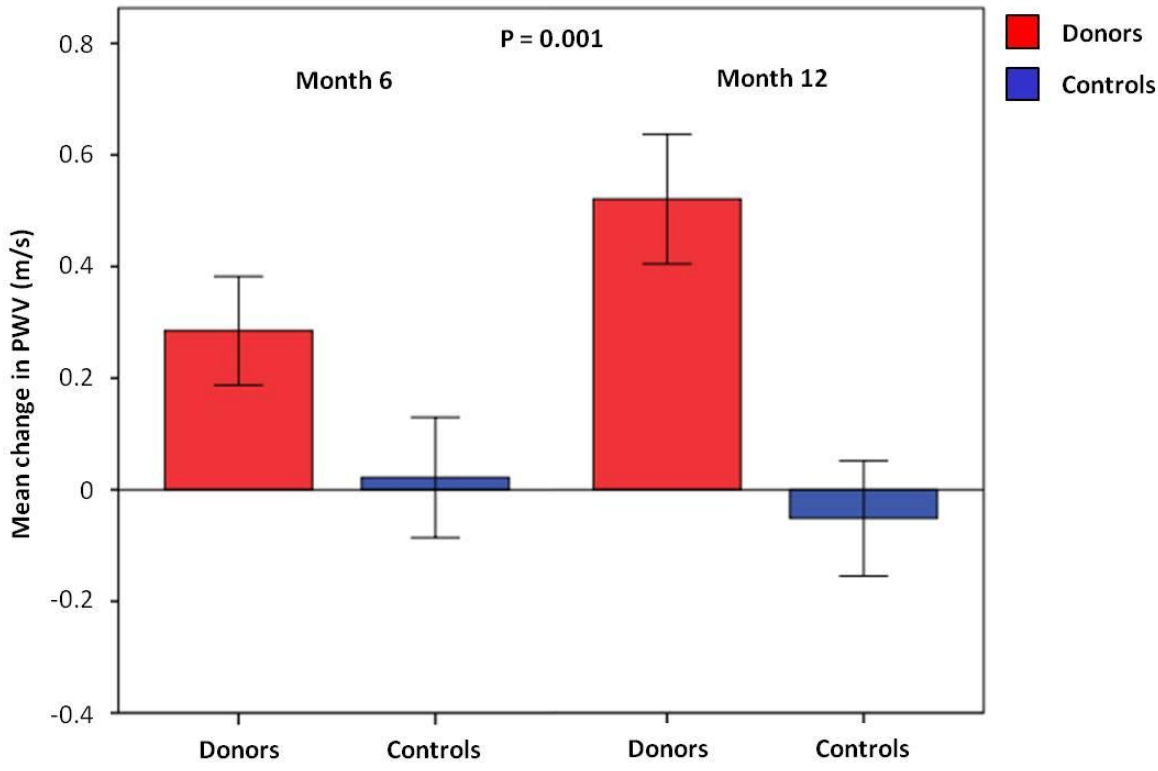

Figure 5-6. 6- and 12-Month Changes in Aortic Pulse Wave Velocity in Donors versus Controls.

Error bars (S.E.M.). Repeated-measures ANOVA with time point (month 0, 6 or 12) as the within-subjects factor and group (control or donor) as the between-subjects factor tested the difference in change over time between groups.

An increase in arterial stiffness was observed in donors versus controls and was independent of blood pressure as confirmed by significant changes in PWV_{adj} (+0.43 ± 0.69 m/s vs. −0.02 ± 0.72 m/s; $P < 0.01$, Table 5–8). Directionally similar but non-significant increases in AIx_{75} were demonstrated at 12 months ($P = 0.07$) (Table 5–8).

Table 5-8. Effect of a Reduction in Renal Function on Arterial Stiffness.

	Donor (N = 59)		Control (N = 48)		
	Month 0	**Month 12**	**Month 0**	**Month 12**	**P Value**
PWV (m/s)	6.8 ± 1.1	7.3 ± 1.5	6.7 ± 1.1	6.7 ± 1.1	<0.001
PWV_{adj} (m/s)	6.7 ± 0.9	7.1 ± 1.1	6.6 ± 1.1	6.6 ± 1.1	0.002
AIx (%)	22 ± 13	23 ± 13	19 ± 13	18 ± 11	0.20
AIx_{75} (%)	16 ± 13	18 ± 12	13 ± 14	13 ± 12	0.07

Data are presented as mean ± SD. N is the number of subjects with available baseline and 12 month data. Repeated-measures ANOVA with time point (month 0 or 12) as the within-subjects factor and group (control or donor) as the between-subjects factor tested the difference in change over time between groups. A two-tailed P value <0.05 was considered statistically significant. Abbreviations: AIx, augmentation index; AIx_{75}, augmentation index adjusted for a heart rate of 75 beats per minute; PWV, aortic pulse wave velocity; PWV_{adj}, aortic pulse wave velocity adjusted for mean arterial pressure.

5.3.8. Effects on Aortic Distensibility

Consistent with the observed changes in PWV, aortic distensibility at the level of the proximal ascending aorta was reduced following nephrectomy in donors compared to controls ($-0.29 \pm 1.38 \times 10^{-3}$ $mmHg^{-1}$ vs. $+0.28 \pm 0.79 \times 10^{-3}$ $mmHg^{-1}$; P = 0.03; Table 5-9). There were however, no differences in distensibility between donors and controls at the level of the proximal descending and distal descending aorta.

5.3.9. Effects on Carotid Intima-Media Thickness

At 12 months, there was no demonstrable change in carotid IMT in donors versus controls (+0.01 ± 0.03 mm vs. 0.00 ± 0.03 mm; P = 0.31; Table 5-9).

5.3.10. Effects on the Left Ventricular Interstitium

Compared with controls, there was a trend towards elevated ECV in donors post-nephrectomy (mean effect size +2.1%) although this result was almost certainly underpowered (n = 13) and did not meet statistical significance (Table 5-9). There was no significant difference between donors and controls in the increases in ultrasonic reflectivity observed at 12 months (as determined by the change in cIBS).

Table 5-9. Effects of a Reduction in Renal Function on Large Artery Structure and Function and Myocardial Tissue Characteristics.

	Donor (N = 45)		Control (N = 43)		
	Month 0	**Month 12**	**Month 0**	**Month 12**	**P Value**
Aortic distensibility					
Proximal ascending aorta (× 10^{-3} $mmHg^{-1}$)	3.75 ± 2.75	3.46 ± 2.32	3.62 ± 2.07	3.90 ± 2.13	0.03
Proximal descending aorta (× 10^{-3} $mmHg^{-1}$)	4.33 ± 2.63	4.10 ± 1.56	3.79 ± 1.30	4.11 ± 1.55	0.18
Distal descending aorta (× 10^{-3} $mmHg^{-1}$)	5.40 ± 2.28	5.64 ± 2.09	5.36 ± 2.31	5.66 ± 1.99	0.99
Arterial structure					
Carotid intima-media thickness (mm)	0.59 ± 0.10	0.60 ± 0.10	0.59 ± 0.11	0.59 ± 0.10	0.31
Myocardial tissue characterization					
Extracellular volume (%)†	25.9 ± 3.9	28.0 ± 3.1	27.8 ± 4.1	27.5 ± 3.0	0.27
Intracellular volume (%)†	74.1 ± 3.9	72.0 ± 3.1	72.2 ± 4.1	72.5 ± 3.0	0.26
Calibrated integrated backscatter (dB)	-28.0 ± 3.0	-25.4 ± 3.7	-27.7 ± 2.0	-25.9 ± 4.4	0.57

Data are presented as mean ± SD. N is the number of subjects with available baseline and 12 month data. Repeated-measures ANOVA with time point (month 0 or 12) as the within-subjects factor and group (control or donor) as the between-subjects factor tested the difference in change over time between groups. †Data available in 13 subjects. A two-tailed P value <0.05 was considered statistically significant.

5.3.11. Effects on Endothelial Function

There was a significant reduction in FMD in donors (the endothelial-dependent response to functional hyperaemia) compared with controls at 12 months (Table 5–10). By contrast, there was no difference between donors and controls in the brachial response to GTN control (the endothelial-independent response).

Table 5-10. Effect of a Reduction in Renal Function on Endothelial Function.

	Donor (N = 30)		**Control (N = 32)**		
	Month 0	**Month 12**	**Month 0**	**Month 12**	**P Value**
*Brachial reactivity**					
FMD	7.02 ± 3.75	6.36 ± 3.32	6.62 ± 3.07	7.50 ± 4.13	0.03
GTN control	15.33 ± 5.63	14.93 ± 6.56	17.79 ± 5.30	17.61 ± 5.55	0.28

*Percentage change in cross-sectional area from baseline. Data are presented as mean ± SD. N is the number of subjects with available baseline and 12 month data. Repeated-measures ANOVA with time point (month 0 or 12) as the within-subjects factor and group (control or donor) as the between-subjects factor tested the difference in change over time between groups. A two-tailed P value <0.05 was considered statistically significant.

Abbreviations: FMD, flow-mediated-dilatation; GTN, glyceryl trinitrate.

5.3.12. Determinants of the Change in Left Ventricular Mass

Univariate analysis showed an association between the increase in LV mass and the decrease in iGFR ($\beta = -0.3$, $R^2 = 0.19$, $P < 0.001$; Table 5-11). This relationship remained significant after adjustment for sex and 12-month changes in aortic PWV and uric acid ($\beta = -0.4$, $R^2 = 0.17$, $P = 0.04$). There was a less strong but still significant association between the reduction in eGFR and increase in LV mass (Figure 5-7). Consistent with the finding that blood pressure did not change in donors versus controls, there was no significant association between 12-month changes in mean arterial pressure and LV mass.

Table 5-11. Univariate and Multivariable Analyses with 12-Month Change in Left Ventricular Mass as the Outcome Variable.

Variable	**Univariate**		**Multivariable**		
	R	**P value**	**β**	**95% CI**	**P value**
Age	0.03	0.76			
Sex	-9.48	0.06	-0.04	-7.24 to 5.56	0.79
Baseline LV mass (g)	-0.12	0.25			
12 month change in iGFR (ml/min/1.73m^2)	-0.44	<0.001	-0.39	-0.51 to -0.01	0.04
12 month change in eGFR (ml/min/1.73m^2)	-0.30	0.004			
12 month change in mean arterial blood pressure (mmHg)	0.06	0.66			
12 month change in aortic PWV (m/s)	0.26	0.02	0.05	-4.09 to 5.38	0.78
12 month change in uric acid (μmol/l)	0.26	0.02	-0.01	-0.09 to 0.08	0.94
12 month change in intact PTH (pg/ml)	-0.02	0.85			

Data analysed using Pearson correlation (univariate) and enter linear regression (multivariable). All variables that correlated with the change in left ventricular mass in univariate analysis were entered into the multivariate regression model. R^2 for model = 0.17, P = 0.04. For gender; 0 = male, 1 = female.

Abbreviations: β, standardised beta coefficient; eGFR, estimated glomerular filtration rate by the CKD-EPI equation; iGFR, isotopic glomerular filtration rate; LV, left ventricular; PTH, parathyroid hormone; PWV, pulse wave velocity; 95% CI, 95% confidence interval.

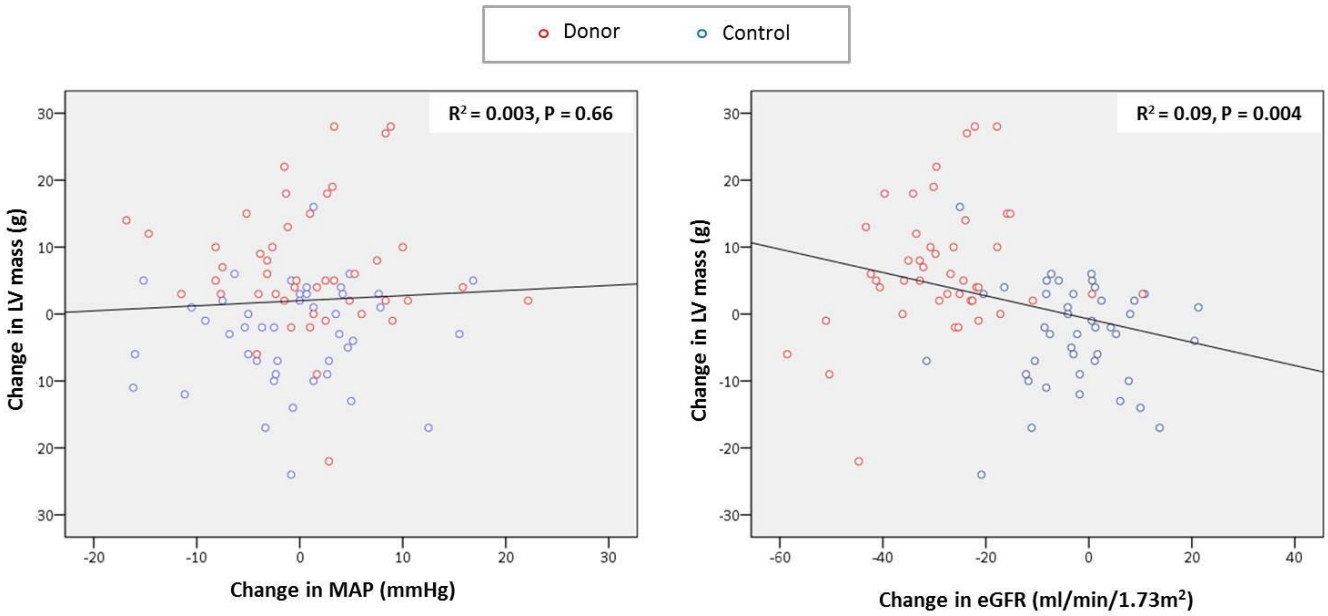

Figure 5-7. Univariate Associations Between Changes in Mean Arterial Blood Pressure and Estimated Glomerular Filtration Rate With Changes in Left Ventricular Mass.

Abbreviations: eGFR, estimated glomerular filtration rate; LV, left ventricular; MAP mean arterial pressure.

5.3.13. Reproducibility

Reproducibility of cardiac MRI derived LV metrics are given in detail in Chapter 3. In brief, the intraobserver and interstudy variability for LV mass was low (ICC [95% CI]; 0.99 [0.98-1.00] and 0.98 [0.91-1.00], respectively).

5.4. Discussion

This study has demonstrated that a modest reduction in GFR caused by unilateral nephrectomy in healthy human subjects causes important structural and functional cardiovascular abnormalities within one year. Left ventricular mass was elevated with a graded independent association between the reduction in GFR and the increase in LV mass even after adjustment for demographic and haemodynamic factors. In addition, there was an increase in LV mass – volume ratio, reduced LV myocardial deformation and increased aortic stiffness. Although ED was observed, there was no effect on atherosclerosis progression as determined by carotid IMT measurement. The prevalence of microalbuminuria and detectable cardiac troponin was increased after donation along with a significant rise in serum hsCRP. These findings provide powerful insights into the pathophysiological effects of CKD on the cardiovascular system suggesting that they are not primarily atherosclerotic but instead mediated via LV hypertrophy and fibrosis together with increased large artery stiffness.

Despite robust epidemiological evidence of an association between reduced eGFR and increased cardiovasscular risk (Matsushita et al., 2010), clear proof of causation has been lacking. The debate has been heightened by an increasing body of opinion suggesting that early stage CKD is benign and that age-related nephron loss should not be “medicalised” (Moynihan et al., 2013). Distinguishing causality from association in CKD is made difficult by the numerous concomitant diseases that

invariably accompany reduced GFR including hypertension, diabetes mellitus, anaemia, dyslipidaemia and vasculitis. By studying kidney donors we were able to isolate the effect of a reduction in renal function on the cardiovascular system, free from such confounding disease processes. The results suggest that reduced GFR is an independent graded risk factor for adverse LV remodelling independent of blood pressure. Because the prevalence of early stage CKD is high (up to 1 in 7 people in the US), it may be a major cause of increased LV mass in the community, a potent risk factor for cardiovascular death and adverse events (Zile et al., 2011). Further investigation is required to identify the mediators of "renal" cardiovascular disease. We have found no evidence to support effects mediated by blood pressure or activation of the renin angiotensin system. On the basis of the results presented in this Chapter, uric acid and PTH and FGF-23 are all worthy of further investigation as mediators of both increased ventricular mass and arterial stiffening (Velagaleti et al., 2008, Faul et al., 2011).

5.4.1. Effects on Cardiovascular Structure and Function

Our findings may have important clinical implications as many of the variables examined are of prognostic importance. Both LV mass and aortic PWV have been consistently associated with increased mortality in both the general population (Willum-Hansen et al., 2006, Cheng et al., 2009) and patients with CKD (Blacher et al., 1999, Foley et al., 1995). While no subject in the current study reached criteria for LV hypertrophy, both LV mass and mass-to-volume ratio have continuous rather

than dichotomous relationships with risk (Zile et al., 2011). Indeed, LV mass is second only to age in its ability to predict cardiovascular events, cardiovascular death, and total mortality (Levy et al., 1990).

There was a marked reduction in global myocardial strain parameters in donors that was not seen in controls; such indices have become increasingly accepted as powerful predictors of cardiac events and may predate changes in gross measures of function such as LV ejection fraction (Cho et al., 2009). The observed increase in carotid-femoral PWV in donors was further supported by the significant reduction in proximal aortic distensibility demonstrated on MRI. Although there were no changes in distensibility at the level of the proximal descending and distal descending aorta, this pattern of disease appears to mimic age-related, regional increases in PWV which primarily affect the proximal aorta (Rogers et al., 2001).

5.4.2. Effects on Cardiac Biomarkers

Compared with controls, there was a 16-fold increase in the risk of developing detectable hsTnT in donors. Detectable troponin (rather than elevated above the 99th centile) has been independently associated with structural heart disease and all-cause mortality in the general population and also predicts adverse cardiovascular outcomes in subjects with CKD stages 1 – 3, highlighting the importance of silent cardiac damage (Scheven et al., 2012, De Lemos et al., 2010, Defilippi et al., 2010). High-sensitivity troponin concentrations have been linked to

the magnitude of hypertrophic response in patients with aortic stenosis (Chin et al., 2014). Consistent with this finding, the release of low quantities of hsTnT in donors may have resulted from concentric remodelling causing a supply–demand mismatch which precipitated a low grade hypoxia (Claeys, 2014, Mishra et al., 2013).

There were also a significant proportion of donors who developed an ACR ≥ 3.0mg/mmol. This finding of increased urinary protein excretion could reflect hyperfiltration in the remaining kidney but might also relate to the early onset of ED that was also evident among donors in the current study. Irrespective of the mechanism, even low levels of urinary albumin excretion have been shown to predict adverse cardiovascular outcomes independent of conventional cardiac risk factors (Klausen et al., 2004, Arnlov et al., 2005). Finally, there was a significant elevation in levels of hsCRP observed in donors and this biomarker has a strong independent association with mortality in healthy subjects as well as in the non-dialysis CKD population (Boekholdt et al., 2006, Vickery et al., 2008).

5.4.3. Implications for Kidney Donors

The practice of living kidney donation is expanding rapidly; to date over 130,000 such procedures have been performed in the US alone (OPTN, 2014). While observational studies of kidney donors have been largely reassuring, (Fehrman-Ekholm et al., 1997, Segev et al., 2010) there can be no complacency about the long-term safety of unilateral nephrectomy. Studies using carefully selected healthy

control groups suggest that there may be a small increase in the risk of cardiovascular events and in the risk of developing ESRD, particularly in non-white ethnic groups (Lentine et al., 2010, Muzaale et al., 2014, Mjoen et al., 2013). Our results provide an explanation of the mechanism by which adverse cardiovascular effects of kidney donation may be mediated. Further research is required to ascertain the natural history of the effects we have demonstrated. In the meantime, the transplant community should be open about the pathophysiological consequences of nephrectomy to subjects considering donation to ensure a process of fully informed consent is maintained. Further prospective clinical registry studies with appropriate control groups are essential to examine the effects of nephrectomy on long term cardiovascular mortality and morbidity (Thiel et al., 2011).

5.4.4. Other Studies

Our results extend those which have been presented in the only other prospective, controlled study of kidney donors to date (Kasiske et al., 2013). Kasiske *et al.* also found no effect of kidney donation on peripheral blood pressure but similar biochemical effects including an increase in parathyroid hormone and uric acid. Both these factors have been associated with adverse cardiovascular outcomes and may themselves have direct adverse effects on LV geometry (Kao et al., 2011, Laflamme et al., 2014).

5.4.5. Limitations

The detailed, prospective, pathophysiological design of this study is its major strength but there are some limitations. While over half of all subjects approached (53%) took part in this study we cannot completely exclude the potential for some selection bias. The number of donors undergoing T1 mapping to quantify ECV was small; while an increase in ECV was demonstrated in donors the result did not reach statistical significance and thus, these preliminary findings require confirmation with larger numbers. Even at 12 months post-nephrectomy, the effects of the operation itself on the cardiovascular system cannot be fully discounted. Finally, the study was not large enough, nor of sufficient duration to provide data on clinical end points in living kidney donors.

5.4.6. Conclusion

In conclusion, kidney donors exhibited adverse changes in LV mass and systolic function, increased aortic stiffness and a less favourable cardiovascular disease biomarker profile at 12 months after donation. The increase in LV mass was independently related to changes in renal function but independent of blood pressure. These findings suggest that reduced GFR should be regarded as an independent causative cardiovascular risk factor.

6. FUTURE STUDIES

6.1. Summary of Main Findings

Even early stage CKD is associated with increased cardiovascular morbidity and mortality, although until now it has been difficult to decipher how many of these excess events are caused by the reduction in GFR or the conventional risk factors that have a propensity to accompany CKD, such as hypertension and diabetes mellitus. In this body of work, we have shown that the modest reduction in GFR caused by kidney donation (approximately 30 ml/min/1.73 m^2) causes increased left ventricular mass and increased arterial stiffness with no effect on blood pressure at 12 months. Increases in LV mass had a graded independent association with the magnitude of the reduction in GFR, even after adjustment for demographic and haemodynamic factors. In addition, there was concentric remodelling, impaired short and long axis systolic function, and increased arterial stiffness. There was no effect on progression of atheromatous disease as measured by carotid IMT. The prevalence of microalbuminuria and detectable cardiac troponin was increased after donation along with a significant rise in serum hsCRP. In summary, these data provide powerful evidence that CKD is an independent causative cardiovascular risk factor exerting adverse effects on the myocardium and large arteries.

I am confident in drawing the above conclusions because of the reliability of the data presented herein. I have presented a peer-reviewed validation of my CMR-FT analyses

against tagging which is the reference standard technique for quantifying myocardial strain. Moreover, there was excellent reproducibility in the blinded LV measurements performed using cardiac MRI.

6.2. Implications of Findings

These findings have major implications for both the general population, in whom early moderate CKD is highly prevalent, as well as for living kidney donors. After age, LV hypertrophy is the most potent risk factor for cardiovascular death and mortality in the community (Levy et al., 1990). Our findings suggest that a reduction in GFR of approximately −30 ml/min/1.73m^2 is sufficient to cause increases in LV mass leading to concentric LV remodelling. It is therefore highly plausible that early stage CKD is a major driver of LV hypertrophy in community dwelling subjects and thereby precipitates a substantial proportion of adverse cardiovascular events in the general population. The work presented in this thesis provides robust evidence that the relationship between CKD and cardiovascular disease is causative, which suggests up to a fifth of major vascular events among those aged over 70 years can be attributed to reduced renal function (Mafham et al., 2011).

There is now a clear requirement for the prospective registration of all living kidney donors (Moody et al., 2012c). It is impossible to randomize an individual to become a living kidney donor (Reese et al., 2015) and for that reason we must continue to strive to generate new knowledge about long-term donor outcomes using an observational

approach with control groups that, while likely still imperfect, will represent improvements over existing work. In our own prospective study presented in this volume of work, we were able to ensure that the nondonor controls used for comparison with donors had equivalent baseline health status, by performing an identical screening protocol for both groups on study entry, as well as detailed cardiovascular and renal assessments. This is the major advantage of our detailed pathophysiological study over the existing data from epidemiological studies. A similar approach will need to be adopted by future prospective large-scale studies if we are to ever confirm or refute the possibility that kidney donation impacts adversely upon cardiovascular risk.

6.3. Future Directions

We hypothesise that although the differences in LV mass and arterial stiffness between donors and controls were small at 12 months after nephrectomy, these may increase with time. Whether these adverse changes to the LV and aorta persist or increase can only be answered with extended follow up. Indeed, one of the major initial aims of this study was to establish a "donor cohort". We plan to repeat ambulatory BP and arterial stiffness measures annually for 5 years whilst repeating cardiac MRI studies to determine LV mass along with functional measures at 3 and 5 years. Long-term longitudinal outcomes and mortality data will also be provided by the registration of participants with the NHS Medical Research Information System (MRIS) and accessing information from the UK National Transplant Register.

6.3.1. Future Analyses

To date, there are no longitudinal data on the effects of nephrectomy on FGF-23 and the results of these assays are eagerly awaited. One cross-sectional study has shown increased FGF-23 at a median time after donation of 5.3 years (Young et al., 2012a). Both serum FGF-23 levels and plasma iPTH levels were significantly higher in donors as compared with controls. If we observe an increase in levels of circulating FGF-23 in donors over 12 months, this would lend support to the theory that the FGF-23 pathway is a key driver in adverse LV remodelling in CKD, and appears to exert its effects via a blood pressure-independent mechanism. This would provide further

impetus for the development of novel compounds to target the FGF-23 pathway with the aim of improving structural and functional cardiovascular parameters in early stage CKD. For example, the non-specific FGF-23 receptor antagonist PD173074, was recently shown to retard the development of LVH in animal models of CKD (Faul et al., 2011).

In the near future, the stored serum of donors and controls will undergo proteomic profiling (SomaLogic, Boulder, CO 80301 USA). There is already a validated panel of proteins available for patients with stable coronary artery disease which has been shown to very accurately stratify cardiovascular risk (SomaScan CVD Panel). Using the same technology, a recent US study examined the influence of circulating factors using heterochronic parabiosis, a surgical technique in which the joining of mice of different ages leads to a shared circulation (Loffredo et al., 2013). After 4 weeks of exposure to the circulation of young mice, LV hypertrophy in old mice significantly regressed. Modified aptamer-based proteomics identified growth differentiation factor 11 (GDF11), a member of the TGF-β superfamily, as a blood-borne factor in young mice that declined with age. Supplementation of old mice with GDF11 restored youthful circulating levels which reversed age-related hypertrophy. Thus, it may prove illuminating to quantify changes in the proteome before and after kidney donation and assess for changes in GDF11 expression. This approach may help identify novel serum biomarkers responsible for the increased LV hypertrophy and excess cardiovascular risk associated with CKD.

A detailed CMR-FT assessment of LV systolic and diastolic function under resting conditions has already been presented in this body of work. In those subjects with appropriate image quality, transthoracic echocardiography was also performed during a progressive submaximal exercise test to derive stress-related changes in LV systolic and diastolic function using TDI and strain measures. Exercise uncovers abnormalities of both systolic and diastolic function in patients with heart failure with preserved ejection fraction (HFpEF), including torsional dyssynchrony which relates to LV hypertrophy as well as exercise capacity (Tan et al., 2013, Tan et al., 2009). In patients with advanced CKD, HFpEF is common and tends to overlap with uraemic cardiomyopathy (Wang et al., 2013). In the current study, subjects were installed on a dedicated semisupine cycling ergometer (Schiller ERG 911 BP/L, Baar, Switzerland). After a 15-minute rest period, each subject underwent an exercise test that included 3 workload stages each of 4 minutes duration, at 20%, 30% and 40% of their maximal aerobic power estimated via the Wasserman equation:

$$\text{Semi-supine VO 2 max} = 0.8*[(\text{body mass } (50.72 – 0.372 \text{ X age}))–350]/10.3$$

The maximal aerobic power was corrected for semisupine position by removing 20% from the normal values (Arena et al., 2009, Doucende et al., 2010). As for previous analyses, changes in TDI and strain measures in donors are to be compared with changes in controls over time. More specifically, left ventricular long-axis function is to

be examined during exercise because it offers important prognostic information (Wang et al., 2015). These data should provide valuable insight into the effects of reduced GFR on cardiac mechanics during stress.

6.3.2. Other Studies in Progress

The blood pressure and PWV data presented in this volume of work are also being entered into the EARNEST Study (Effects of A Reduction in glomerular filtration rate after NEphrectomy on Arterial STiffness). The rationale and methods for this study have been reported in detail (Moody et al., 2014b). EARNEST is a collaborative UK multicentre study with a prospective, longitudinal, parallel group design and is also being led by our group. The study plans to recruit 440 living kidney donors and 440 healthy controls and is powered to detect an increase in peripheral and central blood pressure, and to detect very small increases in arterial stiffness in donors. In regard to the effects of kidney donation on peripheral blood pressure, the data remain inconclusive and the results of this study should therefore prove very informative. These data will also help to confirm or deny the results of the PWV measurements presented in the current work which have been performed by an unblinded observer (W.E.M.).

After submitting an application to UK Transplant during the course of this work, I was granted access to data on over 10,000 UK living kidney donors operated on between

1990 and 2012. Using these data, I have already reported in abstract form that long-term cardiovascular outcomes are superior in UK kidney donors compared with a contemporaneous control group, although this finding may have reflected residual confounding from selection and follow up biases (Moody, 2013). Acknowledging the difficulties in identifying an appropriately matched non-donor control group, the focus of this investigation has changed to examining changes in GFR exclusively in donors; there are marked differences in the extent of the recovery of renal function post-transplant which offers a unique opportunity to examine the association between changes in eGFR and cardiovascular risk. Using linked datasets from the UK Transplant Registry and the NHS Hospital Episodes Statistics database, my aim is to examine the hypothesis that the size of the reduction in renal function associated with nephrectomy independently predicts long-term adverse cardiovascular events in UK living kidney donors. Findings from this study might support the need for intervention studies to help determine whether early cardiovascular risk reduction therapy should be instituted in the vast number of community dwelling subjects with only modestly impaired renal function, as well as in those that have undergone living kidney donation. Moreover, these data may provide yet further evidence that CKD should be regarded as a causative risk factor for cardiovascular disease.

7. REFERENCES

Abhayaratna, W. P., Yew, S. C. & Talaulikar, G. 2010. Effect of Reduced Renal Function after Voluntary Kidney Donation on Cardiac Structure and Function and Arterial Stiffness **Circulation***,* 122 A20745

Adeney, K. L., Siscovick, D. S., Ix, J. H., et al. 2009. Association of serum phosphate with vascular and valvular calcification in moderate CKD. **J Am Soc Nephrol***,* 20 (2): 381-387

Ahmed, R., Dunford, J., Mehran, R., et al. 2014. Pre-eclampsia and future cardiovascular risk among women: a review. **J Am Coll Cardiol***,* 63 (18): 1815-1822

Alam, M., Wardell, J., Andersson, E., et al. 1999. Characteristics of mitral and tricuspid annular velocities determined by pulsed wave Doppler tissue imaging in healthy subjects. **J Am Soc Echocardiogr***,* 12 (8): 618-628

Amabile, N., Guerin, A. P., Leroyer, A., et al. 2005. Circulating endothelial microparticles are associated with vascular dysfunction in patients with end-stage renal failure. **J Am Soc Nephrol***,* 16 (11): 3381-3388

Anderson, R. G., Bueschen, A. J., Lloyd, L. K., et al. 1991. Short-term and long-term changes in renal function after donor nephrectomy. **J Urol***,* 145 (1): 11-13

Annuk, M., Soveri, I., Zilmer, M., et al. 2005. Endothelial function, CRP and oxidative stress in chronic kidney disease. **J Nephrol***,* 18 (6): 721-726

Arena, R., Myers, J., Abella, J., et al. 2009. Determining the preferred percent-predicted equation for peak oxygen consumption in patients with heart failure. **Circ Heart Fail***,* 2 (2): 113-120

Arnlov, J., Evans, J. C., Meigs, J. B., et al. 2005. Low-grade albuminuria and incidence of cardiovascular disease events in nonhypertensive and nondiabetic individuals: the Framingham Heart Study. **Circulation***,* 112 (7): 969-975

Asselbergs, F. W., Diercks, G. F., Hillege, H. L., et al. 2004. Effects of fosinopril and pravastatin on cardiovascular events in subjects with microalbuminuria. **Circulation***,* 110 (18): 2809-2816

Assomull, R. G., Prasad, S. K., Lyne, J., et al. 2006. Cardiovascular magnetic resonance, fibrosis, and prognosis in dilated cardiomyopathy. **J Am Coll Cardiol***,* 48 (10): 1977-1985

Augustine, D., Lewandowski, A. J., Lazdam, M., et al. 2013. Global and regional left ventricular myocardial deformation measures by magnetic resonance feature tracking in healthy volunteers: comparison with tagging and relevance of gender. **J Cardiovasc Magn Reson***,* 15 (1): 8

Avolio, A. P., Van Bortel, L. M., Boutouyrie, P., et al. 2009. Role of pulse pressure amplification in arterial hypertension: experts' opinion and review of the data. **Hypertension***,* 54 (2): 375-383

Babitt, J. L. & Lin, H. Y. 2012. Mechanisms of anemia in CKD. **J Am Soc Nephrol***,* 23 (10): 1631-1634

Bahous, S. A., Stephan, A., Blacher, J., et al. 2006. Aortic stiffness, living donors, and renal transplantation. **Hypertension***,* 47 (2): 216-221

Baigent, C., Landray, M. J., Reith, C., et al. 2011. The effects of lowering LDL cholesterol with simvastatin plus ezetimibe in patients with chronic kidney disease (Study of Heart and Renal Protection): a randomised placebo-controlled trial. **Lancet***,* 377 (9784): 2181-2192

Baksi, A. J., Treibel, T. A., Davies, J. E., et al. 2009. A meta-analysis of the mechanism of blood pressure change with aging. **J Am Coll Cardiol***,* 54 (22): 2087-2092

Balamuthusamy, S., Srinivasan, L., Verma, M., et al. 2008. Renin angiotensin system blockade and cardiovascular outcomes in patients with chronic kidney disease and proteinuria: a meta-analysis. **Am Heart J***,* 155 (5): 791-805

Baltzan, M. A., Ahmed, S., Baltzan, R. B., et al. 1997. Variations in living donor graft rates by dialysis clinic: effect on outcome and cost of chronic renal failure therapy. **Clin Nephrol***,* 47 (6): 351-355

Barri, Y. M., Parker, T., 3rd, Daoud, Y., et al. 2010. Definition of chronic kidney disease after uninephrectomy in living donors: what are the implications? **Transplantation***,* 90 (5): 575-580

Berne, R. M. L., M.N. (ed.) 1993. **Physiology***,* Missouri: Mosby.

Besarab, A., Bolton, W. K., Browne, J. K., et al. 1998. The effects of normal as compared with low hematocrit values in patients with cardiac disease who are receiving hemodialysis and epoetin. **N Engl J Med***,* 339 (9): 584-590

Best, P. J., Reddan, D. N., Berger, P. B., et al. 2004. Cardiovascular disease and chronic kidney disease: insights and an update. **Am Heart J***,* 148 (2): 230-242

Bia, M. J., Ramos, E. L., Danovitch, G. M., et al. 1995. Evaluation of living renal donors. The current practice of US transplant centers. **Transplantation***,* 60 (4): 322-327

Blacher, J., Guerin, A. P., Pannier, B., et al. 1999. Impact of aortic stiffness on survival in end-stage renal disease. **Circulation***,* 99 (18): 2434-2439

Blacher, J., Pannier, B., Guerin, A. P., et al. 1998. Carotid arterial stiffness as a predictor of cardiovascular and all-cause mortality in end-stage renal disease. **Hypertension***,* 32 (3): 570-574

Boehme, M., Kaehne, F., Kuehne, A., et al. 2007. Pentraxin 3 is elevated in haemodialysis patients and is associated with cardiovascular disease. **Nephrol Dial Transplant***,* 22 (8): 2224-2229

Boekholdt, S. M., Hack, C. E., Sandhu, M. S., et al. 2006. C-reactive protein levels and coronary artery disease incidence and mortality in apparently healthy men and women: the EPIC-Norfolk prospective population study 1993-2003. **Atherosclerosis***,* 187 (2): 415-422

Bolton, C. H., Downs, L. G., Victory, J. G., et al. 2001. Endothelial dysfunction in chronic renal failure: roles of lipoprotein oxidation and pro-inflammatory cytokines. **Nephrol Dial Transplant***,* 16 (6): 1189-1197

Bos, M. J., Koudstaal, P. J., Hofman, A., et al. 2006. Uric acid is a risk factor for myocardial infarction and stroke: the Rotterdam study. **Stroke***,* 37 (6): 1503-1507

Boudville, N., Prasad, G. V., Knoll, G., et al. 2006. Meta-analysis: risk for hypertension in living kidney donors. **Ann Intern Med***,* 145 (3): 185-196

Briet, M., Bozec, E., Laurent, S., et al. 2006. Arterial stiffness and enlargement in mild-to-moderate chronic kidney disease. **Kidney Int***,* 69 (2): 350-357

BTS 2005. **British Transplantation Society / the Renal Association United Kingdom Guidelines for Living Kidney Transplantation** - 2nd Ed.

Bro, S. & Olgaard, K. 1997. Effects of excess PTH on nonclassical target organs. **Am J Kidney Dis***,* 30 (5): 606-620

Brown, N. J. 2008. Aldosterone and vascular inflammation. **Hypertension***,* 51 (2): 161-167

Cecelja, M. & Chowienczyk, P. 2009. Dissociation of Aortic Pulse Wave Velocity With Risk Factors for Cardiovascular Disease Other Than Hypertension. A Systematic Review. **Hypertension***,*

Celermajer, D. S., Sorensen, K. E., Gooch, V. M., et al. 1992. Non-invasive detection of endothelial dysfunction in children and adults at risk of atherosclerosis. **Lancet***,* 340 (8828): 1111-1115

Celermajer, D. S., Sorensen, K. E., Spiegelhalter, D. J., et al. 1994. Aging is associated with endothelial dysfunction in healthy men years before the age-related decline in women. **J Am Coll Cardiol***,* 24 (2): 471-476

Chan, D. T., Watts, G. F., Irish, A. B., et al. 2011. Rosiglitazone does not improve vascular function in subjects with chronic kidney disease. **Nephrol Dial Transplant***,*

Chang, J. W., Lee, E. K., Kim, T. H., et al. 2007. Effects of alpha-lipoic acid on the plasma levels of asymmetric dimethylarginine in diabetic end-stage renal disease patients on hemodialysis: a pilot study. **Am J Nephrol***,* 27 (1): 70-74

Chavers, B. M., Michael, A. F., Weiland, D., et al. 1985. Urinary albumin excretion in renal transplant donors. **Am J Surg***,* 149 (3): 343-346

Chen, C. H., Nakayama, M., Nevo, E., et al. 1998. Coupled systolic-ventricular and vascular stiffening with age: implications for pressure regulation and cardiac reserve in the elderly. **J Am Coll Cardiol***,* 32 (5): 1221-1227

Cheng, S., Fernandes, V. R., Bluemke, D. A., et al. 2009. Age-related left ventricular remodeling and associated risk for cardiovascular outcomes: the Multi-Ethnic Study of Atherosclerosis. **Circ Cardiovasc Imaging***,* 2 (3): 191-198

Chertow, G. M., Block, G. A., Correa-Rotter, R., et al. 2012. Effect of cinacalcet on cardiovascular disease in patients undergoing dialysis. **N Engl J Med***,* 367 (26): 2482-2494

Chin, C. W., Shah, A. S., Mcallister, D. A., et al. 2014. High-sensitivity troponin I concentrations are a marker of an advanced hypertrophic response and adverse outcomes in patients with aortic stenosis. **Eur Heart J***,*

Chin, E. H., Hazzan, D., Edye, M., et al. 2009. The first decade of a laparoscopic donor nephrectomy program: effect of surgeon and institution experience with 512 cases from 1996 to 2006. **J Am Coll Surg***,* 209 (1): 106-113

Cho, G. Y., Marwick, T. H., Kim, H. S., et al. 2009. Global 2-dimensional strain as a new prognosticator in patients with heart failure. **J Am Coll Cardiol***,* 54 (7): 618-624

Choi, J. H., Kim, K. L., Huh, W., et al. 2004. Decreased number and impaired angiogenic function of endothelial progenitor cells in patients with chronic renal failure. **Arterioscler Thromb Vasc Biol***,* 24 (7): 1246-1252

Chue, C. D., Edwards, N. C., Ferro, C. J., et al. 2013a. Effects of age and chronic kidney disease on regional aortic distensibility: a cardiovascular magnetic resonance study. **Int J Cardiol***,* 168 (4): 4249-4254

Chue, C. D., Edwards, N. C., Moody, W. E., et al. 2012a. Serum phosphate is associated with left ventricular mass in patients with chronic kidney disease: a cardiac magnetic resonance study. **Heart***,* 98 (3): 219-224

Chue, C. D., Townend, J. N., Moody, W. E., et al. 2013b. Cardiovascular effects of sevelamer in stage 3 CKD. **J Am Soc Nephrol***,* 24 (5): 842-852

Chue, C. D., Townend, J. N., Steeds, R. P., et al. 2010. Arterial stiffness in chronic kidney disease: causes and consequences. **Heart***,* 96 (11): 817-823

Chue, C. D., Wall, N. A., Crabtree, N. J., et al. 2012b. Aortic calcification and femoral bone density are independently associated with left ventricular mass in patients with chronic kidney disease. **PLoS One***,* 7 (6): e39241

Claeys, M. J. 2014. High-sensitivity troponin: does it predict the shape of the iceberg underneath the surface? **Eur Heart J***,* 35 (34): 2273-2275

Cockcroft, D. W. & Gault, M. H. 1976. Prediction of creatinine clearance from serum creatinine. **Nephron***,* 16 (1): 31-41

Coresh, J., Astor, B. C., Greene, T., et al. 2003. Prevalence of chronic kidney disease and decreased kidney function in the adult US population: Third National Health and Nutrition Examination Survey. **Am J Kidney Dis***,* 41 (1): 1-12

Coresh, J., Longenecker, J. C., Miller, E. R., 3rd, et al. 1998. Epidemiology of cardiovascular risk factors in chronic renal disease. **J Am Soc Nephrol***,* 9 (12 Suppl): S24-30

Coresh, J., Selvin, E., Stevens, L. A., et al. 2007. Prevalence of chronic kidney disease in the United States. **JAMA***,* 298 (17): 2038-2047

Cupisti, A., Ghiadoni, L., D'Alessandro, C., et al. 2007. Soy protein diet improves endothelial dysfunction in renal transplant patients. **Nephrol Dial Transplant***,* 22 (1): 229-234

Dai, B., David, V., Martin, A., et al. 2012. A comparative transcriptome analysis identifying FGF23 regulated genes in the kidney of a mouse CKD model. **PLoS One***,* 7 (9): e44161

Davies, J. E., Parker, K. H., Francis, D. P., et al. 2008. What is the role of the aorta in directing coronary blood flow? **Heart***,* 94 (12): 1545-1547

De Lemos, J. A., Drazner, M. H., Omland, T., et al. 2010. Association of troponin T detected with a highly sensitive assay and cardiac structure and mortality risk in the general population. **JAMA***,* 304 (22): 2503-2512

Defilippi, C. R., De Lemos, J. A., Christenson, R. H., et al. 2010. Association of serial measures of cardiac troponin T using a sensitive assay with incident heart failure and cardiovascular mortality in older adults. **JAMA***,* 304 (22): 2494-2502

Del Vecchio, L., Procaccio, M., Vigano, S., et al. 2007. Mechanisms of disease: The role of aldosterone in kidney damage and clinical benefits of its blockade. **Nat Clin Pract Nephrol***,* 3 (1): 42-49

Dellegrottaglie, S., Sands, R. L., Gillespie, B. W., et al. 2011. Association between markers of collagen turnover, arterial stiffness and left ventricular hypertrophy in chronic kidney disease (CKD): the Renal Research Institute (RRI)-CKD study. **Nephrol Dial Transplant***,* 26 (9): 2891-2898

Descamps-Latscha, B., Witko-Sarsat, V., Nguyen-Khoa, T., et al. 2005. Advanced oxidation protein products as risk factors for atherosclerotic cardiovascular events in nondiabetic predialysis patients. **Am J Kidney Dis***,* 45 (1): 39-47

Di Angelantonio, E., Chowdhury, R., Sarwar, N., et al. 2010. Chronic kidney disease and risk of major cardiovascular disease and non-vascular mortality: prospective population based cohort study. **Bmj***,* 341 c4986

Di Marco, G. S., Reuter, S., Hillebrand, U., et al. 2009. The soluble VEGF receptor sFlt1 contributes to endothelial dysfunction in CKD. **J Am Soc Nephrol***,* 20 (10): 2235-2245

Donal, E., Mascle, S., Brunet, A., et al. 2012. Prediction of left ventricular ejection fraction 6 months after surgical correction of organic mitral regurgitation: the value of exercise echocardiography and deformation imaging. **Eur Heart J Cardiovasc Imaging***,* 13 (11): 922-930

Doucende, G., Schuster, I., Rupp, T., et al. 2010. Kinetics of left ventricular strains and torsion during incremental exercise in healthy subjects: the key role of torsional mechanics for systolic-diastolic coupling. **Circ Cardiovasc Imaging***,* 3 (5): 586-594

Downie, P. F., Talwar, S., Squire, I. B., et al. 1999. Assessment of the stability of N-terminal pro-brain natriuretic peptide in vitro: implications for assessment of left ventricular dysfunction. **Clin Sci (Lond)***,* 97 (3): 255-258

Edvardsen, T., Rosen, B. D., Pan, L., et al. 2006. Regional diastolic dysfunction in individuals with left ventricular hypertrophy measured by tagged magnetic resonance imaging--the Multi-Ethnic Study of Atherosclerosis (MESA). **Am Heart J***,* 151 (1): 109-114

Edwards, N. C., Ferro, C. J., Kirkwood, H., et al. 2010. Effect of spironolactone on left ventricular systolic and diastolic function in patients with early stage chronic kidney disease. **Am J Cardiol***,* 106 (10): 1505-1511

Edwards, N. C., Ferro, C. J., Townend, J. N., et al. 2008a. Aortic distensibility and arterial-ventricular coupling in early chronic kidney disease: a pattern resembling heart failure with preserved ejection fraction. **Heart***,* 94 (8): 1038-1043

Edwards, N. C., Hirth, A., Ferro, C. J., et al. 2008b. Subclinical abnormalities of left ventricular myocardial deformation in early-stage chronic kidney disease: the precursor of uremic cardiomyopathy? **J Am Soc Echocardiogr***,* 21 (12): 1293-1298

Edwards, N. C., Moody, W. E., Yuan, M., et al. 2015. Diffuse Interstitial Fibrosis and Myocardial Dysfunction in Early Chronic Kidney Disease. **Am J Cardiol***,*

Edwards, N. C., Steeds, R. P., Chue, C. D., et al. 2012. The safety and tolerability of spironolactone in patients with mild to moderate chronic kidney disease. **Br J Clin Pharmacol**, 73 (3): 447-454

Edwards, N. C., Steeds, R. P., Ferro, C. J., et al. 2006. The treatment of coronary artery disease in patients with chronic kidney disease. **QJM**, 99 (11): 723-736

Edwards, N. C., Steeds, R. P., Stewart, P. M., et al. 2009. Effect of spironolactone on left ventricular mass and aortic stiffness in early-stage chronic kidney disease: a randomized controlled trial. **J Am Coll Cardiol**, 54 (6): 505-512

Eknoyan, G., Lameire, N., Barsoum, R., et al. 2004. The burden of kidney disease: improving global outcomes. **Kidney Int**, 66 (4): 1310-1314

Endemann, D. H. & Schiffrin, E. L. 2004. Endothelial dysfunction. **J Am Soc Nephrol**, 15 (8): 1983-1992

Fang, J. & Alderman, M. H. 2000. Serum uric acid and cardiovascular mortality the NHANES I epidemiologic follow-up study, 1971-1992. National Health and Nutrition Examination Survey. **JAMA**, 283 (18): 2404-2410

Farquharson, C. A. & Struthers, A. D. 2000. Spironolactone increases nitric oxide bioactivity, improves endothelial vasodilator dysfunction, and suppresses vascular angiotensin I/angiotensin II conversion in patients with chronic heart failure. **Circulation**, 101 (6): 594-597

Faul, C., Amaral, A. P., Oskouei, B., et al. 2011. FGF23 induces left ventricular hypertrophy. **J Clin Invest**, 121 (11): 4393-4408

Fehrman-Ekholm, I., Elinder, C. G., Stenbeck, M., et al. 1997. Kidney donors live longer. **Transplantation**, 64 (7): 976-978

Feig, D. I. & Johnson, R. J. 2003. Hyperuricemia in childhood primary hypertension. **Hypertension**, 42 (3): 247-252

Ferreira, J. C., Brum, P. C. & Mochly-Rosen, D. 2011. betaIIPKC and epsilonPKC isozymes as potential pharmacological targets in cardiac hypertrophy and heart failure. **J Mol Cell Cardiol**, 51 (4): 479-484

Ferro, C. J., Chue, C. D., De Belder, M. A., et al. 2015. Impact of renal function on survival after transcatheter aortic valve implantation (TAVI): an analysis of the UK TAVI registry. **Heart**,

Fesler, P., Mourad, G., Du Cailar, G., et al. 2015. Arterial stiffness : an independent determinant of adaptive glomerular hyperfiltration after kidney donation. **Am J Physiol Renal Physiol**, ajprenal 00524 02014

Foley, R. N., Murray, A. M., Li, S., et al. 2005. Chronic kidney disease and the risk for cardiovascular disease, renal replacement, and death in the United States Medicare population, 1998 to 1999. **J Am Soc Nephrol**, 16 (2): 489-495

Foley, R. N., Parfrey, P. S., Harnett, J. D., et al. 1995. The prognostic importance of left ventricular geometry in uremic cardiomyopathy. **J Am Soc Nephrol**, 5 (12): 2024-2031

Foley, R. N., Parfrey, P. S., Morgan, J., et al. 2000. Effect of hemoglobin levels in hemodialysis patients with asymptomatic cardiomyopathy. **Kidney Int**, 58 (3): 1325-1335

Forbat, S. M., Mohiaddin, R. H., Yang, G. Z., et al. 1995. Measurement of regional aortic compliance by MR imaging: a study of reproducibility. **J Magn Reson Imaging**, 5 (6): 635-639

Ford, M. L., Tomlinson, L. A., Chapman, T. P., et al. 2010. Aortic stiffness is independently associated with rate of renal function decline in chronic kidney disease stages 3 and 4. **Hypertension**, 55 (5): 1110-1115

Fox, C. S., Matsushita, K., Woodward, M., et al. 2012. Associations of kidney disease measures with mortality and end-stage renal disease in individuals with and without diabetes: a meta-analysis. **Lancet**, 380 (9854): 1662-1673

Fratz, S., Chung, T., Greil, G. F., et al. 2013. Guidelines and protocols for cardiovascular magnetic resonance in children and adults with congenital heart disease: SCMR expert consensus group on congenital heart disease. **J Cardiovasc Magn Reson**, 15: 51

Frimodt-Moller, M., Nielsen, A. H., Kamper, A. L., et al. 2008. Reproducibility of pulse-wave analysis and pulse-wave velocity determination in chronic kidney disease. **Nephrol Dial Transplant**, 23 (2): 594-600

Funder, J. W. 2010. Minireview: Aldosterone and mineralocorticoid receptors: past, present, and future. **Endocrinology**, 151 (11): 5098-5102

Furchgott, R. F. & Zawadzki, J. V. 1980. The obligatory role of endothelial cells in the relaxation of arterial smooth muscle by acetylcholine. **Nature**, 288 (5789): 373-376

Ganesh, S. K., Stack, A. G., Levin, N. W., et al. 2001. Association of elevated serum PO(4), Ca x PO(4) product, and parathyroid hormone with cardiac mortality risk in chronic hemodialysis patients. **J Am Soc Nephrol**, 12 (10): 2131-2138

Gansevoort, R. T., Verhave, J. C., Hillege, H. L., et al. 2005. The validity of screening based on spot morning urine samples to detect subjects with microalbuminuria in the general population. **Kidney Int Suppl**, (94): S28-35

Garcia, J. F., Ebbe, S. N., Hollander, L., et al. 1982. Radioimmunoassay of erythropoietin: circulating levels in normal and polycythemic human beings. **J Lab Clin Med**, 99 (5): 624-635

Garg, A. X., Meirambayeva, A., Huang, A., et al. 2012. Cardiovascular disease in kidney donors: matched cohort study. **Bmj**, 344 e1203

Garg, A. X., Muirhead, N., Knoll, G., et al. 2006. Proteinuria and reduced kidney function in living kidney donors: A systematic review, meta-analysis, and meta-regression. **Kidney Int**, 70 (10): 1801-1810

Garg, A. X., Nevis, I. F., Mcarthur, E., et al. 2015. Gestational hypertension and preeclampsia in living kidney donors. **N Engl J Med**, 372 (2): 124-133

Garg, A. X., Prasad, G. V., Thiessen-Philbrook, H. R., et al. 2008. Cardiovascular disease and hypertension risk in living kidney donors: an analysis of health administrative data in Ontario, Canada. **Transplantation**, 86 (3): 399-406

Gersch, C., Palii, S. P., Kim, K. M., et al. 2008. Inactivation of nitric oxide by uric acid. **Nucleosides Nucleotides Nucleic Acids**, 27 (8): 967-978

Geyer, H., Caracciolo, G., Abe, H., et al. 2010. Assessment of myocardial mechanics using speckle tracking echocardiography: fundamentals and clinical applications. **J Am Soc Echocardiogr**, 23 (4): 351-369; quiz 453-355

Giannitsis, E., Kurz, K., Hallermayer, K., et al. 2010. Analytical validation of a high-sensitivity cardiac troponin T assay. **Clin Chem***,* 56 (2): 254-261

Go, A. S., Chertow, G. M., Fan, D., et al. 2004. Chronic kidney disease and the risks of death, cardiovascular events, and hospitalization. **N Engl J Med***,* 351 (13): 1296-1305

Goicoechea, M., De Vinuesa, S. G., Gomez-Campdera, F., et al. 2008. Serum fibrinogen levels are an independent predictor of mortality in patients with chronic kidney disease (CKD) stages 3 and 4. **Kidney Int Suppl***,* (111): S67-70

Gossmann, J., Wilhelm, A., Kachel, H. G., et al. 2005. Long-term consequences of live kidney donation follow-up in 93% of living kidney donors in a single transplant center. **Am J Transplant***,* 5 (10): 2417-2424

Greene, E. L., Kren, S. & Hostetter, T. H. 1996. Role of aldosterone in the remnant kidney model in the rat. **J Clin Invest***,* 98 (4): 1063-1068

Groenink, M., De Roos, A., Mulder, B. J., et al. 1998. Changes in aortic distensibility and pulse wave velocity assessed with magnetic resonance imaging following beta-blocker therapy in the Marfan syndrome. **Am J Cardiol***,* 82 (2): 203-208

Grothues, F., Smith, G. C., Moon, J. C., et al. 2002. Comparison of interstudy reproducibility of cardiovascular magnetic resonance with two-dimensional echocardiography in normal subjects and in patients with heart failure or left ventricular hypertrophy. **Am J Cardiol***,* 90 (1): 29-34

Guerin, A. P., Blacher, J., Pannier, B., et al. 2001. Impact of aortic stiffness attenuation on survival of patients in end-stage renal failure. **Circulation***,* 103 (7): 987-992

Guo, Q., Carrero, J. J., Yu, X., et al. 2009. Associations of VEGF and its receptors sVEGFR-1 and -2 with cardiovascular disease and survival in prevalent haemodialysis patients. **Nephrol Dial Transplant***,* 24 (11): 3468-3473

Habibi, M., Chahal, H., Opdahl, A., et al. 2014. Association of CMR-measured LA function with heart failure development: results from the MESA study. **JACC Cardiovasc Imaging***,* 7 (6): 570-579

Hakim, R. M., Goldszer, R. C. & Brenner, B. M. 1984. Hypertension and proteinuria: long-term sequelae of uninephrectomy in humans. **Kidney Int***,* 25 (6): 930-936

Han, S. H., Kang, E. W., Yoon, S. J., et al. 2011. Combined vascular effects of HMG-CoA reductase inhibitor and angiotensin receptor blocker in non-diabetic patients undergoing peritoneal dialysis. **Nephrol Dial Transplant***,*

Hankiewicz, J. H., Goldspink, P. H., Buttrick, P. M., et al. 2008. Principal strain changes precede ventricular wall thinning during transition to heart failure in a mouse model of dilated cardiomyopathy. **Am J Physiol Heart Circ Physiol***,* 294 (1): H330-336

Hanna, E. B., Chen, A. Y., Roe, M. T., et al. 2011. Characteristics and in-hospital outcomes of patients with non-ST-segment elevation myocardial infarction and chronic kidney disease undergoing percutaneous coronary intervention. **JACC Cardiovasc Interv***,* 4 (9): 1002-1008

Harnett, J. D., Parfrey, P. S., Griffiths, S. M., et al. 1988. Left ventricular hypertrophy in end-stage renal disease. **Nephron***,* 48 (2): 107-115

Harrild, D. M., Han, Y., Geva, T., et al. 2012. Comparison of cardiac MRI tissue tracking and myocardial tagging for assessment of regional ventricular strain. **Int J Cardiovasc Imaging***,* 28 (8): 2009-2018

Hekimian, G., Boutten, A., Flamant, M., et al. 2013. Progression of aortic valve stenosis is associated with bone remodelling and secondary hyperparathyroidism in elderly patients--the COFRASA study. **Eur Heart J***,* 34 (25): 1915-1922

Hendel, R. C., Patel, M. R., Kramer, C. M., et al. 2006. ACCF/ACR/SCCT/SCMR/ASNC/NASCI/SCAI/SIR 2006 appropriateness criteria for cardiac computed tomography and cardiac magnetic resonance imaging: a report of the American College of Cardiology Foundation Quality Strategic Directions Committee Appropriateness Criteria Working Group, American College of Radiology, Society of Cardiovascular Computed Tomography, Society for Cardiovascular Magnetic Resonance, American Society of Nuclear Cardiology, North American Society for Cardiac Imaging, Society for Cardiovascular Angiography and Interventions, and Society of Interventional Radiology. **J Am Coll Cardiol***,* 48 (7): 1475-1497

Henry, R. M., Kamp, O., Kostense, P. J., et al. 2005. Mild renal insufficiency is associated with increased left ventricular mass in men, but not in women: an arterial stiffness-related phenomenon--the Hoorn Study. **Kidney Int***,* 68 (2): 673-679

Herzog, C. A., Ma, J. Z. & Collins, A. J. 1998. Poor long-term survival after acute myocardial infarction among patients on long-term dialysis. **N Engl J Med***,* 339 (12): 799-805

Heywood, J. T. B. J. C. J. (ed.) 2012. **The Cardiorenal Syndrome: A Clinician's Guide to Pathophysiology and Management***,* Minneapolis: Cardiotext Publishing.

Hill, N. R., Lasserson, D., Thompson, B., et al. 2014. Benefits of Aldosterone Receptor Antagonism in Chronic Kidney Disease (BARACK D) trial-a multi-centre, prospective, randomised, open, blinded end-point, 36-month study of 2,616 patients within primary care with stage 3b chronic kidney disease to compare the efficacy of spironolactone 25 mg once daily in addition to routine care on mortality and cardiovascular outcomes versus routine care alone: study protocol for a randomized controlled trial. **Trials***,* 15: 160

Hor, K. N., Baumann, R., Pedrizzetti, G., et al. 2011. Magnetic resonance derived myocardial strain assessment using feature tracking. **J Vis Exp***,* (48):

Hor, K. N., Gottliebson, W. M., Carson, C., et al. 2010. Comparison of magnetic resonance feature tracking for strain calculation with harmonic phase imaging analysis. **JACC Cardiovasc Imaging***,* 3 (2): 144-151

Horvat, L. D., Shariff, S. Z. & Garg, A. X. 2009. Global trends in the rates of living kidney donation. **Kidney Int***,* 75 (10): 1088-1098

Hostetter, T. H., Olson, J. L., Rennke, H. G., et al. 1981. Hyperfiltration in remnant nephrons: a potentially adverse response to renal ablation. **Am J Physiol***,* 241 (1): F85-93

Howard, G., Sharrett, A. R., Heiss, G., et al. 1993. Carotid artery intimal-medial thickness distribution in general populations as evaluated by B-mode ultrasound. ARIC Investigators. **Stroke***,* 24 (9): 1297-1304

Huan, Y., Kapoor, S., Deloach, S., et al. 2013. Changes in biomarkers associated with living kidney donation. **Am J Nephrol***,* 38 (3): 212-217

Hudsmith, L. E., Cheng, A. S., Tyler, D. J., et al. 2007. Assessment of left atrial volumes at 1.5 Tesla and 3 Tesla using FLASH and SSFP cine imaging. **J Cardiovasc Magn Reson***,* 9 (4): 673-679

Hudsmith, L. E., Petersen, S. E., Francis, J. M., et al. 2005. Normal human left and right ventricular and left atrial dimensions using steady state free precession magnetic resonance imaging. **J Cardiovasc Magn Reson***,* 7 (5): 775-782

Ibrahim, H. N., Foley, R., Tan, L., et al. 2009. Long-term consequences of kidney donation. **N Engl J Med***,* 360 (5): 459-469

Ibrahim, H. N., Kukla, A., Cordner, G., et al. 2010. Diabetes after kidney donation. **Am J Transplant***,* 10 (2): 331-337

Imaram, W., Gersch, C., Kim, K. M., et al. 2010. Radicals in the reaction between peroxynitrite and uric acid identified by electron spin resonance spectroscopy and liquid chromatography mass spectrometry. **Free Radic Biol Med***,* 49 (2): 275-281

Iskandrian, A. E., Hage, F. G., Shaw, L. J., et al. 2014. Serial myocardial perfusion imaging: defining a significant change and targeting management decisions. **JACC Cardiovasc Imaging***,* 7 (1): 79-96

Ix, J. H., Katz, R., Kestenbaum, B. R., et al. 2012. Fibroblast growth factor-23 and death, heart failure, and cardiovascular events in community-living individuals: CHS (Cardiovascular Health Study). **J Am Coll Cardiol***,* 60 (3): 200-207

Jackson, C. E., Shirodaria, C. C., Lee, J. M., et al. 2009. Reproducibility and accuracy of automated measurement for dynamic arterial lumen area by cardiovascular magnetic resonance. **Int J Cardiovasc Imaging***,* 25 (8): 797-808

Jafar, T. H., Stark, P. C., Schmid, C. H., et al. 2003. Progression of chronic kidney disease: the role of blood pressure control, proteinuria, and angiotensin-converting enzyme inhibition: a patient-level meta-analysis. **Ann Intern Med***,* 139 (4): 244-252

Jalal, D. I., Chonchol, M., Chen, W., et al. 2013. Uric acid as a target of therapy in CKD. **Am J Kidney Dis***,* 61 (1): 134-146

JBS3 2014. Joint British Societies' consensus recommendations for the prevention of cardiovascular disease (JBS3). **Heart***,* 100 Suppl 2 ii1-ii67

Jean, G., Terrat, J. C., Vanel, T., et al. 2009. High levels of serum fibroblast growth factor (FGF)-23 are associated with increased mortality in long haemodialysis patients. **Nephrol Dial Transplant***,* 24 (9): 2792-2796

Jellis, C., Martin, J., Narula, J., et al. 2010. Assessment of nonischemic myocardial fibrosis. **J Am Coll Cardiol***,* 56 (2): 89-97

Jie, K. E., Zaikova, M. A., Bergevoet, M. W., et al. 2010. Progenitor cells and vascular function are impaired in patients with chronic kidney disease. **Nephrol Dial Transplant**, 25 (6): 1875-1882

Joannides, R., Haefeli, W. E., Linder, L., et al. 1995. Nitric oxide is responsible for flow-dependent dilatation of human peripheral conduit arteries in vivo. **Circulation**, 91 (5): 1314-1319

Kalantar-Zadeh, K., Block, G., Humphreys, M. H., et al. 2003. Reverse epidemiology of cardiovascular risk factors in maintenance dialysis patients. **Kidney Int**, 63 (3): 793-808

Kalantar-Zadeh, K., Brennan, M. L. & Hazen, S. L. 2006. Serum myeloperoxidase and mortality in maintenance hemodialysis patients. **Am J Kidney Dis**, 48 (1): 59-68

Kanbay, M., Nicoleta, M., Selcoki, Y., et al. 2010. Fibroblast growth factor 23 and fetuin A are independent predictors for the coronary artery disease extent in mild chronic kidney disease. **Clin J Am Soc Nephrol**, 5 (10): 1780-1786

Kanbay, M., Segal, M., Afsar, B., et al. 2013. The role of uric acid in the pathogenesis of human cardiovascular disease. **Heart**, 99 (11): 759-766

Kanbay, M., Yilmaz, M. I., Sonmez, A., et al. 2011. Serum uric Acid level and endothelial dysfunction in patients with nondiabetic chronic kidney disease. **Am J Nephrol**, 33 (4): 298-304

Kane, G. C., Karon, B. L., Mahoney, D. W., et al. 2011. Progression of left ventricular diastolic dysfunction and risk of heart failure. **JAMA**, 306 (8): 856-863

Kang, D. H., Hughes, J., Mazzali, M., et al. 2001. Impaired angiogenesis in the remnant kidney model: II. Vascular endothelial growth factor administration reduces renal fibrosis and stabilizes renal function. **J Am Soc Nephrol**, 12 (7): 1448-1457

Kao, M. P., Ang, D. S., Gandy, S. J., et al. 2011. Allopurinol benefits left ventricular mass and endothelial dysfunction in chronic kidney disease. **J Am Soc Nephrol**, 22 (7): 1382-1389

Kasiske, B. L., Anderson-Haag, T., Ibrahim, H. N., et al. 2013. A Prospective Controlled Study of Kidney Donors: Baseline and 6-Month Follow-up. **Am J Kidney Dis**, 62 (3): 577-586

KDIGO 2012. Kidney Disease: Improving Global Outcomes (KDIGO) CKD Work Group. KDIGO 2012 Clinical Practice Guideline for the Evaluation and Management of Chronic Kidney Disease. **Kidney Int**, 3 (Suppl 1): S1-150

KDOQI 2006. KDOQI Clinical Practice Guidelines and Clinical Practice Recommendations for Anemia in Chronic Kidney Disease. **Am J Kidney Dis**, 47 (5 Suppl 3): S11-145

Kempny, A., Fernandez-Jimenez, R., Orwat, S., et al. 2012. Quantification of biventricular myocardial function using cardiac magnetic resonance feature tracking, endocardial border delineation and echocardiographic speckle tracking in patients with repaired tetralogy of Fallot and healthy controls. **J Cardiovasc Magn Reson**, 14: 32

Kestenbaum, B., Katz, R., De Boer, I., et al. 2011. Vitamin D, parathyroid hormone, and cardiovascular events among older adults. **J Am Coll Cardiol***,* 58 (14): 1433-1441

Ketteler, M., Bongartz, P., Westenfeld, R., et al. 2003. Association of low fetuin-A (AHSG) concentrations in serum with cardiovascular mortality in patients on dialysis: a cross-sectional study. **Lancet***,* 361 (9360): 827-833

Kielstein, J. T., Boger, R. H., Bode-Boger, S. M., et al. 2002. Marked increase of asymmetric dimethylarginine in patients with incipient primary chronic renal disease. **J Am Soc Nephrol***,* 13 (1): 170-176

Kjekshus, J., Apetrei, E., Barrios, V., et al. 2007. Rosuvastatin in older patients with systolic heart failure. **N Engl J Med***,* 357 (22): 2248-2261

Klausen, K., Borch-Johnsen, K., Feldt-Rasmussen, B., et al. 2004. Very low levels of microalbuminuria are associated with increased risk of coronary heart disease and death independently of renal function, hypertension, and diabetes. **Circulation***,* 110 (1): 32-35

Knoll, G. 2008. Trends in kidney transplantation over the past decade. **Drugs***,* 68 Suppl 1 3-10

Kralisch, S., Ziegelmeier, M., Bachmann, A., et al. 2008. Serum levels of the atherosclerosis biomarker sTWEAK are decreased in type 2 diabetes and end-stage renal disease. **Atherosclerosis***,* 199 (2): 440-444

Krohn, A. G., Ogden, D. A. & Holmes, J. H. 1966. Renal function in 29 healthy adults before and after nephrectomy. **JAMA***,* 196 (4): 322-324

Kumai, Y., Kamouchi, M., Hata, J., et al. 2012. Proteinuria and clinical outcomes after ischemic stroke. **Neurology***,*

Kurth, T., De Jong, P. E., Cook, N. R., et al. 2009. Kidney function and risk of cardiovascular disease and mortality in women: a prospective cohort study. **Bmj***,* 338 b2392

Kuzkaya, N., Weissmann, N., Harrison, D. G., et al. 2005. Interactions of peroxynitrite with uric acid in the presence of ascorbate and thiols: implications for uncoupling endothelial nitric oxide synthase. **Biochem Pharmacol***,* 70 (3): 343-354

Lacolley, P., Labat, C., Pujol, A., et al. 2002. Increased carotid wall elastic modulus and fibronectin in aldosterone-salt-treated rats: effects of eplerenone. **Circulation***,* 106 (22): 2848-2853

Laflamme, M. H., Mahjoub, H., Mahmut, A., et al. 2014. Parathyroid hormone is associated with the LV mass after aortic valve replacement. **Heart***,*

Lajer, M., Tarnow, L., Jorsal, A., et al. 2008. Plasma concentration of asymmetric dimethylarginine (ADMA) predicts cardiovascular morbidity and mortality in type 1 diabetic patients with diabetic nephropathy. **Diabetes Care***,* 31 (4): 747-752

Lang, R. M., Bierig, M., Devereux, R. B., et al. 2005. Recommendations for chamber quantification: a report from the American Society of Echocardiography's Guidelines and Standards Committee and the Chamber Quantification Writing Group, developed in conjunction with the European Association of

Echocardiography, a branch of the European Society of Cardiology. **J Am Soc Echocardiogr**, 18 (12): 1440-1463

Latham, R. D., Westerhof, N., Sipkema, P., et al. 1985. Regional wave travel and reflections along the human aorta: a study with six simultaneous micromanometric pressures. **Circulation**, 72 (6): 1257-1269

Laupacis, A., Keown, P., Pus, N., et al. 1996. A study of the quality of life and cost-utility of renal transplantation. **Kidney Int**, 50 (1): 235-242

Laurent, S., Cockcroft, J., Van Bortel, L., et al. 2006. Expert consensus document on arterial stiffness: methodological issues and clinical applications. **Eur Heart J**, 27 (21): 2588-2605

Lawes, C. M., Vander Hoorn, S. & Rodgers, A. 2008. Global burden of blood-pressure-related disease, 2001. **Lancet**, 371 (9623): 1513-1518

Lentine, K. L., Schnitzler, M. A., Xiao, H., et al. 2010. Racial variation in medical outcomes among living kidney donors. **N Engl J Med**, 363 (8): 724-732

Leskinen, Y., Lehtimaki, T., Loimaala, A., et al. 2003. Carotid atherosclerosis in chronic renal failure-the central role of increased plaque burden. **Atherosclerosis**, 171 (2): 295-302

Levey, A. S., Stevens, L. A., Schmid, C. H., et al. 2009. A new equation to estimate glomerular filtration rate. **Ann Intern Med**, 150 (9): 604-612

Levin, A., Djurdjev, O., Beaulieu, M., et al. 2008. Variability and risk factors for kidney disease progression and death following attainment of stage 4 CKD in a referred cohort. **Am J Kidney Dis**, 52 (4): 661-671

Levin, A., Thompson, C. R., Ethier, J., et al. 1999. Left ventricular mass index increase in early renal disease: impact of decline in hemoglobin. **Am J Kidney Dis**, 34 (1): 125-134

Levy, D., Garrison, R. J., Savage, D. D., et al. 1990. Prognostic implications of echocardiographically determined left ventricular mass in the Framingham Heart Study. **N Engl J Med**, 322 (22): 1561-1566

Lewington, S., Clarke, R., Qizilbash, N., et al. 2002. Age-specific relevance of usual blood pressure to vascular mortality: a meta-analysis of individual data for one million adults in 61 prospective studies. **Lancet**, 360 (9349): 1903-1913

Li, B., Liu, Y., Occleshaw, C. J., et al. 2010. In-line automated tracking for ventricular function with magnetic resonance imaging. **JACC Cardiovasc Imaging**, 3 (8): 860-866

Li, B., Young, A. A. & Cowan, B. R. 2008. GPU accelerated non-rigid registration for the evaluation of cardiac function. **Med Image Comput Comput Assist Interv**, 11 (Pt 2): 880-887

Liabeuf, S., Barreto, D. V., Barreto, F. C., et al. 2010. Free p-cresylsulphate is a predictor of mortality in patients at different stages of chronic kidney disease. **Nephrol Dial Transplant**, 25 (4): 1183-1191

Liese, A. D., Hense, H. W., Lowel, H., et al. 1999. Association of serum uric acid with all-cause and cardiovascular disease mortality and incident myocardial infarction in the MONICA Augsburg cohort. World Health Organization Monitoring Trends and Determinants in Cardiovascular Diseases. **Epidemiology**, 10 (4): 391-397

Lilitkarntakul, P., Dhaun, N., Melville, V., et al. 2011. Blood pressure and not uraemia is the major determinant of arterial stiffness and endothelial dysfunction in patients with chronic kidney disease and minimal co-morbidity. **Atherosclerosis**, 216 (1): 217-225

Lim, K., Lu, T. S., Molostvov, G., et al. 2012. Vascular Klotho deficiency potentiates the development of human artery calcification and mediates resistance to fibroblast growth factor 23. **Circulation**, 125 (18): 2243-2255

Lindeman, R. D., Tobin, J. & Shock, N. W. 1985. Longitudinal studies on the rate of decline in renal function with age. **J Am Geriatr Soc**, 33 (4): 278-285

Litwin, M. & Niemirska, A. 2009. Intima-media thickness measurements in children with cardiovascular risk factors. **Pediatr Nephrol**, 24 (4): 707-719

Litwin, M., Wuhl, E., Jourdan, C., et al. 2008. Evolution of large-vessel arteriopathy in paediatric patients with chronic kidney disease. **Nephrol Dial Transplant**, 23 (8): 2552-2557

Lobysheva, I., Rath, G., Sekkali, B., et al. 2011. Moderate Caveolin-1 Downregulation Prevents NADPH Oxidase-Dependent Endothelial Nitric Oxide Synthase Uncoupling by Angiotensin II in Endothelial Cells. **Arterioscler Thromb Vasc Biol**,

Loffredo, F. S., Steinhauser, M. L., Jay, S. M., et al. 2013. Growth differentiation factor 11 is a circulating factor that reverses age-related cardiac hypertrophy. **Cell**, 153 (4): 828-839

London, G. 2001. Pathophysiology of cardiovascular damage in the early renal population. **Nephrol Dial Transplant**, 16 Suppl 2 3-6

London, G., Guerin, A., Pannier, B., et al. 1992. Increased systolic pressure in chronic uremia. Role of arterial wave reflections. **Hypertension**, 20 (1): 10-19

London, G. M., Guerin, A. P., Marchais, S. J., et al. 1996. Cardiac and arterial interactions in end-stage renal disease. **Kidney Int**, 50 (2): 600-608

Lorenzen, J., David, S., Bahlmann, F. H., et al. 2010. Endothelial progenitor cells and cardiovascular events in patients with chronic kidney disease--a prospective follow-up study. **PLoS One**, 5 (7): e11477

Lote, C. J. (ed.) 2012. **Principles of Renal Physiology**, New York, U.S.: Springer.

Lu, T. M., Ding, Y. A., Leu, H. B., et al. 2004. Effect of rosuvastatin on plasma levels of asymmetric dimethylarginine in patients with hypercholesterolemia. **Am J Cardiol**, 94 (2): 157-161

Ludmer, P. L., Selwyn, A. P., Shook, T. L., et al. 1986. Paradoxical vasoconstriction induced by acetylcholine in atherosclerotic coronary arteries. **N Engl J Med**, 315 (17): 1046-1051

Luksha, N., Luksha, L., Carrero, J. J., et al. 2011. Impaired resistance artery function in patients with end-stage renal disease. **Clin Sci (Lond)**, 120 (12): 525-536

Luther, J. M., Luo, P., Wang, Z., et al. 2012. Aldosterone deficiency and mineralocorticoid receptor antagonism prevent angiotensin II-induced cardiac, renal, and vascular injury. **Kidney Int**,

Lutsey, P. L., Alonso, A., Selvin, E., et al. 2014. Fibroblast growth factor-23 and incident coronary heart disease, heart failure, and cardiovascular mortality:

the Atherosclerosis Risk in Communities study. **J Am Heart Assoc***,* 3 (3): e000936

Maceira, A. M., Prasad, S. K., Khan, M., et al. 2006. Normalized left ventricular systolic and diastolic function by steady state free precession cardiovascular magnetic resonance. **J Cardiovasc Magn Reson***,* 8 (3): 417-426

Mackie, F. E., Rosenberg, A. R., Harmer, J. A., et al. 2010. HMG CoA reductase inhibition and endothelial function in children with chronic kidney disease (CKD)--a pilot study. **Acta Paediatr***,* 99 (3): 457-459

Macwalter, R. S., Wong, S. Y., Wong, K. Y., et al. 2002. Does renal dysfunction predict mortality after acute stroke? A 7-year follow-up study. **Stroke***,* 33 (6): 1630-1635

Mafham, M., Emberson, J., Landray, M. J., et al. 2011. Estimated glomerular filtration rate and the risk of major vascular events and all-cause mortality: a meta-analysis. **PLoS One***,* 6 (10): e25920

Mahmoodi, B. K., Matsushita, K., Woodward, M., et al. 2012. Associations of kidney disease measures with mortality and end-stage renal disease in individuals with and without hypertension: a meta-analysis. **Lancet***,* 380 (9854): 1649-1661

Makita, Z., Radoff, S., Rayfield, E. J., et al. 1991. Advanced glycosylation end products in patients with diabetic nephropathy. **N Engl J Med***,* 325 (12): 836-842

Mallamaci, F., Benedetto, F. A., Tripepi, G., et al. 2008. Vascular endothelial growth factor, left ventricular dysfunction and mortality in hemodialysis patients. **J Hypertens***,* 26 (9): 1875-1882

Mark, P. B., Johnston, N., Groenning, B. A., et al. 2006. Redefinition of uremic cardiomyopathy by contrast-enhanced cardiac magnetic resonance imaging. **Kidney Int***,* 69 (10): 1839-1845

Maron, B. J., Towbin, J. A., Thiene, G., et al. 2006. Contemporary definitions and classification of the cardiomyopathies: an American Heart Association Scientific Statement from the Council on Clinical Cardiology, Heart Failure and Transplantation Committee; Quality of Care and Outcomes Research and Functional Genomics and Translational Biology Interdisciplinary Working Groups; and Council on Epidemiology and Prevention. **Circulation***,* 113 (14): 1807-1816

Martensson, J., Groth, S., Rehling, M., et al. 1998. Chromium-51-EDTA clearance in adults with a single-plasma sample. **J Nucl Med***,* 39 (12): 2131-2137

Martin, A., David, V. & Quarles, L. D. 2012a. Regulation and function of the FGF23/klotho endocrine pathways. **Physiol Rev***,* 92 (1): 131-155

Martin, F. L., Huntley, B. K., Korinek, J., et al. 2008. New Insights into the Kidney-Heart Connection: Mild Renal Insufficiency Induces Cardiac Fibrosis and Diastolic Dysfunction Followed by Late Systolic Impairment. **Circulation***,* 118 S334-S335

Martin, F. L., Mckie, P. M., Cataliotti, A., et al. 2012b. Experimental mild renal insufficiency mediates early cardiac apoptosis, fibrosis, and diastolic

dysfunction: a kidney-heart connection. **Am J Physiol Regul Integr Comp Physiol**, 302 (2): R292-299

Mathew, J. S., Sachs, M. C., Katz, R., et al. 2014. Fibroblast growth factor-23 and incident atrial fibrillation: the Multi-Ethnic Study of Atherosclerosis (MESA) and the Cardiovascular Health Study (CHS). **Circulation**, 130 (4): 298-307

Matsumoto, Y., Mori, Y., Kageyama, S., et al. 2014. Spironolactone reduces cardiovascular and cerebrovascular morbidity and mortality in hemodialysis patients. **J Am Coll Cardiol**, 63 (6): 528-536

Matsushita, K., Van Der Velde, M., Astor, B. C., et al. 2010. Association of estimated glomerular filtration rate and albuminuria with all-cause and cardiovascular mortality in general population cohorts: a collaborative meta-analysis. **Lancet**, 375 (9731): 2073-2081

Mccullough, P. A., Jurkovitz, C. T., Pergola, P. E., et al. 2007. Independent components of chronic kidney disease as a cardiovascular risk state: results from the Kidney Early Evaluation Program (KEEP). **Arch Intern Med**, 167 (11): 1122-1129

Mcgonigle, R. J., Wallin, J. D., Shadduck, R. K., et al. 1984. Erythropoietin deficiency and inhibition of erythropoiesis in renal insufficiency. **Kidney Int**, 25 (2): 437-444

Meier-Kriesche, H. U. & Kaplan, B. 2002. Waiting time on dialysis as the strongest modifiable risk factor for renal transplant outcomes: a paired donor kidney analysis. **Transplantation**, 74 (10): 1377-1381

Meijers, B. K., Bammens, B., De Moor, B., et al. 2008. Free p-cresol is associated with cardiovascular disease in hemodialysis patients. **Kidney Int**, 73 (10): 1174-1180

Menon, V., Greene, T., Wang, X., et al. 2005. C-reactive protein and albumin as predictors of all-cause and cardiovascular mortality in chronic kidney disease. **Kidney Int**, 68 (2): 766-772

Merino, A., Portoles, J., Selgas, R., et al. 2010. Effect of different dialysis modalities on microinflammatory status and endothelial damage. **Clin J Am Soc Nephrol**, 5 (2): 227-234

Miao, Y., Ottenbros, S. A., Laverman, G. D., et al. 2011. Effect of a reduction in uric acid on renal outcomes during losartan treatment: a post hoc analysis of the reduction of endpoints in non-insulin-dependent diabetes mellitus with the Angiotensin II Antagonist Losartan Trial. **Hypertension**, 58 (1): 2-7

Michels, W. M., Grootendorst, D. C., Verduijn, M., et al. 2010. Performance of the Cockcroft-Gault, MDRD, and new CKD-EPI formulas in relation to GFR, age, and body size. **Clin J Am Soc Nephrol**, 5 (6): 1003-1009

Mishra, R. K., Li, Y., Defilippi, C., et al. 2013. Association of cardiac troponin T with left ventricular structure and function in CKD. **Am J Kidney Dis**, 61 (5): 701-709

Mitani, H., Ishizaka, N., Aizawa, T., et al. 2002. In vivo klotho gene transfer ameliorates angiotensin II-induced renal damage. **Hypertension**, 39 (4): 838-843

Mjoen, G., Hallan, S., Hartmann, A., et al. 2013. Long-term risks for kidney donors. **Kidney Int***,*

Mjoen, G., Midtvedt, K., Holme, I., et al. 2010. One- and five-year follow-ups on blood pressure and renal function in kidney donors. **Transpl Int***,*

Mjoen, G., Reisaeter, A., Hallan, S., et al. 2012. Overall and cardiovascular mortality in Norwegian kidney donors compared to the background population. **Nephrol Dial Transplant***,* 27 (1): 443-447

Moody, W. E., Begaj, I., Banerjee, A., Chue, C.D., Edwards, N.C., Steeds, R.P., Ferro, C.J., Townend, J.N. 2013. Long-term cardiovascular outcomes in UK living kidney donors. **Eur Heart J***,* 34 (suppl 1): P5161

Moody, W. E., Chue, C. D., Inston, N. G., et al. 2012a. Understanding the effects of chronic kidney disease on cardiovascular risk: are there lessons to be learnt from healthy kidney donors? **J Hum Hypertens***,* 26 (3): 141-148

Moody, W. E., Edwards, N. C., Chue, C. D., et al. 2013. Arterial disease in chronic kidney disease. **Heart***,* 99 (6): 365-372

Moody, W. E., Edwards, N. C., Chue, C. D., et al. 2015. Variability in Cardiac Magnetic Resonance Measurement of Left Ventricular Ejection Fraction, Volumes and Mass in Healthy Adults: Defining a Significant Change at One Year. **Br J Radiol***,* 20140831

Moody, W. E., Edwards, N. C., Madhani, M., et al. 2012b. Endothelial dysfunction and cardiovascular disease in early-stage chronic kidney disease: Cause or association? **Atherosclerosis***,*

Moody, W. E., Ferro, C. J., Chue, C. D., et al. 2012c. Invite all donors to participate in follow-up studies. **Bmj***,* 344 e2724

Moody, W. E., Taylor, R. J., Edwards, N. C., et al. 2014a. Comparison of magnetic resonance feature tracking for systolic and diastolic strain and strain rate calculation with spatial modulation of magnetization imaging analysis. **J Magn Reson Imaging***,*

Moody, W. E., Tomlinson, L. A., Ferro, C. J., et al. 2014b. Effect of A Reduction in glomerular filtration rate after NEphrectomy on arterial STiffness and central hemodynamics: Rationale and design of the EARNEST study. **Am Heart J***,* 167 (2): 141-149 e142

Moody, W. E. & Townend, J. N. 2014. The importance of selecting controls in kidney donor outcome studies. **Kidney Int***,* 85 (5): 1241

Moon, J. C., Lorenz, C. H., Francis, J. M., et al. 2002. Breath-hold FLASH and FISP cardiovascular MR imaging: left ventricular volume differences and reproducibility. **Radiology***,* 223 (3): 789-797

Moon, J. C., Messroghli, D. R., Kellman, P., et al. 2013. Myocardial T1 mapping and extracellular volume quantification: a Society for Cardiovascular Magnetic Resonance (SCMR) and CMR Working Group of the European Society of Cardiology consensus statement. **J Cardiovasc Magn Reson***,* 15 92

Moore, C. C., Lugo-Olivieri, C. H., Mcveigh, E. R., et al. 2000. Three-dimensional systolic strain patterns in the normal human left ventricle: characterization with tagged MR imaging. **Radiology***,* 214 (2): 453-466

Mor-Avi, V., Lang, R. M., Badano, L. P., et al. 2011. Current and evolving echocardiographic techniques for the quantitative evaluation of cardiac mechanics: ASE/EAE consensus statement on methodology and indications endorsed by the Japanese Society of Echocardiography. **J Am Soc Echocardiogr***,* 24 (3): 277-313

Morena, M., Terrier, N., Jaussent, I., et al. 2006. Plasma osteoprotegerin is associated with mortality in hemodialysis patients. **J Am Soc Nephrol***,* 17 (1): 262-270

Morton, G., Schuster, A., Jogiya, R., et al. 2012. Inter-study reproducibility of cardiovascular magnetic resonance myocardial feature tracking. **J Cardiovasc Magn Reson***,* 14 43

Moynihan, R., Glassock, R. & Doust, J. 2013. Chronic kidney disease controversy: how expanding definitions are unnecessarily labelling many people as diseased. **Bmj***,* 347 f4298

Muscholl, M. W., Schunkert, H., Muders, F., et al. 1998. Neurohormonal activity and left ventricular geometry in patients with essential arterial hypertension. **Am Heart J***,* 135 (1): 58-66

Muzaale, A. D., Massie, A. B., Wang, M. C., et al. 2014. Risk of end-stage renal disease following live kidney donation. **JAMA***,* 311 (6): 579-586

Nagueh, S. F., Appleton, C. P., Gillebert, T. C., et al. 2009. Recommendations for the evaluation of left ventricular diastolic function by echocardiography. **J Am Soc Echocardiogr***,* 22 (2): 107-133

Nakahara, T., Takata, Y., Hirayama, Y., et al. 2007. Left ventricular hypertrophy and geometry in untreated essential hypertension is associated with blood levels of aldosterone and procollagen type III amino-terminal peptide. **Circ J***,* 71 (5): 716-721

Nakashima, A., Carrero, J. J., Qureshi, A. R., et al. 2010. Effect of circulating soluble receptor for advanced glycation end products (sRAGE) and the proinflammatory RAGE ligand (EN-RAGE, S100A12) on mortality in hemodialysis patients. **Clin J Am Soc Nephrol***,* 5 (12): 2213-2219

Nanayakkara, P. W., Kiefte-De Jong, J. C., Ter Wee, P. M., et al. 2009. Randomized placebo-controlled trial assessing a treatment strategy consisting of pravastatin, vitamin E, and homocysteine lowering on plasma asymmetric dimethylarginine concentration in mild to moderate CKD. **Am J Kidney Dis***,* 53 (1): 41-50

Nanayakkara, P. W., Van Guldener, C., Ter Wee, P. M., et al. 2007. Effect of a treatment strategy consisting of pravastatin, vitamin E, and homocysteine lowering on carotid intima-media thickness, endothelial function, and renal function in patients with mild to moderate chronic kidney disease: results from the Anti-Oxidant Therapy in Chronic Renal Insufficiency (ATIC) Study. **Arch Intern Med***,* 167 (12): 1262-1270

NHSBT. 2013. **NHS Blood & Transplant Organ Donation and Transplantation Activity Report 2012/13**. Available: https://nhsbtmediaservices.blob.core.windows.net/organ-donation-assets/pdfs/activity_report_2012_13.pdf [Accessed 27th February, 2015]

NICE. 2015. **Chronic kidney disease: early identification and management of chronic kidney disease in adults in primary and secondary care**. Available: http://www.nice.org.uk/guidance/cg182/resources/guidance-chronic-kidney-disease-pdf [Accessed 27th Februaury, 2015]

Nitta, K., Akiba, T., Uchida, K., et al. 2003. The progression of vascular calcification and serum osteoprotegerin levels in patients on long-term hemodialysis. **Am J Kidney Dis***,* 42 (2): 303-309

Nogueira, J. M., Weir, M. R., Jacobs, S., et al. 2009. A study of renal outcomes in African American living kidney donors. **Transplantation***,* 88 (12): 1371-1376

O'Connor, C. M. G. S., W.; Gheorghiade, M.; Adams Jr, K. F. (ed.) 2005. **Managing acute decompensated heart failure***,* Oxon: Taylor Francis.

O'Rourke, M. F. & Safar, M. E. 2005. Relationship between aortic stiffening and microvascular disease in brain and kidney: cause and logic of therapy. **Hypertension***,* 46 (1): 200-204

Okamoto, M., Akioka, K., Nobori, S., et al. 2009. Short- and long-term donor outcomes after kidney donation: analysis of 601 cases over a 35-year period at Japanese single center. **Transplantation***,* 87 (3): 419-423

OPTN 2014. Organ Procurement and Transplantation Network. Available: http://optn.transplant.hrsa.gov/ [Accessed 27th February, 2015]

Palmer, T. M., Nordestgaard, B. G., Benn, M., et al. 2013. Association of plasma uric acid with ischaemic heart disease and blood pressure: mendelian randomisation analysis of two large cohorts. **Bmj***,* 347 f4262

Panichi, V., Rizza, G. M., Paoletti, S., et al. 2008. Chronic inflammation and mortality in haemodialysis: effect of different renal replacement therapies. Results from the RISCAVID study. **Nephrol Dial Transplant***,* 23 (7): 2337-2343

Parfrey, P. S., Foley, R. N., Harnett, J. D., et al. 1996. Outcome and risk factors for left ventricular disorders in chronic uraemia. **Nephrol Dial Transplant***,* 11 (7): 1277-1285

Parfrey, P. S., Foley, R. N., Wittreich, B. H., et al. 2005. Double-blind comparison of full and partial anemia correction in incident hemodialysis patients without symptomatic heart disease. **J Am Soc Nephrol***,* 16 (7): 2180-2189

Parfrey, P. S., Lauve, M., Latremouille-Viau, D., et al. 2009. Erythropoietin therapy and left ventricular mass index in CKD and ESRD patients: a meta-analysis. **Clin J Am Soc Nephrol***,* 4 (4): 755-762

Pascual, J., Teruel, J. L., Moya, J. L., et al. 1991. Regression of left ventricular hypertrophy after partial correction of anemia with erythropoietin in patients on hemodialysis: a prospective study. **Clin Nephrol***,* 35 (6): 280-287

Pfeffer, M. A., Burdmann, E. A., Chen, C. Y., et al. 2009. A trial of darbepoetin alfa in type 2 diabetes and chronic kidney disease. **N Engl J Med***,* 361 (21): 2019-2032

Picano, E., Pelosi, G., Marzilli, M., et al. 1990. In vivo quantitative ultrasonic evaluation of myocardial fibrosis in humans. **Circulation***,* 81 (1): 58-64

Piovesan, A., Molineri, N., Casasso, F., et al. 1999. Left ventricular hypertrophy in primary hyperparathyroidism. Effects of successful parathyroidectomy. **Clin Endocrinol (Oxf)***,* 50 (3): 321-328

Pitt, B., Zannad, F., Remme, W. J., et al. 1999. The effect of spironolactone on morbidity and mortality in patients with severe heart failure. Randomized Aldactone Evaluation Study Investigators. **N Engl J Med***,* 341 (10): 709-717

Poggio, E. D., Wang, X., Greene, T., et al. 2005. Performance of the modification of diet in renal disease and Cockcroft-Gault equations in the estimation of GFR in health and in chronic kidney disease. **J Am Soc Nephrol***,* 16 (2): 459-466

Poterucha, J. T., Kutty, S., Lindquist, R. K., et al. 2012. Changes in left ventricular longitudinal strain with anthracycline chemotherapy in adolescents precede subsequent decreased left ventricular ejection fraction. **J Am Soc Echocardiogr***,* 25 (7): 733-740

Prasad, G. V., Lipszyc, D., Huang, M., et al. 2008. A prospective observational study of changes in renal function and cardiovascular risk following living kidney donation. **Transplantation***,* 86 (9): 1315-1318

Quarles, L. D. 2013. Reducing cardiovascular mortality in chronic kidney disease: something borrowed, something new. **J Clin Invest***,* 123 (2): 542-543

Rajagopalan, S., Duquaine, D., King, S., et al. 2002. Mineralocorticoid receptor antagonism in experimental atherosclerosis. **Circulation***,* 105 (18): 2212-2216

Ravani, P., Tripepi, G., Malberti, F., et al. 2005. Asymmetrical dimethylarginine predicts progression to dialysis and death in patients with chronic kidney disease: a competing risks modeling approach. **J Am Soc Nephrol***,* 16 (8): 2449-2455

Rebholz, C. M., Grams, M. E., Coresh, J., et al. 2015. Serum fibroblast growth factor-23 is associated with incident kidney disease. **J Am Soc Nephrol***,* 26 (1): 192-200

Recio-Mayoral, A., Banerjee, D., Streather, C., et al. 2011. Endothelial dysfunction, inflammation and atherosclerosis in chronic kidney disease--a cross-sectional study of predialysis, dialysis and kidney-transplantation patients. **Atherosclerosis***,* 216 (2): 446-451

Reese, P. P., Bloom, R. D., Feldman, H. I., et al. 2015. Selecting appropriate controls for kidney donors--reply. **Am J Transplant***,* 15 (1): 287-288

Reule, S., Matas, A. & Ibrahim, H. N. 2013. Selection of controls in kidney donor outcome studies: an admirable effort. **Am J Kidney Dis***,* 61 (2): 194-196

Rizvi, S. A., Naqvi, S. A., Jawad, F., et al. 2005. Living kidney donor follow-up in a dedicated clinic. **Transplantation***,* 79 (9): 1247-1251

Rizzoni, D., Porteri, E., Guelfi, D., et al. 2001. Structural alterations in subcutaneous small arteries of normotensive and hypertensive patients with non-insulin-dependent diabetes mellitus. **Circulation***,* 103 (9): 1238-1244

Rogacev, K. S., Seiler, S., Zawada, A. M., et al. 2011. CD14++CD16+ monocytes and cardiovascular outcome in patients with chronic kidney disease. **Eur Heart J***,* 32 (1): 84-92

Rogers, W. J., Hu, Y. L., Coast, D., et al. 2001. Age-associated changes in regional aortic pulse wave velocity. **J Am Coll Cardiol***,* 38 (4): 1123-1129

Ronco, C., Mccullough, P., Anker, S. D., et al. 2010. Cardio-renal syndromes: report from the consensus conference of the acute dialysis quality initiative. **Eur Heart J**, 31 (6): 703-711
Rossi, M., Campbell, K. L., Johnson, D. W., et al. 2014. Uremic toxin development in living kidney donors: a longitudinal study. **Transplantation**, 97 (5): 548-554
Rugale, C., Du Cailar, G., Fesler, P., et al. 2013. Effect of early stage kidney disease on cardiac mass: comparison to post-donation renal function. **Am J Nephrol**, 38 (2): 168-173
Saeki, A., Recchia, F. & Kass, D. A. 1995. systolic flow augmentation in hearts ejecting into a model of stiff aging vasculature. Influence on myocardial perfusion-demand balance. **Circ Res**, 76 (1): 132-141
Saito, H., Kusano, K., Kinosaki, M., et al. 2003. Human fibroblast growth factor-23 mutants suppress Na+-dependent phosphate co-transport activity and 1alpha,25-dihydroxyvitamin D3 production. **J Biol Chem**, 278 (4): 2206-2211
Saleh, F. N., Schirmer, H., Sundsfjord, J., et al. 2003. Parathyroid hormone and left ventricular hypertrophy. **Eur Heart J**, 24 (22): 2054-2060
Saltzman, A. J., Stone, G. W., Claessen, B. E., et al. 2011. Long-term impact of chronic kidney disease in patients with ST-segment elevation myocardial infarction treated with primary percutaneous coronary intervention: the HORIZONS-AMI (Harmonizing Outcomes With Revascularization and Stents in Acute Myocardial Infarction) trial. **JACC Cardiovasc Interv**, 4 (9): 1011-1019
Sanchez-Lozada, L. G., Tapia, E., Lopez-Molina, R., et al. 2007. Effects of acute and chronic L-arginine treatment in experimental hyperuricemia. **Am J Physiol Renal Physiol**, 292 (4): F1238-1244
Saran, R., Marshall, S. M., Madsen, R., et al. 1997. Long-term follow-up of kidney donors: a longitudinal study. **Nephrol Dial Transplant**, 12 (8): 1615-1621
Sautin, Y. Y., Nakagawa, T., Zharikov, S., et al. 2007. Adverse effects of the classic antioxidant uric acid in adipocytes: NADPH oxidase-mediated oxidative/nitrosative stress. **Am J Physiol Cell Physiol**, 293 (2): C584-596
Savage, M. T., Ferro, C. J., Pinder, S. J., et al. 2002. Reproducibility of derived central arterial waveforms in patients with chronic renal failure. **Clin Sci (Lond)**, 103 (1): 59-65
Savoia, C., Touyz, R. M., Endemann, D. H., et al. 2006. Angiotensin receptor blocker added to previous antihypertensive agents on arteries of diabetic hypertensive patients. **Hypertension**, 48 (2): 271-277
Scheven, L., De Jong, P. E., Hillege, H. L., et al. 2012. High-sensitive troponin T and N-terminal pro-B type natriuretic peptide are associated with cardiovascular events despite the cross-sectional association with albuminuria and glomerular filtration rate. **Eur Heart J**, 33 (18): 2272-2281
Schiffrin, E. L., Lipman, M. L. & Mann, J. F. 2007. Chronic kidney disease: effects on the cardiovascular system. **Circulation**, 116 (1): 85-97
Schiller, N. B., Shah, P. M., Crawford, M., et al. 1989. Recommendations for quantitation of the left ventricle by two-dimensional echocardiography. American Society of Echocardiography Committee on Standards,

Subcommittee on Quantitation of Two-Dimensional Echocardiograms. **J Am Soc Echocardiogr**, 2 (5): 358-367

Schluter, K. D. & Piper, H. M. 1998. Cardiovascular actions of parathyroid hormone and parathyroid hormone-related peptide. **Cardiovasc Res**, 37 (1): 34-41

Schmitt, M., Avolio, A., Qasem, A., et al. 2005. Basal NO locally modulates human iliac artery function in vivo. **Hypertension**, 46 (1): 227-231

Schrier, R. W. 2010. Aldosterone 'escape' vs 'breakthrough'. **Nat Rev Nephrol**, 6 (2): 61

Schuster, A., Kutty, S., Padiyath, A., et al. 2011a. Cardiovascular magnetic resonance myocardial feature tracking detects quantitative wall motion during dobutamine stress. **J Cardiovasc Magn Reson**, 13 58

Schuster, A., Paul, M., Bettencourt, N., et al. 2011b. Cardiovascular magnetic resonance myocardial feature tracking for quantitative viability assessment in ischemic cardiomyopathy. **Int J Cardiol**,

Schwarz, U., Buzello, M., Ritz, E., et al. 2000. Morphology of coronary atherosclerotic lesions in patients with end-stage renal failure. **Nephrol Dial Transplant**, 15 (2): 218-223

Schwedler, S. B., Metzger, T., Schinzel, R., et al. 2002. Advanced glycation end products and mortality in hemodialysis patients. **Kidney Int**, 62 (1): 301-310

Segev, D. L., Muzaale, A. D., Caffo, B. S., et al. 2010. Perioperative mortality and long-term survival following live kidney donation. **JAMA**, 303 (10): 959-966

Seiler, S., Reichart, B., Roth, D., et al. 2010. FGF-23 and future cardiovascular events in patients with chronic kidney disease before initiation of dialysis treatment. **Nephrol Dial Transplant**, 25 (12): 3983-3989

Shahul, S., Rhee, J., Hacker, M. R., et al. 2012. Subclinical left ventricular dysfunction in preeclamptic women with preserved left ventricular ejection fraction: a 2D speckle-tracking imaging study. **Circ Cardiovasc Imaging**, 5 (6): 734-739

Shapiro, L. M., Moore, R. B., Logan-Sinclair, R. B., et al. 1984. Relation of regional echo amplitude to left ventricular function and the electrocardiogram in left ventricular hypertrophy. **Br Heart J**, 52 (1): 99-105

Shimada, T., Hasegawa, H., Yamazaki, Y., et al. 2004. FGF-23 is a potent regulator of vitamin D metabolism and phosphate homeostasis. **J Bone Miner Res**, 19 (3): 429-435

Shlipak, M. G., Matsushita, K., Arnlov, J., et al. 2013. Cystatin C versus creatinine in determining risk based on kidney function. **N Engl J Med**, 369 (10): 932-943

Simonetti, O. P. & Raman, S. V. 2010. Straining to justify strain measurement. **JACC Cardiovasc Imaging**, 3 (2): 152-154

Simpson, R. U., Hershey, S. H. & Nibbelink, K. A. 2007. Characterization of heart size and blood pressure in the vitamin D receptor knockout mouse. **J Steroid Biochem Mol Biol**, 103 (3-5): 521-524

Singh, A. K., Szczech, L., Tang, K. L., et al. 2006. Correction of anemia with epoetin alfa in chronic kidney disease. **N Engl J Med**, 355 (20): 2085-2098

Stam, F., Van Guldener, C., Becker, A., et al. 2006. Endothelial dysfunction contributes to renal function-associated cardiovascular mortality in a

population with mild renal insufficiency: the Hoorn study. **J Am Soc Nephrol**, 17 (2): 537-545

Stenvinkel, P., Carrero, J. J., Axelsson, J., et al. 2008. Emerging biomarkers for evaluating cardiovascular risk in the chronic kidney disease patient: how do new pieces fit into the uremic puzzle? **Clin J Am Soc Nephrol**, 3 (2): 505-521

Stenvinkel, P., Heimburger, O. & Jogestrand, T. 2002. Elevated interleukin-6 predicts progressive carotid artery atherosclerosis in dialysis patients: association with Chlamydia pneumoniae seropositivity. **Am J Kidney Dis**, 39 (2): 274-282

Stenvinkel, P., Heimburger, O., Paultre, F., et al. 1999. Strong association between malnutrition, inflammation, and atherosclerosis in chronic renal failure. **Kidney Int**, 55 (5): 1899-1911

Stevens, L. A., Coresh, J., Greene, T., et al. 2006. Assessing kidney function--measured and estimated glomerular filtration rate. **N Engl J Med**, 354 (23): 2473-2483

Stewart, G. A., Gansevoort, R. T., Mark, P. B., et al. 2005. Electrocardiographic abnormalities and uremic cardiomyopathy. **Kidney Int**, 67 (1): 217-226

Storsley, L. J., Young, A., Rush, D. N., et al. 2010. Long-term medical outcomes among Aboriginal living kidney donors. **Transplantation**, 90 (4): 401-406

Struthers, A. D. 2004. The clinical implications of aldosterone escape in congestive heart failure. **Eur J Heart Fail**, 6 (5): 539-545

Struthers, A. D. & Macdonald, T. M. 2004. Review of aldosterone- and angiotensin II-induced target organ damage and prevention. **Cardiovasc Res**, 61 (4): 663-670

Sui, Y., Zhao, H. L., Ma, R. C., et al. 2007. Pancreatic islet beta-cell deficit and glucose intolerance in rats with uninephrectomy. **Cell Mol Life Sci**, 64 (23): 3119-3128

Sundstrom, J., Sullivan, L., D'Agostino, R. B., et al. 2005. Relations of serum uric acid to longitudinal blood pressure tracking and hypertension incidence. **Hypertension**, 45 (1): 28-33

Sviglerova, J., Kuncova, J., Nalos, L., et al. 2010. Cardiovascular parameters in rat model of chronic renal failure induced by subtotal nephrectomy. **Physiol Res**, 59 Suppl 1 S81-88

Tan, J. C., Ho, B., Busque, S., et al. 2010. Imprecision of creatinine-based GFR estimates in uninephric kidney donors. **Clin J Am Soc Nephrol**, 5 (3): 497-502

Tan, Y. T., Wenzelburger, F., Lee, E., et al. 2009. The pathophysiology of heart failure with normal ejection fraction: exercise echocardiography reveals complex abnormalities of both systolic and diastolic ventricular function involving torsion, untwist, and longitudinal motion. **J Am Coll Cardiol**, 54 (1): 36-46

Tan, Y. T., Wenzelburger, F. W., Sanderson, J. E., et al. 2013. Exercise-induced torsional dyssynchrony relates to impaired functional capacity in patients with heart failure and normal ejection fraction. **Heart**, 99 (4): 259-266

Taylor, R. J., Moody, W. E., Umar, F., et al. 2015. Myocardial strain measurement with feature-tracking cardiovascular magnetic resonance: normal values. **Eur Heart J Cardiovasc Imaging**,

Terasaki, P. I., Cecka, J. M., Gjertson, D. W., et al. 1995. High survival rates of kidney transplants from spousal and living unrelated donors. **N Engl J Med***,* 333 (6): 333-336

Thadhani, R., Appelbaum, E., Pritchett, Y., et al. 2012. Vitamin D therapy and cardiac structure and function in patients with chronic kidney disease: the PRIMO randomized controlled trial. **JAMA***,* 307 (7): 674-684

Thambyrajah, J., Landray, M. J., Mcglynn, F. J., et al. 2000. Abnormalities of endothelial function in patients with predialysis renal failure. **Heart***,* 83 (2): 205-209

Thiel, G. T., Nolte, C. & Tsinalis, D. 2011. Prospective Swiss cohort study of living-kidney donors: study protocol. **BMJ Open***,* 1 (2): e000202

Tonelli, M., Muntner, P., Lloyd, A., et al. 2012. Risk of coronary events in people with chronic kidney disease compared with those with diabetes: a population-level cohort study. **Lancet***,*

Tong, M., Carrero, J. J., Qureshi, A. R., et al. 2007. Plasma pentraxin 3 in patients with chronic kidney disease: associations with renal function, protein-energy wasting, cardiovascular disease, and mortality. **Clin J Am Soc Nephrol***,* 2 (5): 889-897

Touboul, P. J., Hennerici, M. G., Meairs, S., et al. 2012. Mannheim carotid intima-media thickness and plaque consensus (2004-2006-2011). An update on behalf of the advisory board of the 3rd, 4th and 5th watching the risk symposia, at the 13th, 15th and 20th European Stroke Conferences, Mannheim, Germany, 2004, Brussels, Belgium, 2006, and Hamburg, Germany, 2011. **Cerebrovasc Dis***,* 34 (4): 290-296

Tousoulis, D., Andreou, I., Tsiatas, M., et al. 2011. Effects of rosuvastatin and allopurinol on circulating endothelial progenitor cells in patients with congestive heart failure: the impact of inflammatory process and oxidative stress. **Atherosclerosis***,* 214 (1): 151-157

Tripepi, G., Mallamaci, F. & Zoccali, C. 2005. Inflammation markers, adhesion molecules, and all-cause and cardiovascular mortality in patients with ESRD: searching for the best risk marker by multivariate modeling. **J Am Soc Nephrol***,* 16 Suppl 1 S83-88

Ugander, M., Oki, A. J., Hsu, L. Y., et al. 2012. Extracellular volume imaging by magnetic resonance imaging provides insights into overt and sub-clinical myocardial pathology. **Eur Heart J***,* 33 (10): 1268-1278

Urakawa, I., Yamazaki, Y., Shimada, T., et al. 2006. Klotho converts canonical FGF receptor into a specific receptor for FGF23. **Nature***,* 444 (7120): 770-774

USRDS 2011. U S Renal Data System, Annual Data Report: Atlas of Chronic Kidney Disease and End-Stage Renal Disease in the United States, National Institutes of Health, National Institute of Diabetes and Digestive and Kidney Diseases, Bethesda, MD, 2011.

Van Biesen, W., De Bacquer, D., Verbeke, F., et al. 2007. The glomerular filtration rate in an apparently healthy population and its relation with cardiovascular mortality during 10 years. **Eur Heart J***,* 28 (4): 478-483

Van Guldener, C., Janssen, M. J., Lambert, J., et al. 1998. Endothelium-dependent vasodilatation is impaired in peritoneal dialysis patients. **Nephrol Dial Transplant**, 13 (7): 1782-1786

Van Guldener, C., Lambert, J., Janssen, M. J., et al. 1997. Endothelium-dependent vasodilatation and distensibility of large arteries in chronic haemodialysis patients. **Nephrol Dial Transplant**, 12 Suppl 2 14-18

Van Popele, N. M., Grobbee, D. E., Bots, M. L., et al. 2001. Association between arterial stiffness and atherosclerosis: the Rotterdam Study. **Stroke**, 32 (2): 454-460

Vaz, S., Falkmer, T., Passmore, A. E., et al. 2013. The case for using the repeatability coefficient when calculating test-retest reliability. **PLoS One**, 8 (9): e73990

Velagaleti, R. S., Gona, P., Levy, D., et al. 2008. Relations of biomarkers representing distinct biological pathways to left ventricular geometry. **Circulation**, 118 (22): 2252-2258, 2255p following 2258

Vickery, S., Webb, M. C., Price, C. P., et al. 2008. Prognostic value of cardiac biomarkers for death in a non-dialysis chronic kidney disease population. **Nephrol Dial Transplant**, 23 (11): 3546-3553

Vitart, V., Rudan, I., Hayward, C., et al. 2008. SLC2A9 is a newly identified urate transporter influencing serum urate concentration, urate excretion and gout. **Nat Genet**, 40 (4): 437-442

Voelkl, J., Alesutan, I., Leibrock, C. B., et al. 2013. Spironolactone ameliorates PIT1-dependent vascular osteoinduction in klotho-hypomorphic mice. **J Clin Invest**, 123 (2): 812-822

Von Elm, E., Altman, D. G., Egger, M., et al. 2007. The Strengthening the Reporting of Observational Studies in Epidemiology (STROBE) statement: guidelines for reporting observational studies. **Epidemiology**, 18 (6): 800-804

Vukusich, A., Kunstmann, S., Varela, C., et al. 2010. A randomized, double-blind, placebo-controlled trial of spironolactone on carotid intima-media thickness in nondiabetic hemodialysis patients. **Clin J Am Soc Nephrol**, 5 (8): 1380-1387

Wang, A. Y., Wang, M., Lam, C. W., et al. 2013. Heart failure with preserved or reduced ejection fraction in patients treated with peritoneal dialysis. **Am J Kidney Dis**, 61 (6): 975-983

Wang, J., Fang, F., Wai-Kwok Yip, G., et al. 2015. Left ventricular long-axis performance during exercise is an important prognosticator in patients with heart failure and preserved ejection fraction. **Int J Cardiol**, 178 131-135

Wang, J. J., O'Brien, A. B., Shrive, N. G., et al. 2003. Time-domain representation of ventricular-arterial coupling as a windkessel and wave system. **Am J Physiol Heart Circ Physiol**, 284 (4): H1358-1368

Wang, M. C., Tsai, W. C., Chen, J. Y., et al. 2005. Stepwise increase in arterial stiffness corresponding with the stages of chronic kidney disease. **Am J Kidney Dis**, 45 (3): 494-501

Wei, W., Tolle, M., Zidek, W., et al. 2010. Validation of the mobil-O-Graph: 24 h-blood pressure measurement device. **Blood Press Monit**, 15 (4): 225-228

Weiner, D. E., Tighiouart, H., Elsayed, E. F., et al. 2008. The relationship between nontraditional risk factors and outcomes in individuals with stage 3 to 4 CKD. **Am J Kidney Dis***,* 51 (2): 212-223

Weir, J. P. 2005. Quantifying test-retest reliability using the intraclass correlation coefficient and the SEM. **J Strength Cond Res***,* 19 (1): 231-240

Weiss, W., Gohlisch, C., Harsch-Gladisch, C., et al. 2012. Oscillometric estimation of central blood pressure: validation of the Mobil-O-Graph in comparison with the SphygmoCor device. **Blood Press Monit***,* 17 (3): 128-131

Wever, R., Boer, P., Hijmering, M., et al. 1999. Nitric oxide production is reduced in patients with chronic renal failure. **Arterioscler Thromb Vasc Biol***,* 19 (5): 1168-1172

Wheeler, D. C., Townend, J. N. & Landray, M. J. 2003. Cardiovascular risk factors in predialysis patients: baseline data from the Chronic Renal Impairment in Birmingham (CRIB) study. **Kidney Int Suppl***,* (84): S201-203

Wiesmann, F., Petersen, S. E., Leeson, P. M., et al. 2004. Global impairment of brachial, carotid, and aortic vascular function in young smokers: direct quantification by high-resolution magnetic resonance imaging. **J Am Coll Cardiol***,* 44 (10): 2056-2064

Wilkinson, I. B., Fuchs, S. A., Jansen, I. M., et al. 1998. Reproducibility of pulse wave velocity and augmentation index measured by pulse wave analysis. **J Hypertens***,* 16 (12 Pt 2): 2079-2084

Wilkinson, I. B. & Webb, D. J. 2001. Venous occlusion plethysmography in cardiovascular research: methodology and clinical applications. **Br J Clin Pharmacol***,* 52 (6): 631-646

Willum-Hansen, T., Staessen, J. A., Torp-Pedersen, C., et al. 2006. Prognostic value of aortic pulse wave velocity as index of arterial stiffness in the general population. **Circulation***,* 113 (5): 664-670

Wolf, M., Shah, A., Gutierrez, O., et al. 2007. Vitamin D levels and early mortality among incident hemodialysis patients. **Kidney Int***,* 72 (8): 1004-1013

Yeon, S. B., Reichek, N., Tallant, B. A., et al. 2001. Validation of in vivo myocardial strain measurement by magnetic resonance tagging with sonomicrometry. **J Am Coll Cardiol***,* 38 (2): 555-561

Yildiz, A., Oflaz, H., Pusuroglu, H., et al. 2003. Left ventricular hypertrophy and endothelial dysfunction in chronic hemodialysis patients. **Am J Kidney Dis***,* 41 (3): 616-623

Yilmaz, B. A., Caliskan, Y., Yilmaz, A., et al. 2014. Cardiovascular-Renal Changes After Kidney Donation: One-Year Follow-Up Study. **Transplantation***,*

Yilmaz, M. I., Axelsson, J., Sonmez, A., et al. 2009. Effect of renin angiotensin system blockade on pentraxin 3 levels in type-2 diabetic patients with proteinuria. **Clin J Am Soc Nephrol***,* 4 (3): 535-541

Yilmaz, M. I., Carrero, J. J., Martin-Ventura, J. L., et al. 2010a. Combined therapy with renin-angiotensin system and calcium channel blockers in type 2 diabetic hypertensive patients with proteinuria: effects on soluble TWEAK, PTX3, and flow-mediated dilation. **Clin J Am Soc Nephrol***,* 5 (7): 1174-1181

Yilmaz, M. I., Sonmez, A., Ortiz, A., et al. 2011a. Soluble TWEAK and PTX3 in nondialysis CKD patients: impact on endothelial dysfunction and cardiovascular outcomes. **Clin J Am Soc Nephrol***,* 6 (4): 785-792

Yilmaz, M. I., Sonmez, A., Saglam, M., et al. 2010b. Reduced proteinuria using ramipril in diabetic CKD stage 1 decreases circulating cell death receptor activators concurrently with ADMA. A novel pathophysiological pathway? **Nephrol Dial Transplant***,* 25 (10): 3250-3256

Yilmaz, M. I., Stenvinkel, P., Sonmez, A., et al. 2011b. Vascular health, systemic inflammation and progressive reduction in kidney function; clinical determinants and impact on cardiovascular outcomes. **Nephrol Dial Transplant***,*

Young, A., Hodsman, A. B., Boudville, N., et al. 2012a. Bone and mineral metabolism and fibroblast growth factor 23 levels after kidney donation. **Am J Kidney Dis***,* 59 (6): 761-769

Young, A. A., Axel, L., Dougherty, L., et al. 1993. Validation of tagging with MR imaging to estimate material deformation. **Radiology***,* 188 (1): 101-108

Young, A. A., Cowan, B. R., Thrupp, S. F., et al. 2000. Left ventricular mass and volume: fast calculation with guide-point modeling on MR images. **Radiology***,* 216 (2): 597-602

Young, A. A., Imai, H., Chang, C. N., et al. 1994. Two-dimensional left ventricular deformation during systole using magnetic resonance imaging with spatial modulation of magnetization. **Circulation***,* 89 (2): 740-752

Young, A. A., Li, B., Kirton, R. S., et al. 2012b. Generalized spatiotemporal myocardial strain analysis for DENSE and SPAMM imaging. **Magn Reson Med***,* 67 (6): 1590-1599

Zannad, F., Mcmurray, J. J., Krum, H., et al. 2011. Eplerenone in patients with systolic heart failure and mild symptoms. **N Engl J Med***,* 364 (1): 11-21

Zile, M. R., Gottdiener, J. S., Hetzel, S. J., et al. 2011. Prevalence and Significance of Alterations in Cardiac Structure and Function in Patients With Heart Failure and a Preserved Ejection Fraction. **Circulation***,*

Zoccali, C., Benedetto, F. A., Maas, R., et al. 2002. Asymmetric dimethylarginine, C-reactive protein, and carotid intima-media thickness in end-stage renal disease. **J Am Soc Nephrol***,* 13 (2): 490-496

8. APPENDIX I: LIST OF ABSTRACTS RELATED TO THIS WORK

Oral communications

- **Moody WE**, Ferro CJ, Edwards NC, Chue CD, Lin ES, Taylor RJ,Cockwell P, Steeds RP, Townend JN. Effects of Nephrectomy on Cardiovascular Structure and Function in Living Kidney Donors. Finalist for **American College of Cardiology Scientific Sessions Young Investigator Research Award in Physiology, Pharmacology and Pathology, San Diego, March 2015.**

- Edwards NC, **Moody WE**, Yuan M, Flanagan S, Ferro CJ, Townend JN, Steeds RP. Early stage chronic kidney disease: a paradigm for diffuse fibrosis and clinical progression. *J Cardiovasc Magn Reson* 2014, 16(Suppl 1):O66.

- **Moody WE**, Lin LS, Bloxham N, Fraser H, Taylor RJ, Edwards NC, Holloway B, Ferro CJ, Townend JN, Steeds RP. Real-world relative utility of stress testing and coronary calcium score for the detection of coronary artery disease in prospective renal transplant recipients. *Eur Heart J Cardiovasc Imaging* 2013; 14(suppl 2): P839. **Winner of the British Nuclear Cardiology Society Young Investigator Award 2013**.

- Taylor RJ, Umar F, **Moody WE**, Meyyapan C, Stegemann B, Townend JN *et al*. Feature-tracking cardiovascular magnetic resonance as a novel technique for the assessment of mechanical dyssynchrony. Europace 2013; 15(suppl 2): ii2-ii5.

- **Moody WE**, Chue CD, Ludman PF, Chan YC, Narayan G, Millington JM, Townend JN, Doshi SN. Bleeding outcomes in patients undergoing routine transradial primary angioplasty for acute myocardial infarction treated with eptifibatide and unfractionated heparin: a single centre real-world experience. *EuroIntervention* 2012; 8N: 047.

- McNulty CL, Gorecki J, Kloss D, Knott I, Lee R, Robinson A, **Moody WE**, Fisher JP. Haemodynamic responses to muscle metaboreceptor activation in humans. *Physiology* 2012; C18.

- Chue CD, Townend JN, **Moody WE**, Edwards NC, Steeds RP, Ferro CJ. Effects of sevelamer carbonate on arterial stiffness and left ventricular mass in patients with stage 3 chronic kidney disease: results of a randomized controlled trial. AHA Elizabeth Barrett-Connor Research Award for Young Investigators in Training Finalist. *Circulation* 2012; 126: A9529.

Poster communications

- **Moody WE**, Lin ELS, Ferro, CJ, Edwards NC, Holloway B, Townend JN, Steeds RP. Prognostic Value of Calcium Scoring as an Adjunct to Stress Myocardial Perfusion Scintigraphy in End-Stage Renal Disease. Accepted for presentation at American College of Cardiology's 2015 Scientific Sessions.

- **Moody WE**, Edwards NC, Chue CD, Taylor RJ, Li AK, Ferro CJ, Townend JN, Steeds RP. Normative annual changes in left ventricular volumes, mass and function among healthy adults: a prospective cardiac magnetic resonance imaging study. *J Cardiovasc Magn Reson* 2014, 16(suppl 1): P99.

- Edwards NC, Yuan M, Good IK, **Moody WE**, Steeds RP. Optimum management of asymptomatic moderate-severe degenerative mitral regurgitation: a role for T1 mapping in risk stratification? *J Cardiovasc Magn Reson* 2014, 16(suppl 1): P238.

- Taylor RJ, Umar F, Lin L, Ahmed A, **Moody WE**, Stegemann B, Townend JN, Steeds RP, Leyva F. Mechanical effects of midwall fibrosis in non-ischemic dilated cardiomyopathy. *J Cardiovasc Magn Reson* 2014, 16(suppl 1): P308.

- **Moody WE**, Begaj I, Banerjee A, Chue CD, Edwards NC, Steeds RP, Ferro CJ, Townend JN. Long-term cardiovascular outcomes in UK living kidney donors. *Eur Heart J* 2013, 34(suppl 1): P5161.

- **Moody WE**, Taylor RJ, Edwards NC, Umar F, Chue CD, Taylor TJ, Ferro CJ, Townend JN, Leyva F, Steeds RP. Comparison of magnetic resonance feature tracking for longitudinal strain calculation with spatial modulation of magnetization imaging analysis. *J Cardiovasc Magn Reson* 2013; 14(suppl 1): P123.

- Taylor RJ, **Moody WE**, Umar F, Edwards NC, Taylor TJ, Townend JN, Steeds RP, Leyva F. The effects of age and gender on myocardial strain: A feature tracking cardiac magnetic resonance study. *Eur Heart J Cardiovasc Imaging* 2013; 14(suppl 2): P1243.

- Taylor RJ, Umar F, **Moody WE**, Townend JN, Steeds RP, Leyva F. The reproducibility and analysis time of cardiac magnetic resonance feature tracking: potential for clinical application. *Heart* 2013; 99(suppl 2): A64.

- Edwards NC, Noori A, Chue CD, **Moody WE**, Ferro CJ, Townend JN, Steeds RP. Impaired circumferential and longitudinal myocardial deformation in early stage chronic kidney disease: the earliest features of uremic cardiomyopathy. *J Cardiovasc Magn Reson* 2013, 15(suppl 1): P153.

9. APPENDIX II: LIST OF PUBLICATIONS ARISING DIRECTLY FROM THIS WORK

- **Moody WE**, Edwards NC, Chue CD, Taylor RJ, Ferro CJ, Townend JN, Steeds RP. Variability in Cardiac Magnetic Resonance Measurement of Left Ventricular Ejection Fraction, Volumes and Mass in Healthy Adults: Defining a Significant Change at One Year. *Br J Radiol* 2015 Feb 24:20140831. [Epub ahead of print]

- Taylor RJ,* **Moody WE**,* Umar F, Edwards NC, Taylor TJ, Stegemann B, Townend JN, Hor KN, Steeds RP, Mazur W, Leyva F. Myocardial strain measurement with feature-tracking cardiovascular magnetic resonance: normal values. *Eur Heart J Cardiovasc Imaging* 2015 Feb 23. pii: jev006. [Epub ahead of print]

  **Joint first authors*

- **Moody WE**, Taylor RJ, Edwards NC, Chue CD, Umar F, Taylor T, Young A, Ferro CJ, Townend JN, Leyva F, Steeds RP. Comparison of magnetic resonance feature tracking for systolic and diastolic strain and strain rate calculation with spatial modulation of magnetization imaging analysis. *J Magn Reson Imaging* 2014 Mar 28. doi: 10.1002/jmri.24623. [Epub ahead of print]

- **Moody WE**, Tomlinson LA, Ferro CJ, Steeds RP, Mark PB, Zehnder D, Tomson CR, Cockcroft JR, Wilkinson IB, Townend JN. Effect of A Reduction in glomerular filtration rate after NEphrectomy on arterial STiffness and central hemodynamics: Rationale and design of the EARNEST study. *Am Heart* J 2014; 167: 141-149.e2.

- **Moody WE**, Ferro, CJ, Townend JN. The EARNEST Study: Interarm blood pressure differences should also be recorded. *Am Heart J* 2014; 168:e9.

- **Moody WE**, Townend JN. The importance of selecting controls in kidney donor outcome studies. *Kidney Int* 2014; 85:1241.

- **Moody WE**, Edwards NC, Chue CD, Ferro CJ, Townend JN. Arterial disease in chronic kidney disease. *Heart* 2013; 99: 365-72.

- **Moody WE**, Edwards NC, Townend JN. Letter by Moody *et al*. regarding article "Prevalence and significance of alterations in cardiac structure and function in patients with heart failure and a preserved ejection fraction". *Circulation* 2012; 126: e62.

- **Moody WE**, Ferro CJ, Chue CD, Edwards NC, Steeds RP, Townend JN. Invite all donors to participate in follow-up studies. *BMJ* 2012; 344: e2724.

- **Moody WE**, Edwards NC, Madhani M, Chue CD, Steeds RP, Ferro CJ, Townend JN. Endothelial dysfunction and cardiovascular disease in early-stage chronic kidney disease: Cause or association? *Atherosclerosis* 2012; 223: 86-94.

- **Moody WE**, Chue CD, Inston NG, Edwards NC, Steeds RP, Ferro CJ, Townend JN. Understanding the effects of chronic kidney disease on cardiovascular risk: are there lessons to be learnt from healthy kidney donors? *J Hum Hypertens* 2012; 26: 141-8.

10. APPENDIX III: LIST OF OTHER PUBLICATIONS RELATED TO THIS WORK

- Edwards NC, **Moody WE**, Yuan M, Hayer MK, Ferro CJ, Townend JN, Steeds RP. Diffuse Interstitial Fibrosis and Myocardial Dysfunction in Early Chronic Kidney Disease. Am J Cardiol. 2015 Feb 12. [Epub ahead of print]

- Bashir A, **Moody WE**, Edwards NC, Ferro CJ, Townend JN, Steeds RP. Coronary Artery Calcium Assessment in Chronic Kidney Disease: Utility in Cardiovascular Disease Risk Assessment and Treatment? Am J Kidney Dis. Mar 6 2015. [Epub ahead of print]

- Yuan M, **Moody WE**, Townend JN. Central Blood Pressure in Chronic Kidney Disease: Latest Evidence and Clinical Relevance. Curr Hypertens Rev. Dec 31 2014. [Epub ahead of print]

- Edwards NC, **Moody WE**, Yuan M, Weale P, Neil D, Townend J, Steeds RP. Quantification of Left Ventricular Interstitial Fibrosis in Asymptomatic Chronic Primary Degenerative Mitral Regurgitation. Circ Cardiovasc Imaging. Aug 19 2014. [Epub ahead of print]

- Oxborough D, Ghani S, Harkness A, Lloyd G, **Moody WE**, Ring R, Sandoval J, Senior R, Sheikh N, Stout M, Utomi V, Willis J, Zaidi A, Steeds RP. Impact of Methodology and the use of Allometric Scaling on the Echocardiographic Assessment of the Aortic Root and Arch. *Echo Res Pract* 2014; 1:1-9.

- Edwards NC, **Moody WE**, Chue CD, Ferro CJ, Townend JN, Steeds RP. Defining the Natural History of Uremic Cardiomyopathy in Chronic Kidney Disease – the role of cardiovascular magnetic resonance imaging. JACC Cardiovasc Imaging 2014; 7:703-14.

- Taylor RJ, Umar F, **Moody WE**, Meyyappan C, Stegemann B, Townend JN, Hor KN, Miszalski-Jamka T, Mazur W, Steeds RP, Leyva F. Feature-tracking cardiovascular magnetic resonance as a novel technique for the assessment of mechanical dyssynchrony. *Int J Cardiol* 2014; 175:120-5.

- McNulty CL, **Moody WE**, Wagenmakers AJ, Fisher JP. Effect of muscle metaboreflex activation on central hemodynamics and cardiac function in humans. Accepted for publication. *Appl Physiol Nutr Metab* 2014; 39:861-70.

- Ng KP, **Moody WE**, Chue CD, Edwards NC, Savage T, Tomson CR, Steeds RP, Townend JN, Ferro CJ. Central pulse pressure in patients with chronic kidney disease and in renal transplant recipients. J Hum Hypertens 2014; 28: 180-5.

- Chue CD, Townend JN, **Moody WE**, Zehnder D, Wall NA, Harper L, Edwards NC, Steeds RP, Ferro CJ. Cardiovascular effects of sevelamer in stage 3 CKD. J Am Soc Nephrol 2013; 24: 842-52.

- Chue CD, **Moody WE**, Steeds RP, Townend JN, Ferro CJ. Unexpected benefits of participation in a clinical trial: abdominal aortic aneurysms in patients with chronic kidney disease. *QJM* 2012; 105(12): 1213-6.

- Chue CD, Wall NA, Crabtree NJ, Zehnder D, **Moody WE**, Edwards NC, Steeds RP, Townend JN, Ferro CJ. Aortic calcification and femoral bone density are independently associated with left ventricular mass in patients with chronic kidney disease. *PLoS One* 2012; 7: e39241.

- Chue CD, Edwards NC, **Moody WE**, Steeds RP, Townend JN, Ferro CJ. Serum phosphate is associated with left ventricular mass in patients with chronic kidney disease: a cardiac magnetic resonance study. *Heart* 2012; 98: 219-24.

11. APPENDIX IV: LIST OF PERSONAL AWARDS ARISING DIRECTLY FROM THIS WORK

- Finalist for Young Investigator Research Award in Physiology, Pharmacology and Pathology. Oral presentation at American College of Cardiology Scientific Sessions, San Diego, March 2015.
- Joint British Cardiovascular Society and American College of Cardiology Multi-Modality Imaging Preceptorship. Cedars-Sinai, Los Angeles, June 2014.
- British Heart Foundation Clinical Research Training Fellowship FS/11/17/28700. April 2011 – April 2014.